

An evaluation, characterization and comparison of pressure balancing
valves, tempering valves, automatic mixing valves
and anti-scald type shower valves

by

George Randall Wandling

A thesis submitted to the graduate faculty
in partial fulfillment of the requirements for the degree of
MASTER OF SCIENCE

Major: Mechanical Engineering
Major Professor: Donald R. Flugrad, Jr.

Iowa State University

Ames, Iowa

1996

Copyright © George Randall Wandling, 1996. All rights reserved.

Graduate College
Iowa State University

This is to certify that the Master's thesis of
George Randall Wandling
has met the thesis requirements of Iowa State University

Signatures have been redacted for privacy

TABLE OF CONTENTS

| | |
|---|------|
| LIST OF TABLES | v |
| LIST OF FIGURES | vi |
| ACKNOWLEDGEMENTS | xiii |
| CHAPTER 1. INTRODUCTION | 1 |
| Research Goals | 4 |
| Thesis Organization | 5 |
| CHAPTER 2. LITERATURE REVIEW | 7 |
| CHAPTER 3. STUDIES OF THERMAL INJURIES | 12 |
| CHAPTER 4. RESIDENTIAL REQUIREMENTS FOR HOT WATER | 16 |
| CHAPTER 5. STANDARDS AND CODES | 18 |
| CHAPTER 6. PRESSURE BALANCED BATH VALVES | 19 |
| Valve Design | 19 |
| System Modeling | 25 |
| System Testing | 48 |
| CHAPTER 7. TEMPERING VALVES | 80 |
| Valve Design | 80 |
| System Modeling | 84 |
| System Testing | 97 |
| CHAPTER 8. ANTI-SCALD VALVES | 115 |
| Valve Design | 115 |
| System Modeling | 121 |
| System Testing | 133 |
| CHAPTER 9. THERMOSTATIC MIXING VALVES | 147 |

| | |
|---------------------------------|-----|
| Valve Design | 147 |
| System Modeling | 153 |
| System Testing | 172 |
| CHAPTER 10. CONCLUSIONS | 202 |
| Recommendations for Future Work | 204 |
| REFERENCES | 206 |

LIST OF TABLES

| | | |
|------------|---|-----|
| Table 3.1: | Time-surface temperature thresholds for thermal injury of human adult skin. | 14 |
| Table 6.1: | Mix temperature vs. position of rotational limit stop | 20 |
| Table 6.2: | Effective orifice plate area as a function of handle position | 38 |
| Table 6.3: | Pressure valve response, cold supply pressure drop | 70 |
| Table 7.1: | Thermostat length as a function of temperature | 85 |
| Table 7.2: | Thermostat length as a function of time and ΔT | 87 |
| Table 7.3: | Tempering valve response, cold supply pressure drop | 100 |
| Table 7.4: | Tempering valve response, hot supply temperature increase | 107 |
| Table 8.1: | Thermostat length as a function of temperature | 125 |
| Table 9.1: | Thermostat length as a function of temperature | 159 |
| Table 9.2: | Thermostat length as a function of time and ΔT | 161 |
| Table 9.3 | Mixing valve response, cold supply pressure drop | 177 |
| Table 9.4 | Mixing valve response, cold supply pressure drop | 184 |
| Table 9.5 | Mixing valve response, hot supply temperature increase | 196 |

LIST OF FIGURES

| | | |
|--------------|--|----|
| Figure 3.1: | Time-surface temperature thresholds for second & third degree reaction of human adult and child skin | 15 |
| Figure 6.1: | Cross section view of pressure balance valve | 22 |
| Figure 6.2: | Cross section view of pressure balance valve | 24 |
| Figure 6.3: | Pressure valve orifice plate and supply flow lines | 26 |
| Figure 6.4: | Cold supply spool inlet and outlet area | 34 |
| Figure 6.5: | Hot supply spool inlet and outlet area | 35 |
| Figure 6.6: | Orifice plate flow area as a function of handle position | 36 |
| Figure 6.7: | Orifice plate flow area graphed as a function of handle position | 37 |
| Figure 6.8: | Ψ_c and Ψ_h plotted as a function of spool position | 44 |
| Figure 6.9: | Λ_c and Λ_h plotted as a function of spool position | 45 |
| Figure 6.10: | Spool pressure plotted as a function of spool position | 46 |
| Figure 6.11: | Supply flow plotted as a function of spool position | 47 |
| Figure 6.12: | Piping schematic for valve tests | 50 |
| Figure 6.13: | Pressure valve test, results of the hot and cold supply flow as a function of time | 53 |
| Figure 6.14: | Pressure valve test, supply flow as a function of valve handle position | 54 |
| Figure 6.15: | Pressure valve test, mix temperature as a function of valve handle position | 55 |

| | | |
|--------------|---|----|
| Figure 6.16: | Pressure valve model, hot and cold supply flow as a function of valve handle position | 56 |
| Figure 6.17: | Pressure valve model and test, mix temperature as a function of valve handle position | 57 |
| Figure 6.18: | Pressure valve model and test, flow rate as a function of valve handle position | 58 |
| Figure 6.19: | Pressure valve test, increase in hot supply temperature, supply and mix temperatures | 60 |
| Figure 6.20: | Pressure valve test, increase in hot supply temperature, supply pressure | 61 |
| Figure 6.21: | Pressure valve test, increase in hot supply temperature, supply flow rates | 62 |
| Figure 6.22: | Pressure valve test, decrease in cold supply pressure, supply pressure | 64 |
| Figure 6.23: | Pressure valve test, decrease in cold supply pressure, supply flow rates | 65 |
| Figure 6.24: | Pressure valve test, decrease in cold supply pressure, supply and mix temperatures | 66 |
| Figure 6.25: | Pressure valve model, decrease in cold supply pressure, spool position | 71 |
| Figure 6.26: | Pressure valve model, decrease in cold supply pressure, spool velocity | 72 |
| Figure 6.27: | Pressure valve model, decrease in cold supply pressure, spool acceleration | 73 |
| Figure 6.28: | Pressure valve model, decrease in cold supply pressure, mix temperature | 74 |
| Figure 6.29: | Pressure valve model, decrease in cold supply pressure, spool pressure | 75 |
| Figure 6.30: | Pressure valve model, decrease in cold supply pressure, supply flow rates | 76 |
| Figure 6.31: | Pressure balance valve test and model, cold supply pressure decrease, mix temperature | 77 |
| Figure 6.32: | Pressure balance valve test and model, cold supply pressure decrease, supply pressure | 78 |

| | | |
|--------------|---|-----|
| Figure 6.33: | Pressure balance valve test and model, cold supply pressure decrease, supply flow | 79 |
| Figure 7.1: | Cross section view of tempering valve | 82 |
| Figure 7.2: | Cross section view of tempering valve | 83 |
| Figure 7.3: | Thermostat length as a function of temperature, test and model | 87 |
| Figure 7.4: | Thermostat response when exposed to hot water bath, test and model | 89 |
| Figure 7.5: | Poppet valve extension (Ds) as a function of thermostat temperature, model equation (7.4) | 91 |
| Figure 7.6: | Cold supply flow as a function of thermostat temperature | 95 |
| Figure 7.7: | Mix temperature as a function of thermostat temperature | 96 |
| Figure 7.8: | Tempering valve test, cold supply pressure drop, supply and mix pressure | 98 |
| Figure 7.9: | Tempering valve test, cold supply pressure drop, supply and mix temperature | 99 |
| Figure 7.10: | Tempering valve model, cold supply pressure drop, orifice area | 101 |
| Figure 7.11: | Tempering valve model, cold supply pressure drop, mix and thermostat temperature | 102 |
| Figure 7.12: | Tempering valve model, cold supply pressure drop, supply pressure | 103 |
| Figure 7.13: | Tempering valve model, cold supply pressure drop, hot and cold supply flow rate | 104 |
| Figure 7.14: | Tempering valve test and model, cold supply pressure drop, mix temperature | 105 |
| Figure 7.15: | Tempering valve test, hot supply temperature increase, supply and mix temperature | 108 |
| Figure 7.16: | Tempering valve test, hot supply temperature increase, supply and mix pressure | 109 |
| Figure 7.17: | Tempering valve test, hot supply temperature increase, supply flow rates | 110 |

| | | |
|--------------|---|-----|
| Figure 7.18: | Tempering valve model, hot supply temperature increase, orifice area | 111 |
| Figure 7.19: | Tempering valve model, hot supply temperature increase, mix and thermostat temperature | 112 |
| Figure 7.20: | Tempering valve model, hot supply temperature increase, supply flow rates | 113 |
| Figure 7.21: | Tempering valve test and model, hot supply temperature increase, mix temperature | 114 |
| Figure 8.1: | Cross section view of anti-scald valve | 117 |
| Figure 8.2: | Anti-scald valve system components | 118 |
| Figure 8.3: | Anti-scald valve cage housing design | 119 |
| Figure 8.4: | Valve orifice area as a function of actuator position | 123 |
| Figure 8.5: | Actuator spring length as a function of temperature, test and model | 127 |
| Figure 8.6: | Actuator spring force as a function of actuator position, model | 128 |
| Figure 8.7: | Return spring force as a function of actuator position, model | 129 |
| Figure 8.8: | Actuator equilibrium equation as a function of position ranging from $0.00 < x < 0.030$, model | 131 |
| Figure 8.9: | Actuator equilibrium equation as a function of position ranging from $0.03 < x < 0.065$, model | 132 |
| Figure 8.10: | Anti-Scald valve test, gradual temperature increase, supply and mix temperature | 135 |
| Figure 8.11: | Anti-Scald valve test, gradual temperature increase, mix pressure | 136 |
| Figure 8.12: | Anti-Scald valve test, gradual temperature increase, supply flow | 137 |
| Figure 8.13: | Anti-Scald valve model, force equation for the actuator ball, actuator spring temperature 108°F | 138 |
| Figure 8.14: | Anti-Scald valve test, increase in mix temperature, mix temperature | 140 |

| | | |
|--------------|--|-----|
| Figure 8.15: | Anti-Scald valve test, increase in mix temperature, mix pressure | 141 |
| Figure 8.16: | Anti-Scald valve model, increase in mix temperature, mix and actuator spring temperature | 143 |
| Figure 8.17: | Anti-Scald valve model, increase in mix temperature, actuator position | 144 |
| Figure 8.18: | Anti-Scald valve test and model, increase in mix temperature, supply mix pressure | 145 |
| Figure 8.19: | Anti-Scald valve test and model, increase in mix temperature, supply mix flow | 146 |
| Figure 9.1: | Cross section view of mixing valve | 149 |
| Figure 9.2: | Cross section view of mixing valve components | 150 |
| Figure 9.3: | Cross section view of mixing valve | 152 |
| Figure 9.4: | Spool casing cold supply inlet and outlet area, model | 156 |
| Figure 9.5: | Spool casing hot supply inlet and outlet area, model | 157 |
| Figure 9.6: | Thermostat length as a function of temperature, test and model | 160 |
| Figure 9.7: | Thermostat dynamic reaction to a 190°F water bath, test and model | 162 |
| Figure 9.8: | Hot and cold supply flow area as a function of thermostat length and valve handle position | 164 |
| Figure 9.9: | Λ plotted as a function of thermostat temperature | 168 |
| Figure 9.10: | Mix temperature as a function of thermostat temperature | 171 |
| Figure 9.11: | Mixing valve test, cold supply pressure drop, supply flow | 174 |
| Figure 9.12: | Mixing valve test, cold supply pressure drop, supply and mix temperature | 175 |

| | | |
|--------------|---|-----|
| Figure 9.13: | Mixing valve response, 10 psi cold supply pressure drop, spool velocity | 176 |
| Figure 9.14: | Mixing valve model, cold supply pressure drop, spool pressure | 178 |
| Figure 9.15: | Mixing valve model, cold supply pressure drop, spool acceleration | 179 |
| Figure 9.16: | Mixing valve model, cold supply pressure drop, spool velocity | 180 |
| Figure 9.17: | Mixing valve model, cold supply pressure drop, spool position | 181 |
| Figure 9.18: | Mixing valve model, cold supply pressure drop, supply flow | 182 |
| Figure 9.19: | Mixing valve model, cold supply pressure drop, mix and thermostat temperature | 183 |
| Figure 9.20: | Mixing valve model, cold supply pressure drop, spool and spool casing position | 185 |
| Figure 9.21: | Mixing valve model, cold supply pressure drop, supply flow | 186 |
| Figure 9.22: | Mixing valve model, cold supply pressure drop, mix and thermostat temperature | 187 |
| Figure 9.23: | Mixing valve test and model, cold supply pressure drop, supply flows | 188 |
| Figure 9.24: | Mixing valve test and model, cold supply pressure drop, mix temperature | 189 |
| Figure 9.25: | Mixing valve test, hot supply temperature increase, supply and mix temperatures | 193 |
| Figure 9.26: | Mixing valve test, hot supply water temperature increase, supply pressure | 194 |
| Figure 9.27: | Mixing valve test, hot supply water temperature increase, supply flow | 195 |
| Figure 9.28: | Mixing valve response, hot supply temperature increase, spool and case position | 197 |
| Figure 9.29: | Mixing valve response, hot supply temperature increase, supply flow | 198 |

| | |
|--|-----|
| Figure 9.30: Mixing valve model, hot supply temperature increase, supply, mix and thermostat temperature | 198 |
| Figure 9.31: Mixing valve test and model, hot supply temperature increase, mix temperature | 200 |
| Figure 9.32: Mixing valve test and model, hot supply temperature increase, supply flow rates | 201 |

ACKNOWLEDGEMENTS

I owe a great deal to my wife, Mary, and my children: Chip, Daniel, Elizabeth and Alyse for the support they have given me. They have been supportive in allowing me to dedicate time to this pursuit; time, once past, we will never have again.

I dedicate this work to my parents, Don and Beverly Wandling, who have provided me the technical guidance, advice, time, as well as moral and financial support to complete this work.

I express my sincere thanks to Professor Donald Flugrad, Jr. for being my major professor and advisor.

Many thanks to Professor Ron Nelson and Professor Loren Zachary for serving on the committee and taking their valuable time to read and comment on my thesis.

CHAPTER 1. INTRODUCTION

The closed plumbing system has transformed the availability of potable hot water in our homes from a luxury to a necessity. In the early 1900's, hot water used for washing clothes, dishes, and personal and home hygiene was often heated in an open pot on the stove. Many tasks involving the warming of water were accomplished through a significant amount of human effort.

Today, energy efficient gas fired water heaters, copper tubing, faucets, and automatic valves provide the capability to deliver stored hot water to automatic dishwashers, clothes washing machines, bath tubs, showers, kitchen and bathroom sinks. The utility of hot water delivered with such a system is truly tremendous.

During the same period of technological improvements concerning the conveyance and availability of heated water, the hazards associated with the generation, distribution and use of hot water have been dramatically reduced. These hazards have been reduced to the point where people can deliver and use hot water with reasonable safety.

The utility of hot water requires that it be heated and stored at a temperature higher than would be suitable for bathing. Cold water must be added to the hot water in order to achieve a water temperature that meets the users needs and desires. A simple hot

and cold faucet valve has been used successfully for many years to mix cold and hot water to satisfy needs.

One hazard that exists with the use of hot water is that of scalding. Tap water scald injuries have received a great deal of attention in recent years. Infants, the elderly, and the infirm have been susceptible to tap water scalds. One method that has been prescribed to limit access to hot water and reduce tap water scalds is the use of automatic tempering valves, pressure balancing valves, automatic mixing valves or anti-scald valves.

Automatic tempering control valves sense the temperature of the output water and controls the output water temperature to the setting of the control handle. A thermostatic element in the valve reacts to the temperature of the output water and moves in response to temperature changes to maintain a selected temperature. As the temperature of the thermostat element is raised, the movement of the thermostat increases the flow area for the cold water supply; therefore, tempering of the output water is increased. As the temperature of the thermostat element is decreased, the movement of the thermostat decreases the flow area for the cold water supply; therefore, tempering of the output water is decreased.

Pressure changes in the cold or the hot water supply to a shower control are caused by plumbing and piping restrictions and sizing problems. The piping will not supply all of the water needed in the house - a reduction in supply pressure is the result. This occurs when water is used at other locations after the shower is turned on. Variation in water pressure due to water use and plumbing interior to the house can cause a loss of cold water flow

or a loss of hot water flow. The result can be a sudden reduction of cold or hot water being supplied to the shower control. Thus, the shower temperature becomes suddenly hot or cold.

The pressure balance control automatically moves to decrease the flow of the higher pressure water and increase the flow of the lower pressure water. The purpose of the pressure balance valve is to prevent sudden variations of temperature from that selected by the user.

This valve has a spool that meters the hot and cold water in response to pressure changes in the hot or cold supply water entering the valve. The control is turned on - the user can select a handle position that gives all cold water, all hot water, or any combination between. The user adjusts the control to mix cold and hot water to achieve a temperature of choice. If there are no changes in the pressure, the spool does not move. If the cold pressure decreases, the spool moves to decrease the hot flow and increase the cold flow, thus maintaining the same mix of hot and cold supply water.

Mixing valves, which can be manual or automatic, mix the hot supply and cold supply water to a temperature selected by the user. These valves come in various designs and may have: 1) two valve controls - one for the hot supply water and one for the cold supply water, 2) a single lever or handle to control the temperature and/or the flow rate, 3) a single lever or handle with an adjustable high limit stop, 4) two valve controls - a valve to adjust the flow rate and a control to adjust the output water temperature. Other designs are possible. A mixing valve may just simply mix the hot

and cold supply water which is manually adjusted by the user. Any temperature or pressure changes in the hot or cold supply to the valve may affect the output mix temperature and/or flow rate. Mixing valves may also incorporate thermostatic and spool elements to address changes in water supply pressure and temperature.

Anti-Scald valves are furnished with an automatic thermostatic control having thermal elements. These elements will reduce the flow of water to a specified amount when a maximum water temperature is achieved.

Research Goals

This work presents an evaluation, characterization and comparison of pressure balancing valves, automatic tempering valves, automatic mixing valves and anti-scald type shower valves. The devices will be evaluated on water outlet temperature based on variable inlet water temperatures and pressures. These valves have been developed to allow adjustment of the temperature of water distributed in potable water systems. This work is to develop an understanding of the capability of such valves to reduce or eliminate hazards from hot water in residential potable water systems resulting in thermal shock and tap water scalds.

The specific goals of this study are:

1. To develop mathematical modeling using differential equations to characterize the dynamic response of each of the valves evaluated.
2. To develop a methodology to test the valves in an environment which is representative of the plumbing systems found in residential hot and cold water potable plumbing systems in the United States.
3. To evaluate the capability of each of the valves to control output water temperature based on changes in supply temperature and pressure.

Thesis Organization

The second chapter of the thesis presents a literature review. The review focus is on the following areas: performance standards for thermal-shock-preventing devices and systems, medical studies of thermal injuries, the requirements for hot water in residential hot water heating systems, and plumbing standards and codes which establish recommendations and requirements for the design of potable hot water heating and distribution systems.

Chapter 2 lists the standards and requirements for thermal-shock-preventing devices and systems. Details regarding the research and data on the time-temperature relationship to produce second and third degree burns in children and adults is provided in

Chapter 3. The requirements for hot water for various uses in our homes is described in Chapter 4. Chapter 5 explains the standards and plumbing code requirements for potable hot water heating and distribution systems. Chapter 6 addresses the design, system modeling and testing of a pressure balanced valve. Chapter 7 addresses the design, system modeling and testing of a tempering valve. Chapter 8 addresses the design, system modeling and testing of an anti-scald valve. Chapter 9 addresses the design, system modeling and testing of a mixing valve. The conclusions and scope for future work are summarized in Chapter 10.

CHAPTER 2. LITERATURE REVIEW

The literature review accomplished in this thesis can be broadly categorized into 4 areas: 1) understanding of the time-temperature threshold required to produce irreversible burn injuries, 2) residential requirements for hot water, 3) standards and codes which address the generation and delivery of hot water, and 4) standards which address the design and performance of thermal-shock-preventing devices. The first three areas are discussed in greater depth in the individual chapters that follow.

The American Society for Testing and Materials has published a standard consumer safety specification for Scald-Preventing Devices and Systems in Bathing Areas F444-88 [1988]. This safety specification is directed towards scalds. The standard is intended to establish a maximum allowable discharge temperature and to provide for automatic compensation if that temperature is exceeded.

The minimum performance requirements for scald preventing devices or systems are "the maximum allowable temperature at the water outlet to the bathing area shall be 120 °F or, if the temperature of the water discharging from the water outlet of the devices or systems exceeds 120 °F, the flow shall automatically be reduced to 0.5 gal/min in 5 seconds or less".

Full instructions for installing, adjusting and maintaining the devices are required to be packaged with each device or system.

The installation instructions should state that the responsibility for adjustment in accordance with the manufacturer's instructions lies with the installer. The installation instructions should also include information on temperature settings based on cold water variations and hot water capabilities as a guide to allow the installer to properly set the maximum water-outlet temperature (if required).

For mixing valves, if the valve is not equipped with an integral shut-off or if there is a shut-off installed after the mixing valve - there are to be stop and check valves on the inlets or in the water distribution piping to the valve.

The American Society for Testing and Materials has also published a standard consumer safety specification for Thermal-Shock-Preventing Devices and Systems in Showering Areas F445-88 [1988]. This safety specification addresses certain hazards in connection with shower areas and is directed toward thermal shock. The standard is intended to establish a maximum allowable discharge temperature. It provides for automatic compensation if that temperature is exceeded, or it limits temperature changes that are potentially dangerous or both.

The minimum performance requirements for thermal-shock-preventing devices and systems are that "the maximum allowable temperature at the water outlet to the fixture shall be 120 °F for maximum safety". The temperature of the water discharging from the water outlet of the devices or systems shall automatically be

controlled for maximum safety against rapid fluctuations within a total variation of +/- 5 °F of the adjusted temperature.

In a similar fashion to the ASTM F444 standard the following also applies: complete instructions for installing, adjusting and maintaining the devices are required to be packaged with each device or system. The installation instructions should state that the responsibility for adjustment in accordance with the manufacturer's instructions lies with the installer. The installation instructions should also include information on temperature settings based on cold water variations and hot water capabilities as a guide to allow the installer to properly set the maximum water-outlet temperature (if required).

For mixing valves, if the valve is not equipped with an integral shut-off or if there is a shut-off installed after the mixing valve, there are to be stop and check valves on the inlets or in the water distribution piping to the valve.

The American Society of Sanitary Engineering has published a standard addressing the performance requirements for Temperature Actuated Mixing Valves for Primary Domestic Use, Standard Number 1017 [1979]. This standard provides performance requirements for primary domestic temperature actuated mixing valves which are intended to mix hot and cold water to reduce high service water temperature to building distribution piping. This standard addresses valves used for controlling line water temperature in domestic potable hot water systems which are intended to be

installed at the hot water source. This standard is not intended for end use applications.

The capacity of the valves range from 3 gallons per minute (gpm) to 200 gpm at 10 psi differential or 6 gpm to 400 gpm at 45 psi differential. The hot water inlet temperature ranges from 120°F to 180°F and the cold water inlet temperature ranges from 39°F to 70°F. The valve should have the capability of supplying hot water temperature within a range at least part of which must fall between 100 °F to 140 °F.

The performance requirements for the valve when operating at a flow of 3-5 gpm and at a 10 psi differential is to have a temperature variation of 3 °F above or below the set point. The method of testing the valve is defined in the standard. A suggested piping schematic for the valve test is defined in the standard and includes specifications for the location of pressure gauges, thermocouples and flow meters.

The American Society of Sanitary Engineering has published a standard addressing the performance requirements for Individual Thermostatic Pressure Balancing and Combination Control for Bathing Facilities, Standard Number 1016 [1990]. This standard provides performance requirements for "individual control valves, which will provide the user reasonable protection against exposure to excessive water temperature or excessive outlet temperature fluctuations resulting from a variation in the inlet water pressure up to fifty (50) percent".

The standard applies only to individual control valves for bathing facilities which are thermostatic, pressure balancing or a combination thermostatic and pressure balancing. The valve shall be capable of being adjusted from full cold up to a minimum of 105 °F. The hot water inlet temperature range will be from 120 °F to 180 °F and the cold water inlet temperature range shall be from 39 °F to 70 °F. Performance requirements are that water temperature shall be automatically maintained within a variation of +/- 3 °F.

Test conditions for pressure balance valves entail a change of normal supply pressure by 50 percent of either the hot or cold supply. Test conditions for thermostatic valves include changes in supply pressure of 20% and a hot water supply temperature increase of 25 °F. Test conditions for combination thermostatic and pressure balance valves include changes in supply pressure of 50% and a hot water supply temperature increase of 25 °F.

All control valves shall, when the cold water supply fails, automatically reduce the discharge such that the outlet temperature does not exceed 120 °F prior to a reduction in the flow to 0.5 gpm. The time to accomplish this is to be less than 5 seconds. A piping schematic for the valve test is defined and includes specifications for the location of pressure gauges, thermocouples and flow meters.

CHAPTER 3. STUDIES OF THERMAL INJURIES

There are relatively few studies of the relationship between the temperature of water exposed to human skin and the amount of time to produce a burn. Yet, it is common knowledge that there is an inverse relationship between the temperature of hot water and the amount of time required to produce a burn.

Henriques and Moritz [1947] conducted an investigation regarding the effects on human skin of exposure to hot water and hot oil. The investigation established the time-temperature thresholds for first, second and third degree burns. This was accomplished by experimenting on pigs that were shown to have skin similar to humans with regard to thermal injury. A number of exposures were also conducted on human skin to establish a relationship between the two.

Reactions to exposure that were of insufficient temperature or time to cause complete destruction of the epidermis (skin) were identified as first degree burns. Reactions that resulted in full-thickness destruction of skin were designated as second or third degree burns and were based on the depth of which the skin was affected.

These experiments showed that the degree of reaction varied inversely with the temperature. Second and third degree burns are considered to cause irreversible injury of the skin. A series of 33 exposures were made on human volunteers to determine the extent to

which the experiments on pigs were applicable to man. The results of the human experiments are summarized in Table 3.1.

The results of the experiments on pig and human skin showed that at similar water temperature, there was little or no difference in the susceptibility of the two skin types with regards to thermal injury. At any given surface temperature, the time to destroy pig skin is approximately the same as that required to destroy adult human skin.

Equations were developed by Henriques [1947] to support estimates of burning times based on water temperature, time and skin thickness. Adult burning times are based on a thigh skin thickness of 2.5 mm. Feldman [1983] states that different body area skin thickness' of children range from 0.5 to 1 mm. Figure 3.1 compares adult full thickness burn time based on a thigh skin thickness of 2.5 mm with the skin of a child 0.5 mm thick.

For this thesis, the curve established for children with 0.5 mm skin thickness will be used as the time-temperature threshold criteria for an irreversible injury.

Table 3.1: Time-surface temperature thresholds for thermal injury of human adult skin

| Test | Temperature °F | Duration | | | Second & Third Degree Reaction |
|------|-------------------|----------|------|------|-----------------------------------|
| | | Hrs. | Min. | Sec. | |
| 3 | 111 | 6 | | | X |
| 4* | (111.2) | 6 | | | X |
| 6* | 113 | 3 | | | X |
| 7 | | 3 | | | X |
| 8* | 117 | | 18 | | X |
| 12 | (116.6) | | 25 | | X |
| 13* | | | 40 | | X |
| 14 | | | 40 | | X |
| 15 | | | 45 | | X |
| 17 | 118 | | 15 | | X |
| 18 | (118.4) | | 18 | | X |
| 21 | 120 | | 9 | 30 | X |
| 22* | (120.2) | | 10 | | X |
| 23 | | | 11 | | X |
| 24 | | | 15 | | X |
| 26 | 124 | | 4 | | X |
| 27 | (123.8) | | 6 | | X |
| 29 | 127 | | 1 | 30 | X |
| 31 | 131 | | | 30 | X |
| 33* | 140 | | | 5 | X |

* Oil Heat source instead of water

Source: A. R. Moritz, M.D. and F. C. Henriques, Jr. "Studies of Thermal Injuries - The Relative Temperature of Time and Surface Temperature in the Causation of Cutaneous Burns". The American Journal of Pathology, Vol. 23:695, September, 1947

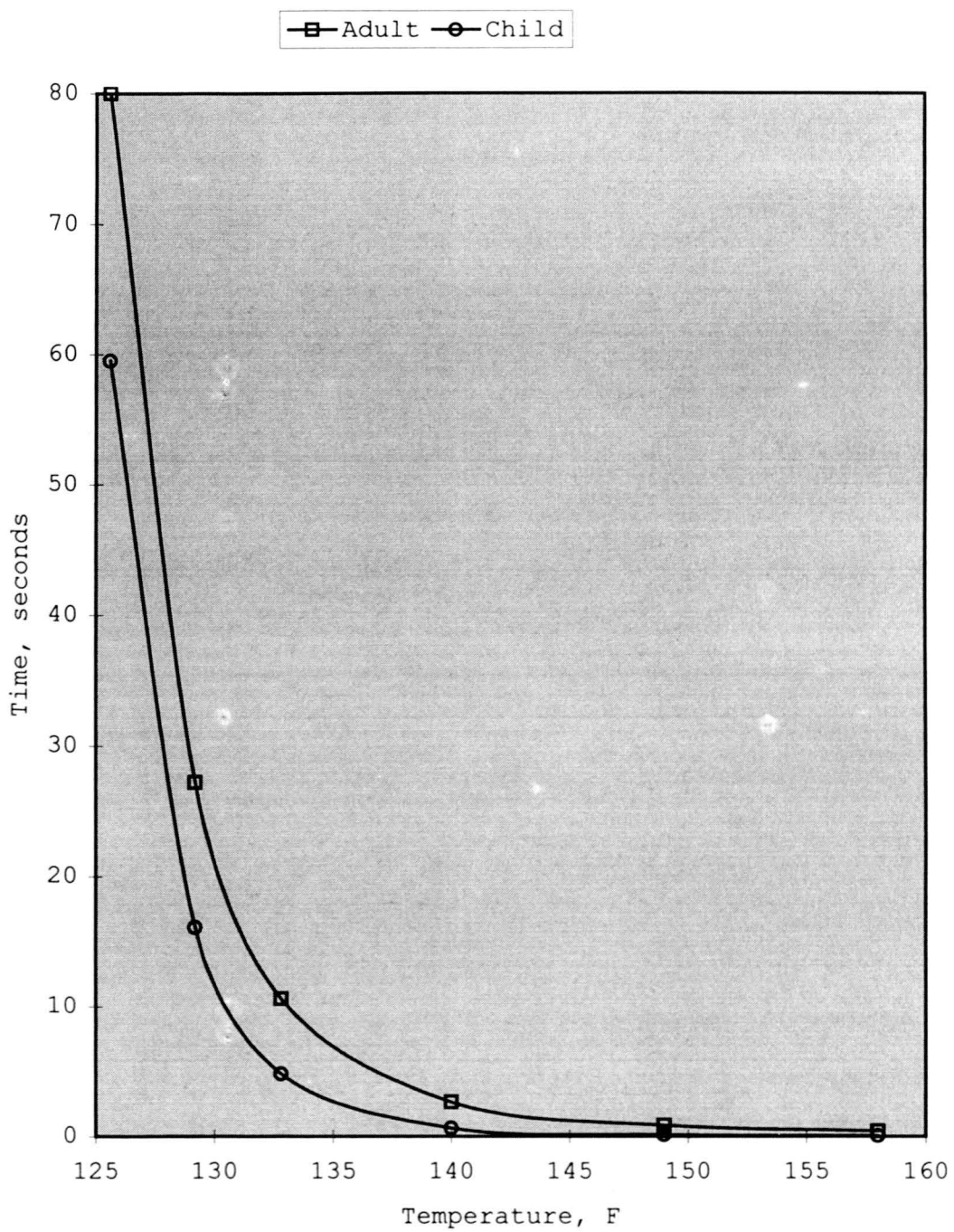


Figure 3.1: Time-surface temperature thresholds for second & third degree reaction of human adult and child skin

CHAPTER 4. RESIDENTIAL REQUIREMENTS FOR HOT WATER

Hot water is used in our homes for washing clothes, dishes and personal and home hygiene. Requirements for hot water were identified by 1) surveying appliance manufacturers of automatic laundry washers and dishwashers, 2) surveying laundry and dishwasher detergent manufacturers, and identifying sanitation and health requirements for hot water.

Manufacturers of laundry washers (KitchenAid [1989], Speed Queen [1987], Maytag [1982], Whirlpool [1979], GE [1990]) and manufacturers of dishwashers (Kitchen-Aid [1977], Whirlpool [1991], Tappan [1992], Sears [1992], Roper [1989], Maytag [1993], GE [1994]) recommend hot water in the appliance ranging in temperature from 130 °F to 160 °F. LemMon [1982] explains that for proper laundering performance, the water heater in the home should be set to deliver 140 °F at the tap. At this setting, the wash water in the washer will be approximately 130°F when the washer controls are set on "Hot". Ten degrees of water temperature are lost as a result of raising the temperature of the washer components and clothes in the wash basket. The Consumer and Food Economics Research Division of the United States Department of Agriculture [1971] explains that both time and temperature are important in killing bacteria: it takes 3 to 5 minutes at 212 °F to kill Staphylococci, or 20 minutes

at a water temperature of 140 °F. Manufacturers of laundry detergents and dishwasher detergents (Colgate-Palmolive [1991], Proctor & Gamble [1986], Lever Brothers [1992]) recommend hot water ranging in temperature from 130°F to 160°F. Peet et al. [1975] explains that water of the correct temperature for effective dish washing ranges from 150 °F to 160 °F. In addition, dishes still soiled after washing, spots and film on the dishes, or dishes that do not dry may be caused by low water temperature. The United States Department of Agriculture [1965] found that soaps removed about one third more soil in hot water (140°F) than in warm water (100°F).

The American Society of Plumbing Engineers [Steel, 1988] recommend setting residential hot water heaters above 140°F to limit the growth of *Legionella pneumophila* in service hot water systems. In addition, the United States Department of Health, Education and Welfare [Knauer, 1974] has recommended that when there is sickness in the family - or when washing diapers, sheets, pajamas and other clothing soiled with human waste, blood or pus - to use hot water (140°F) in the washing machine to kill germs.

CHAPTER 5. STANDARDS AND CODES

The American National Standard Institute (ANSI) has established national standards for gas appliance thermostats and for automatic storage type water heaters.

The ANSI standard for gas appliance thermostats, ANSI Z21.23 - 1993, recommends minimum and maximum dial temperature markings for water heater controls, a calibration point, and a tolerance on a set point. The recommended dial temperature markings for water heaters are 100°F minimum and 180°F maximum, the calibration reference point is 140°F, and the tolerance on the set point is +/- 10°F.

The ANSI standard for automatic storage type water heaters, ANSI Z21.10.1-1993, recommends a maximum thermostat temperature of 180°F, warning labels that address scald hazards, a marking on the thermostat consistent with 120°F, instructions to the installer that the thermostat is set at the lowest position when shipped from the factory, and instructions that the 120°F marking is the preferred starting point for setting the temperature control.

State and local codes generally adopt national plumbing codes from the Uniform Plumbing Code, National Standard Plumbing Code, or the Building Officials & Code Administrators (BOCA) National Building Code. Each of these codes require a hot water heater that is to be installed in residential plumbing systems to meet the requirements of ANSI Z21.10.1.

CHAPTER 6. PRESSURE BALANCED BATH VALVE

Pressure balanced bath valves are designed to minimize the effects of outlet water temperature changes due to inlet pressure changes. These changes may be caused by toilets, sink faucets, washing machines, dishwashers and other points of use found in residential plumbing systems. The purpose of the pressure balance valve is to prevent sudden variations of temperature from that selected by the user. A pressure balance valve has a spool that meters the hot and cold water in response to pressure changes in the hot or cold supply water entering the valve. This type of valve may require adjustment and testing of the valve assembly during installation. In addition, inspection and maintenance of the valve may be required when the hot water heater control temperature is changed. Furthermore, if there is failure of other temperature controlling devices elsewhere in the plumbing system, or if there is lime, rust, sand or other contaminants that affect the operation of the valve, periodic inspection and maintenance will likewise be required.

Valve Design

A commercially available pressure balance bath valve was obtained which would allow the user to set a rotational limit stop

to one of 11 positions. These positions adjust the output mix temperature based upon varying inlet temperatures and are listed in Table 6.1. The cold inlet temperature listed in the instructions varied from 50 degrees Fahrenheit (°F) to 85 °F, and the hot inlet temperature listed varied from 120 °F to 180 °F.

Table 6.1: Mix temperature vs. position of rotational limit stop

| Inlet | Cold/Hot 50°F/120°F | Cold/Hot 50°F/140°F | Cold/Hot 50°F/160°F | Cold/Hot 70°F/160°F | Cold/Hot 40°F/180°F |
|-------------|--|------------------------|------------------------|------------------------|------------------------|
| Position 1 | Shut off zone: no flow 0-20 degrees of handle rotation | | | | |
| Position 2 | 50°F | 50°F | 50°F | 70°F | 40°F |
| Position 3 | 61°F | 67°F | 74°F | 89°F | 70°F |
| Position 4 | 68°F | 75°F | 84°F | 97°F | 84°F |
| Position 5 | 74°F | 85°F | 91°F | 104°F | 95°F |
| Position 6 | 79°F | 91°F | 99°F | 110°F | 103°F |
| Position 7 | 82°F | 97°F | 104°F | 115°F | 109°F |
| Position 8 | 85°F | 104°F | 108°F | 118°F | 115°F |
| Position 9 | 89°F | 117°F | 115°F | 124°F | 124°F |
| Position 10 | 98°F | 134°F | 128°F | 136°F | 140°F |
| Position 11 | 111°F | 138°F | 149°F | 151°F | 165°F |

Instructions regarding the adjustment of the rotational limit stop specify to rotate the stop clockwise to raise the mix temperature. The user should test the mix water temperature with a thermometer until the desired temperature is obtained. If the water temperature is above 120 °F, the user is instructed to rotate the stop counterclockwise. The user is not instructed to ensure that the water heater has recently completed a heating cycle prior to the adjustment of the rotational limit stop.

Figure 6.1 is a cross sectional view of the pressure balance valve. The key components of the valve assembly are: 1) a valve body, 2) a hot and cold spool valve housing, 3) a spool valve casing, 4) a spool, 5) an orifice plate 6) a control handle shaft, 7) a rotational limit, 8) an adjustable stop, 9) a cap assembly, and 10) a control handle (not shown).

Hot and cold half inch copper supply lines are attached to the left and right inlets of the valve body. A half inch copper output line for a shower head, a tub spout or both is also attached to the valve body during installation. Once assembled, hot and cold supply water enters the valve through the supply lines and is directed into the hot and cold spool valve housing assembly. Cold water enters through inlet "A" and hot water enters inlet "B" (See Figure 6.2). The hot and cold supply water is prevented from mixing throughout the valve assembly until both lines discharge past the orifice plate. At the supply entrance of the hot and cold valve housing assembly, there is an elastic diaphragm check valve installed ("C").

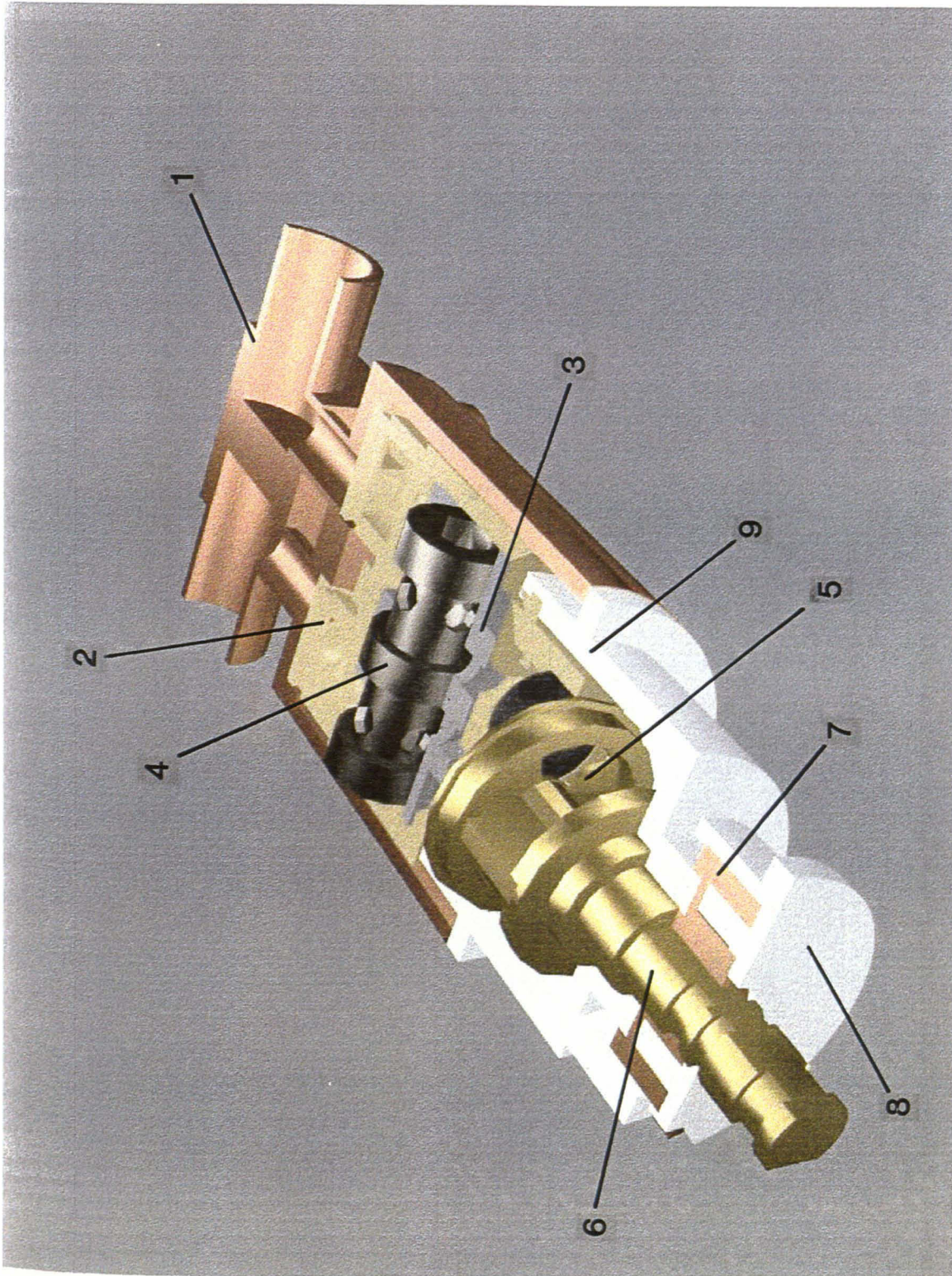


Figure 6.1: Cross section view of pressure balance valve

This diaphragm prevents the backflow of water due to any pressure differential between the hot and cold supply lines. Once past the diaphragm check valve, the supply water passes down a cylindrical cavity and through an orifice ("D") to the cavity which holds the spool valve casing and spool. The spool valve casing has six inlet ("E") and four outlet orifices ("F") for the cold water supply and six inlet ("G") and four outlet orifices ("H") for the hot water supply.

A spool ("I") is located inside the spool valve casing and is free to move axially. The spool will move axially due to a difference in pressure seen between the hot water side and cold water side of the spool casing cavity. The axial movement of the spool affects the inlet and outlet orifice openings of both the hot and cold water supply and thus has an effect on the flow of each supply line.

The supply water enters the spool valve inlet orifices, it flows axially in the spool valve casing and then out of the spool valve outlet orifices. Once past the spool valve outlet orifices, the supply water passes through an orifice ("J") in the spool valve housing and down a cylindrical cavity to the end of the spool valve housing. At the end of the spool valve housing, an orifice plate ("K") is positioned against the hot and cold water spool valve housing outlets.

The orifice plate has two openings; one opening is designed to move past the cold water spool valve housing outlet and one opening is designed to move past the hot water spool valve outlet. As the valve handle is turned, the orifice plate varies the area which

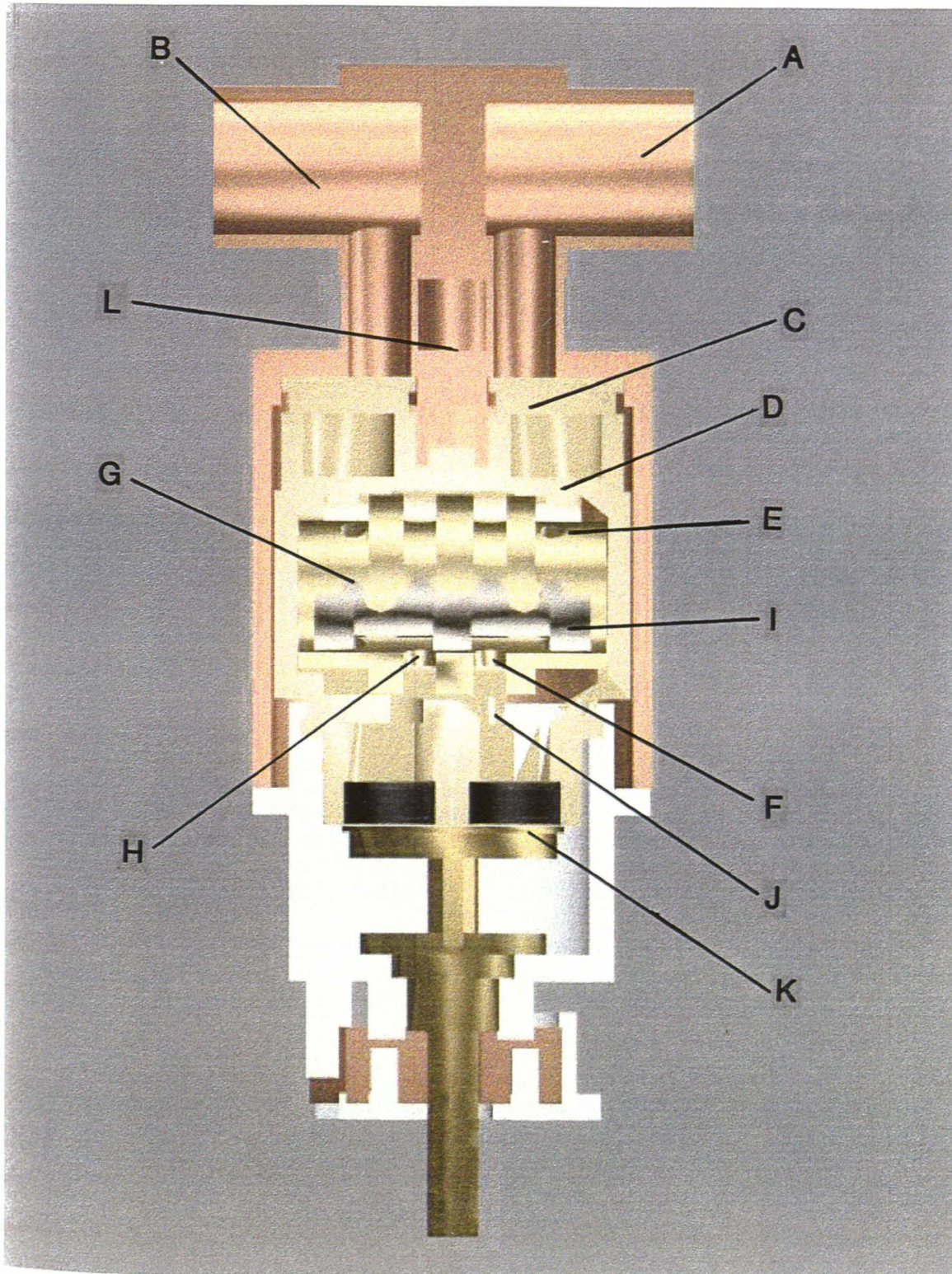


Figure 6.2: Cross section view of pressure balance valve

rotates past the hot and cold spool valve housing outlets. This change in area has an effect on the flow of hot and cold supply water. The orifice plate is attached to the valve handle shaft and the position of the orifice plate is adjusted by the user by turning the valve handle. The valve handle and the attached orifice plate may be rotated through an angle of 134 degrees. Figure 6.3 shows the position of the orifice plate in relation to the hot and cold spool valve housing outlets as the valve handle is rotated.

Once the hot and cold supply water pass the orifice plate, both supplies are mixed in the valve body. The mix then exits the valve assembly through an orifice ("L") to the copper outlet line for the shower nozzle or tub spout.

System Modeling

Fox and McDonald [1978] define incompressible flow as the condition where the density variations within a flow are negligible. Most liquid flows are essentially incompressible. The bulk modulus of elasticity is a measure of the lack of compressibility of a fluid. The bulk modulus of elasticity is defined as:

$$\beta = -(\Delta P / \Delta V) * V_0 \quad (6.1)$$

where:

β = Bulk modulus of elasticity, psi

ΔP = Change in fluid pressure, psi

ΔV = Change in fluid volume, cubic inches

V_0 = Initial fluid volume, cubic inches

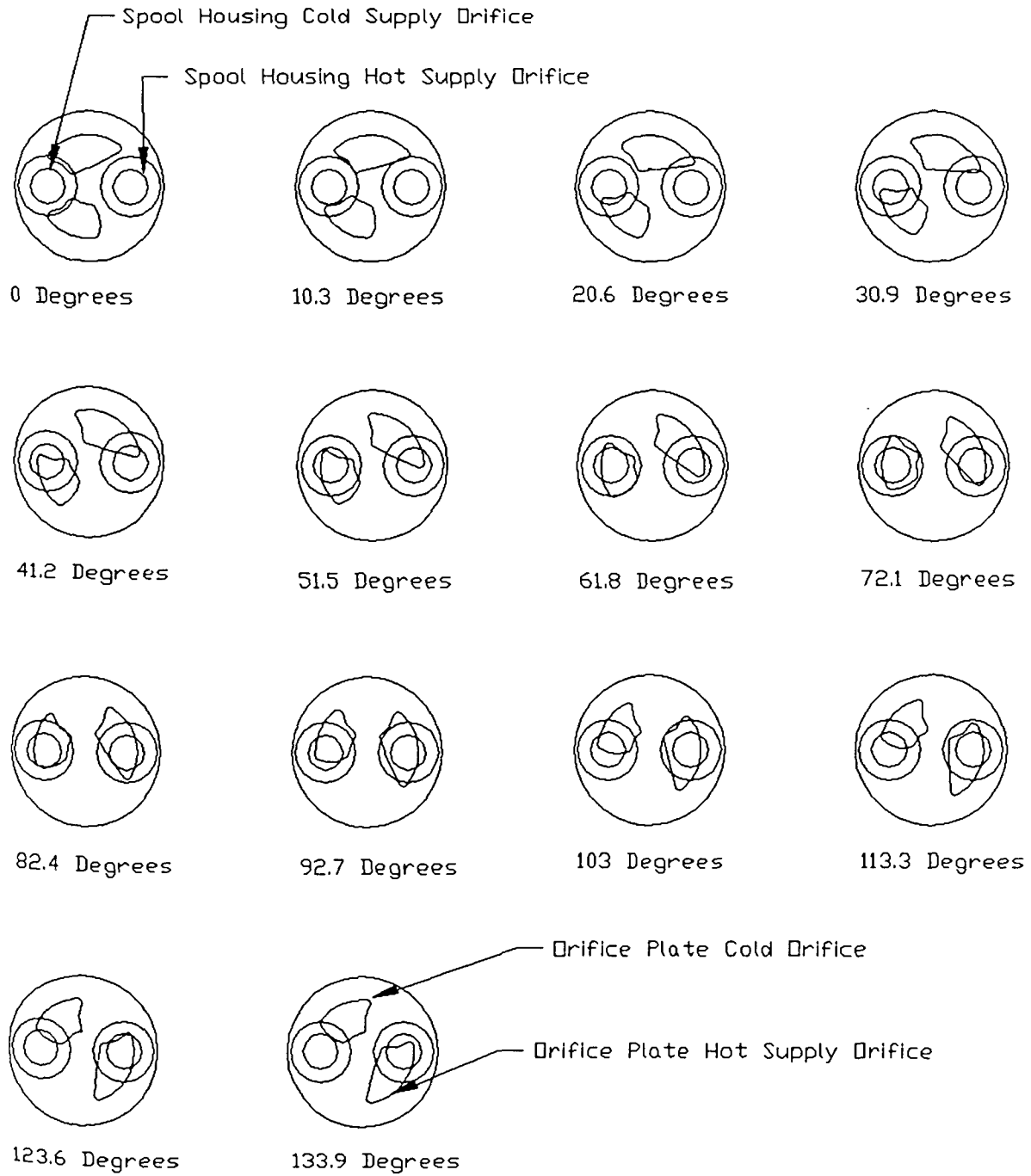


Figure 6.3: Pressure valve orifice plate and supply flow lines

The higher the bulk modulus, the less compressible the fluid. Water has a bulk modulus of 324,800 psi. This means for a 100 psi pressure change on 1 cubic inch of water, the volume of the water will change 0.00031 cubic inches. The total amount of water contained in the valve during operation is in the order of several cubic inches. Considering that water is the operating fluid, that the typical operating pressures found in residential plumbing systems are under 100 psi, and that the bulk modulus of elasticity for water is 324,800 psi - incompressible flow is a good assumption. For incompressible, steady, frictionless flow along a streamline, the density of the fluid is constant and the following equation is constant for the fluid flow. This equation is called the Bernoulli equation:

$$P/\rho + gz + V^2/2 = \text{constant} \quad (6.2)$$

where:

P = Static pressure, pound/ft² (psf)

ρ = Fluid density, slugs/ft³

g = Standard acceleration of gravity on Earth, ft/sec²

z = Vertical elevation, ft

V = Fluid velocity, ft/sec

Bernoulli's equation states that in a system in which no work is being added or subtracted the pressure at any point is the sum of 1) the system pressure, 2) the elevation of the point of interest, and 3) the velocity head at the point of interest. This equation is valid only for a particular point of interest when examining systems

which have frictional losses. Keller [1978] applies Bernoulli's equation to any pair of points in a liquid continuum by adding the pressure loss due to the flow friction between the two points. The pressure total is then a constant for all points of the system.

$$P = \text{constant} = P_s + \rho * g * z + \rho * V^2 / 2 + P_f \quad (6.3)$$

where:

P_s = Static Pressure, psf

P_f = Pressure loss due to friction, psf

Keller [1978] further develops the basic equation for a circular submerged orifice which relates the flow of a fluid to an orifice coefficient, density and the pressure across the orifice:

$$Q = c * A * (2 * \Delta P / \rho)^{0.5} \quad (6.4)$$

where:

Q = Fluid flow, ft³/sec

c = Orifice Coefficient

A = Orifice area, ft²

ΔP = Pressure delta across the orifice, psf

ρ = Fluid density, slugs/ft³

The orifice coefficient is experimentally determined. The coefficient varies based on the ratio of the orifice diameter to the pipe diameter and upon the Reynolds number which is based on upstream flow conditions. For Reynolds numbers greater than 2000 and for orifice to pipe diameter ratios below 0.4, the orifice

coefficient is approximately 0.59. The Reynolds Number is a dimensionless number and is defined as:

$$Re = V \cdot D / \nu \quad (6.5)$$

where:

Re = Reynolds Number

V = Average fluid velocity, ft/sec

D = Pipe diameter, ft

ν = Kinematic viscosity, ft²/sec

For water ranging in temperatures from 50°F to 160°F, the kinematic viscosity ranges from $1.29(10^{-5})$ ft²/s to $4.3(10^{-6})$ ft²/s.

Standard one half inch copper tubing typically found in residential homes has an internal diameter of 0.55 inch. Therefore, the minimum average fluid velocity to achieve a Reynolds Number of 2000 is 0.19 ft/s or 0.14 gallons per minute (gpm) of flow. Since most shower head and tub spigots flow at a much greater rate than 0.14 gpm, a constant orifice coefficient will be used in the modeling of the valve.

Supply water flow through the valve may be calculated using the orifice equation, and the pressure drop across each orifice may also be calculated. The pressure drop across each orifice is also known as "head loss". Modeling of the valve requires defining each orifice in the valve and the associated input flow area, orifice area and the corresponding orifice coefficient. The following are the orifices in the valve that will create head losses in the supply flow:

Orifice 1: Copper piping into the valve body

Orifice 2: Valve body into the spool valve housing inlet

Orifice 3: Spool valve housing inlet into spool casing inlet

Orifice 4: Spool inlet

Orifice 5: Spool outlet

Orifice 6: Spool casing outlet into spool valve housing outlet

Orifice 7: Spool valve housing outlet past the orifice plate

Orifice 8: Valve body into the outlet copper piping

Each of these orifices are shown in Figure 6.2. Three of the orifices will vary depending on conditions of flow and the rotational position of the valve handle.

The spool inlet and outlet orifices will vary depending on the position of the spool. When the spool is centered axially in the spool valve casing, this position may be defined as $x = 0$ inches. The total travel of the spool will then range from $-0.080 < x < 0.080$ inches. The spool inlet and outlet area is dependent on the position of the spool, and therefore is a function of x . The spool orifices are circular openings. The effective orifice area is determined by the position of the spool as the spool lands passes by the circular orifice (see Figure 6.2). For the cold water spool inlet, the orifice area may be defined as follows:

$$A_{ic} = 0.0 \quad \text{For } -0.080 < x < -0.051 \quad (6.6)$$

$$A_{ic} = A_{im} - N_i \cdot r^2 \cdot \arccos[(r+x-0.051)/r] \quad (6.7)$$

$$\text{For } -0.051 < x < 0.073$$

$$A_{ic} = A_{im} \quad \text{For } 0.073 < x < 0.080 \quad (6.8)$$

where:

A_{ic} = Area of cold water spool inlet, ft^2

A_{im} = Maximum area of inlet orifices, ft^2

x = Spool position, inches

r = Radius of inlet orifices, ft

N_i = Number of inlet orifices

For the cold water spool outlet, the orifice area may be defined as follows:

$$A_{oc} = A_{om} \quad \text{For } -0.080 < x < 0.012 \quad (6.9)$$

$$A_{oc} = A_{om} - N_o * r^2 * \arccos[(r - x + 0.012)/r] \quad (6.10)$$

$$\text{For } 0.012 < x < 0.080$$

where:

A_{oc} = Area of cold water spool outlet, ft^2

A_{om} = Maximum area of outlet orifices, ft^2

x = Spool position, inches

r = Radius of outlet orifices, ft

N_o = Number of outlet orifices

For the hot water spool inlet the orifice area may be defined as follows:

$$A_{ih} = A_{im} \quad \text{For } -0.080 < x < -0.073 \quad (6.11)$$

$$A_{ih} = A_{im} - N_i * r^2 * \arccos[(r - x - 0.051)/r] \quad (6.12)$$

$$\text{For } -0.073 < x < 0.051$$

$$A_{ih} = 0.0 \quad \text{For } 0.051 < x < 0.080 \quad (6.13)$$

where:

A_{ih} = Area of hot water spool inlet, ft^2

A_{im} = Maximum area of inlet orifices, ft^2

x = Spool position, inches

r = Radius of inlet orifices, ft

N_i = Number of inlet orifices

For the hot water spool outlet the orifice area may be defined as follows:

$$A_{oh} = A_{om} \quad \text{For } -0.012 < x < 0.080 \quad (6.14)$$

$$A_{oh} = A_{om} - N_o * r^2 * \arccos[(r + x + 0.012)/r] \quad (6.15)$$

$$\text{For } -0.080 < x < -0.012$$

where:

A_{oh} = Area of hot water spool outlet, ft^2

A_{om} = Maximum area of outlet orifices, ft^2

x = Spool position, inches

r = Radius of outlet orifices, ft

N_o = Number of outlet orifices

The spool valve has 6 inlet orifices and 4 outlet orifices for both the hot and cold supply lines. As the spool moves axially in the spool casing, the effective area of the inlet and outlet orifices are affected. When the spool is positioned axially in the center of the spool casing, the spool position is denoted $x = 0$. The spool may travel 0.080 inch towards the hot supply side (x being negative) and may travel 0.080 inch towards the cold supply side (x

being positive). The area of the hot inlets and hot outlets are graphed in Figure 6.4 and Figure 6.5 as a function of x .

The area of the cold and hot spool housing exit orifices are determined by the rotational position of the orifice plate. The orifice plate is attached to the valve handle and the user adjusts the valve handle to a handle position θ . The area for the cold and hot spool housing exit is therefore a function of θ . The area for the hot and cold spool housing exit was determined graphically. Figure 6.6 shows the effective orifice area as the valve handle is rotated through its maximum stroke. Table 6.2 summarizes the orifice area for the hot and cold supply flow and Figure 6.7 graphs the orifice area as a function of handle position. The area of the hot spool housing exit, A_{sph} , and the area of the cold spool housing exit, A_{spc} , are graphed as a function of handle position θ .

To define the characteristic equation for the pressure balance valve, the following system variables are defined:

P_c = Cold input supply pressure to the valve, psf

P_h = Hot input supply pressure to the valve, psf

P_m = Mix output pressure to the shower head or tub spout, psf

θ = Valve handle position, degrees

x = Spool position, inches

Q_c = Cold water supply flow, ft^3/sec

Q_h = Hot water supply flow, ft^3/sec

P_{sc} = Pressure on cold supply side of spool, psf

P_{sh} = Pressure on hot supply side of spool, psf

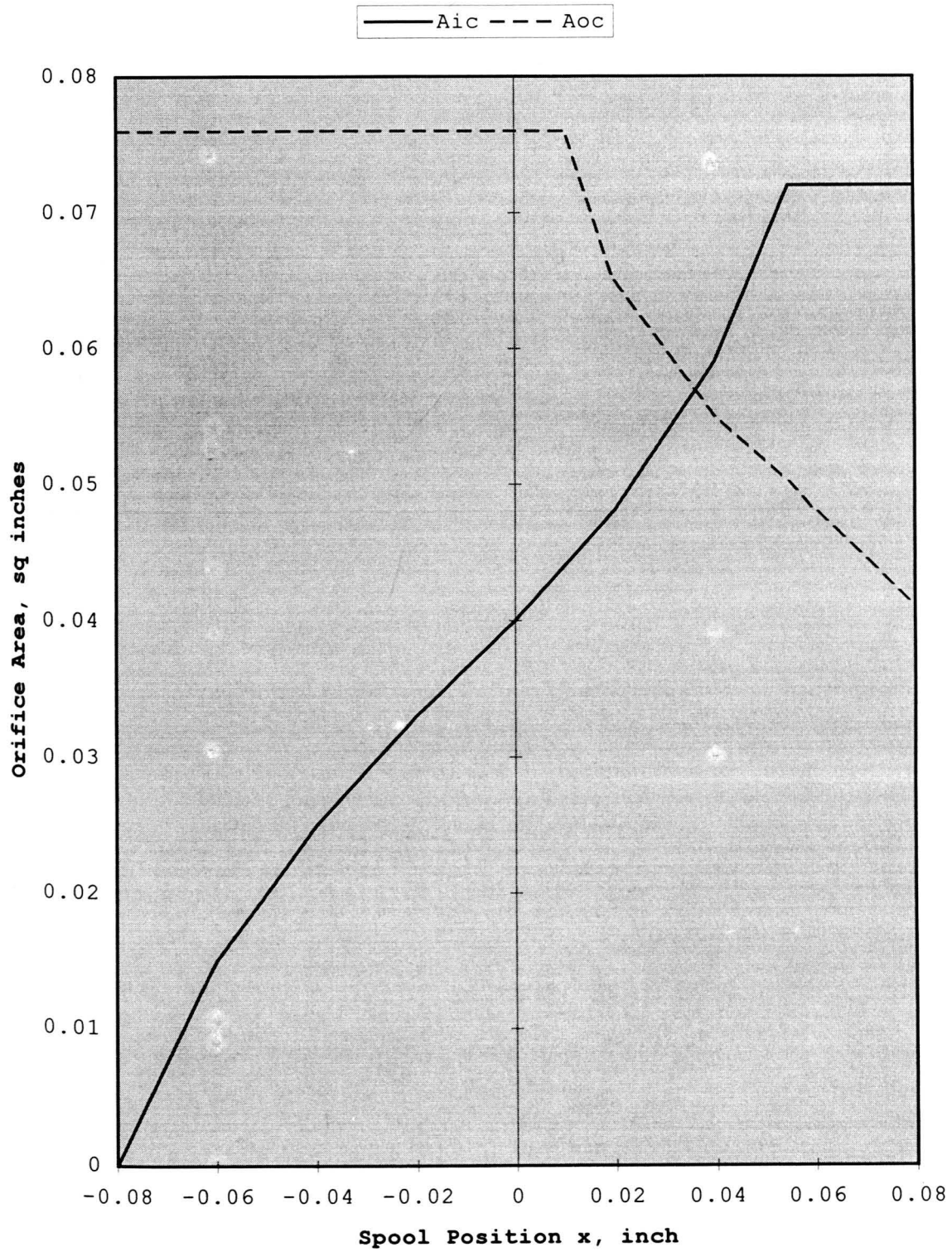


Figure 6.4: Cold supply spool inlet and outlet area

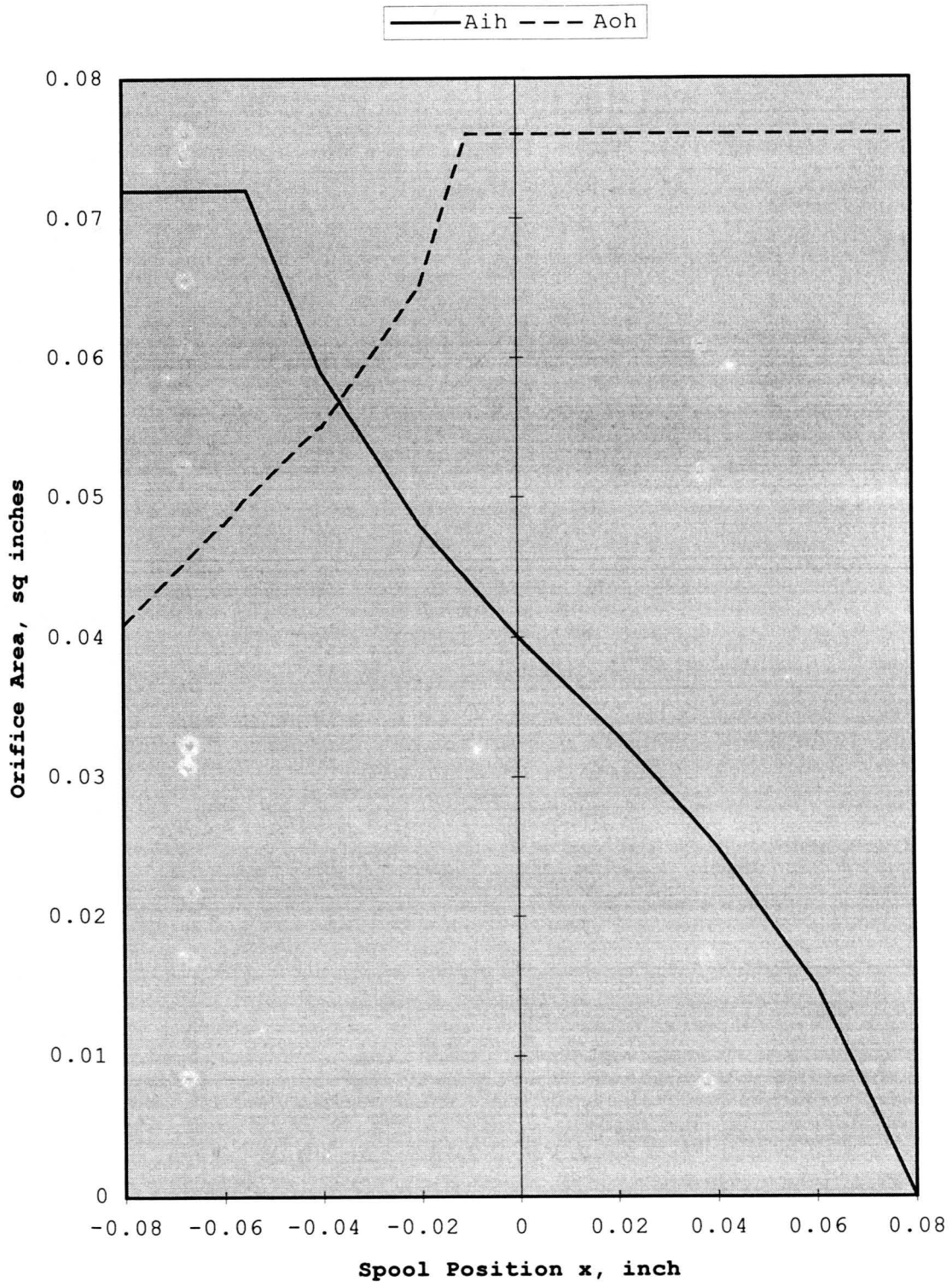


Figure 6.5: Hot supply spool inlet and outlet area

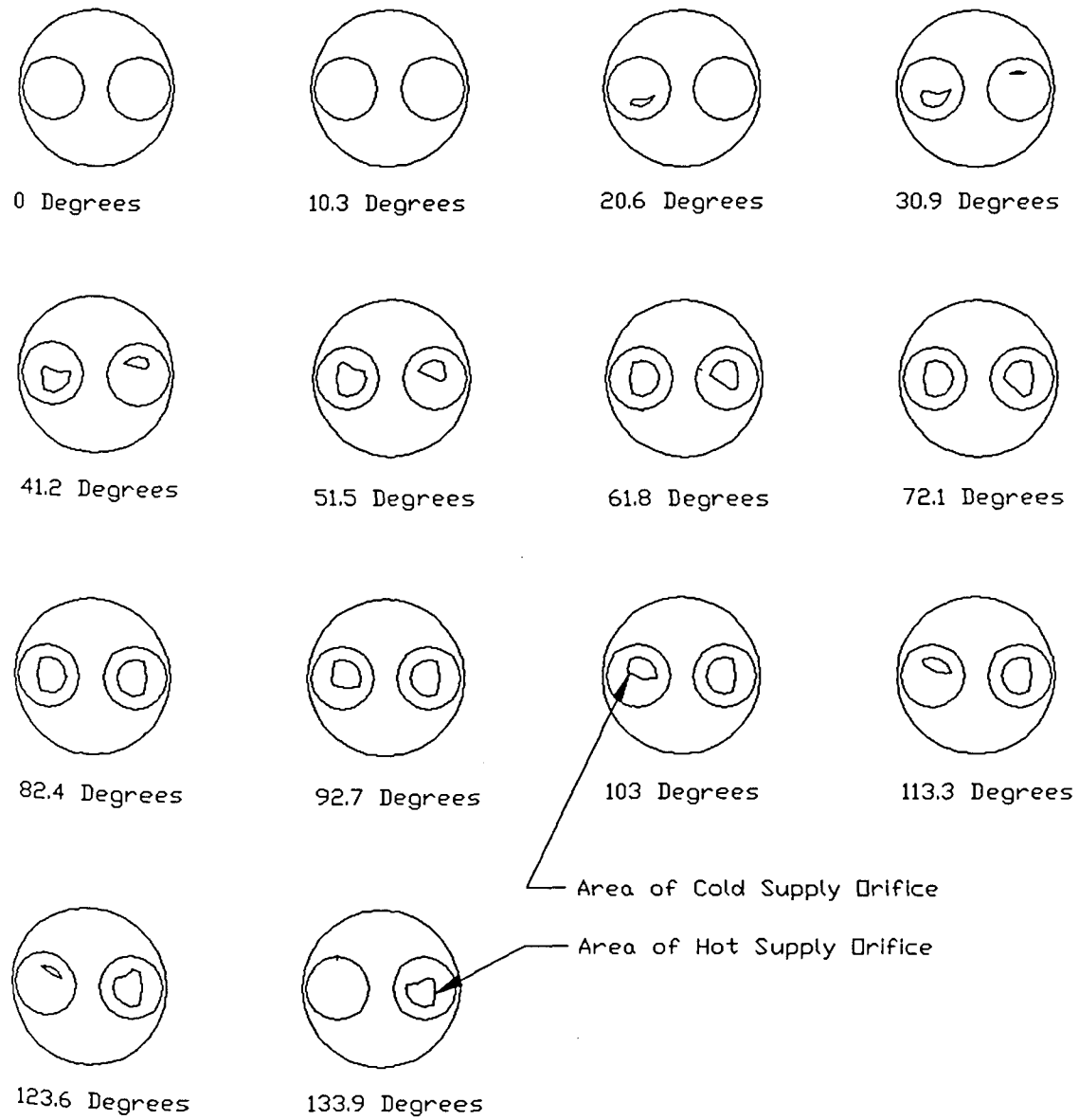
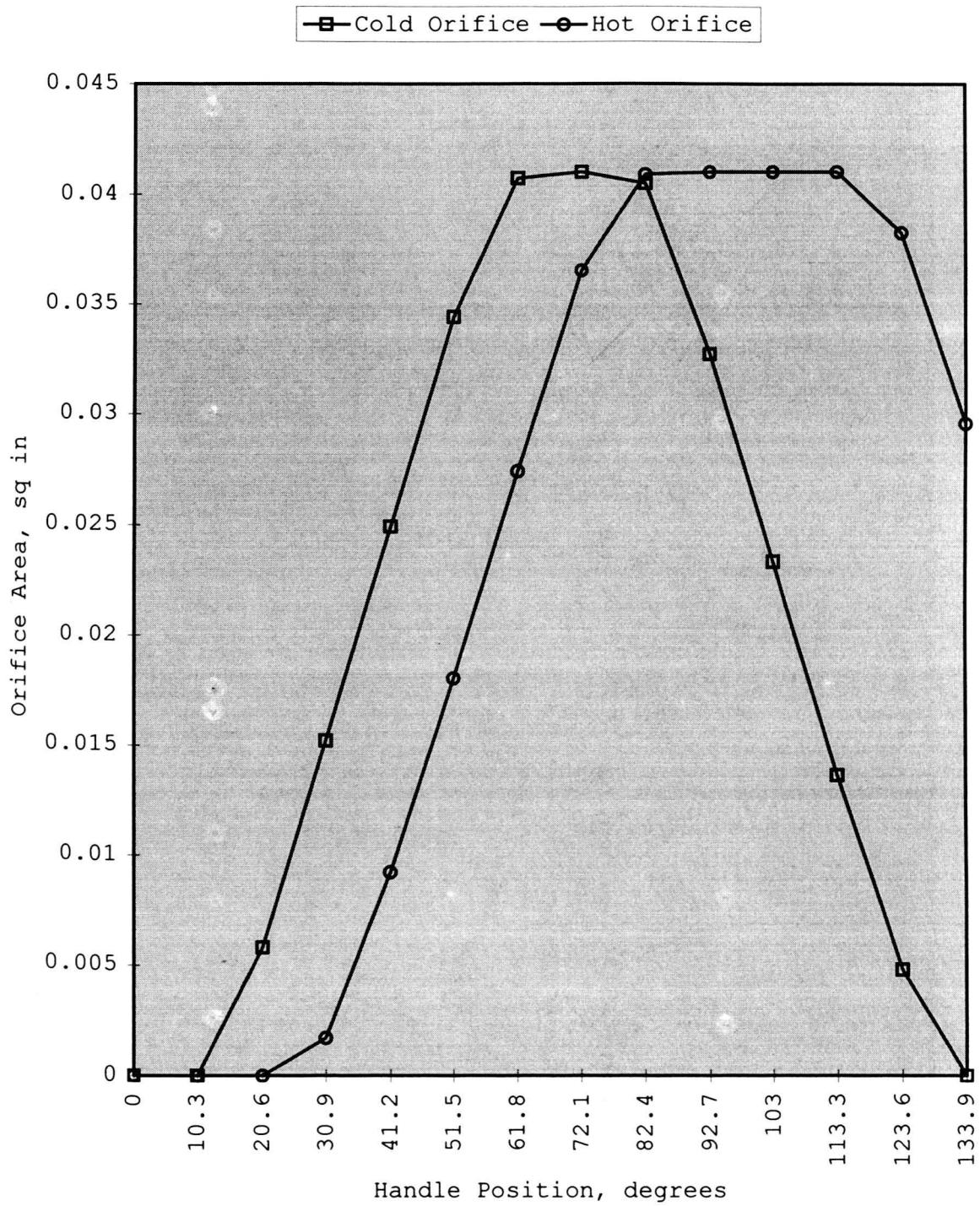


Figure 6.6: Orifice plate flow area as a function of handle position



6.7: Orifice plate flow area graphed as a function of handle position

Table 6.2 - Effective Orifice Plate Area as a Function of Handle Position

| Handle Rotation (degrees) | Cold Supply Orifice (sq inches) | Hot Supply Orifice (sq inches) |
|------------------------------|------------------------------------|-----------------------------------|
| 0.0 | 0.000 | 0.000 |
| 10.3 | 0.000 | 0.000 |
| 20.6 | 0.006 | 0.000 |
| 30.9 | 0.015 | 0.002 |
| 41.2 | 0.025 | 0.009 |
| 51.5 | 0.034 | 0.018 |
| 61.8 | 0.041 | 0.027 |
| 72.1 | 0.041 | 0.037 |
| 82.4 | 0.041 | 0.041 |
| 92.7 | 0.033 | 0.041 |
| 103.0 | 0.023 | 0.041 |
| 113.3 | 0.014 | 0.041 |
| 123.6 | 0.005 | 0.038 |
| 133.9 | 0.000 | 0.030 |

P_{cc} = Pressure in valve where hot and cold supplies mix, psf

ρ = Density of water, slugs/ft³

C = Orifice coefficient

A_o = Area of orifice, ft²

D_p = Hot and cold supply and mix output pipe diameter, ft

A_s = Area of spool which supply pressure acts upon, ft²

M_s = Mass of spool, slugs

Applying the orifice flow equation for orifice 1:

$$Q_c = \{2*(P_c - P_1)^2 / [\rho * (1/A_o * C)^2]\}^{0.5} \quad (6.16)$$

where:

$$A_{1o} = 0.0707/144 \text{ ft}^2$$

$$C = 0.59$$

$P_c - P_1$ = Pressure drop across orifice, psf

Applying the orifice flow equation (6.4) for orifice 2:

$$Q_c = \{2*(P_1 - P_2)^2 / [\rho*(1/A_{2o}*C)^2]\}^{0.5} \quad (6.17)$$

where:

$$A_{2o} = 0.0466/144 \text{ ft}^2$$

$$C = 0.59$$

$P_1 - P_2$ = Pressure drop across orifice, psf

Applying the orifice flow equation for orifice 3:

$$Q_c = \{2*(P_2 - P_3)^2 / [\rho*(1/A_{3o}*C)^2]\}^{0.5} \quad (6.4)$$

where:

$$A_{3o} = 0.0225/144 \text{ ft}^2$$

$$C = 0.59$$

$P_2 - P_3$ = Pressure drop across orifice, psf

Applying the orifice flow equation for orifice 4:

$$Q_c = \{2*(P_3 - P_4)^2 / [\rho*(1/A_{4c}*C)^2]\}^{0.5} \quad (6.18)$$

where:

$$A_{4c} = \text{Area of cold water spool inlet, ft}^2 \quad (6.6, 6.7, 6.8)$$

$$C = 0.59$$

$P_3 - P_4$ = Pressure drop across orifice, psf

Applying the orifice flow equation for orifice 5:

$$Q_c = \{2*(P_4 - P_5)^2 / [\rho*(1/A_{oc}*C)^2]\}^{0.5} \quad (6.19)$$

where:

$$A_{oc} = \text{Area of cold water spool outlet, ft}^2 \quad (6.9, 6.10)$$

$$C = 0.59$$

$P_4 - P_5$ = Pressure drop across orifice, psf

Applying the orifice flow equation for orifice 6:

$$Q_c = \{2*(P_5 - P_6)^2 / [\rho*(1/A_{6o}*C)^2]\}^{0.5} \quad (6.20)$$

where:

$$A_{6o} = .043/144 \text{ ft}^2$$

$$C = 0.59$$

$P_5 - P_6$ = Pressure drop across orifice, psf

Applying the orifice flow equation for orifice 7:

$$Q_c = \{2*(P_6 - P_7)^2 / [\rho*(1/A_{7hc}*C)^2]\}^{0.5} \quad (6.21)$$

where:

A_{7hc} = Area of the cold spool housing exit

$$C = 0.59$$

$P_6 - P_7$ = Pressure drop across orifice, psf

Applying the orifice flow equation for orifice 8:

$$Q_c = \{2*(P_7 - P_o)^2 / [\rho*(1/A_{8o}*C)^2]\}^{0.5} \quad (6.22)$$

where:

$$A_{8o} = 0.0707/144 \text{ ft}^2$$

$$C = 0.59$$

$P_7 - P_o$ = Pressure drop across orifice, psf

P_o = Pressure of the mix output, psf

Since the fluid is incompressible Q_c is equal for each of the eight orifices. Thus the flow equations may be written:

$$P_c - P_1 = \{[Q_c \cdot A_{1o} \cdot C]^2 \cdot \rho\} / 2 \quad (6.23)$$

$$P_1 - P_2 = \{[Q_c \cdot A_{2o} \cdot C]^2 \cdot \rho\} / 2 \quad (6.24)$$

The pressure drop from P_c to P_2 may be written:

$$P_c - P_2 = (Q_c^2 / 2) \cdot \rho \cdot [(A_{1o} \cdot C)^2 + (A_{2o} \cdot C)^2] \quad (6.25)$$

Or solving for flow:

$$Q_c = \{[2 \cdot (P_c - P_2) / \rho] \cdot [1 / (A_{1o} \cdot C)^2 + 1 / (A_{2o} \cdot C)^2]\}^{0.5} \quad (6.26)$$

Expanding this through the valve to the cavity where the hot and cold supply mix yields:

$$Q_c = [2 \cdot (P_c - P_{cc}) / \rho]^{0.5} \cdot \Psi_c^{-0.5} \quad (6.27)$$

where:

$$\Psi_c = 1 / (A_{1o} \cdot C)^2 + 1 / (A_{2o} \cdot C)^2 + 1 / (A_{3o} \cdot C)^2 + 1 / (A_{ic} \cdot C)^2 + \\ 1 / (A_{oc} \cdot C)^2 + 1 / (A_{6o} \cdot C)^2 + 1 / (A_{shc} \cdot C)^2 \quad (6.28)$$

Applying a similar process to the hot supply side of the valve yields:

$$Q_h = [2 \cdot (P_h - P_{cc}) / \rho]^{0.5} \cdot \Psi_h^{-0.5} \quad (6.29)$$

where:

$$\Psi_h = 1 / (A_{1o} \cdot C)^2 + 1 / (A_{2o} \cdot C)^2 + 1 / (A_{3o} \cdot C)^2 + 1 / (A_{ih} \cdot C)^2 + \\ 1 / (A_{oh} \cdot C)^2 + 1 / (A_{6o} \cdot C)^2 + 1 / (A_{shh} \cdot C)^2 \quad (6.30)$$

The flow equation for the mix output of the valve is:

$$Q_m = [2*(P_{cc} - P_m) / \rho]^{0.5} * (A_{8o}*C) \quad (6.31)$$

Figure 6.8 graphs the functions Ψ_h and Ψ_c as functions of x at a valve handle positions of $\theta = 82.4$ degrees.

In a similar fashion the flow equation may be written for the pressure difference between the supply pressure and the pressure that is exerted on the spool. For the cold supply this equation may be written:

$$Q_c = [2*(P_c - P_o) / \rho]^{0.5} * \Lambda_c^{-0.5} \quad (6.32)$$

where:

$$\Lambda_c = \frac{1}{(A_{1o}*C)^2} + \frac{1}{(A_{2o}*C)^2} + \frac{1}{(A_{3o}*C)^2} + \frac{1}{(A_{ic}*C)^2} \quad (6.33)$$

Thus:

$$P_{sc} = P_c - (Q_c^2 * \rho * \Lambda_c) / 2 \quad (6.34)$$

Applying a similar philosophy to the hot supply side of the valve yields:

$$Q_h = [2*(P_h - P_o) / \rho]^{0.5} * \Lambda_h^{-0.5} \quad (6.35)$$

where:

$$\Lambda_h = \frac{1}{(A_{1o}*C)^2} + \frac{1}{(A_{2o}*C)^2} + \frac{1}{(A_{3o}*C)^2} + \frac{1}{(A_{ih}*C)^2} \quad (6.36)$$

Therefore:

$$P_{sh} = P_h - \frac{Q_c^2 * \rho * \Lambda_h}{2} \quad (6.37)$$

Figure 6.9 graphs the functions Λ_h and Λ_c as a function of x based on a valve handle position of 82.4 degrees. Figure 6.10 plots P_{sh} and P_{sc} as a function of spool position for supply pressure of 50

psi, a supply mixing cavity pressure of 11 psi, an output mix pressure of 1 psi, and a valve handle position of 82.4 degrees. Figure 6.11 plots both hot and cold supply flow as a function of spool position for supply pressure of 50 psi, a supply mixing cavity pressure of 11 psi, an output mix pressure of 1 psi, and a valve handle position of 82.4 degrees.

Forces may be summed axially on the spool to obtain the differential equations of motion for the spool. Summing the forces axially results in:

$$M_s x'' = A_s (P_{sh} - P_{sc}) - c x' - f_s \quad (6.38)$$

where:

M_s = Mass of the spool, slugs

x'' = Acceleration of the spool, ft/s^2

x' = Velocity of the spool, ft/s

A_s = Area of the spool, ft^2

P_{sh} = Pressure on the spool due to the hot supply water, psf

P_{sc} = Pressure on the spool due to the cold supply water, psf

c = Damping coefficient due to relative motion of the spool,
slugs/sec

f_s = Frictional force on the spool ($\mu M_s g$), lbf

Baumeister et al. [1978] describe typical values of kinetic coefficient of friction for lubricated hard steel on hard steel. A coefficient of friction (μ) of 0.08 will be used for the modeling. The damping coefficient was varied in the modeling to evaluate the

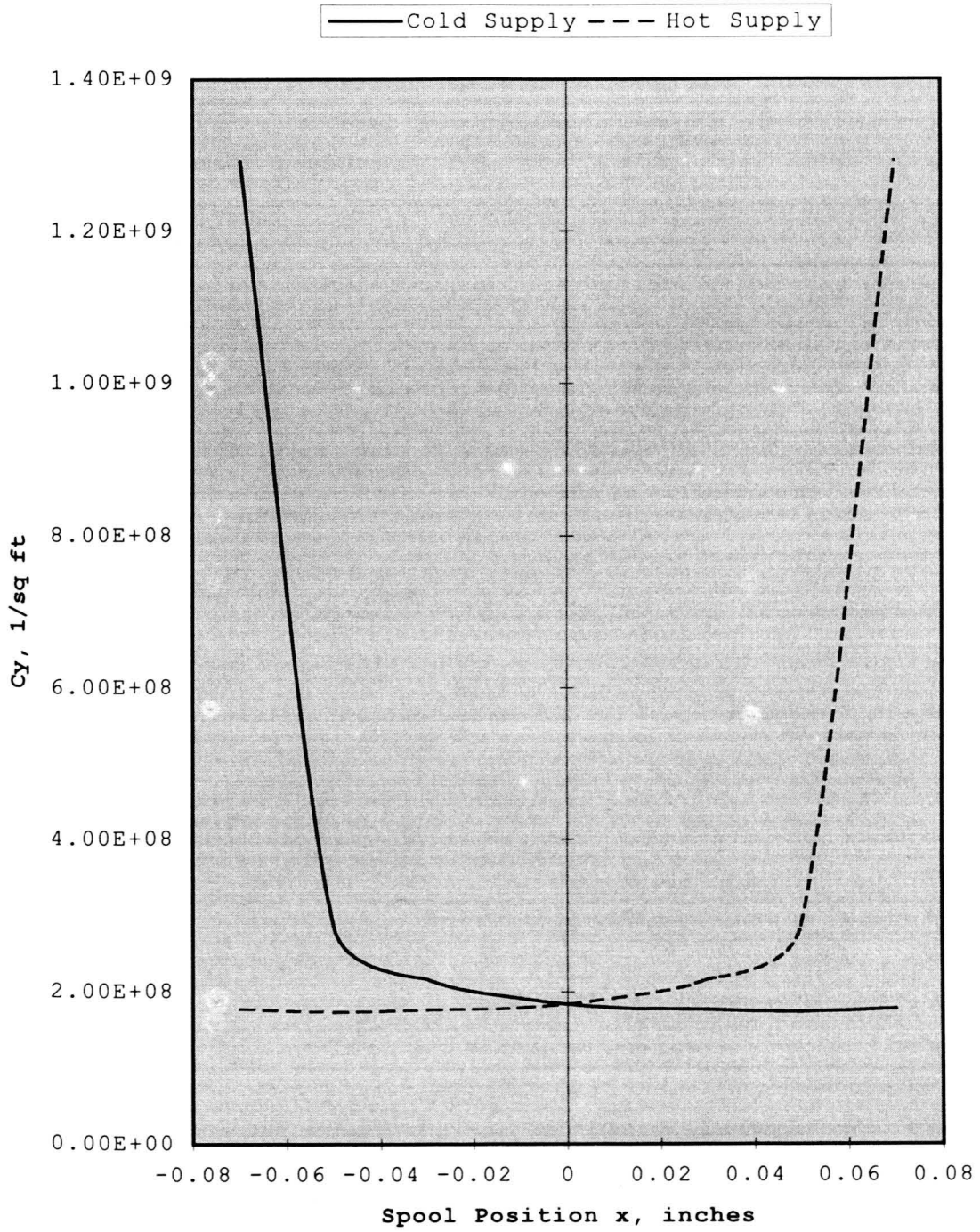
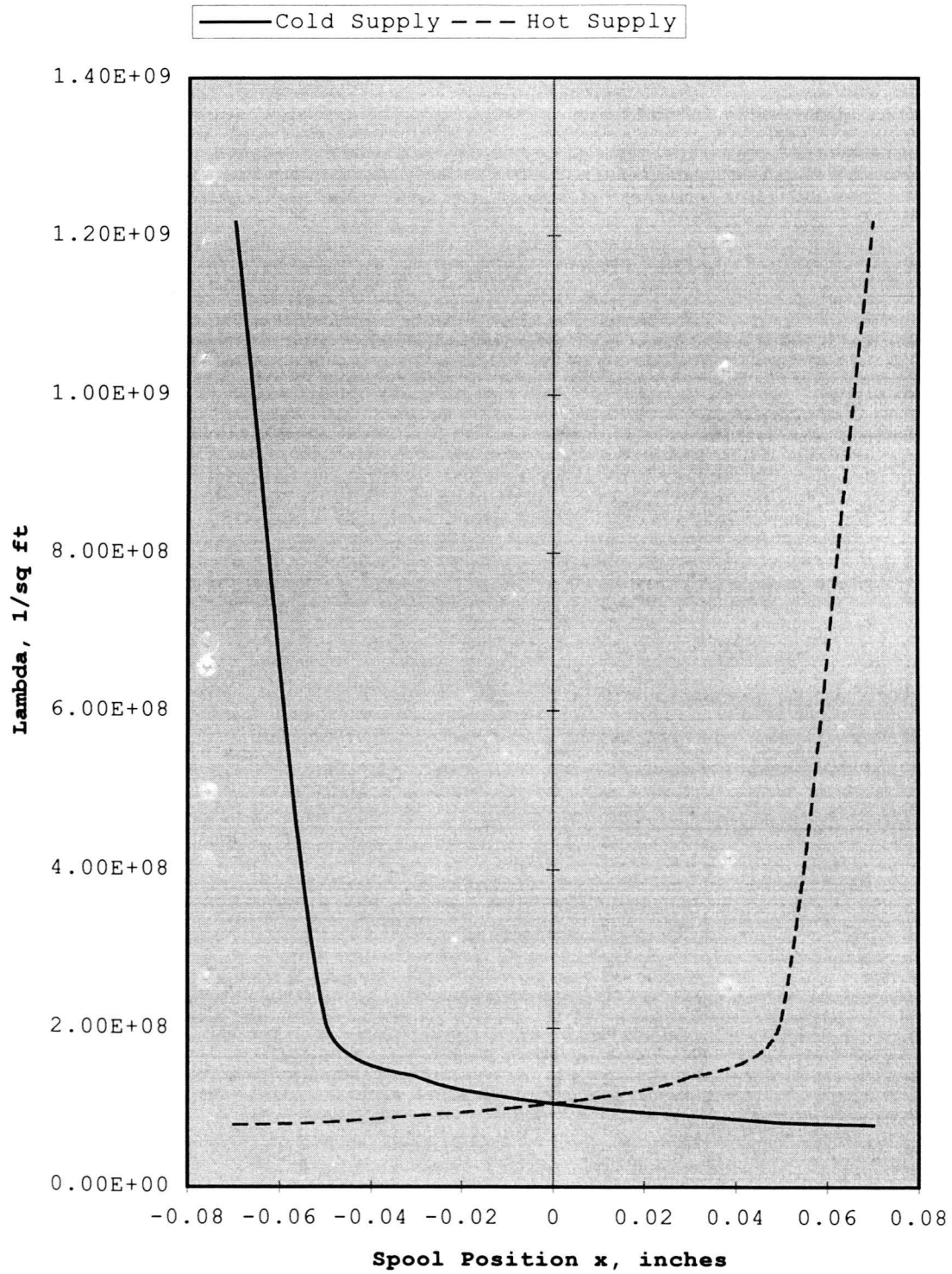


Figure 6.8: Ψ_c and Ψ_h plotted as a function of spool position

Figure 6.9: A_c and A_h plotted as a function of spool position

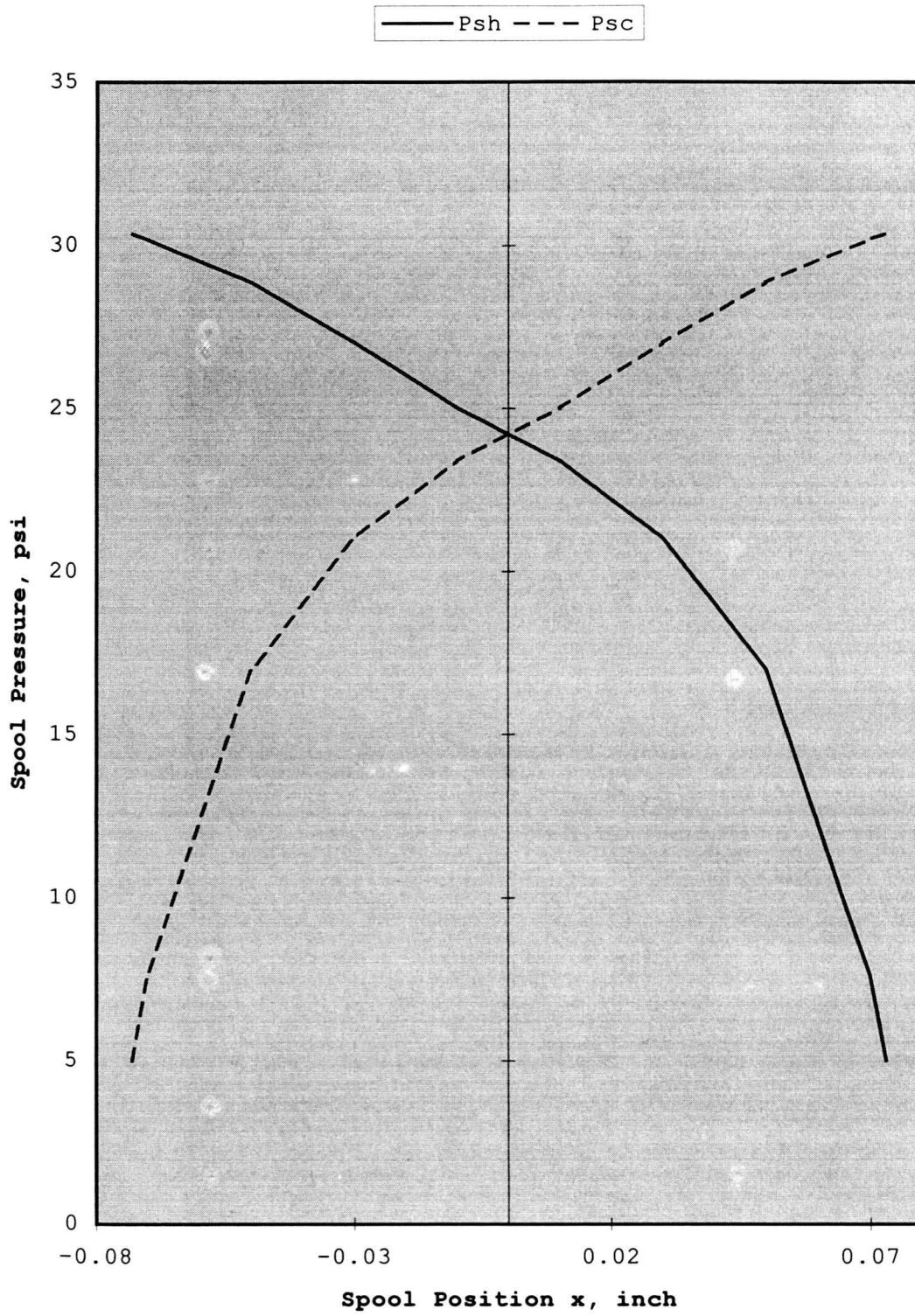


Figure 6.10: Spool pressure plotted as a function of spool position

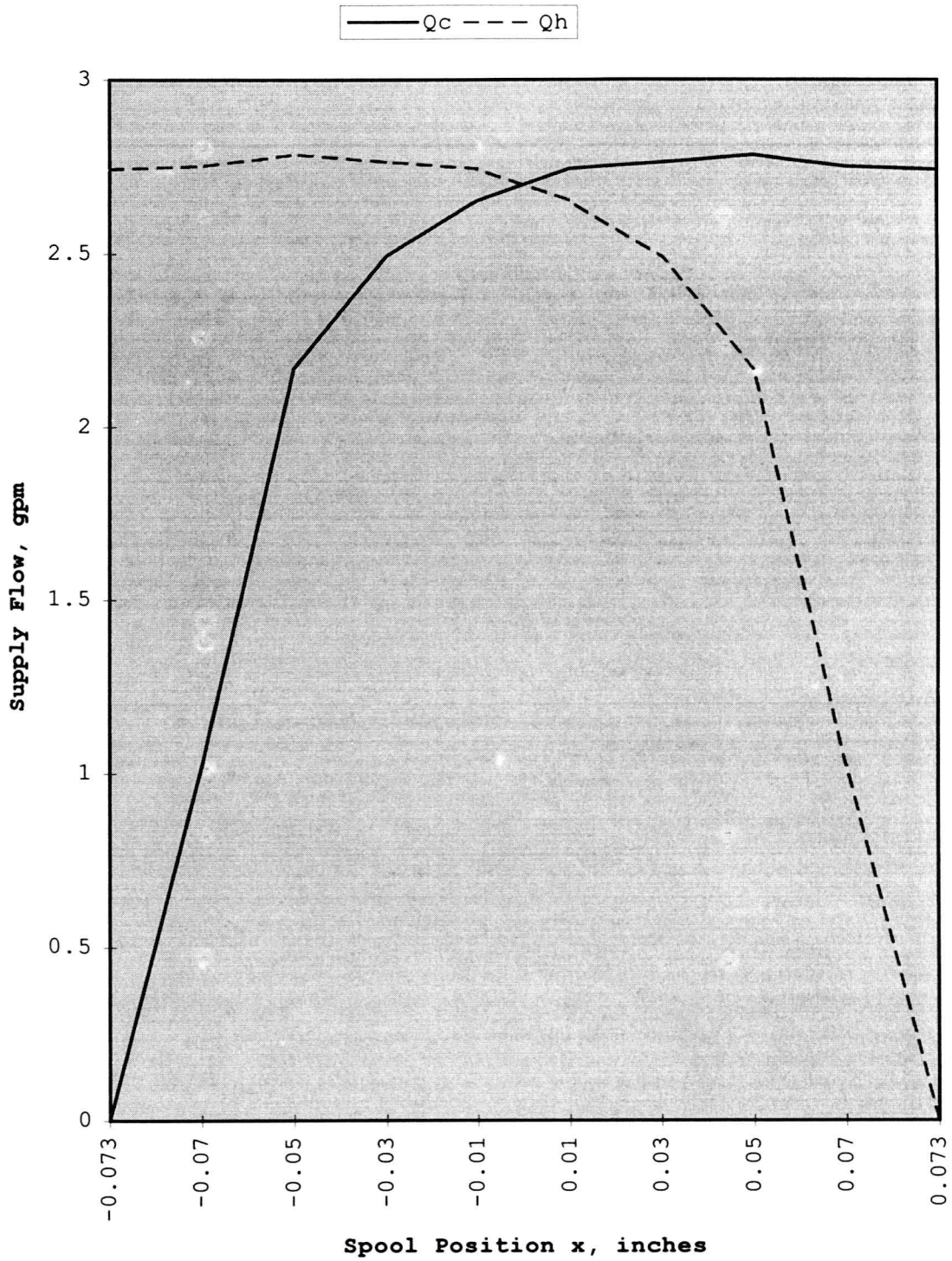


Figure 6.11: Supply flow plotted as a function of spool position

effects on the motion of the spool. Expanding the equation by inserting the expanded form of Psh and Psc results in:

$$x'' = \frac{As}{Ms} \left(\frac{Qc^2 * \rho * \Lambda c - Qh^2 * \rho * \Lambda h}{2} \right) - \frac{cx'}{Ms} - \mu * g \quad (6.39)$$

This is the equation of motion for the spool and involves solving a nonlinear differential equation.

Based upon the laws of conservation of energy and conservation of mass, the following defines the relationship between the hot and cold supply water flow, hot and cold supply water temperature, and the resulting mix flow and temperature:

$$Tm = \frac{Qc * Tc + Qh * Th}{Qm} \quad (6.40)$$

where:

Qm = Mix output flow, ft³/sec

Tm = Temperature of the mix output flow, °F

Qc = Cold supply flow, ft³/sec

Tc = Temperature of the cold supply flow, °F

Qh = Hot supply flow, ft³/sec

Th = Temperature of the hot supply flow, °F

System Testing

A system test environment was developed to test the valves and to meet the requirements of the valve tests suggested in the American Society of Sanitary Engineering standards 1016 and 1017.

The piping schematic for the test environment is detailed in Figure 6.12. Thermocouples were installed next to the valve supply inlets and to the mix outlet. The thermocouples were fine tip thermocouple probes with an accuracy of 1°F. The response time of the thermocouples to moving water was less than 0.5 seconds. The response time was obtained by measuring the time required for the thermocouple to reach 90% of its final temperature - when exposed to 212°F running water, with an initial temperature of 100°F.

Pressure transducers were installed next to the valve supply inlets and to the mix outlet. The response time of the pressure transducers was 0.001 second. The range of the pressure transducers was from 0 psig to 100 psig.

Flow meters were installed next to the supply inlets. The flow meters were capable of measuring water flows from 0.15 to 20 gallons per minute (gpm). The flow meters generated a pulsed output, there were 151.4 pulses to one gallon of flow. The pulsed output of the flow meter fed into a ratemeter. The ratemeter had a 2 second delay factor and normalized (averaged) the data received.

Due to the flow meter delay factor and the normalizing process, accurate flow measurements were only obtained during steady state conditions; trends in flow were obtained during dynamic response periods. Data was collected through the use of a personal computer with a data collection board. Data from the thermocouples, pressure transducers and flow meters was collected and recorded to a disk file every 0.5 seconds.

Tests were conducted on the pressure balanced bath valve to

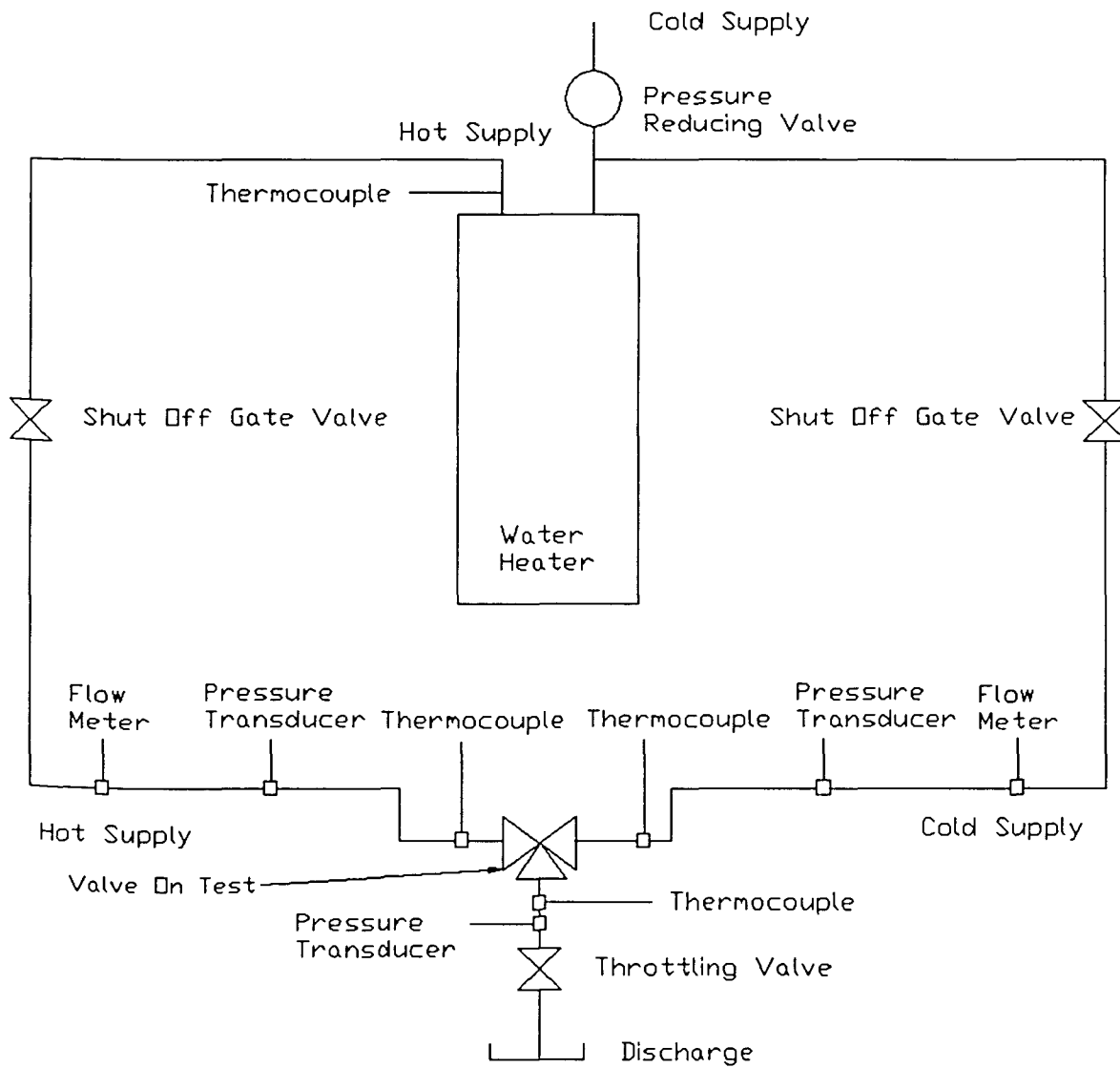


Figure 6.12: Piping schematic for valve tests

obtain characteristic flow curves for the valve and to obtain information on the dynamic response of the valve. Figure 6.13 is a plot of the test results for the hot and cold supply flow as the valve handle was turned through its maximum stroke. The valve handle was rotated counterclockwise from 0 to 133.9 degrees in 13 increments of 10.3 degrees. The system was allowed to reach a steady state condition at each rotational position. Figure 6.14 graphs the supply flow as a function of the valve handle position. Figure 6.15 graphs the mix temperature. The operating parameters were approximately:

$$P_h = P_c = 50 \text{ psi}$$

$$P_o = 2 \text{ psi}$$

$$T_h = 160^\circ\text{F}$$

$$T_c = 50^\circ\text{F}$$

To calculate the steady state flow conditions using the characteristic equations, an iterative approach is required. An estimate is made of the spool position (x) and of the pressure of the common mixing cavity (P_{cc}). Flow calculations of the hot water supply, cold water supply and the mix output are calculated using equations 6.27, 6.29 and 6.31. Pressure on the spool due to the hot water supply and the cold water supply are calculated using equations 6.34 and 6.37. Based on the supply and mix flows, the estimated pressure in the common mixing cavity (P_{cc}) may be updated. If the mix flow is lower than the combination of the hot and cold supply flow, P_{cc} is increased. If the mix flow is higher than the combination of the hot and cold supply flow, P_{cc} is decreased.

Based on the spool pressures (P_{sh} and P_{sc}), the spool position may be updated. If the hot supply spool pressure (P_{sh}) is higher than the cold supply pressure (P_{sc}), x is increased. If the hot supply spool pressure is lower than the cold supply spool pressure, x is decreased. This process is repeated until the hot and cold supply flow rates are equal to the mix flow rate and the cold supply spool pressure is equal to the hot supply spool pressure.

Based on the model developed for the pressure balanced valve, the hot and cold supply flows were calculated. The operating parameters for the model were the hot supply, cold supply, and mix output pressures which were recorded in the test. Figure 6.16 graphs the hot and cold supply flow as a function of the valve handle position (θ). Figure 6.17 graphs the mix temperature of the test and model flows based on the input supply temperatures. Figure 6.18 graphs the supply flow based on the model and test. Evaluation of the test supply flow curves to the model supply flow curves show the cold supply model characterizes the test flow to within 6% at a valve handle position of 51.5 degrees. The hot supply model characterizes the test flow to within 14% at a valve handle position of 82.4 degrees. It appears that that the graphical analysis of the hot supply orifice location was shifted approximately 10 degrees relative to the valve handle position.

Tests were conducted to record the response of the valve given a change in the hot water supply temperature. Steady state pressure, temperature, and flow conditions were established prior to

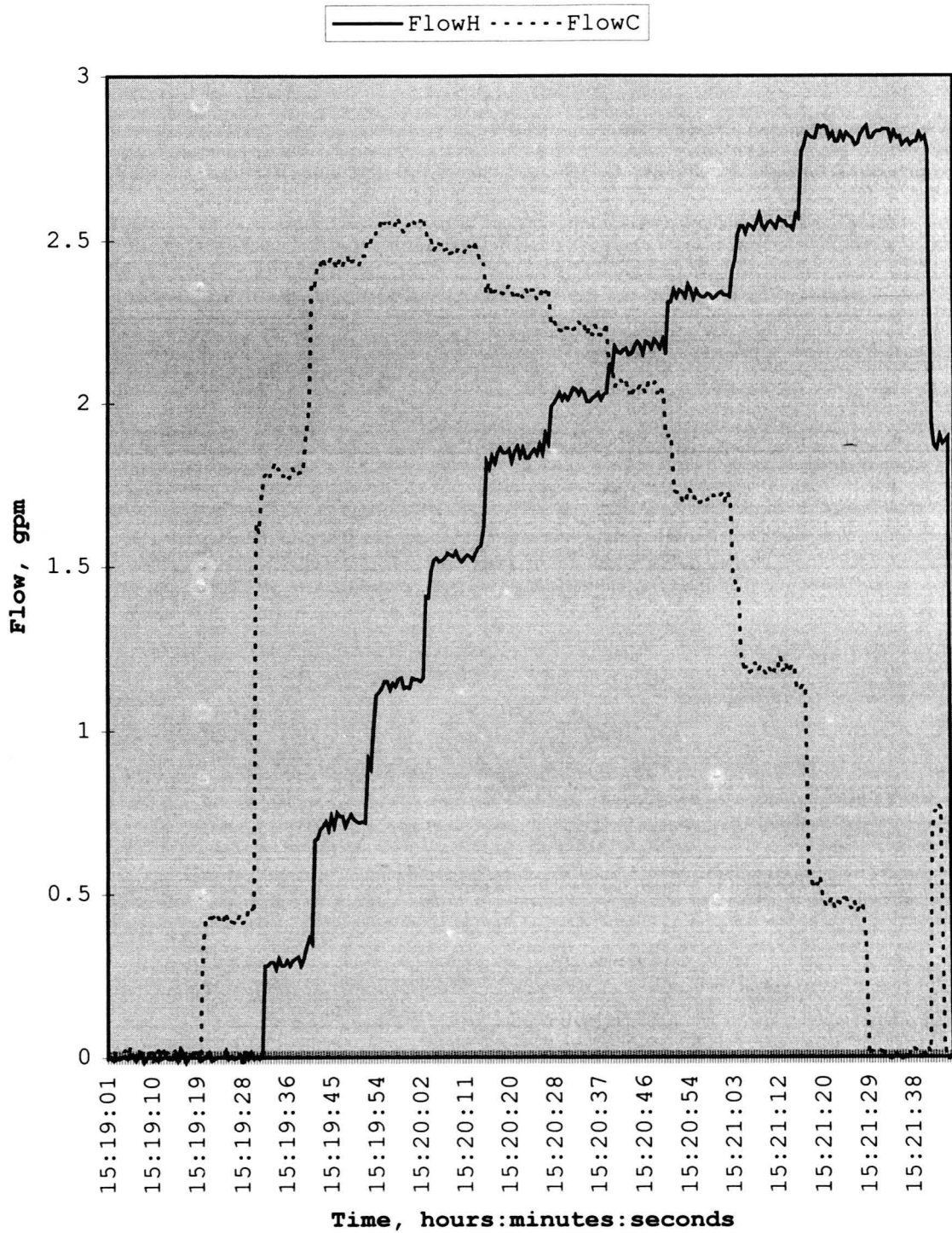


Figure 6.13: Pressure Valve test, results of the hot and cold supply flow as a function of time

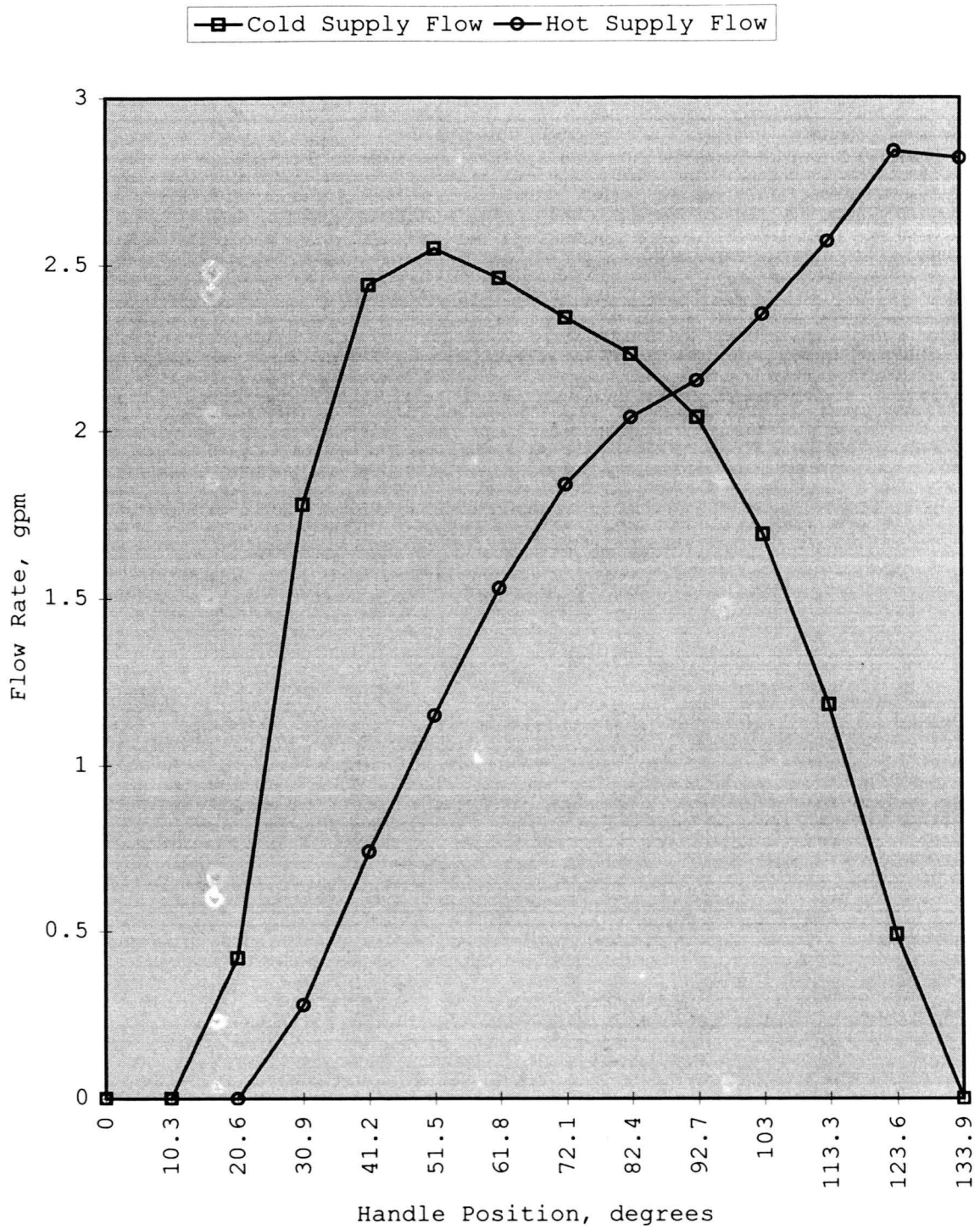


Figure 6.14: Pressure Valve test, supply flow as a function of valve handle position

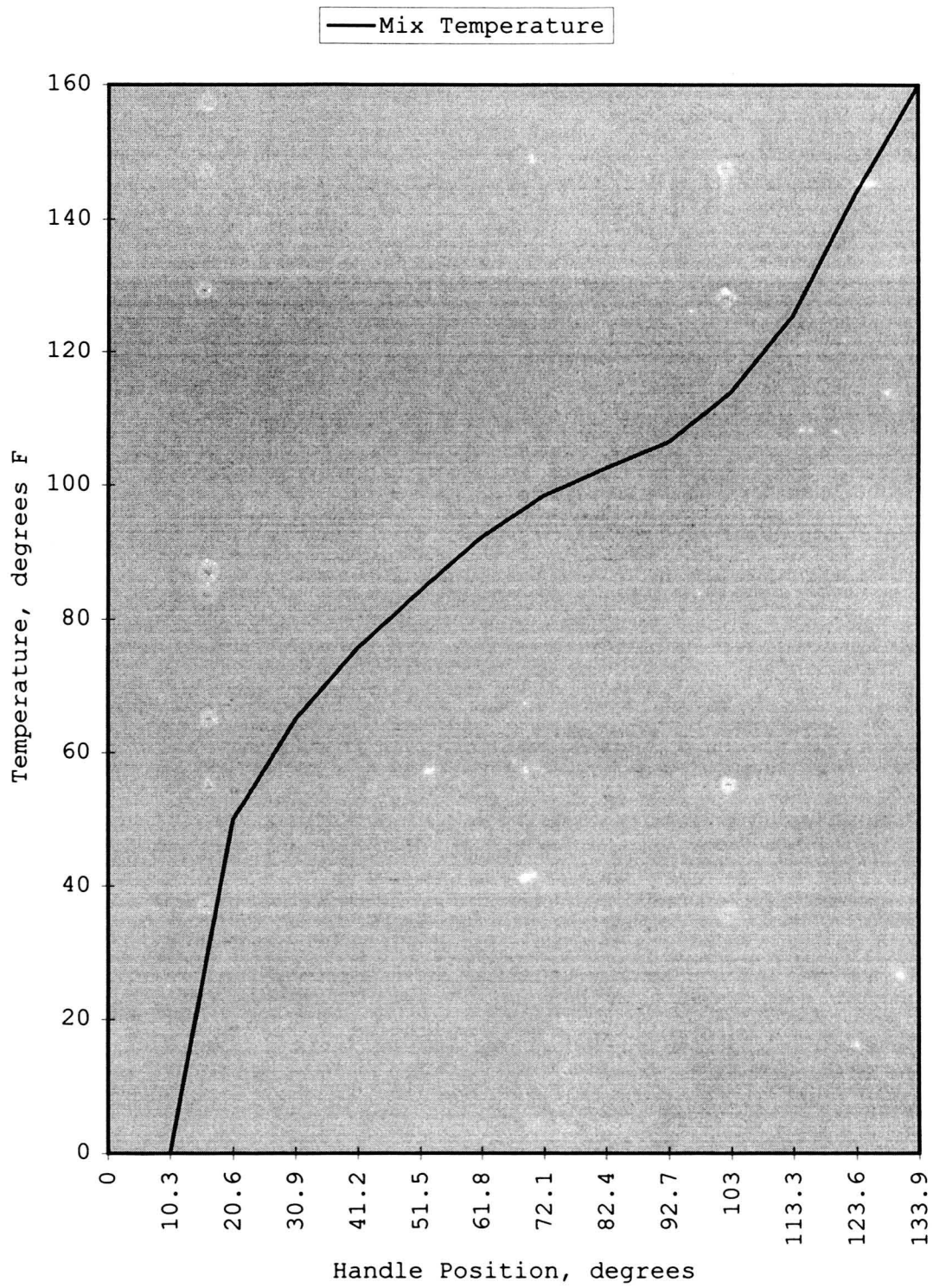


Figure 6.15: Pressure valve test, mix temperature as a function of valve handle position

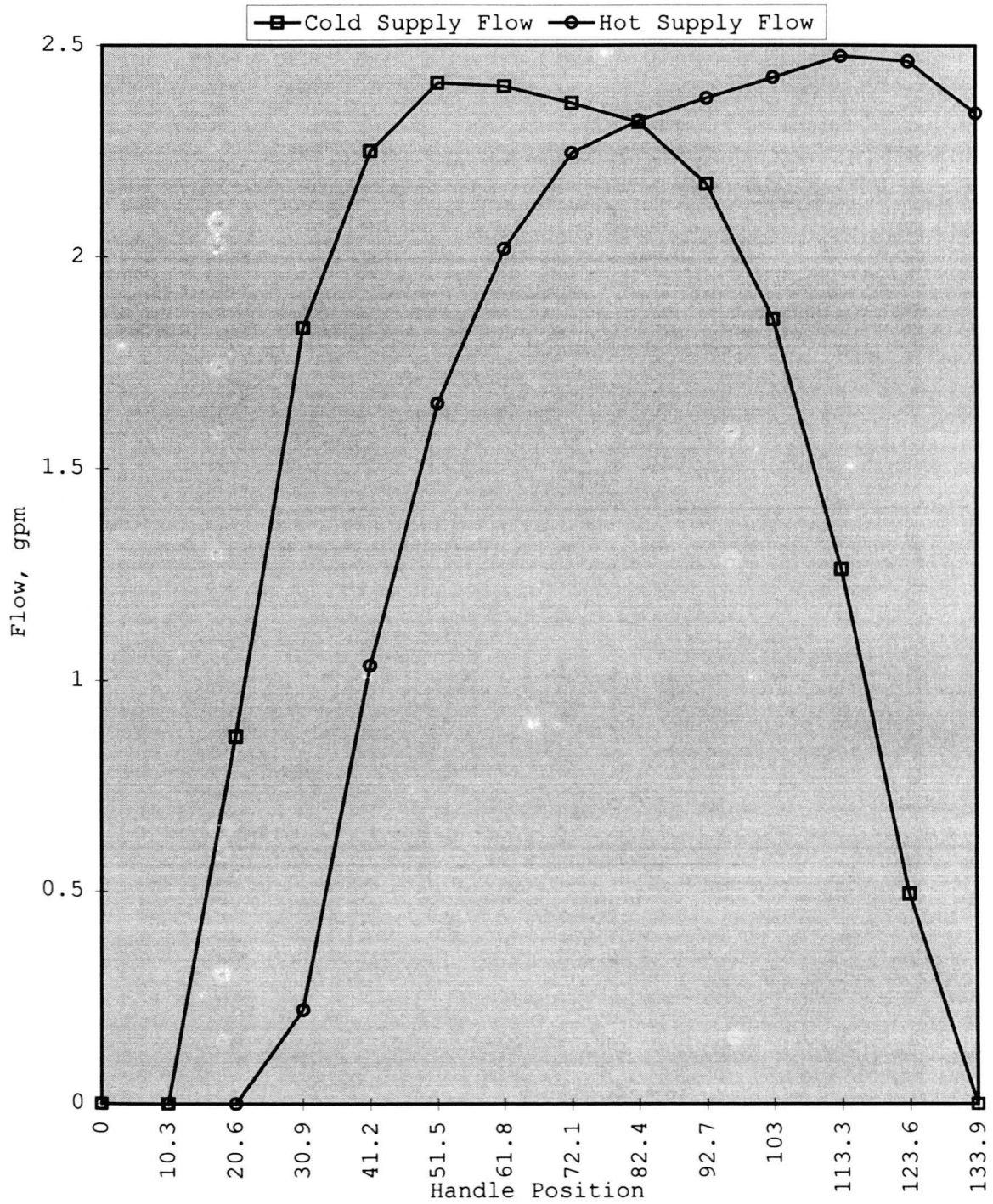


Figure 6.16: Pressure Valve model, hot and cold supply flow as a function of valve handle position

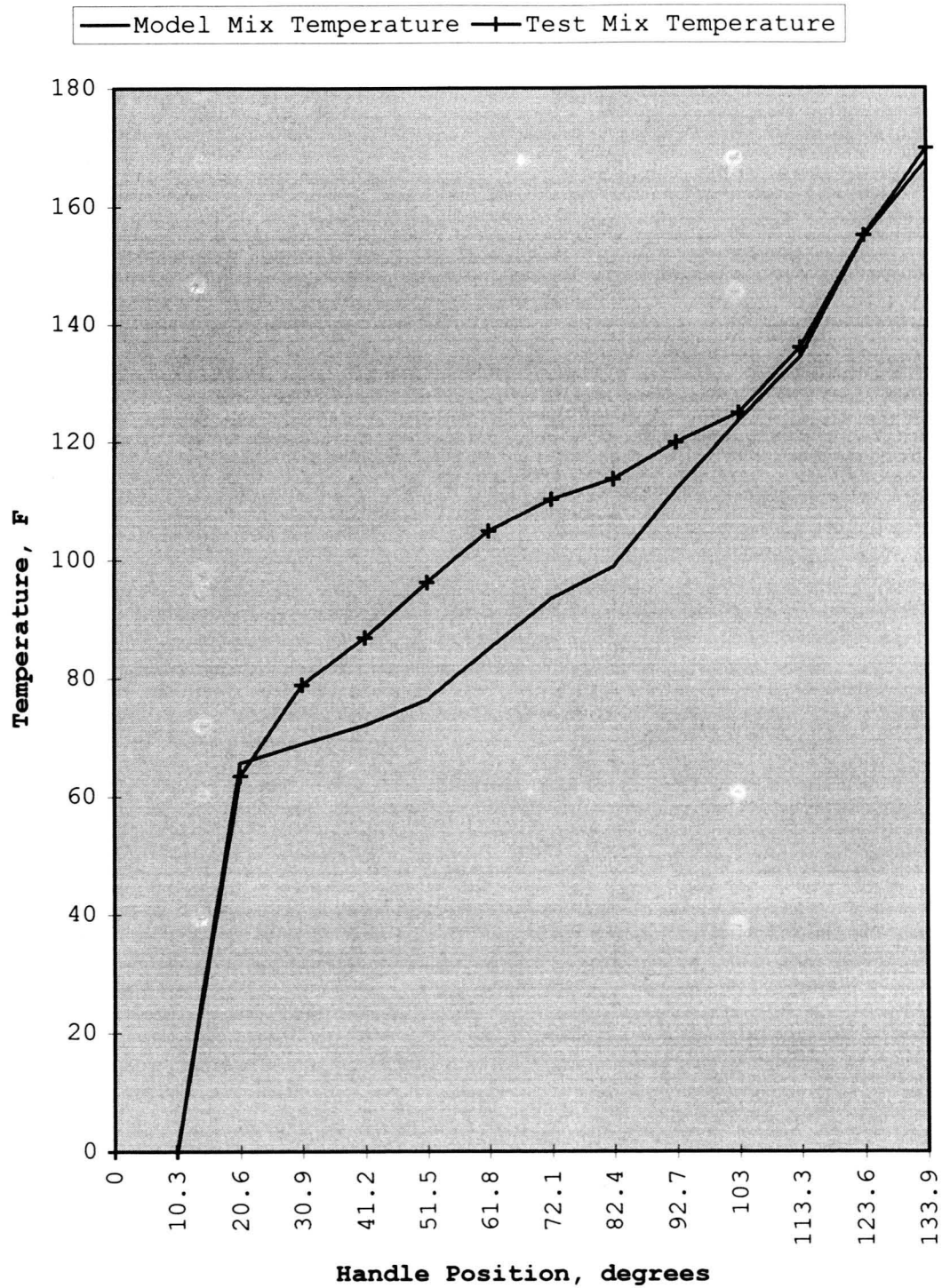


Figure 6.17: Pressure valve model and test, mix temperature as a function of valve handle position

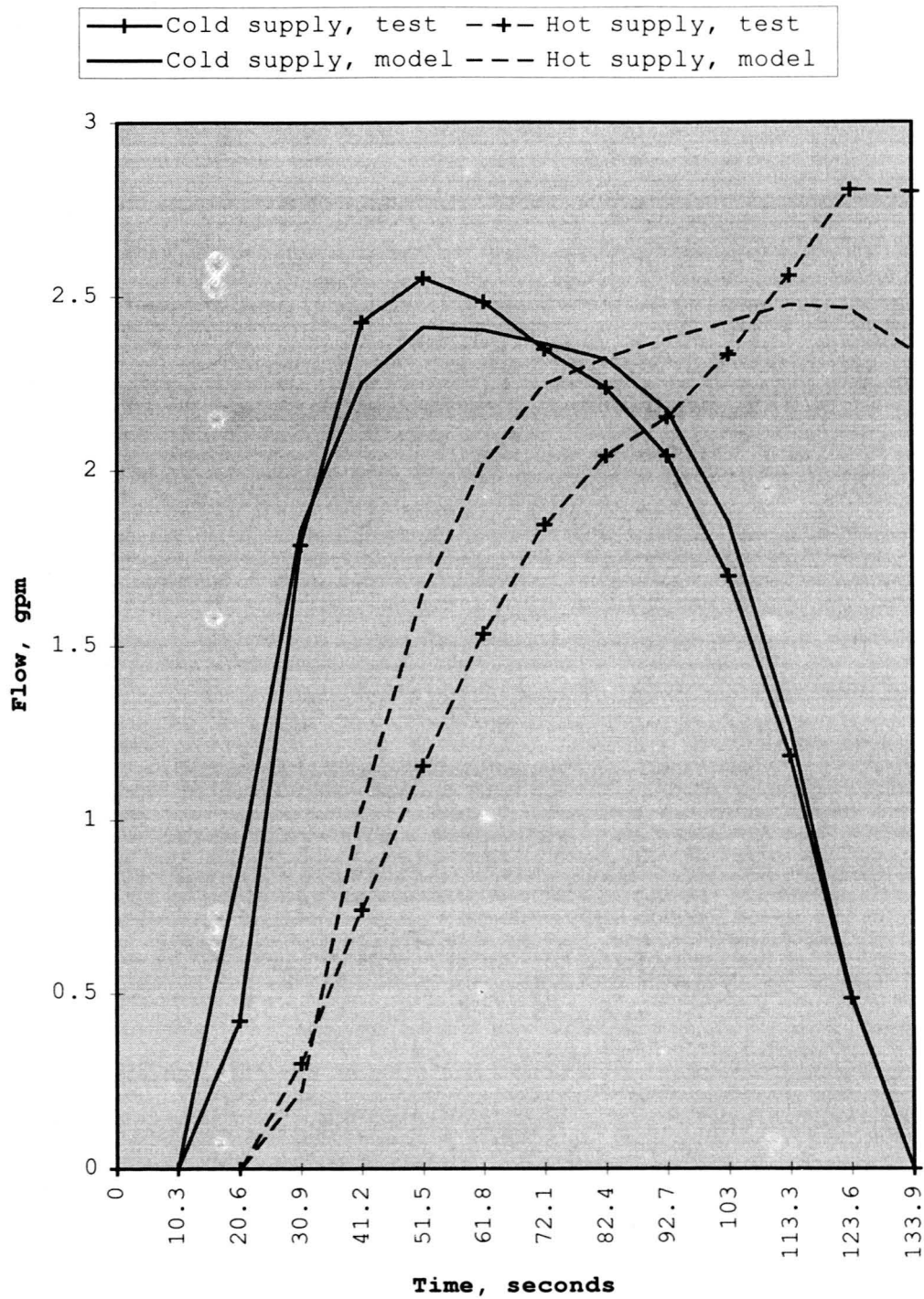


Figure 6.18: Pressure valve model and test, flow rate as a function of valve handle position

changing the hot water supply temperature. The temperature of the hot water supply was allowed to reach room temperature prior to the test. The water heater was set to deliver water at approximately 160°F. The valve handle was then turned to 82.4 degrees. Supply pressure was not changed during the test. Figure 6.19 graphs the hot and cold supply temperature and the resulting mix temperature. A steady state condition is established at the location of the "Y" axis. Figure 6.20 graphs the supply pressure of the hot and cold supply pressure. Figure 6.21 is a graph of the supply flow.

The following is the model for the response of the valve given the initial test conditions of steady state flow and pressure, then increasing the hot water supply temperature. Given the following at time $t = 0$:

$$P_c = 47 \text{ psi}$$

$$T_c = 60 \text{ }^\circ\text{F}$$

$$P_h = 47 \text{ psi}$$

$$T_h = 75 \text{ }^\circ\text{F}$$

$$P_o = 5 \text{ psi}$$

$$\theta = 72.1 \text{ degrees}$$

For steady state flow at time $t = 0$:

$$Q_c = [2*(P_c - P_o)/(\rho*\Psi_c)]^{0.5} \quad (6.41)$$

Similarly for the hot supply flow:

$$Q_h = [2*(P_h - P_o)/(\rho*\Psi_h)]^{0.5} \quad (6.42)$$

The hot and cold supply flow is unaffected by a change in supply temperature. For a sudden supply temperature increase (step

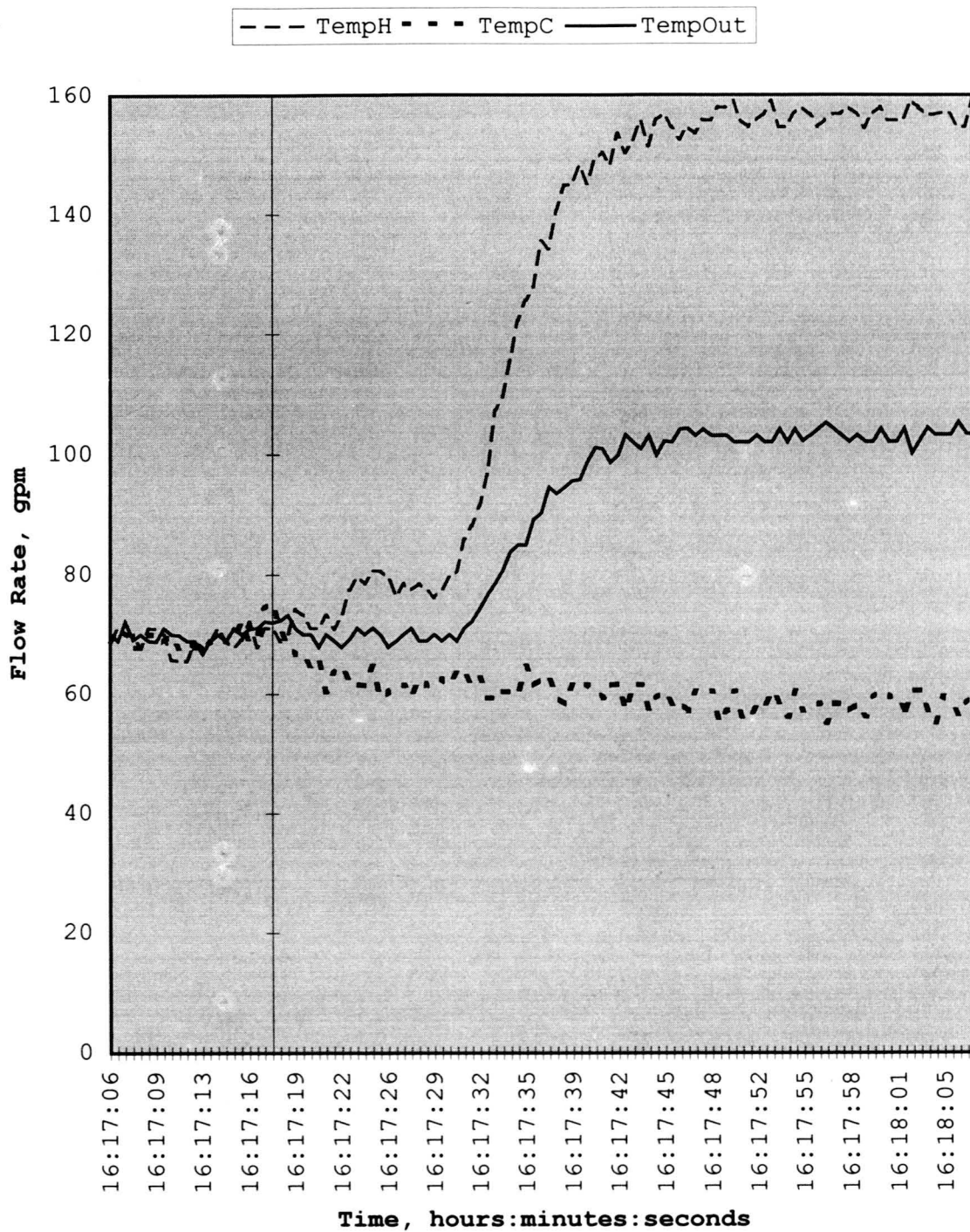


Figure 6.19: Pressure Valve test, increase in hot supply temperature, supply and mix temperatures

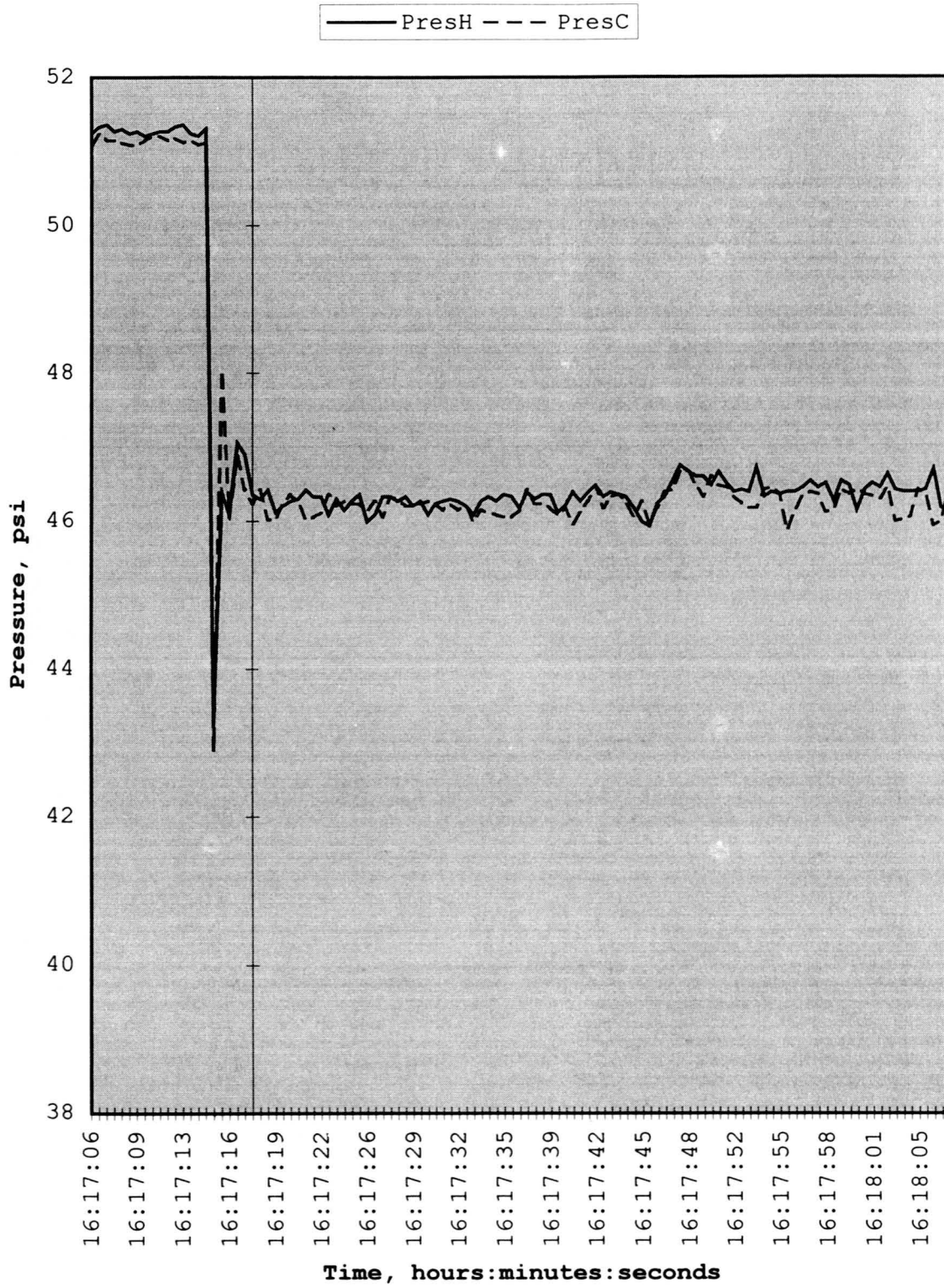


Figure 6.20: Pressure Valve test, increase in hot supply temperature, supply pressure

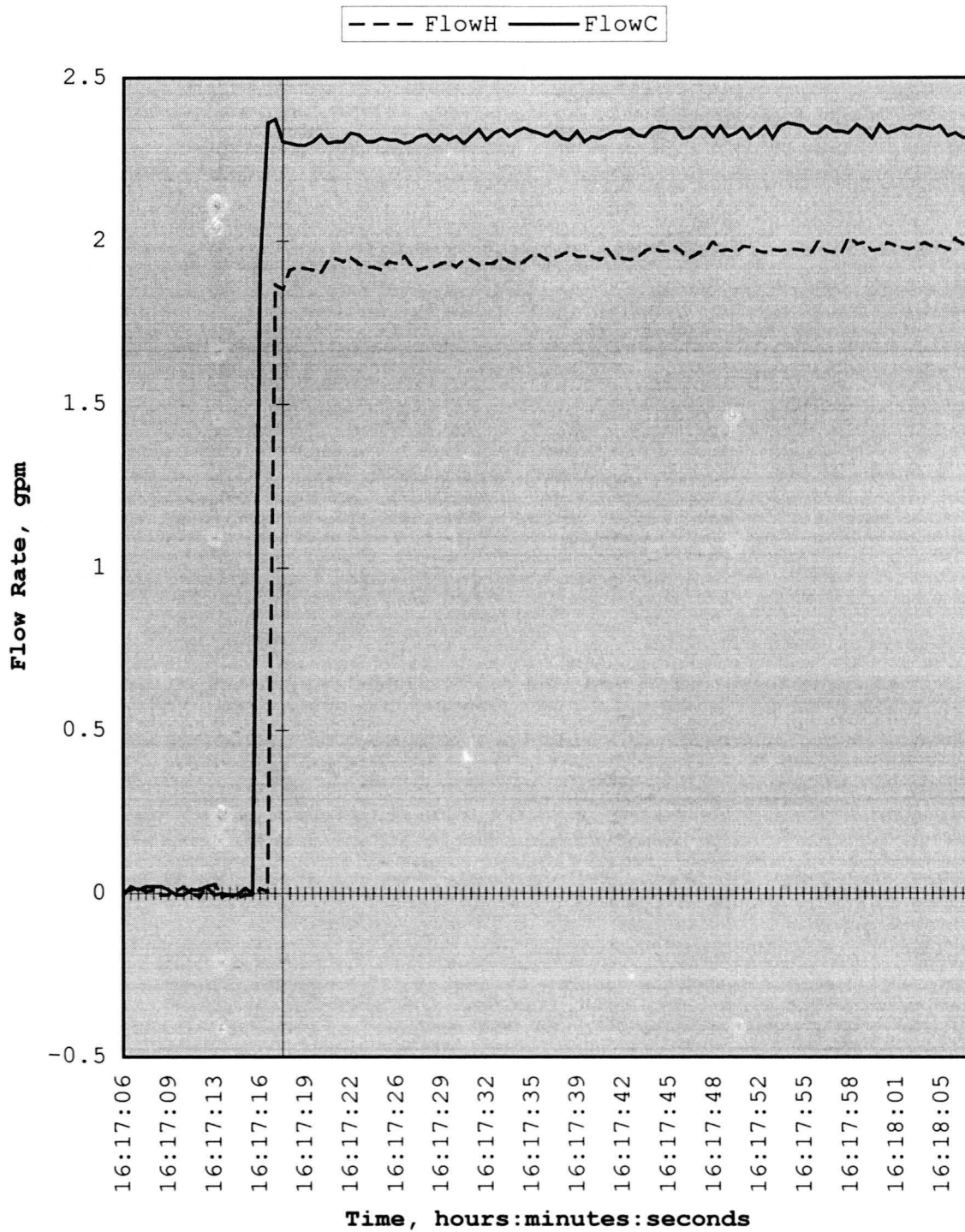


Figure 6.21: Pressure Valve test, increase in hot supply temperature, supply flow rates

function) to 160 °F in the hot supply, there is no effect on the spool pressure for either the hot or cold supply and thus there is no change in the spool position. The resulting mix temperature will simply be:

$$T_m = \frac{Q_c * T_c + Q_h * T_h'}{Q_c + Q_h} \quad (6.43)$$

where:

T_h' = current hot supply temperature, °F

The pressure balance valve has a dynamic response to address changes in the hot and cold supply pressure, but has no dynamic response to address changes in the hot and cold supply temperature. The characteristic equations for the pressure balance valve predict that there will be no change in the supply flow rates with a change in supply flow temperature; this was verified in the previous temperature test and can be seen in Figures 6.20 and 6.21.

Tests were conducted to record the response of the valve given a change in the cold water supply pressure. Steady state pressure, temperature and flow conditions were established prior to changing the cold water supply pressure. The pressure balance valve handle was set at 82.4 degrees and steady state conditions were established. The upstream shut off valve for the cold water supply was then partially closed to produce a cold supply pressure drop. Supply temperature was not changed and the cold supply pressure was dropped. Figure 6.22 graphs the hot and cold supply pressure as a function of time. A steady state condition is established at the location of the "Y" axis. Figure 6.23 graphs the supply flow and Figure 6.24 graphs the hot supply, cold supply and mix temperature.

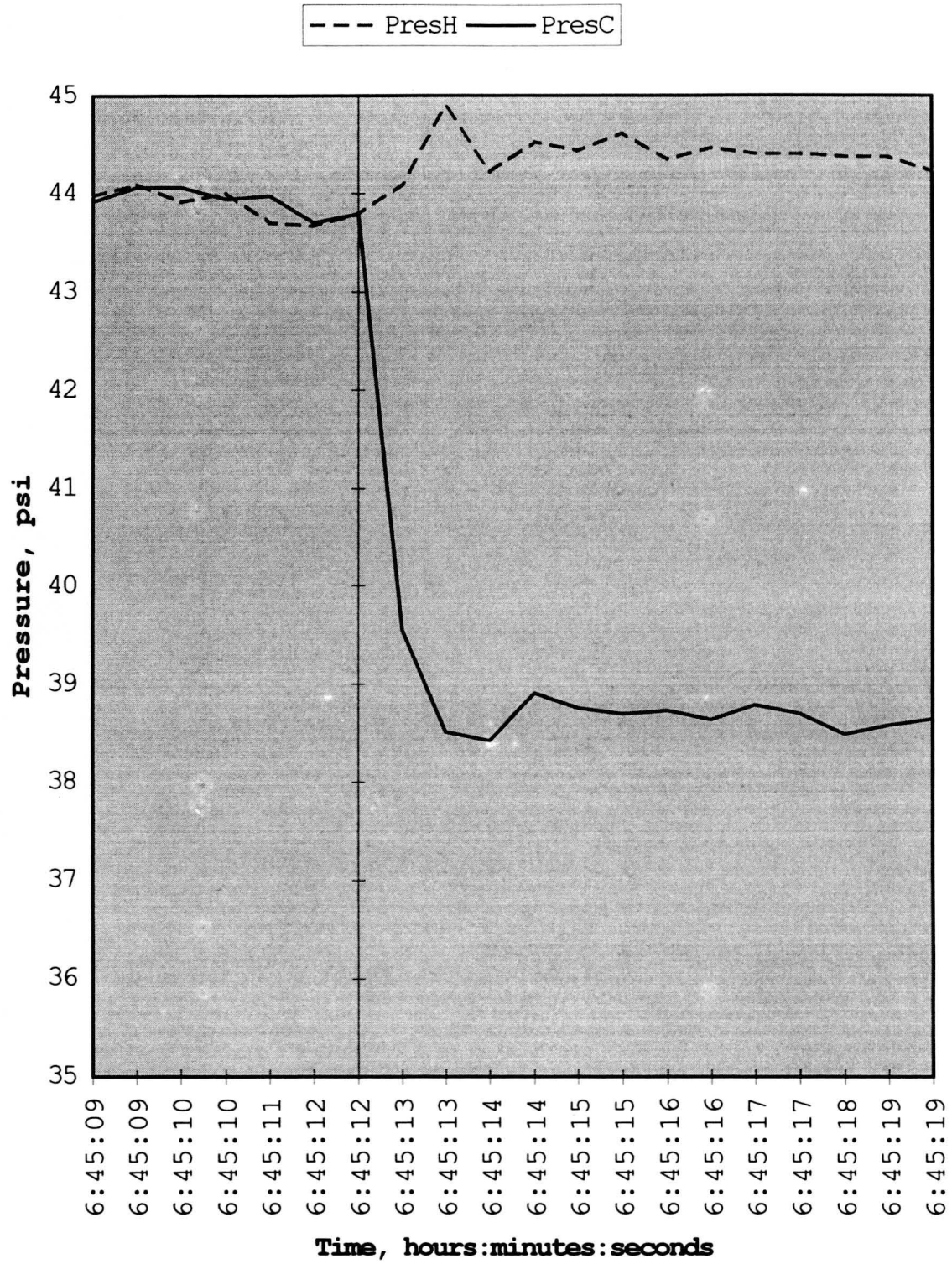


Figure 6.22: Pressure Valve test, decrease in cold supply pressure, supply pressure

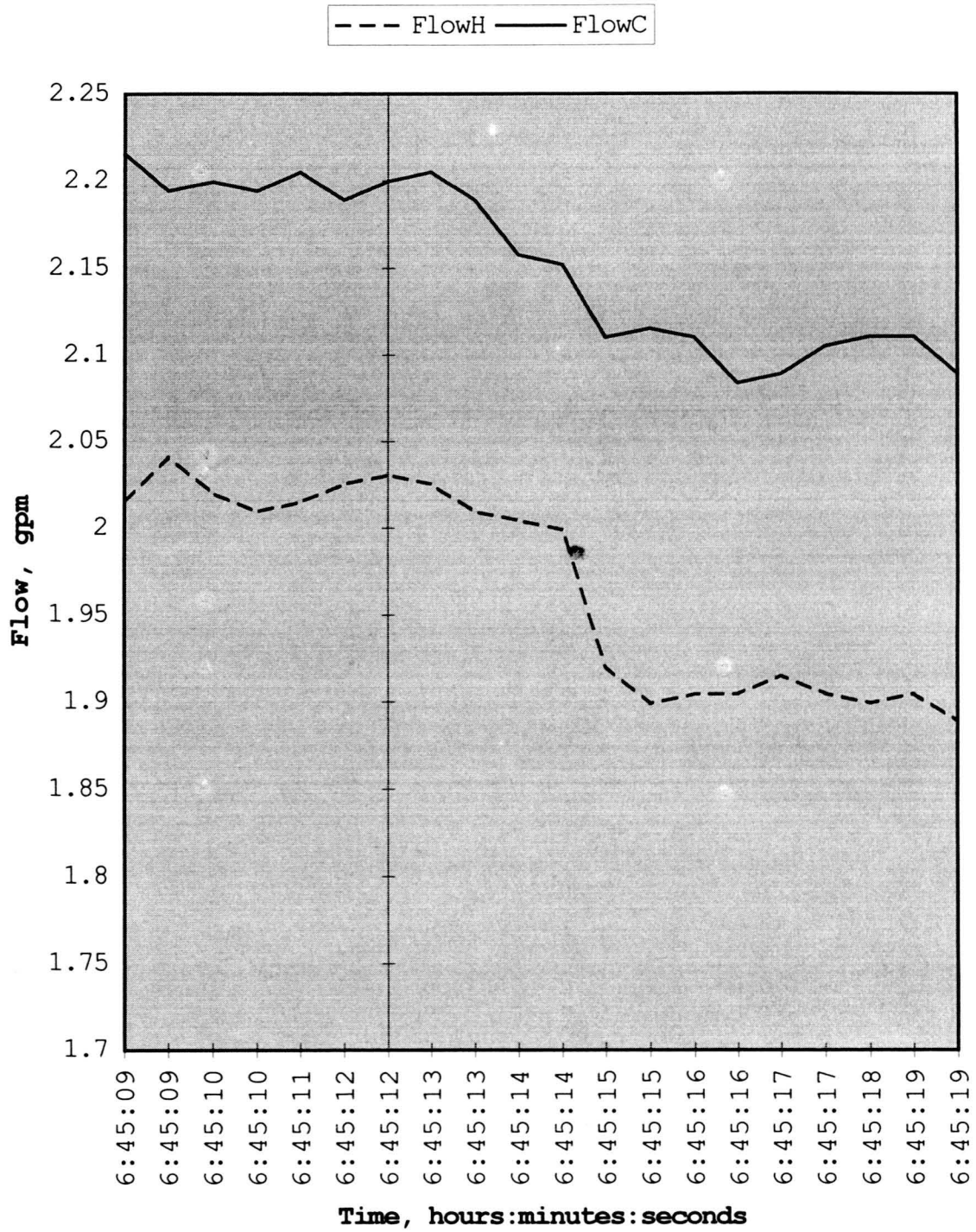


Figure 6.23: Pressure Valve test, decrease in cold supply pressure, supply flow rates

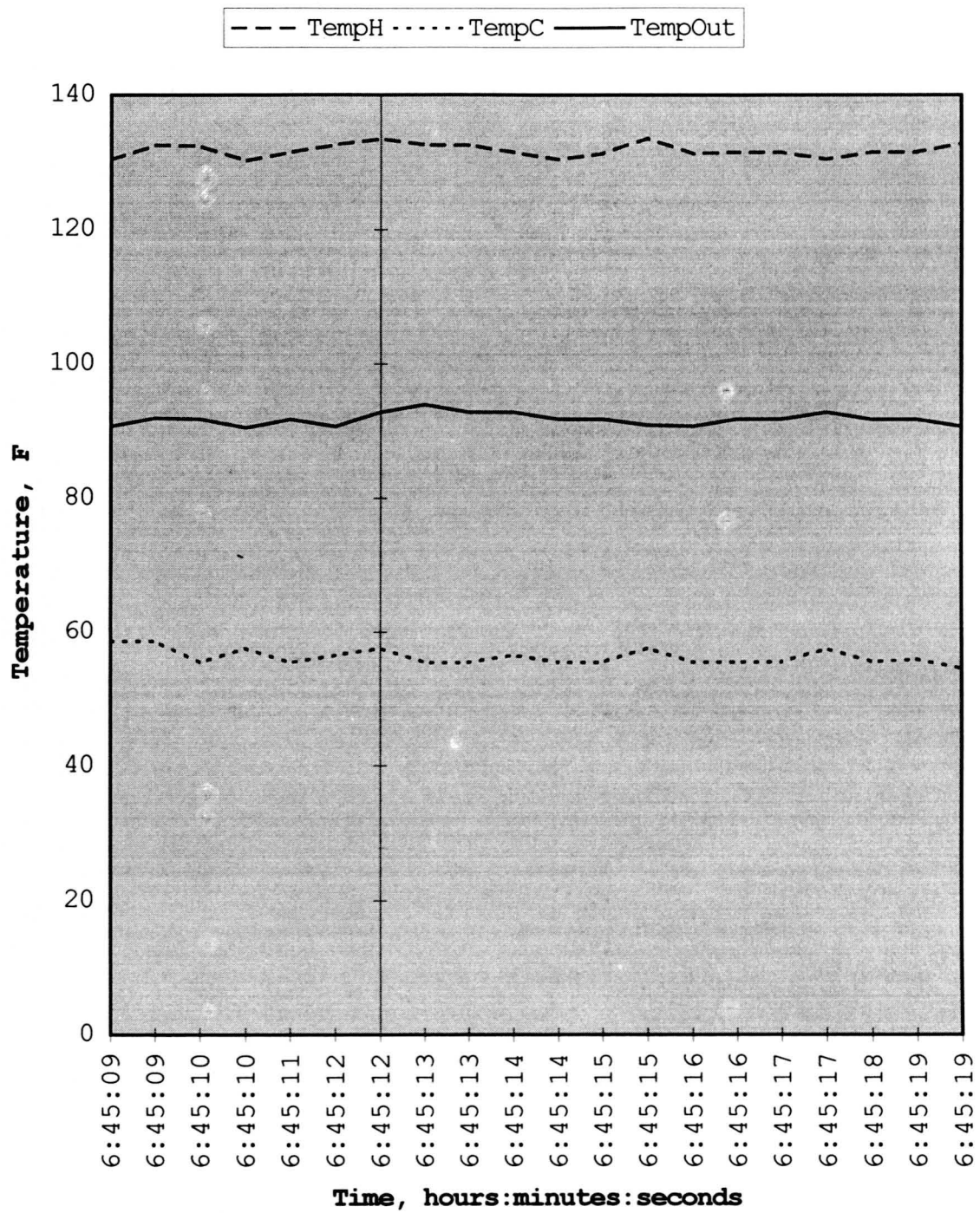


Figure 6.24: Pressure Valve test, decrease in cold supply pressure, supply and mix temperatures

The test pressure and temperature supplies will be used in the characteristic equations to evaluate the dynamic response of the valve. Given an initial set of steady state flow and pressure conditions, the cold water supply pressure is changed. Given the following at time $t < 0$:

$$P_c = 44 \text{ psi}$$

$$T_c = 55^\circ\text{F}$$

$$P_h = 44 \text{ psi}$$

$$T_h = 132^\circ\text{F}$$

$$P_o = 2.9 \text{ psi}$$

$$\theta = 84.4 \text{ degrees}$$

For steady state flow at time $t = 0$:

$$Q_c = [2*(P_c - P_o)/(\rho*\Psi_c)]^{0.5} \quad (6.45)$$

$$Q_c = 2.31 \text{ gpm}$$

$$P_{sc} = P_c - (Q_c^2*\rho*\Lambda_c/2) \quad (6.46)$$

$$P_{sc} = 25.2 \text{ psi}$$

Similarly for the hot supply flow:

$$Q_h = [2*(P_h - P_o)/(\rho*\Psi_h)]^{0.5} \quad (6.47)$$

$$Q_h = 2.31 \text{ gpm}$$

$$P_{sh} = P_h - Q_h^2*\rho*\Lambda_h/2 \quad (6.48)$$

$$P_{sh} = 25.2 \text{ psi}$$

For a sudden supply pressure drop (step function) in the cold supply flow, the previous equations for Q_c (6.27), Q_h (6.29), Q_m (6.31), P_{sc} (6.34), P_{sh} (6.37), and x'' (6.39) will be used as time

is incremented by 0.0005 seconds. A standard differential equation solver cannot be used since the common mix pressure is unknown and must be established through an iteration process. The following equations will be used to calculate the velocity and position of the spool.

$$x'(t+0.0005) = x'(t) + 0.0005 \cdot x''(t) \quad (6.49)$$

$$x(t+0.0005) = x(t) + 0.0005 \cdot [x'(t) + x'(t+0.0005)]/2 \quad (6.50)$$

The effects of friction on the movement of the spool are negligible when compared to the pressure differences on the spool; they were eliminated from the calculations. A damping coefficient of $0.45/M_s$ (where M_s is the mass of the spool) was used in the characteristic equations. A summary of the results from this modeling is listed in Table 6.3.

Spool position graphed as a function of time may be found in Figure 6.25, spool velocity is graphed in Figure 6.26, spool acceleration is graphed in Figure 6.27, mix temperature is graphed in Figure 6.28, spool pressure is graphed in Figure 6.29, and supply flow rates are graphed in Figure 6.30. This model shows that the dynamic response of the valve due to a change in pressure occurs in approximately 0.01 seconds. Figure 6.28 shows the valve reacts to level the fluctuation in mix temperature to less than 0.5 degrees in approximately 0.01 seconds.

Figure 6.31 graphs the test results and the model results of the mix temperature when the valve experiences a pressure drop in the cold supply. Fluctuations of $\pm 1.5^\circ\text{F}$ were consistently found with the test mix temperature. These fluctuations could be a result

of incomplete mixing of the hot and cold supply flows and could be a result of variations in the hot and cold water supply temperatures. Figure 6.32 is a comparison of the test results of the supply pressures and the supply pressures used in the modeling. Figure 6.33 is a comparison of the test and model supply flow rates.

Table 6.3 - Pressure Valve Response, Cold Supply Pressure Drop

Tc = 50°F, Th = 160°F

| Time (sec) | x'' (ft/s ²) | x' (ft/s) | x (inch) | Qc (gpm) | Psc (psi) | Qh (gpm) | Psh (psi) | Qm (gpm) | Tm (F) |
|---------------|-----------------------------|--------------|-------------|-------------|--------------|-------------|--------------|-------------|-----------|
| -0.0005 | 0 | 0.000 | 0.0000 | 2.31 | 25.2 | 2.31 | 25.2 | 4.62 | 93.5 |
| 0.0000 | 437 | 0.000 | 0.0000 | 2.14 | 22.6 | 2.33 | 24.8 | 4.47 | 95.2 |
| 0.0005 | 341 | 0.219 | 0.0007 | 2.14 | 22.6 | 2.33 | 24.9 | 4.46 | 95.1 |
| 0.0010 | 239 | 0.389 | 0.0025 | 2.15 | 22.8 | 2.33 | 24.6 | 4.48 | 95.0 |
| 0.0015 | 136 | 0.509 | 0.0050 | 2.16 | 22.8 | 2.31 | 24.5 | 4.47 | 94.8 |
| 0.0020 | 40 | 0.577 | 0.0084 | 2.17 | 22.9 | 2.30 | 24.2 | 4.47 | 94.6 |
| 0.0025 | -51 | 0.597 | 0.0120 | 2.17 | 23.1 | 2.28 | 24.1 | 4.51 | 94.4 |
| 0.0030 | -150 | 0.571 | 0.0155 | 2.18 | 23.5 | 2.26 | 23.8 | 4.43 | 94.2 |
| 0.0035 | -213 | 0.496 | 0.0187 | 2.18 | 23.7 | 2.24 | 23.6 | 4.42 | 94.0 |
| 0.0040 | -250 | 0.390 | 0.0213 | 2.19 | 23.8 | 2.23 | 23.2 | 4.41 | 93.8 |
| 0.0045 | -262 | 0.265 | 0.0233 | 2.19 | 23.8 | 2.22 | 22.9 | 4.41 | 93.7 |
| 0.0050 | -251 | 0.134 | 0.0245 | 2.20 | 23.9 | 2.21 | 22.8 | 4.41 | 93.6 |
| 0.0055 | -219 | 0.008 | 0.0249 | 2.20 | 23.8 | 2.21 | 22.7 | 4.41 | 93.6 |
| 0.0060 | -169 | -0.101 | 0.0246 | 2.20 | 23.8 | 2.21 | 22.7 | 4.41 | 93.6 |
| 0.0065 | -110 | -0.186 | 0.0238 | 2.20 | 23.7 | 2.22 | 22.8 | 4.41 | 93.7 |
| 0.0070 | -53 | -0.241 | 0.0225 | 2.20 | 23.7 | 2.23 | 23.0 | 4.42 | 93.8 |
| 0.0075 | 0 | -0.267 | 0.0210 | 2.19 | 23.6 | 2.24 | 23.1 | 4.43 | 93.9 |
| 0.0080 | 48 | -0.267 | 0.0194 | 2.19 | 23.5 | 2.24 | 23.3 | 4.43 | 94.0 |
| 0.0085 | 83 | -0.243 | 0.0178 | 2.19 | 23.5 | 2.25 | 23.4 | 4.44 | 94.1 |
| 0.0090 | 107 | -0.201 | 0.0165 | 2.18 | 23.4 | 2.26 | 23.6 | 4.44 | 94.2 |
| 0.0095 | 116 | -0.148 | 0.0155 | 2.18 | 23.4 | 2.26 | 23.7 | 4.45 | 94.2 |
| 0.0100 | 116 | -0.090 | 0.0147 | 2.18 | 23.3 | 2.27 | 23.8 | 4.44 | 94.3 |
| 0.0105 | 104 | -0.032 | 0.0144 | 2.18 | 23.3 | 2.27 | 23.8 | 4.44 | 94.3 |
| 0.0110 | 86 | 0.020 | 0.0143 | 2.18 | 23.3 | 2.27 | 23.8 | 4.44 | 94.3 |
| 0.0115 | 63 | 0.064 | 0.0146 | 2.18 | 23.4 | 2.27 | 23.8 | 4.44 | 94.3 |
| 0.0120 | 38 | 0.095 | 0.0151 | 2.18 | 23.4 | 2.26 | 23.8 | 4.44 | 94.3 |

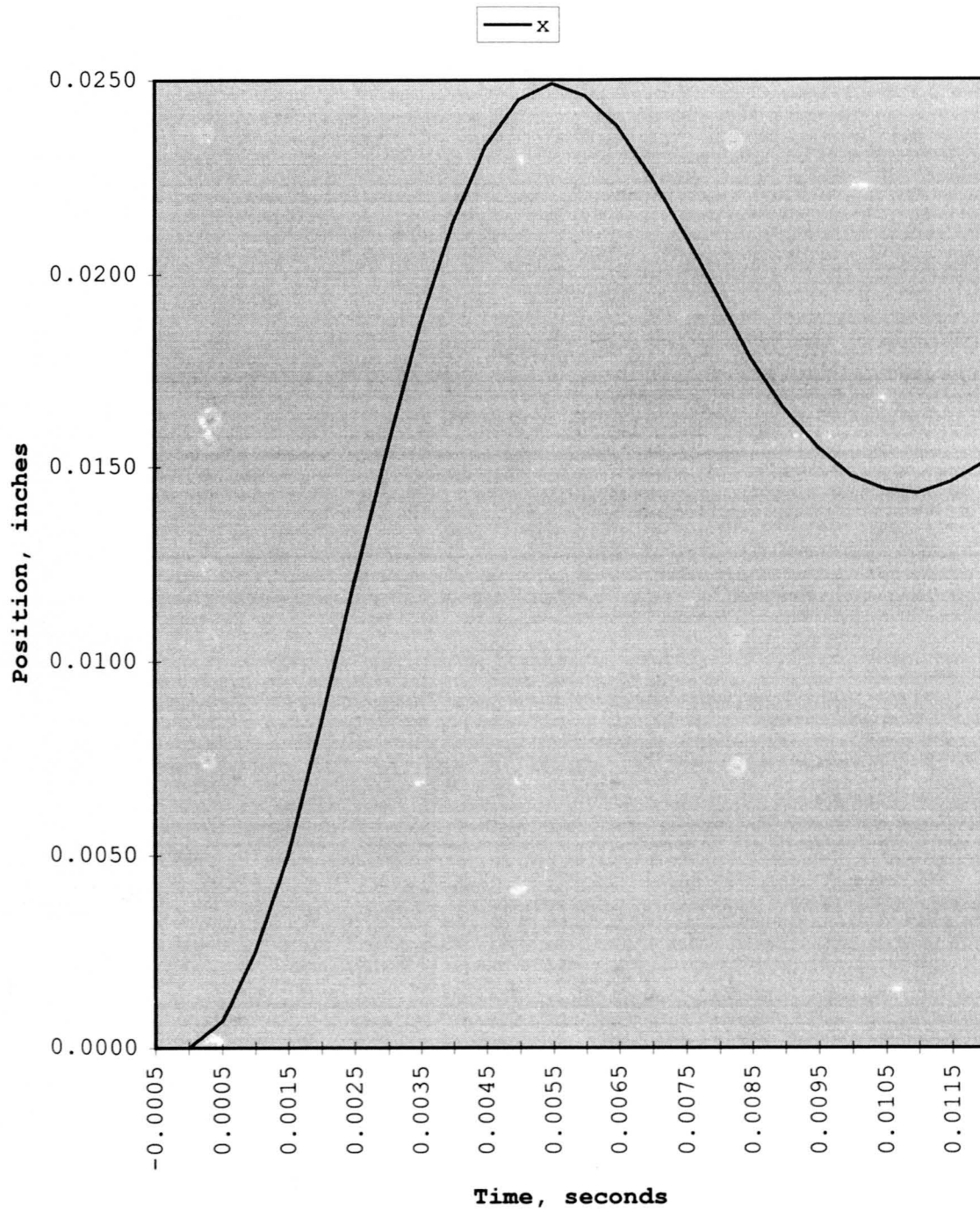


Figure 6.25: Pressure valve model, decrease in cold supply pressure, spool position

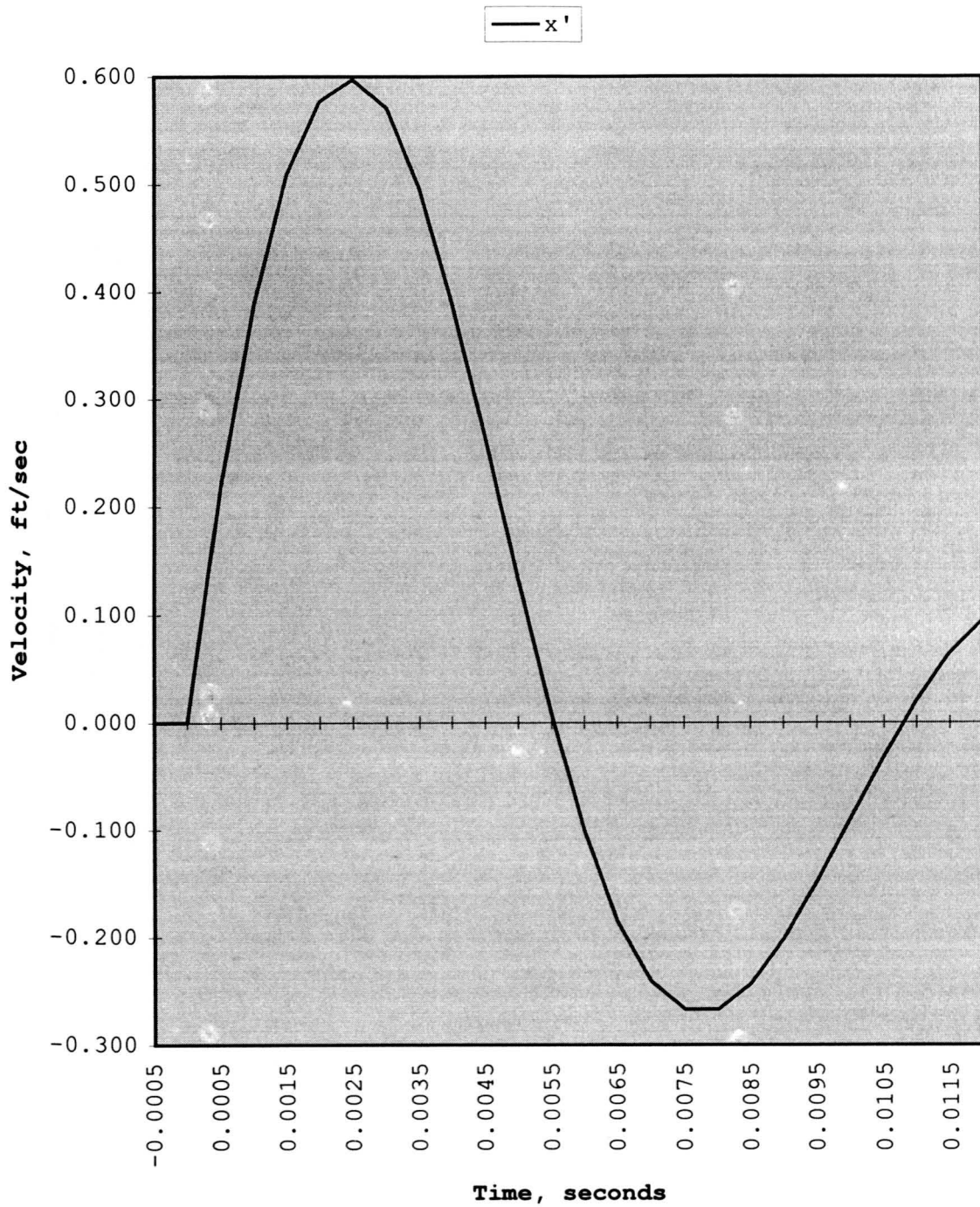


Figure 6.26: Pressure valve response, decrease in cold supply pressure, spool velocity

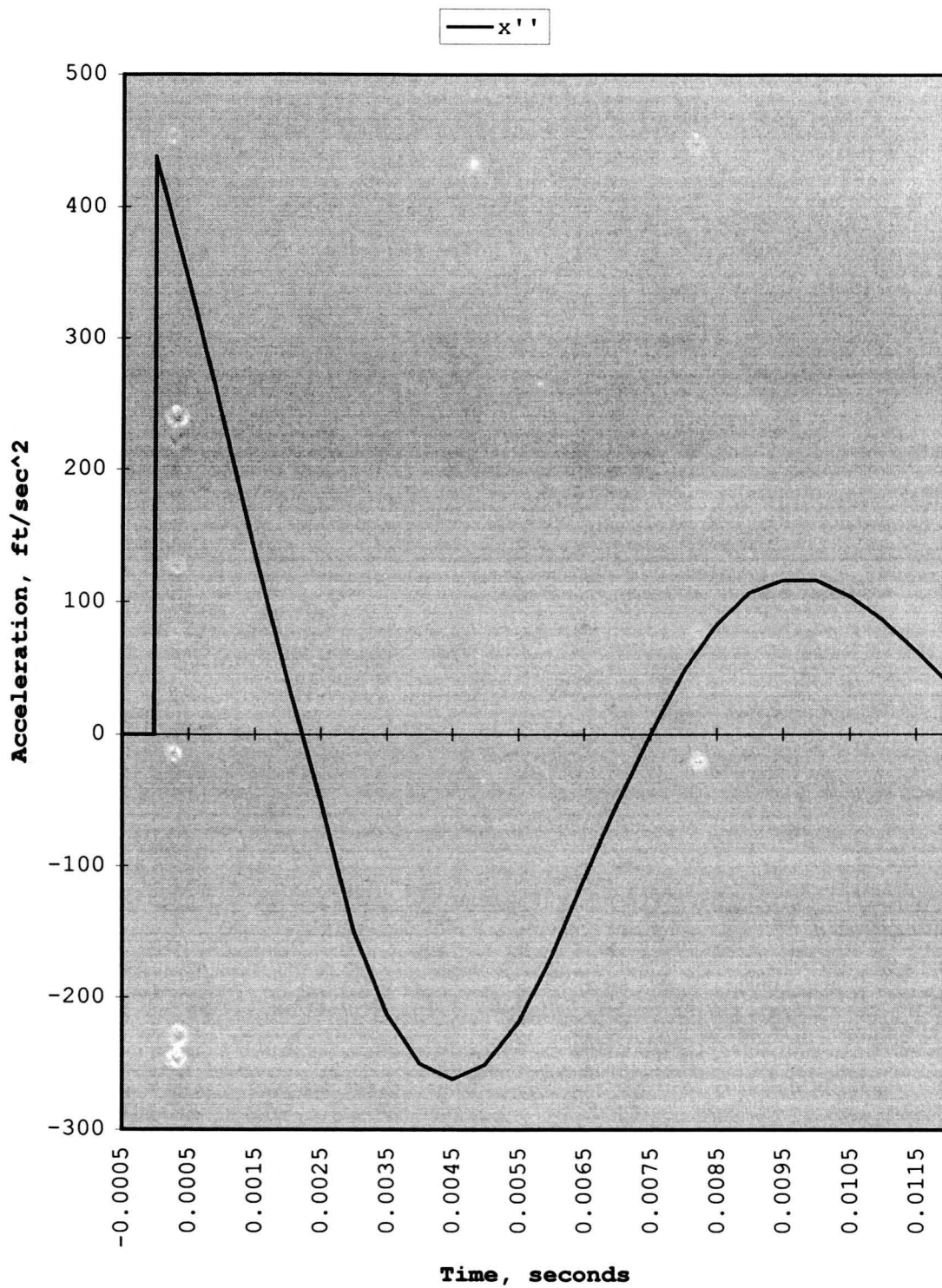


Figure 6.27: Pressure valve response, decrease in cold supply pressure, spool acceleration

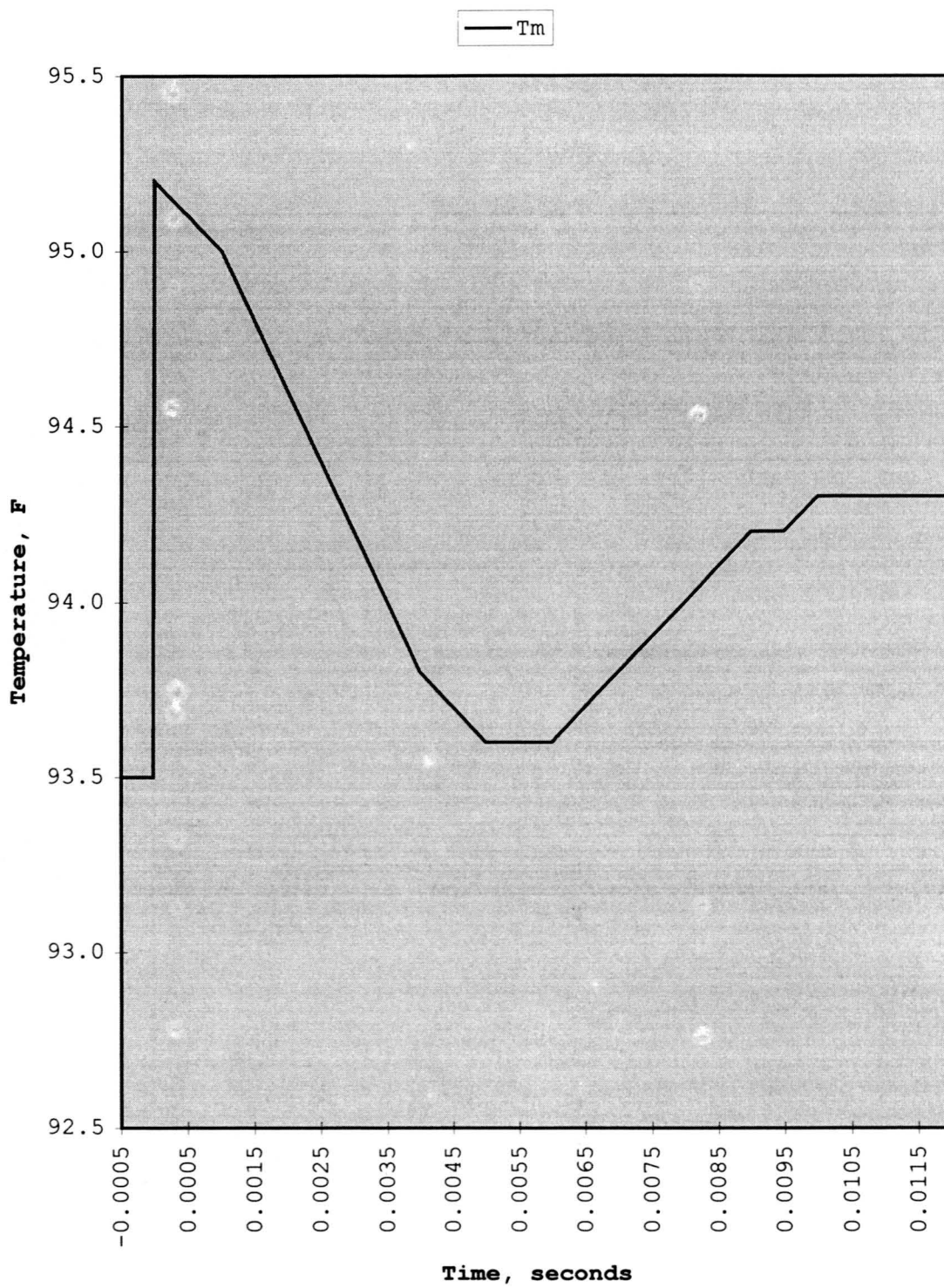


Figure 6.28: Pressure valve response, decrease in cold supply pressure, mix temperature

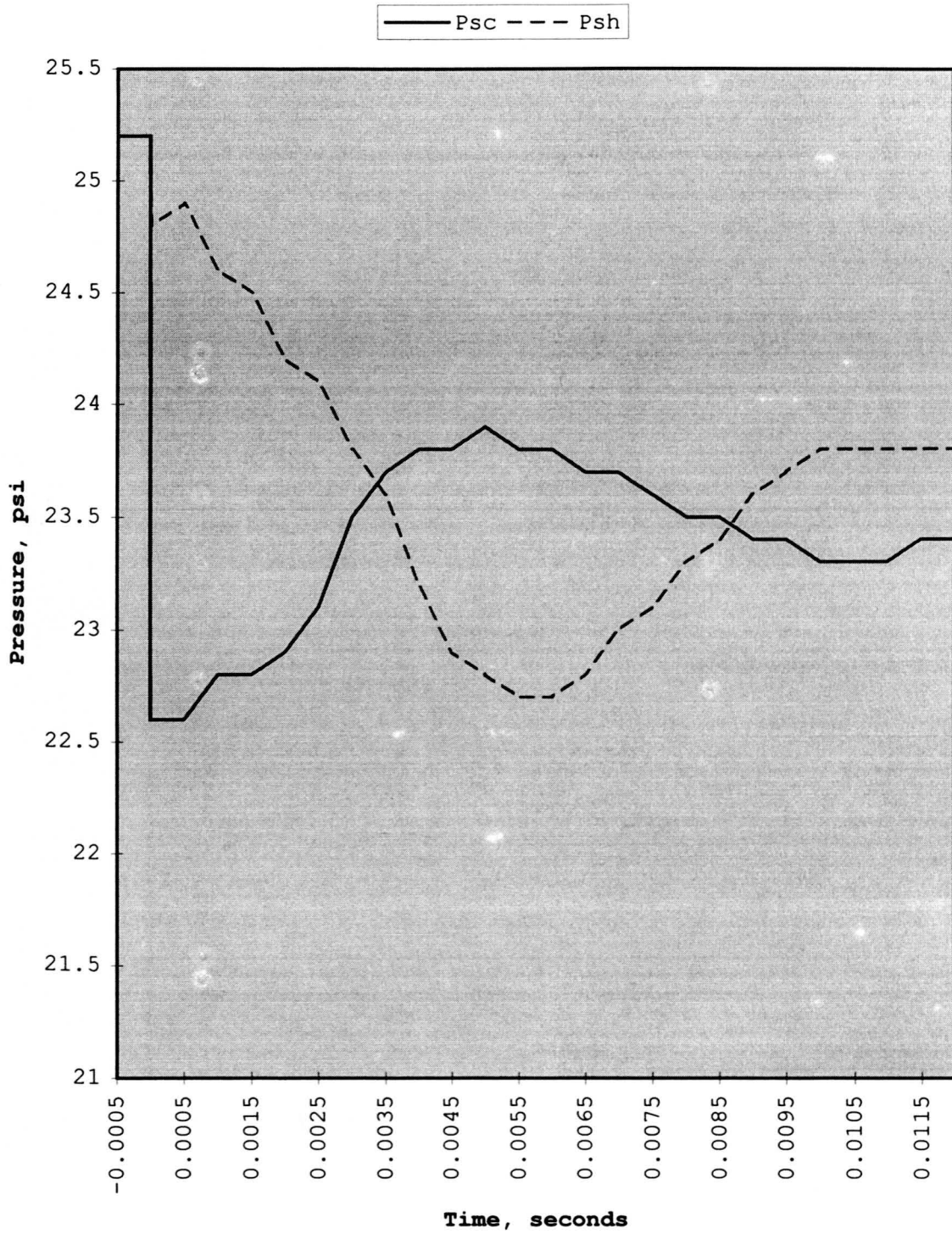


Figure 6.29: Pressure valve response, decrease in cold supply pressure, spool pressure

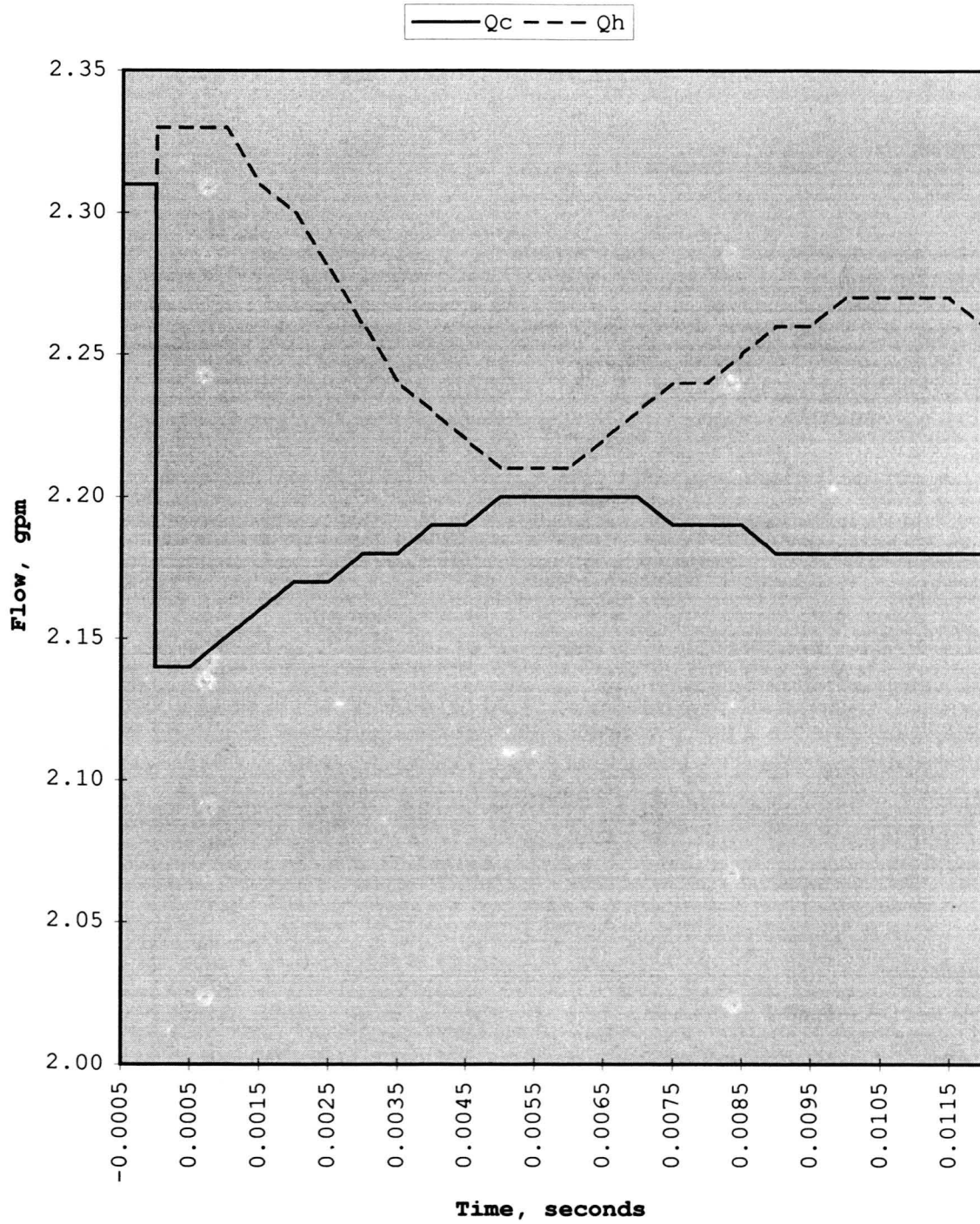


Figure 6.30: Pressure valve response, decrease in cold supply pressure, supply flow rates

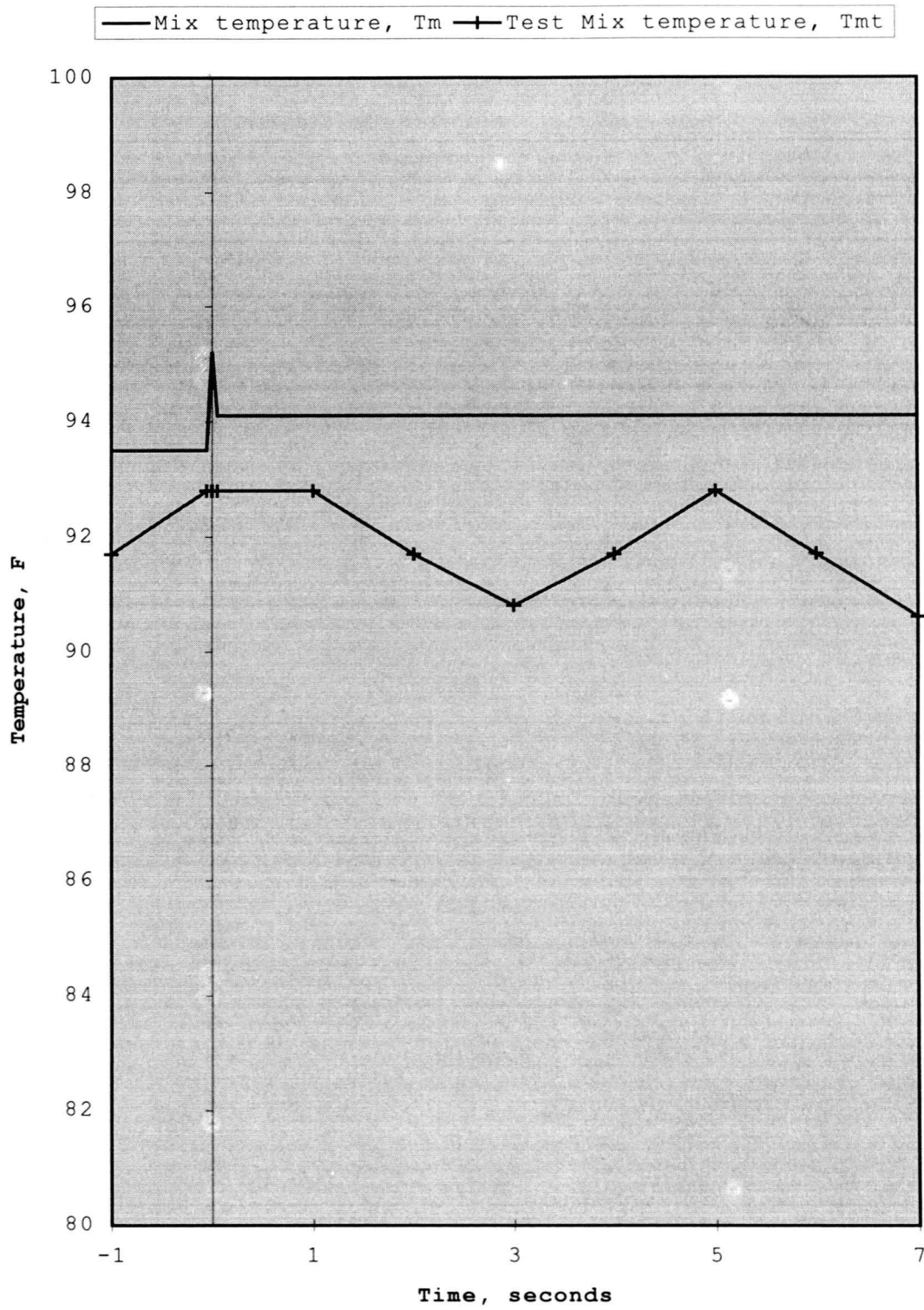


Figure 6.31: Pressure balance valve test and model, cold supply pressure decrease, mix temperature

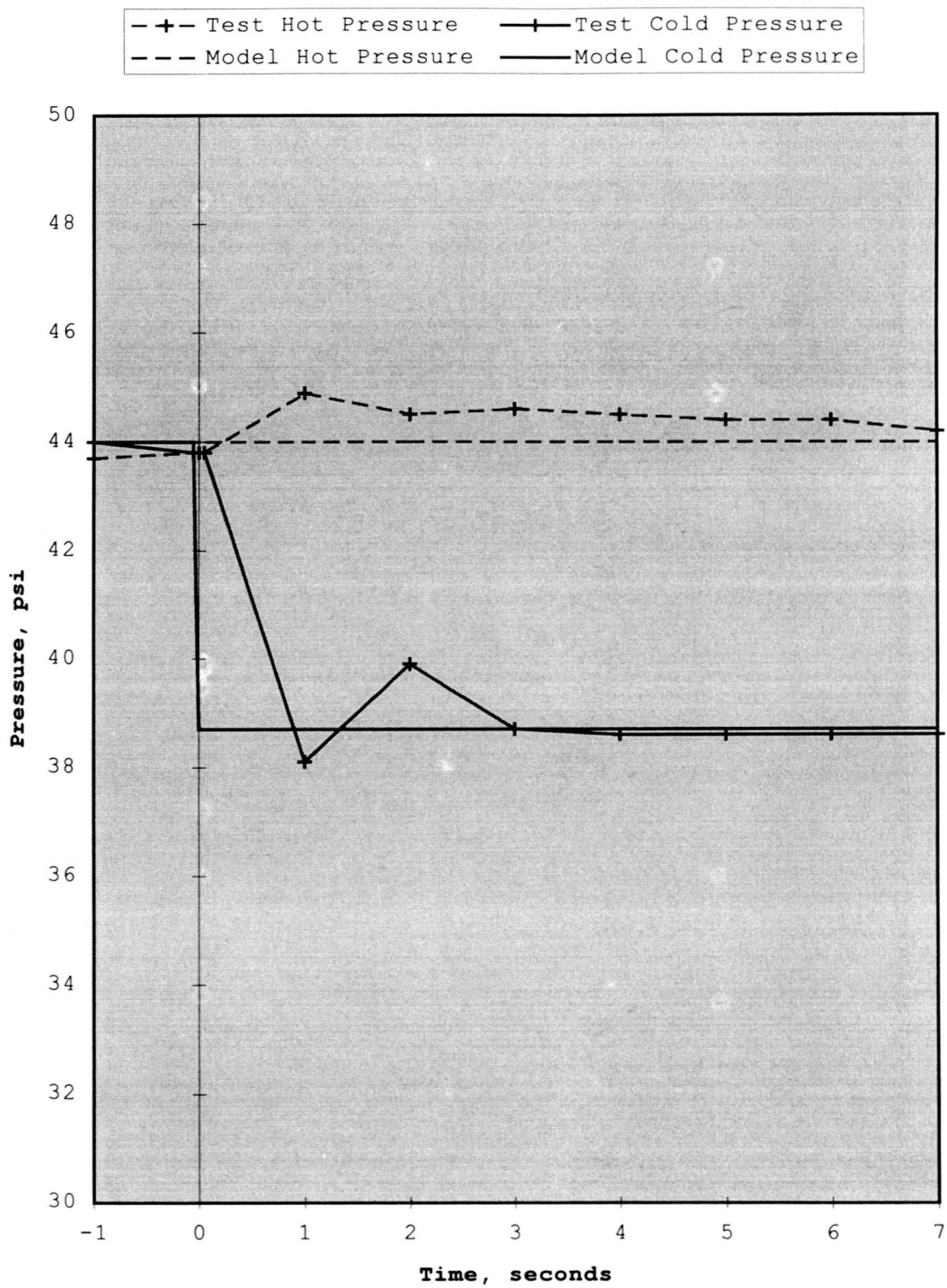


Figure 6.32: Pressure balance valve test and model, cold supply pressure decrease, supply pressure

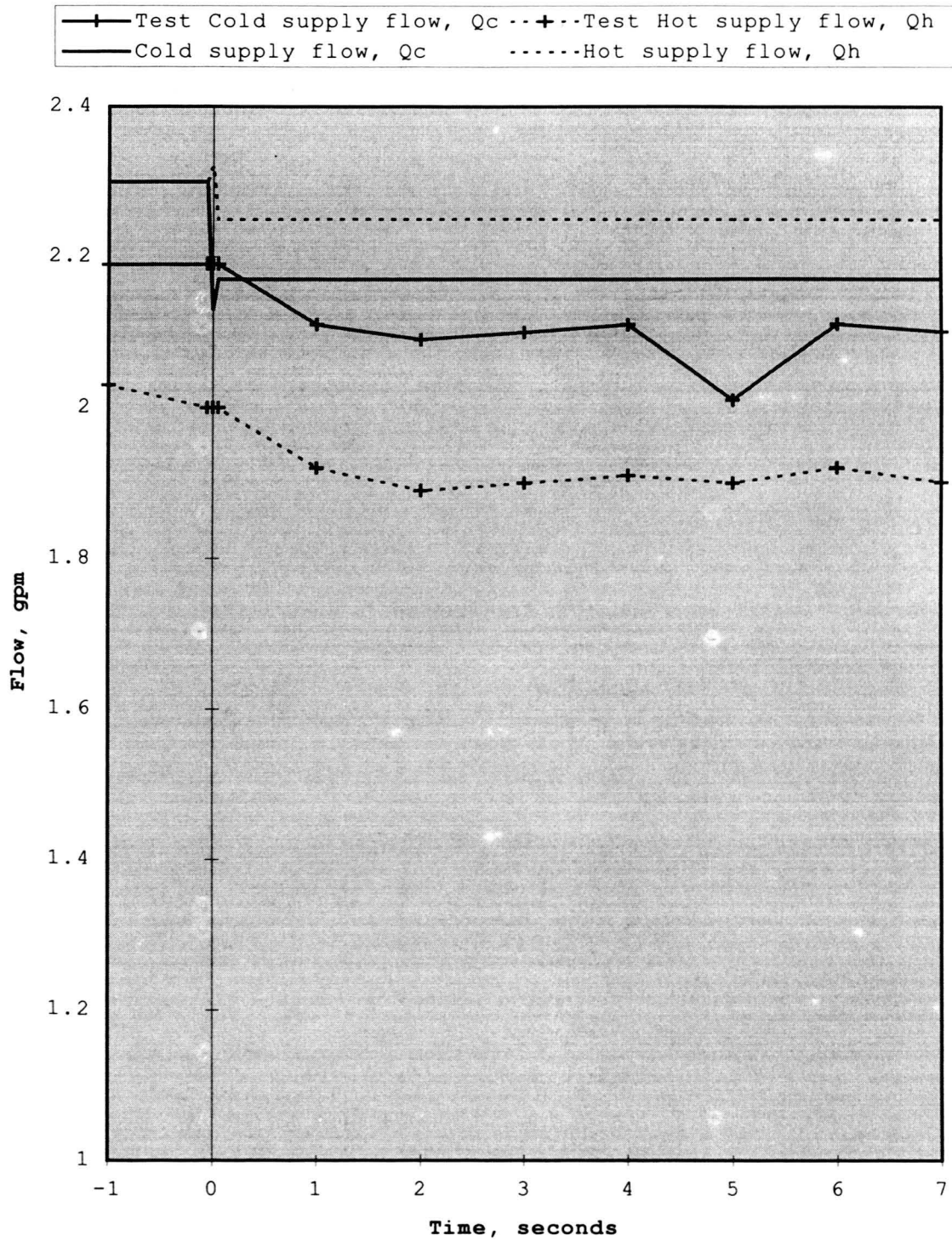


Figure 6.33: Pressure balance valve test and model, cold supply pressure decrease, supply flow

CHAPTER 7. TEMPERING VALVES

Tempering valves are designed to be installed near the water heater and are intended to maintain a constant mix temperature as fluctuations occur in system pressure and temperature. The valve is typically installed on the output line of the water heater and has a cold supply line. This line allows cold water to be added to the hot water supply, thus tempering the mix that is delivered for use. This type of valve is not intended to be used at various points of use, but typically tempers water that is delivered to several points of use.

Periodic inspection of the valve by a licensed contractor is recommended to ensure the valve is maintained and operating properly. Corrosive water conditions, temperatures over 210°F, unauthorized adjustments or repairs can render the valve ineffective for the type of service intended. Regular cleaning and checking of the thermostat assembly are required to obtain proper function and maximum life of this type of valve.

Valve Design

A commercially available tempering valve was obtained which would allow the user to adjust a dial thus adjusting the output mix

temperature. A label on the dial instructs the user to turn the dial counterclockwise to adjust the temperature of the mix towards 130°F, and to turn the dial clockwise to adjust the temperature of the mix towards 100°F. There were no hot supply water temperature requirements, ranges, or limits listed in the installation instructions for the valve. A minimum flow requirement of 2 gallons per minute was outlined to maintain a set mix temperature.

Figure 7.1 is a cross sectional view of the tempering valve. The key components of the valve assembly are: 1) a valve body having hot and cold supply inlets and a mix output , 2) a thermostat assembly, 3) a bonnet assembly, and 4) a poppet valve.

Hot and cold three quarter inch supply lines are attached to the valve body and enter the valve as shown in Figure 7.2 ("H" & "C"). A three quarter inch mix output line ("M") is also attached to the valve body. Hot supply water enters the valve and passes through an orifice ("A") to the mixing chamber. In this chamber there is a thermostat assembly that reacts to the temperature of the mix of hot and cold water. When the temperature of the thermostat assembly increases, fluid inside the thermostat ("B") expands. The expansion of the fluid forces a pin out of the thermostat assembly against the poppet valve. As the poppet valve opens, the orifice area increases and cold supply flow increases. As the temperature of the thermostat assembly continues to increase, the pin continues to extend, the poppet valve continues to open and the flow of cold supply water increases. As the temperature of the mix decreases, the fluid in the thermostat contracts, the thermostat pin retracts

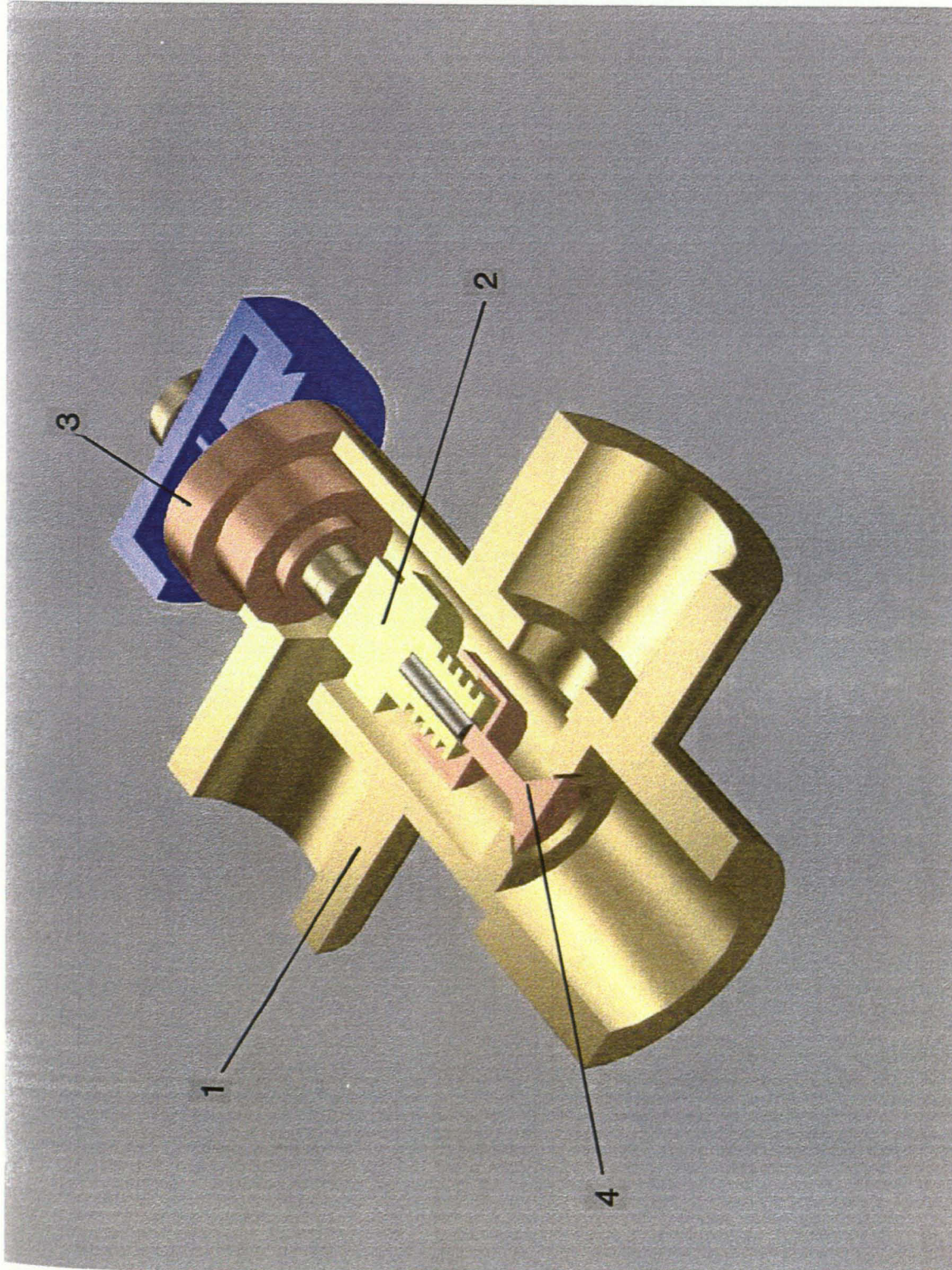


Figure 7.1: Cross section view of tempering valve

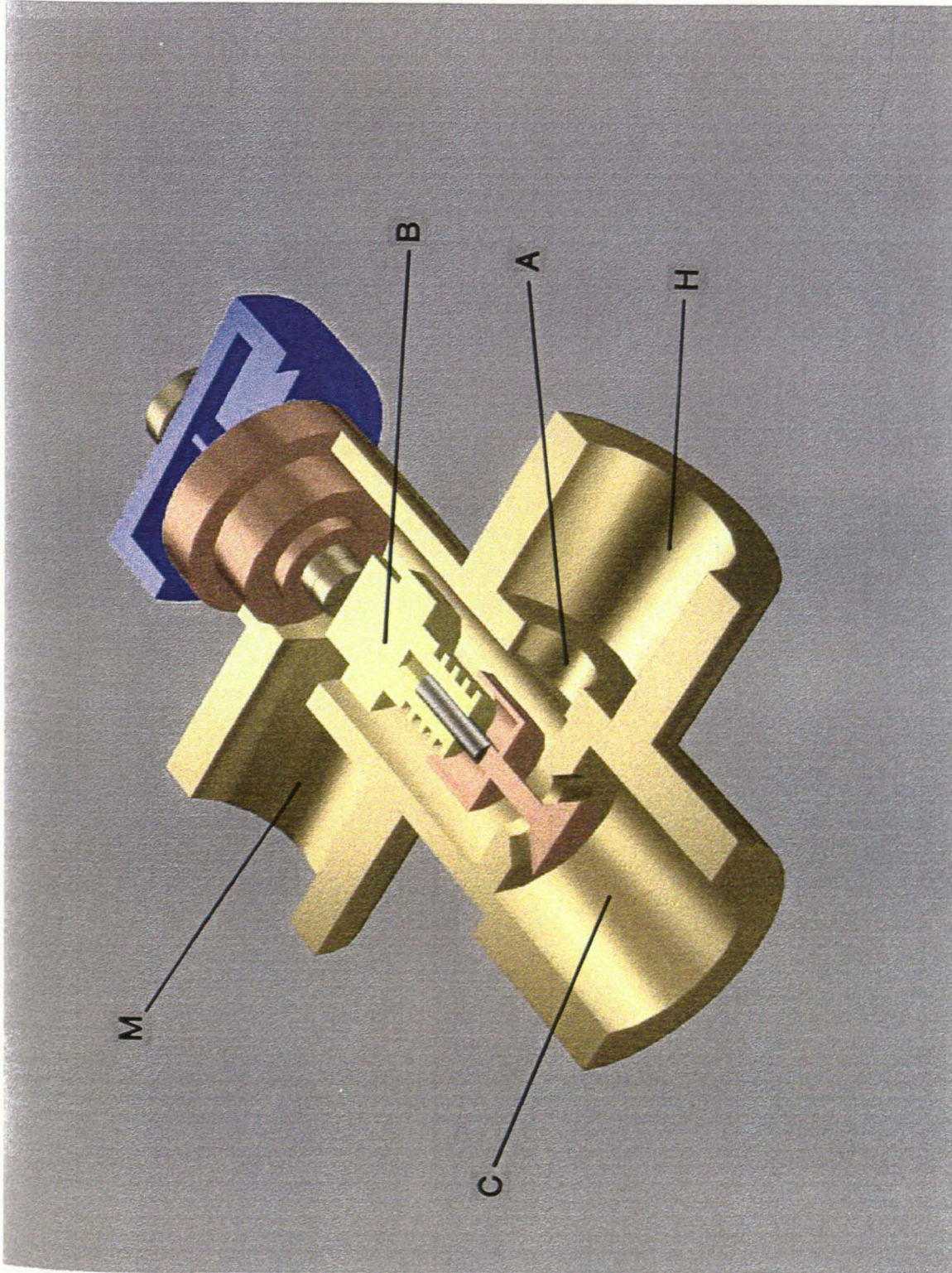


Figure 7.2: Cross section view of tempering valve

and the poppet valves closes; this decreases the flow of the cold supply water.

The bonnet assembly has a dial which allows the user to adjust the mixing valve. The bonnet assembly has a stop which allows the dial to be rotated a total of 360 degrees. Rotation of the dial adjusts the position of the thermostat assembly in the tempering valve. This affects the temperature at which the thermostat will start to open the poppet valve for the cold supply flow. Turning the dial counterclockwise moves the thermostat assembly away from the poppet valve and will result in raising the maximum mix temperature. Turning the dial clockwise moves the thermostat assembly towards the poppet valve and will result in lowering the maximum mix temperature. The dial will adjust the thermostat a total stroke of 0.110 inch relative to the poppet valve.

System Modeling

Once again, assuming incompressible flow, the orifice equation will be used to define the flow across the orifices. Since the minimum flow requirements for proper operation of the valve are 2 gallons per minute, the Reynolds Number for the upstream flow is sufficiently high to allow the use of a constant orifice coefficient. For the hot supply flow the orifice coefficient is approximately 0.68, and for the cold supply flow the orifice coefficient is approximately 0.59. The difference in the orifice coefficients is due to the size of the hot orifice being larger than

the cold orifice when compared to each supply pipe diameter. The mixing chamber has an orifice to the output mix line. The orifice coefficient for the exit of the mixing chamber is approximately 0.72

The model of the valve will have one orifice for the hot supply flow and one orifice for the cold supply flow. There will be pressure head loss through the mixing chamber that will need to be evaluated experimentally.

The thermostat assembly of the tempering valve was removed to characterize its operation. The thermostat was placed in water at various temperatures, and the total length of the assembly was recorded. Table 7.1 summarizes the results.

Table 7.1: Thermostat length as a function of temperature

| | | | | | | |
|------------------|-------|-------|-------|-------|-------|-------|
| Temperature (°F) | 126 | 135 | 147 | 173 | 190 | 212 |
| Length (inches) | 1.120 | 1.125 | 1.140 | 1.165 | 1.175 | 1.190 |

Hogben [1987] defines a methodology for calculating a least squares approximation for data defined by a linear equation. Assuming that the relationship of the thermostat length is a linear function of temperature, the data is characterized by an equation using a least squares data fit. The equation for the length of the thermostat assembly is:

$$L = 1.105 + 0.000842 \cdot T_s \quad (7.1)$$

where:

L = Length of the thermostat assembly, inches

T_s = Temperature of the thermostat

Figure 7.3 is a plot of the raw data and the characteristic equation from the least squares data fit.

The thermostat assembly was placed in a hot water bath at various temperatures. The length of the assembly was measured as a function of time. The initial thermostat temperature and bath water temperature were recorded. Table 7.2 summarizes the results.

Table 7.2: Thermostat Length as a Function of Time and ΔT

| | | | | | | |
|------------------------|------------------|------|------|------|------|-------|
| L_o^1 = 0.975 inches | L_f^2 = 1.175 | | | | | |
| T_o^3 = 95 °F | T_f^4 = 190 °F | | | | | |
| Time (seconds) | 0 | 3 | 6 | 11 | 21 | 50 |
| Length (inches) | 0.975 | 1.00 | 1.05 | 1.10 | 1.15 | 1.173 |

¹ L_o = Initial thermostat length, inches

² L_f = Final thermostat length, inches

³ T_o = Initial thermostat temperature, °F

⁴ T_f = Final thermostat temperature, °F

Karlekar and Desmond [1977] define a class of transient heat transfer problems that lend themselves most readily to analysis as being those with negligible internal resistance to the flow of heat. In such problems, the convective resistance at the system boundary is very large when compared to the internal resistance due

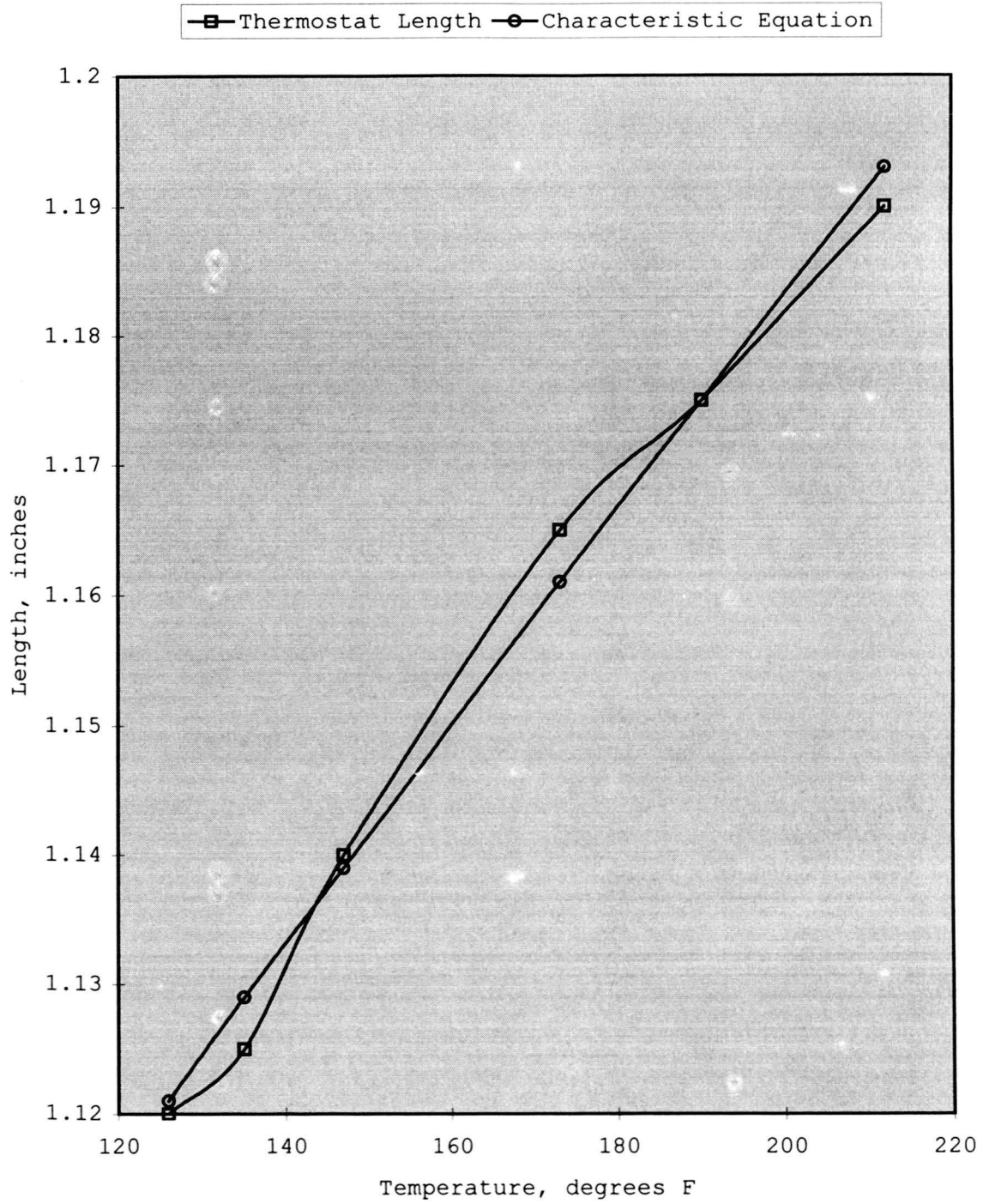


Figure 7.3: Thermostat length as a function of temperature, test and model

to conduction. The solid behaves as though it has an infinite thermal conductivity in that the temperature through the entire solid is always uniform and varies only with time. With such systems the following equation characterizes the temperature of the solid:

$$T = T_f - (T_f - T_o) * e^{-k*t} \quad (7.2)$$

where:

T = Temperature of the body, °F

T_f = Temperature of the convective environment, °F

T_o = Initial temperature of the body, °F

k = Time constant of the system, 1/sec

t = Time, sec

Rearranging this equation and taking the natural log of both sides will give a linear relationship between the variables. Using a least squares approximation for data defined by a linear equation gives the following relationship:

$$L = L_f - (L_f - L_o) * e^{-.093*t} \quad (7.3)$$

where:

L = Length of the thermostat assembly, inches

L_f = Length of the thermostat at the convective environment temperature, inches

L_o = Initial length of thermostat, inches

t = time exposed to the convective environment, seconds

Figure 7.4 plots the raw data and the resulting equation from the least squares data fit with L_f = 1.175 inch and L_o = 0.975 inch.

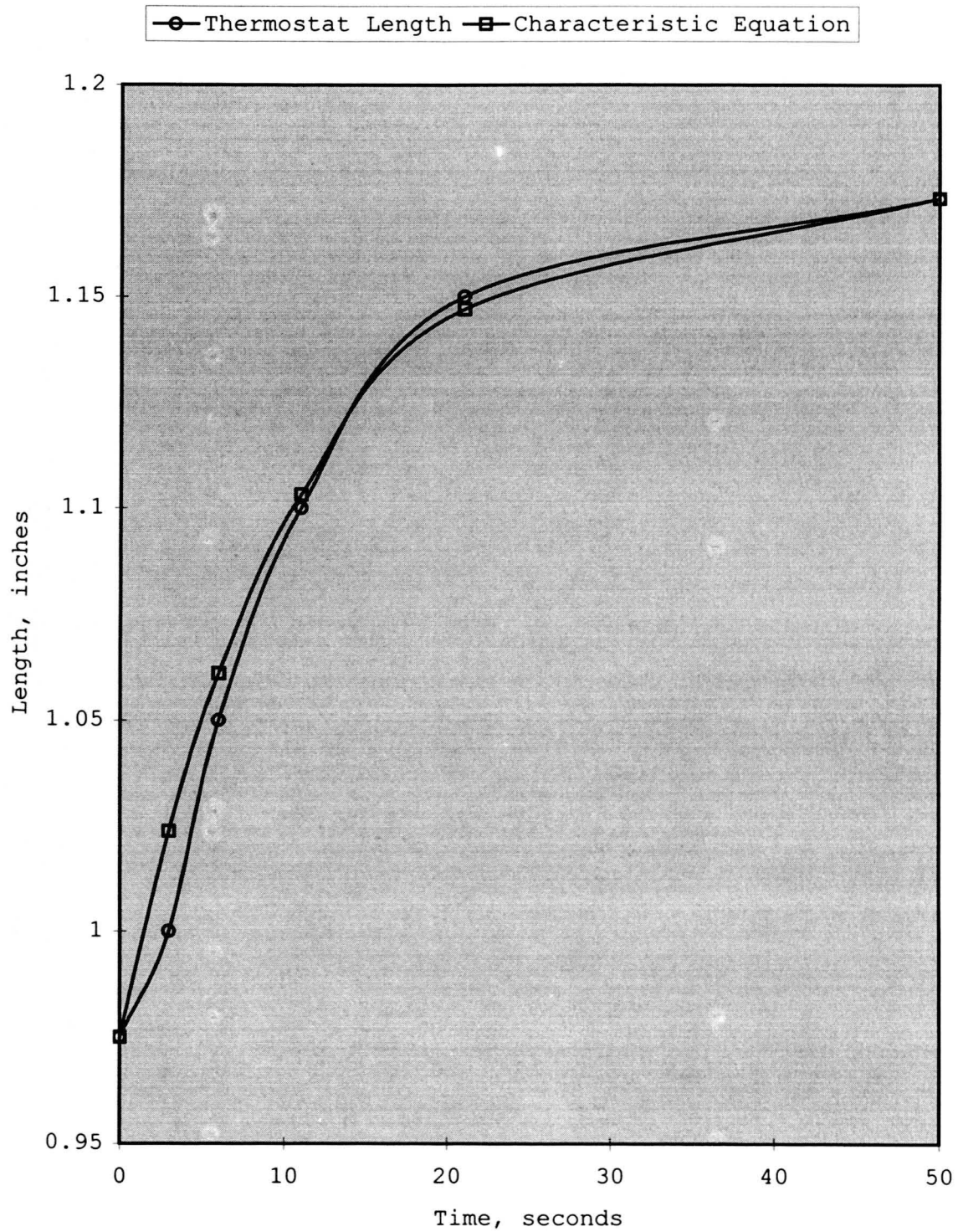


Figure 7.4: Thermostat response when exposed to hot water bath, test and model

Measuring the physical dimensions of the valve, the poppet valve and the bonnet assembly, the following relationship was developed to describe the distance the poppet valve is moved axially from the valve seat:

$$D_s = L_t + B_e - 1.113 \quad (7.4)$$

where:

D_s = Distance poppet valve removed from valve seat, inch

L_t = Length of the thermostat, inches

B_e = Bonnet extension, inches

The distance the poppet valve is removed from the valve seat is a function of thermostat temperature and of the bonnet extension. The bonnet extension is defined by the following:

$$B_e = \frac{0.11 * \theta}{2 * 180} \quad (7.5)$$

where:

B_e = Bonnet extension, inches

θ = Position of bonnet dial, degrees

The distance the poppet valve is from the valve seat is graphed as a function of mix temperature at various bonnet dial positions in Figure 7.5. The convention for the position of the bonnet dial is when $\theta = 0$, the dial is turned completely counterclockwise (at the 130°F mark).

The flow equation for the hot water supply for the tempering valve is the following:

$$Q_h = [2(P_h - P_{cc}) / \rho]^{0.5} * [1 / (C_h * A_h)^2]^{-0.5} \quad (7.6)$$

where:

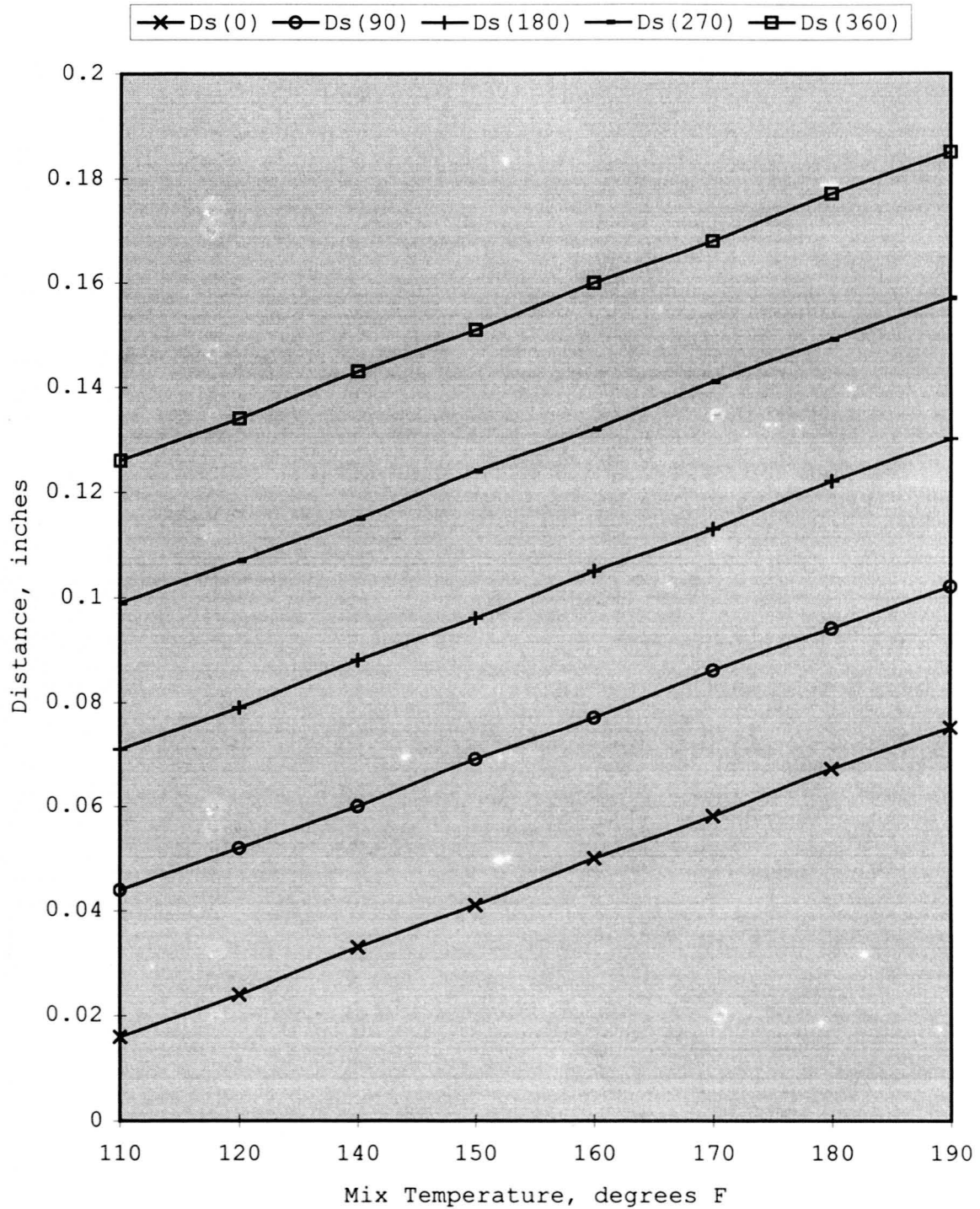


Figure 7.5: Poppet valve extension (Ds) as a function of thermostat temperature, model equation (7.4)

Q_h = Hot supply flow rate, ft^3/sec

P_h = Hot supply pressure, psf

P_{cc} = Common cavity mix pressure, psf

C_h = Hot supply orifice coefficient

A_h = Hot supply orifice area, ft^2

The flow equation for the cold water supply for the tempering valve is the following:

$$Q_c = [2(P_c - P_{cc})/\rho]^{0.5} * [1/(C_c * A_c)^2]^{-0.5} \quad (7.7)$$

where:

Q_c = Cold supply flow rate, ft^3/sec

P_c = Cold supply pressure, psf

P_{cc} = Common cavity mix pressure, psf

C_c = Cold supply orifice coefficient

A_c = Cold supply orifice area, ft^2

The mix flow out of the valve mixing cavity and into the outlet pipe is:

$$Q_m = [2(P_{cc} - P_m)/\rho]^{0.5} * [1/(C_o * A_o)^2]^{-0.5} \quad (7.8)$$

where:

Q_m = Mix flow rate, ft^3/sec

P_{cc} = Common cavity mix pressure, psf

P_m = Mix pressure, psf

C_o = Mix orifice coefficient

A_o = Mix orifice area, ft^2

The area of the cold supply orifice is the following:

$$A_c = \pi \left\{ \left(\frac{d_p}{2} \right)^2 - \left[\left(\frac{d_p}{2} \right) - D_s \right]^2 \right\} \quad (7.9)$$

where:

A_c = Orifice area, ft^2

d_p = Poppet valve diameter, ft

D_s = Poppet Valve distance from valve seat, ft

To calculate the steady state flow conditions using the characteristic equations, an iterative approach is required. An estimate is made of the pressure of the common mixing cavity (P_{cc}) and of the thermostat temperature (T_s). Flow calculations of the hot water supply, cold water supply and the mix output are calculated using equations 7.6, 7.7 and 7.8. Based on the supply and mix flows, the estimated pressure in the common mixing cavity (P_{cc}) may be updated. If the mix flow is lower than the combination of the hot and cold supply flow, P_{cc} is increased. If the mix flow is higher than the combination of the hot and cold supply flow, P_{cc} is decreased. The mix temperature is based upon the following relationship which was established in Chapter 6:

$$T_m = \frac{Q_c \cdot T_c + Q_h \cdot T_h}{Q_m} \quad (7.10)$$

The thermostat temperature is then compared to the mix temperature. If the thermostat temperature is higher than the mix temperature, the thermostat temperature is lowered. If the thermostat temperature is lower than the mix temperature, the thermostat temperature is raised. This process is repeated until the hot and

cold supply flow rates are equal to the mix flow rate and the thermostat temperature is equal to the mix temperature.

The following a solution for the valve given an initial set of steady state flow and pressure conditions. Given the following at $t < 0$:

$$P_c = 50 \text{ psi}$$

$$T_c = 50 \text{ }^\circ\text{F}$$

$$P_h = 50 \text{ psi}$$

$$T_h = 160 \text{ }^\circ\text{F}$$

$$P_{cc} = 49 \text{ psi}$$

$$P_m = 48 \text{ psi}$$

$$\theta = 360 \text{ degrees}$$

For steady state flow at time $t = 0$ the hot supply flow is:

$$Q_h = [2 * (P_h - P_{cc}) / \rho]^{0.5} * [1 / (C_h * A_h)^2]^{-0.5}$$

$$Q_h = 4.10 \text{ gpm}$$

Similarly for the cold supply flow:

$$Q_c = [2 * (P_c - P_{cc}) / \rho]^{0.5} * [1 / (C_c * A_c)^2]^{-0.5}$$

$$Q_c = 0.71 \text{ gpm}$$

For the mix flow:

$$Q_m = [2 * (P_{cc} - P_m) / \rho]^{0.5} * [1 / (C_o * A_o)^2]^{-0.5}$$

$$Q_m = 4.83 \text{ gpm}$$

Figure 7.6 graphs the cold supply flow as a function of the thermostat temperature; flow curves for θ equal to 0, 180 and 360 degrees are plotted. Figure 7.7 is a graph of the mix temperature based on the calculated hot supply flow and following equation 7.10.

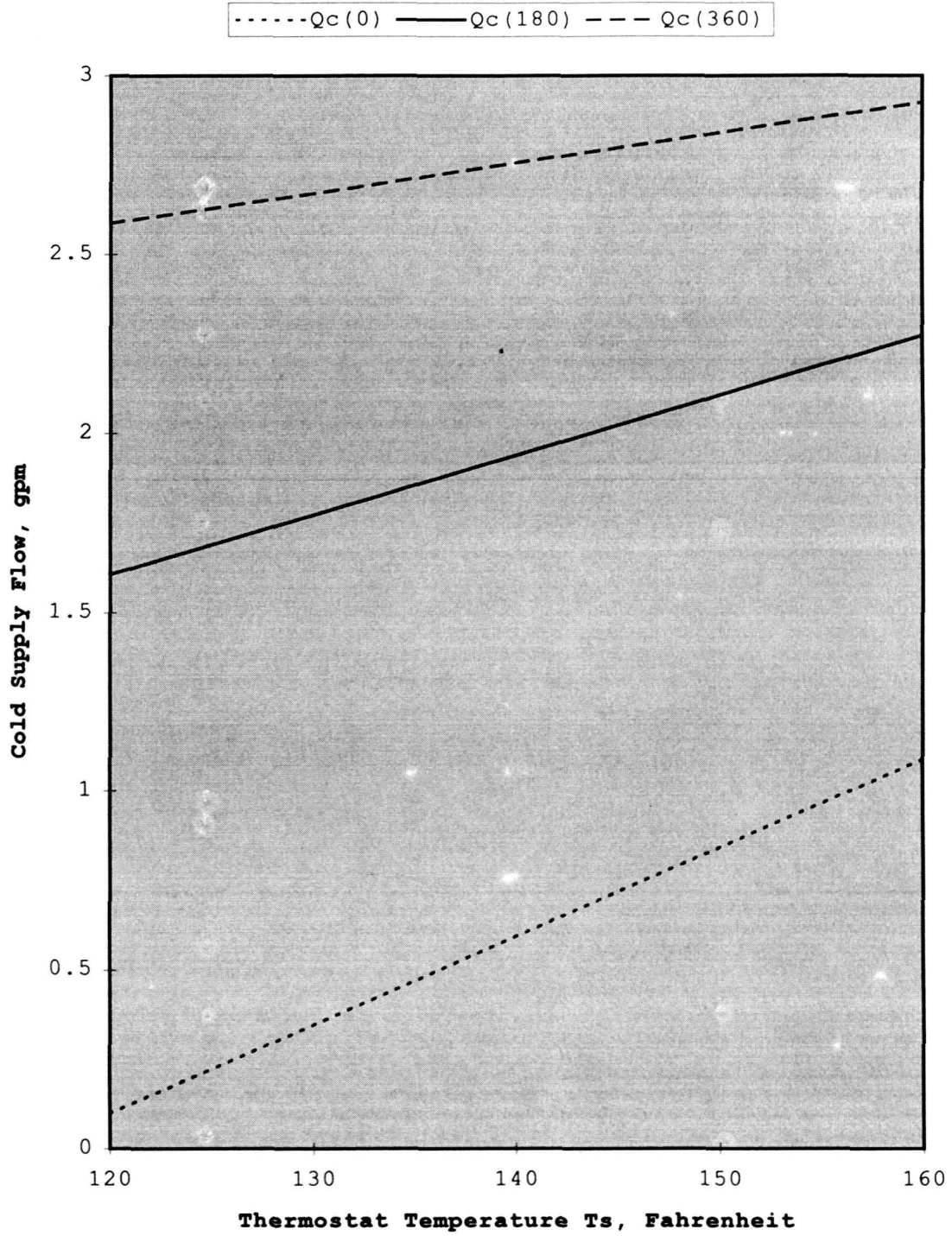


Figure 7.6: Cold supply flow as a function of thermostat temperature

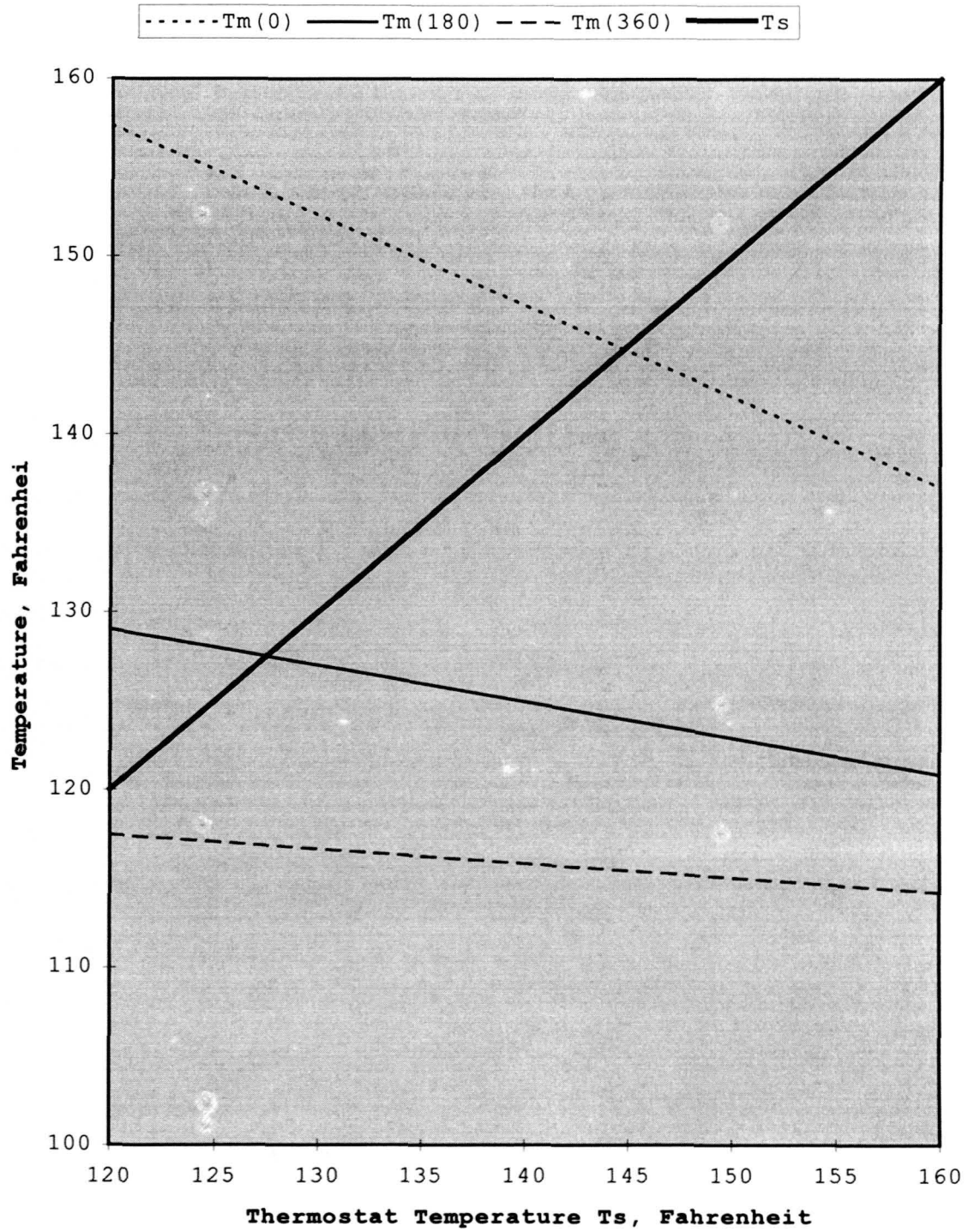


Figure 7.7: Mix temperature as a function of thermostat temperature

The point of equilibrium is where the mix temperature is equal to the thermostat temperature. For the mix temperature curve for which θ is equal to 0 degrees: this temperature is 143.8°F. Referring to Figure 7.6, at a thermostat temperature of 143.8°F, the cold supply flow is 0.71 gpm.

System Testing

Tests were conducted on the tempering valve to obtain characteristic flow curves for the valve and to obtain information on the dynamic response of the valve. Steady state pressure, temperature and flow conditions were established prior to changing the cold supply pressure; the valve bonnet dial was set at 0 degrees (corresponding to 130 °F setting). The upstream shut off valve for the cold water supply was then partially closed to produce a cold supply pressure drop. Figure 7.8 graphs the hot supply, cold supply and mix pressure for the test. Figure 7.9 graphs the hot supply, cold supply and mix temperature for the test. A steady state condition is established at the location of the "Y" axis.

For a sudden supply pressure drop in the cold supply flow, the previous equations for A_c (7.9), Q_c (7.7), Q_h (7.6), Q_m (7.8), T_s (7.2), and T_m (7.10) were used to evaluate the dynamic response of the valve. After a specified period (in this case a 2 second period), the new position of the poppet valve is calculated based on being exposed to the mix temperature for the specified period of time. The area of the cold supply orifice is then calculated and

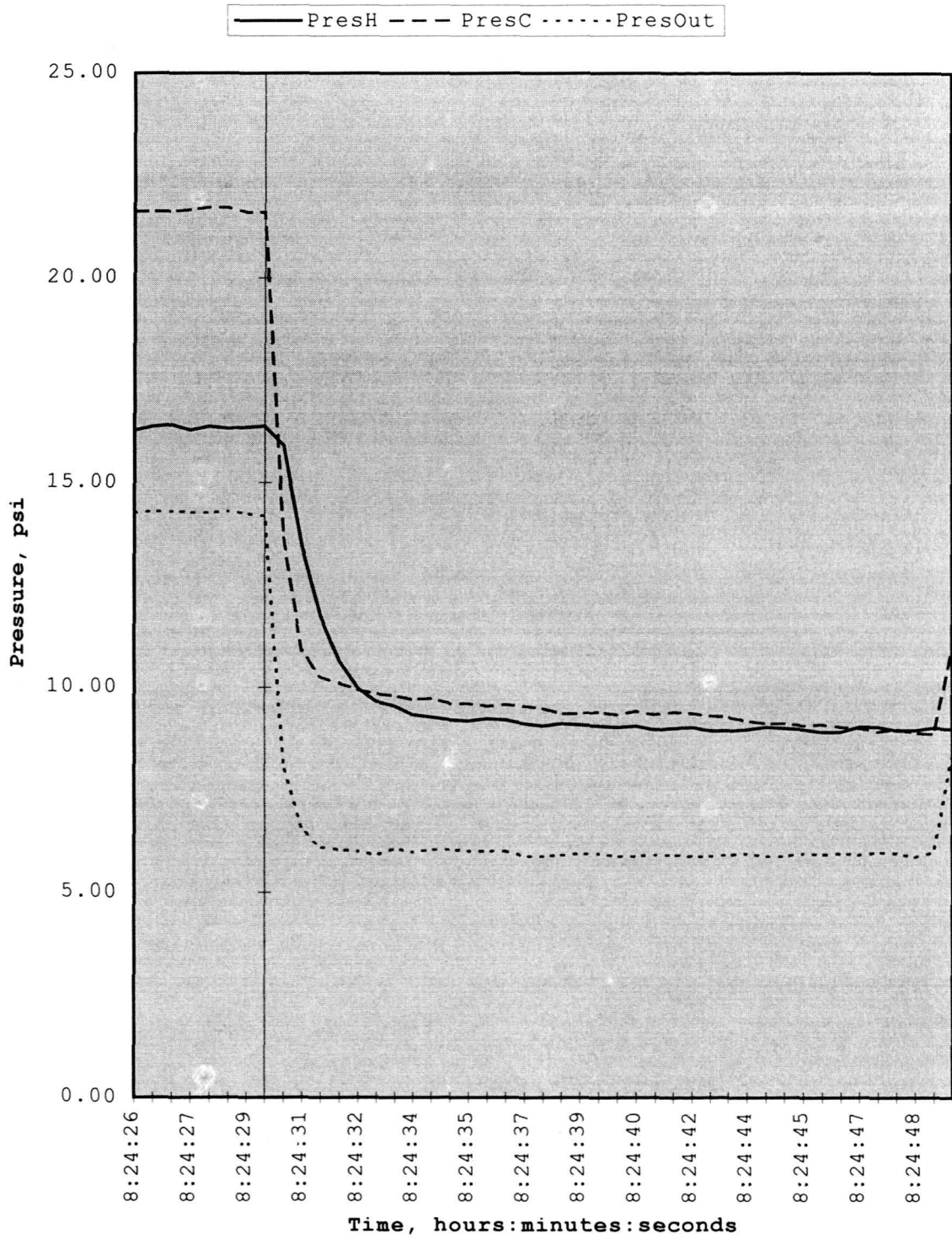


Figure 7.8: Tempering valve test, cold supply pressure drop, supply and mix pressure

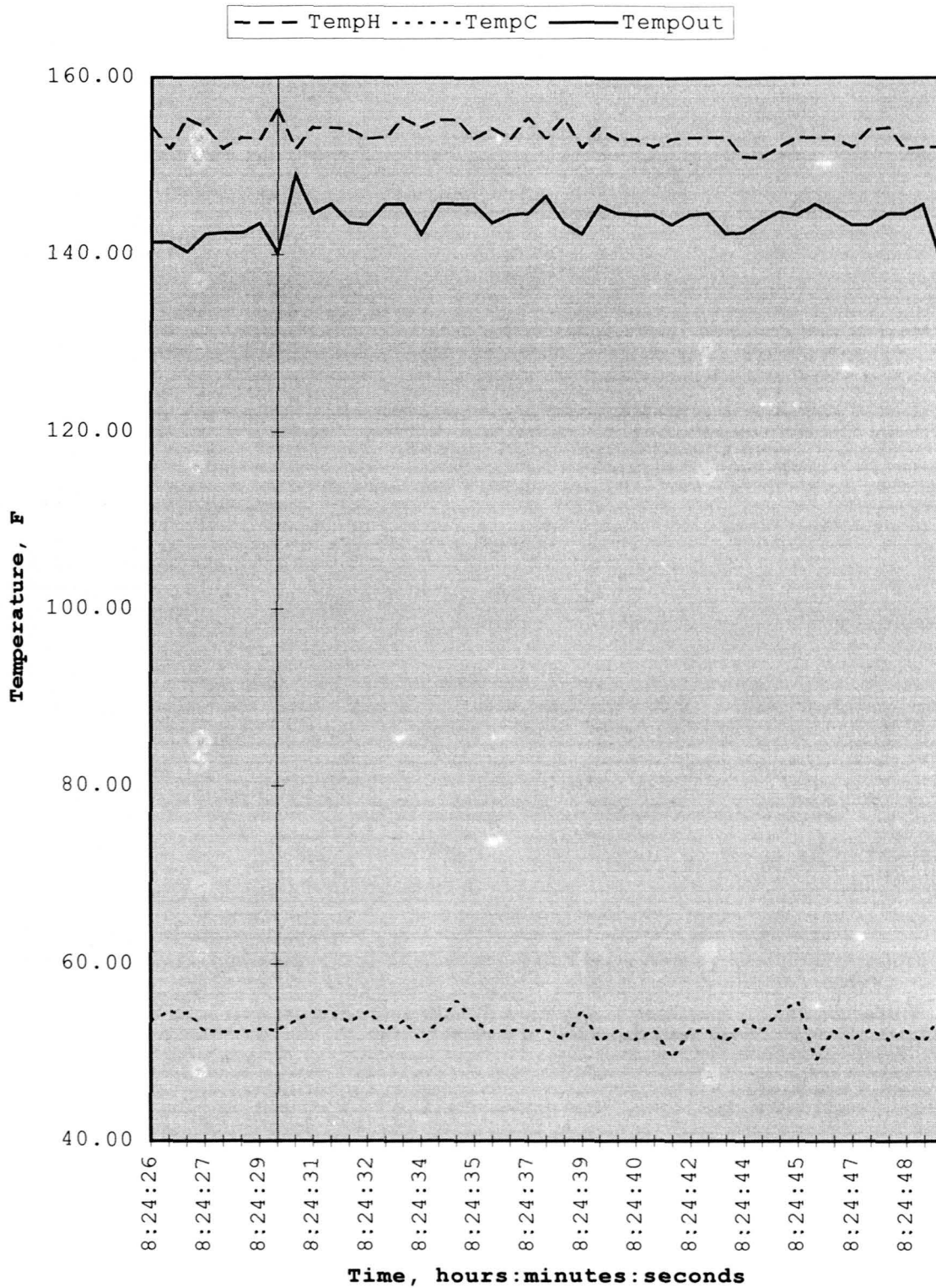


Figure 7.9: Tempering valve test, cold supply pressure drop, supply and mix temperature

the cold flow rate is evaluated. Based on the new cold flow rate, an updated mix temperature is evaluated and the process is repeated for the next time increment.

Table 7.3 summarizes the dynamic response of the tempering valve due to a sudden drop in the cold supply pressure. The operating conditions utilized in the modeling were those established during the test: hot and cold supply pressure, hot and cold supply temperature and mix output pressure.

Table 7.3 Tempering valve response, cold supply pressure drop

| Time (sec) | Ac (sq in) | Pc (psi) | Qc (gpm) | Ph (psi) | Qh (gpm) | Ts (deg F) | Tm (deg F) |
|---------------|---------------|-------------|-------------|-------------|-------------|---------------|---------------|
| -1 | 0.0168 | 21.60 | 0.973 | 16.40 | 4.91 | 139.4 | 139.4 |
| 0 | 0.0168 | 21.60 | 0.973 | 16.40 | 4.91 | 139.4 | 139.4 |
| 1 | 0.0168 | 13.66 | 0.697 | 15.89 | 9.74 | 141.1 | 145.4 |
| 2 | 0.0173 | 10.24 | 0.623 | 11.74 | 8.30 | 141.1 | 147.3 |
| 3 | 0.0178 | 9.94 | 0.668 | 9.97 | 6.90 | 141.4 | 144.4 |
| 4 | 0.0181 | 9.79 | 0.668 | 9.54 | 6.45 | 141.8 | 145.8 |
| 5 | 0.0184 | 9.73 | 0.687 | 9.27 | 6.22 | 142.1 | 145.1 |
| 6 | 0.0187 | 9.60 | 0.686 | 9.18 | 6.17 | 142.2 | 143.1 |
| 7 | 0.0188 | 9.57 | 0.685 | 9.21 | 6.21 | 142.2 | 143.0 |
| 8 | 0.0189 | 9.36 | 0.672 | 9.12 | 6.21 | 142.5 | 145.2 |
| 9 | 0.0191 | 8.39 | 0.684 | 9.05 | 6.10 | 142.6 | 143.9 |
| 10 | 0.0192 | 8.42 | 0.697 | 9.05 | 6.15 | 142.6 | 142.7 |

The poppet orifice area is plotted as a function of time in Figure 7.10, the mix output temperature and thermostat temperature are plotted in Figure 7.11, the cold and hot supply pressure are plotted in Figure 7.12, and the hot and cold supply flow are plotted in Figure 7.13. The mix temperature of the test and the model are plotted in Figure 7.14. Figure 7.14 shows the fluctuations of +/-

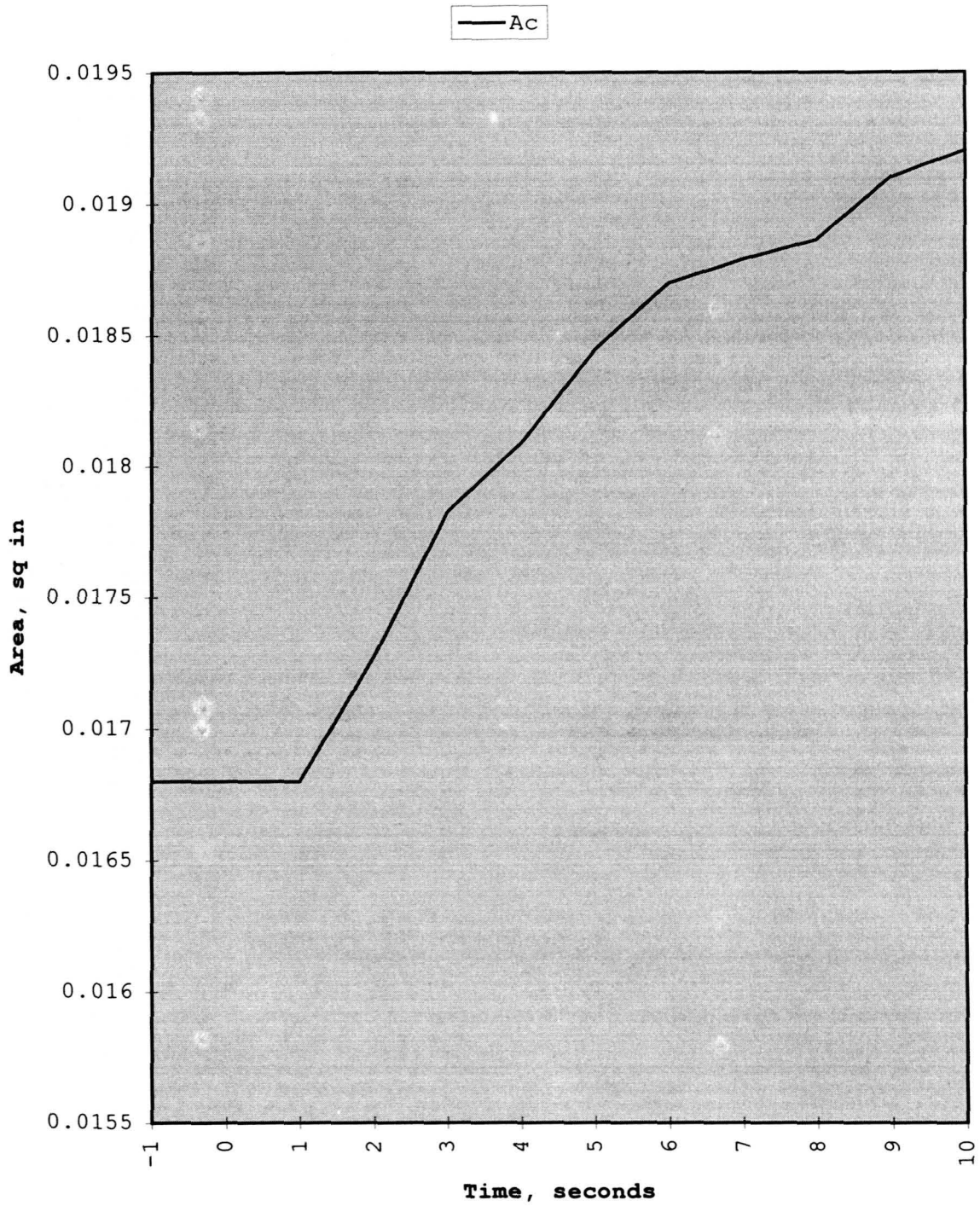


Figure 7.10: Tempering valve model, cold supply pressure drop, orifice area

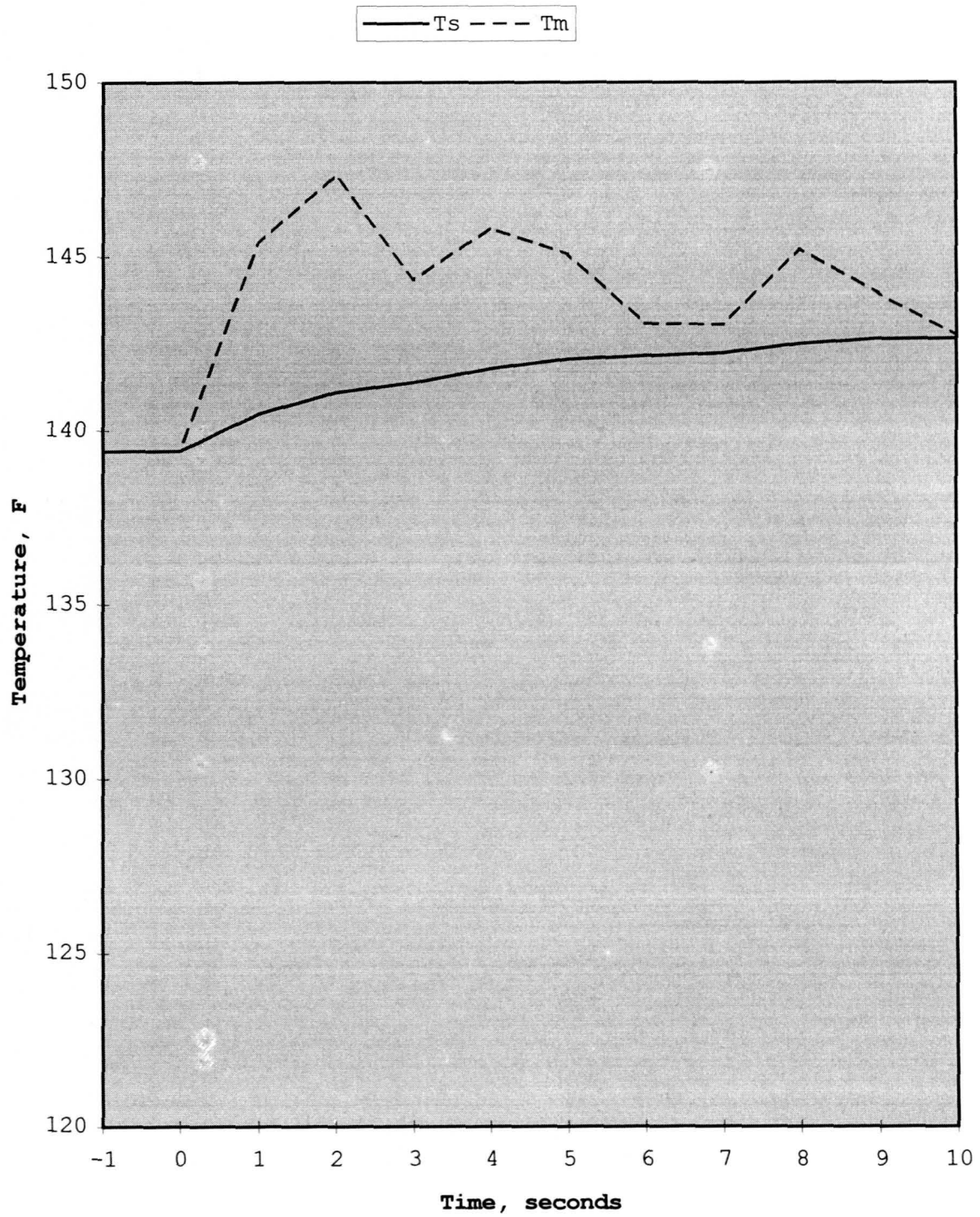


Figure 7.11: Tempering valve model, cold supply pressure drop, mix and thermostat temperature

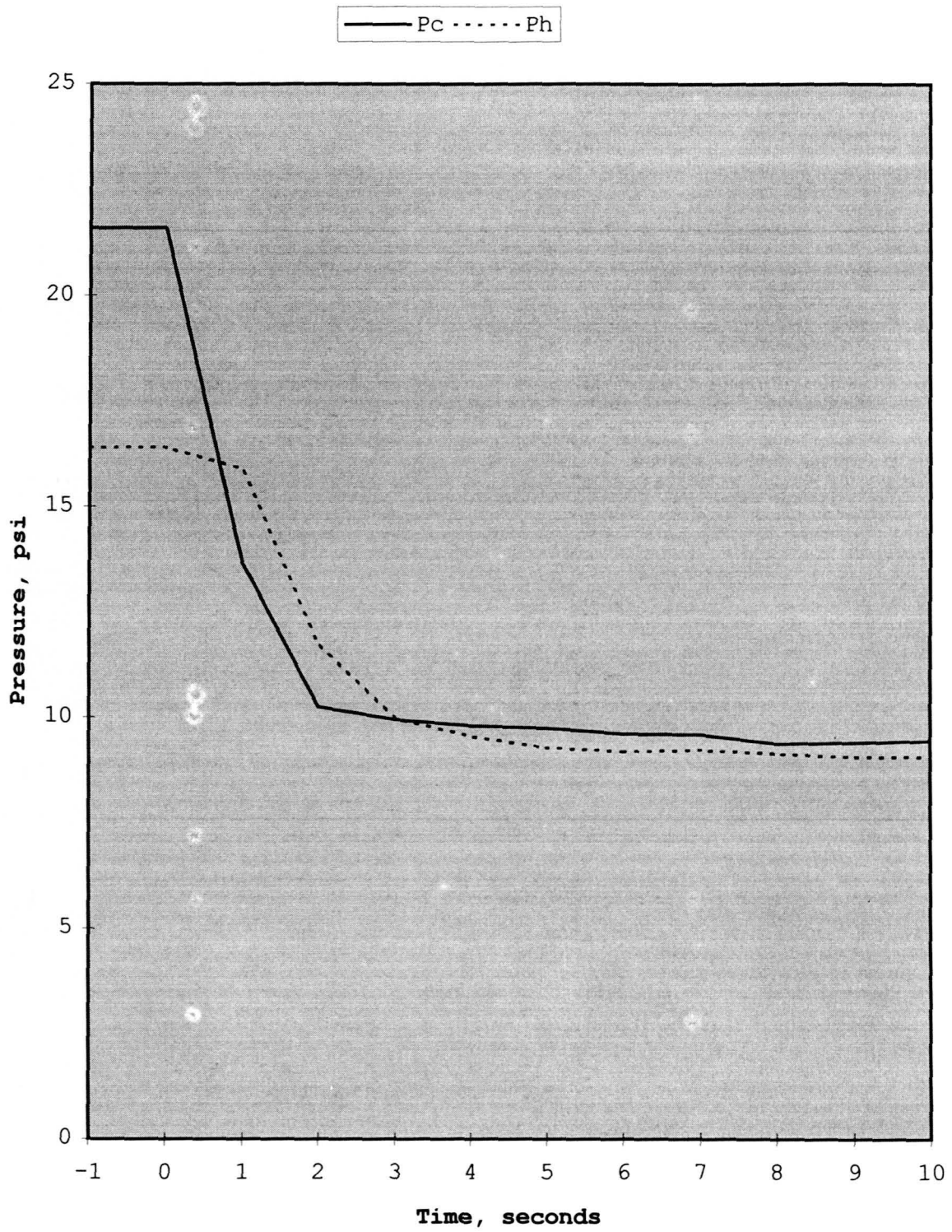


Figure 7.12: Tempering valve model, cold supply pressure drop, supply pressure

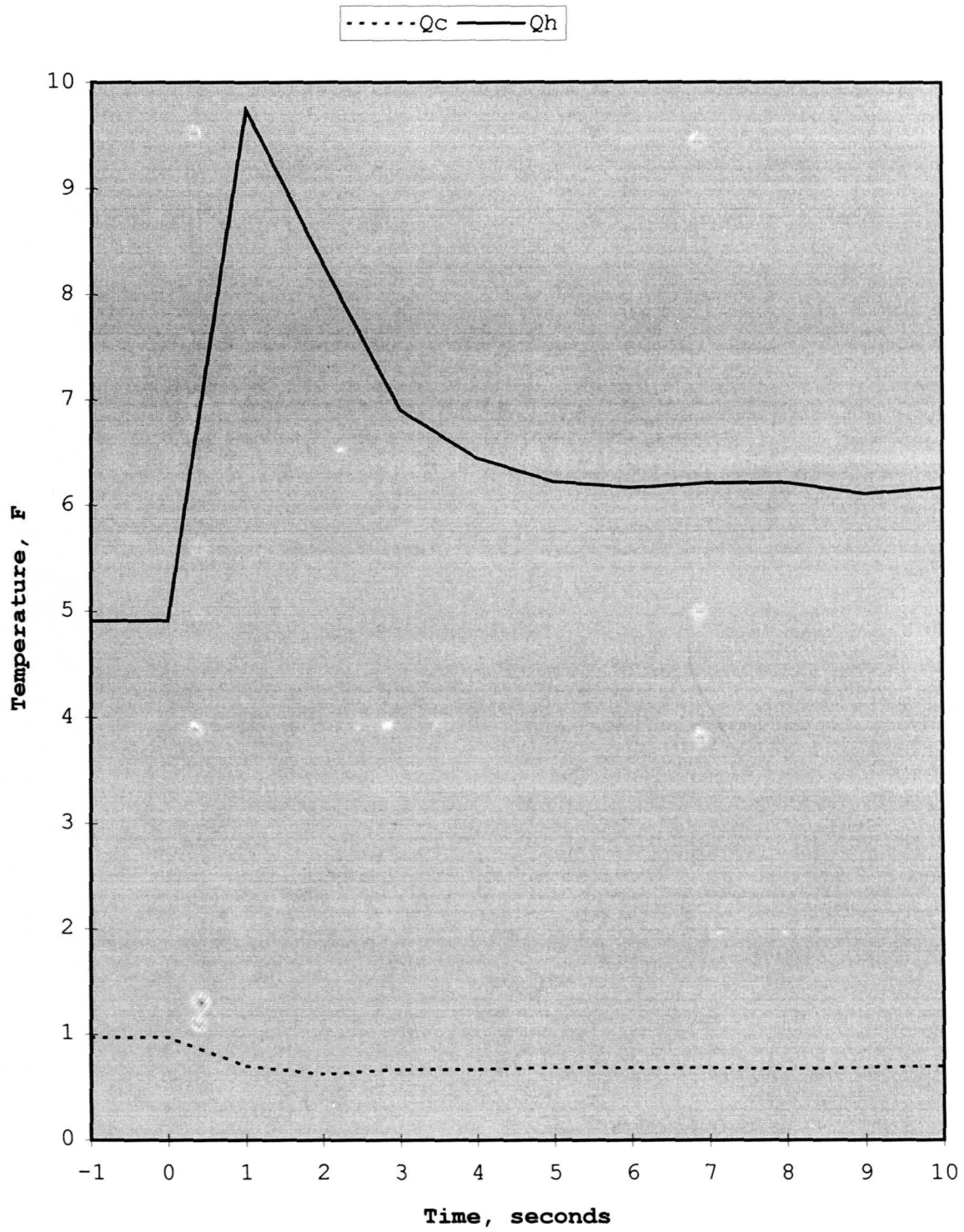


Figure 7.13: Tempering valve model, cold supply pressure drop, hot and cold supply flow rate

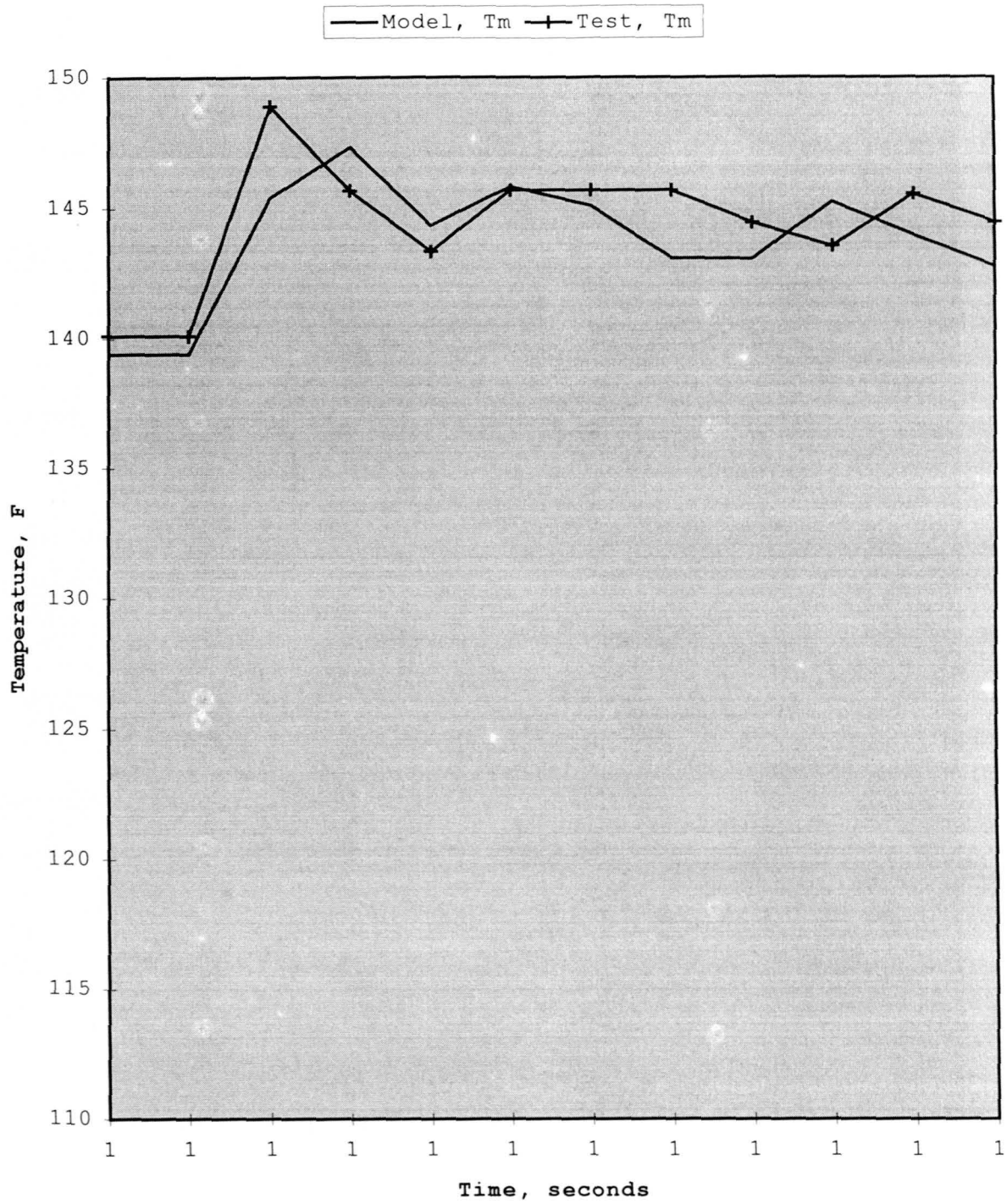


Figure 7.14: Tempering valve test and model, cold supply pressure drop, mix temperature

1.5°F found with the test mix temperature. The model accurately reflects the several degree rise in mix temperature found in the testing and the time required to establish a new temperature output.

Tests were conducted to record the response of the tempering valve given a change in the hot water supply temperature. The temperature of the hot water supply was allowed to reach room temperature prior to the test. The water heater was set to deliver water at approximately 160°F. The valve dial was set 0 degrees (corresponding to the 130°F setting. Supply pressure was not changed during the test. Figure 7.15 graphs the hot supply, cold supply and mix temperature for the test. A steady state condition is established at the location of the "Y" axis. Figure 7.16 graphs the hot supply, cold supply and mix pressure for the test and Figure 7.17 graphs the hot and cold supply flow.

The same methodology used to evaluate the pressure drop in the cold supply line was used to evaluate the dynamic response of the valve. The operating conditions utilized in the modeling were those established during the test: hot and cold supply pressure, hot and cold supply temperature and mix output pressure. Table 7.4 summarizes the dynamic response of the tempering valve due to a sudden increase in temperature of the hot supply water. The poppet orifice area is plotted as a function of time in Figure 7.18, the model mix output temperature and the thermostat temperature are plotted in Figure 7.19, the model supply flow rates are plotted in Figure 7.20 and the test and model mix temperature are plotted in

Figure 7.21. Figure 7.21 shows that the model accurately predicts the response of the valve with regards to the final steady state mix temperature (at 32 seconds) and also with regards to the mix temperature during the dynamic response period (0 to 32 seconds).

Table 7.4 Tempering valve response, hot supply temperature increase

| Time (sec) | Ac (sq in) | Pc (psi) | Qc (gpm) | Tc (°F) | Ph (psi) | Qh (gpm) | Th (°F) | Ts (°F) | Tm (°F) |
|---------------|---------------|-------------|-------------|------------|-------------|-------------|------------|------------|------------|
| 0 | 0.0000 | 23.30 | 0.00 | 63.8 | 19.40 | 8.10 | 66.0 | 66.0 | 66.0 |
| 2 | 0.0000 | 23.10 | 0.00 | 62.8 | 19.04 | 7.72 | 88.4 | 66.0 | 88.4 |
| 4 | 0.0000 | 22.90 | 0.00 | 61.7 | 18.91 | 7.69 | 143.2 | 70.0 | 143.2 |
| 6 | 0.0000 | 22.73 | 0.00 | 62.8 | 19.07 | 7.69 | 156.1 | 82.5 | 156.1 |
| 8 | 0.0000 | 22.45 | 0.00 | 63.9 | 19.04 | 7.72 | 159.3 | 95.0 | 159.3 |
| 10 | 0.0000 | 22.36 | 0.00 | 63.0 | 19.01 | 8.01 | 156.1 | 105.9 | 156.1 |
| 12 | 0.0000 | 22.12 | 0.00 | 63.7 | 18.73 | 8.03 | 159.3 | 114.5 | 159.3 |
| 14 | 0.0056 | 21.97 | 0.34 | 62.8 | 18.55 | 8.00 | 159.5 | 122.1 | 155.6 |
| 16 | 0.0191 | 21.91 | 0.66 | 62.8 | 18.49 | 7.88 | 159.5 | 127.8 | 152.1 |
| 18 | 0.0148 | 21.87 | 0.89 | 62.8 | 18.33 | 7.82 | 159.3 | 131.9 | 149.5 |
| 20 | 0.0176 | 21.57 | 1.01 | 60.7 | 18.33 | 7.54 | 157.2 | 134.9 | 145.8 |
| 22 | 0.0192 | 21.42 | 1.08 | 62.8 | 18.39 | 7.33 | 161.5 | 136.7 | 148.9 |
| 24 | 0.0211 | 21.39 | 1.16 | 60.5 | 18.39 | 7.09 | 159.5 | 138.8 | 145.6 |
| 26 | 0.0220 | 21.42 | 1.20 | 58.7 | 18.55 | 7.09 | 159.3 | 139.9 | 144.8 |
| 28 | 0.0229 | 21.45 | 1.24 | 57.5 | 18.64 | 7.15 | 158.3 | 140.8 | 143.4 |
| 30 | 0.0233 | 21.29 | 1.25 | 56.6 | 18.67 | 7.30 | 160.4 | 141.2 | 145.2 |
| 32 | 0.0238 | 21.29 | 1.25 | 55.4 | 18.70 | 7.01 | 158.3 | 141.9 | 142.6 |

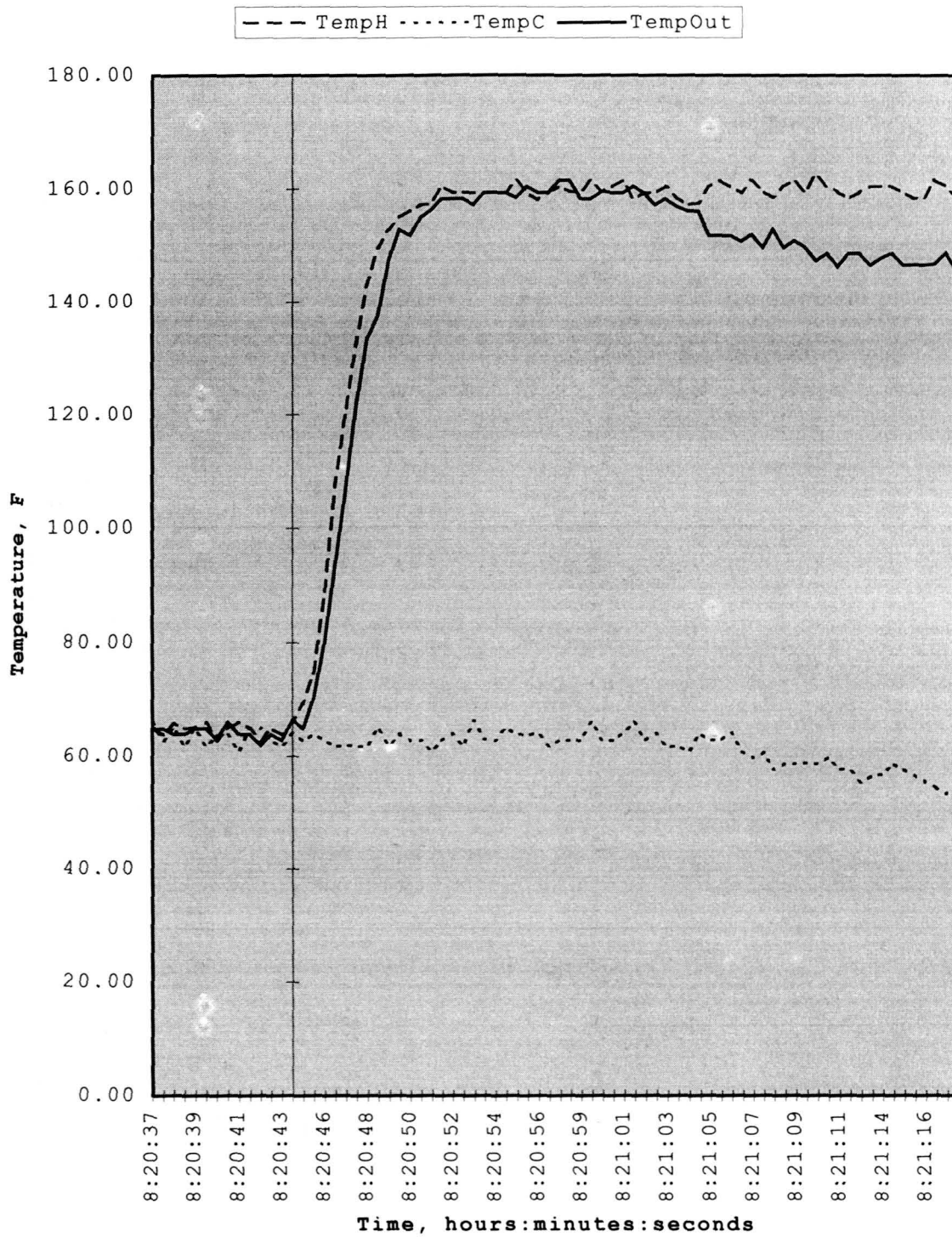


Figure 7.15: Tempering valve test, hot supply temperature increase, supply and mix temperature

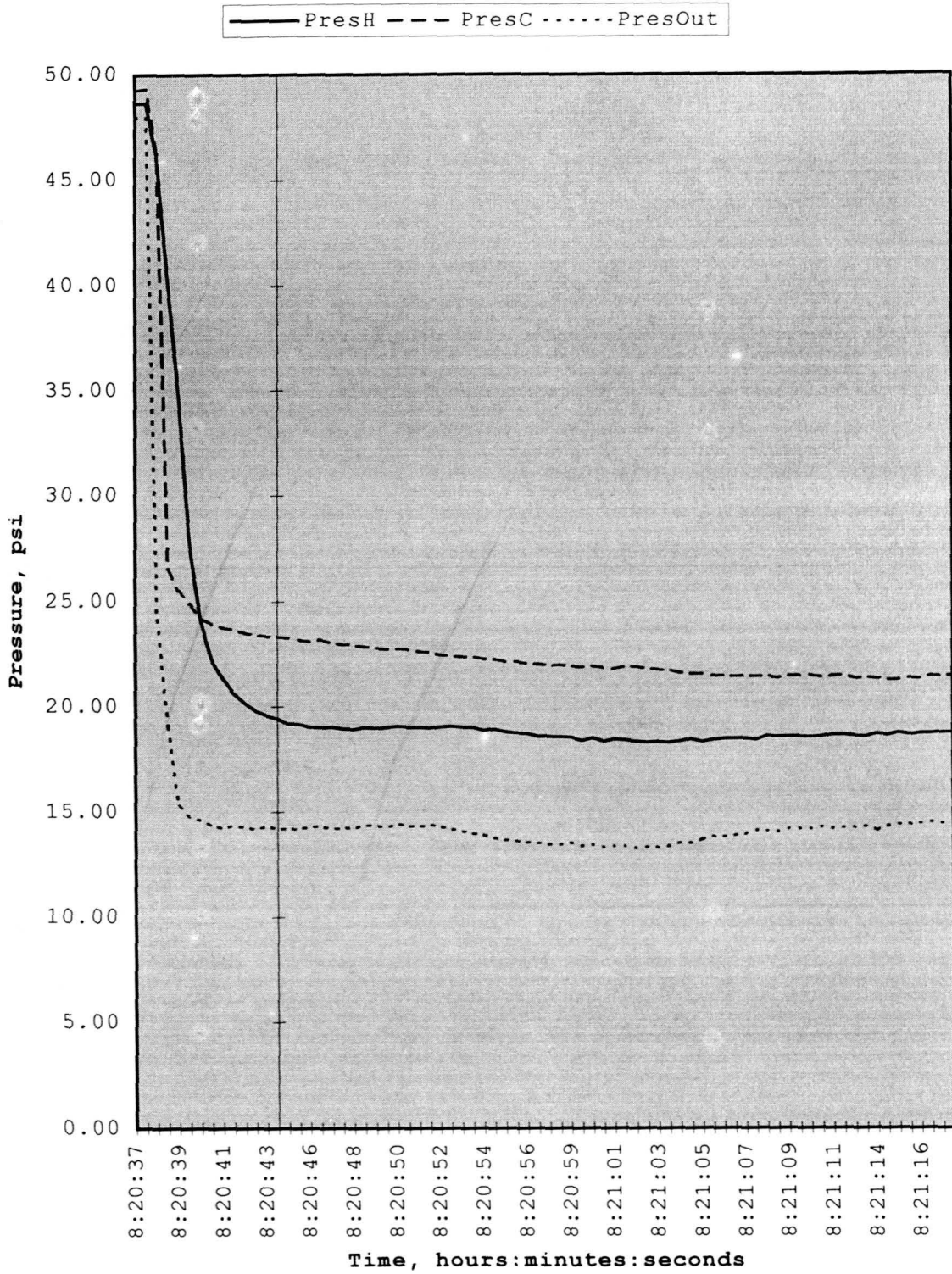


Figure 7.16: Tempering valve test, hot supply temperature increase, supply and mix pressure

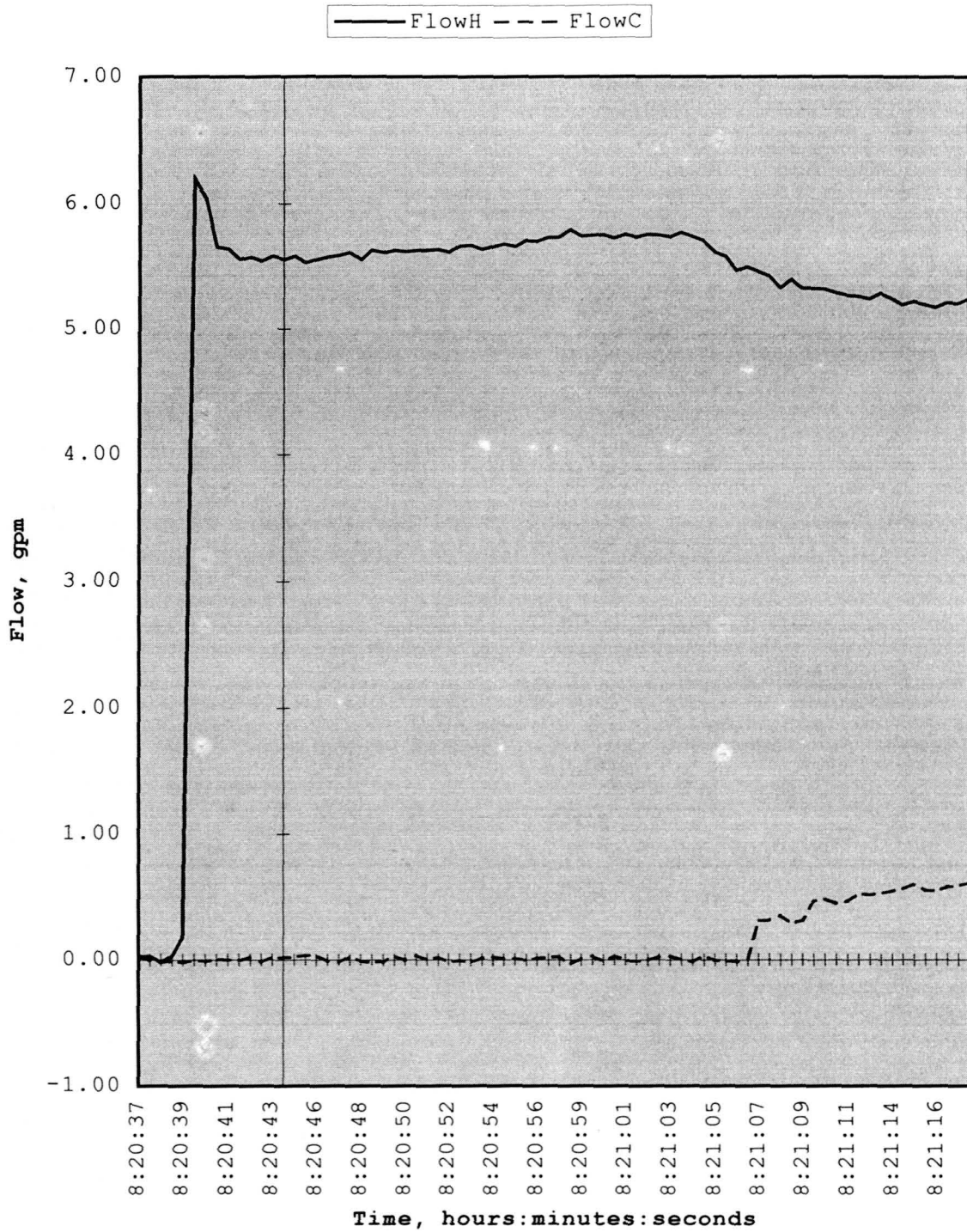


Figure 7.17: Tempering valve test, hot supply temperature increase, supply flow rates

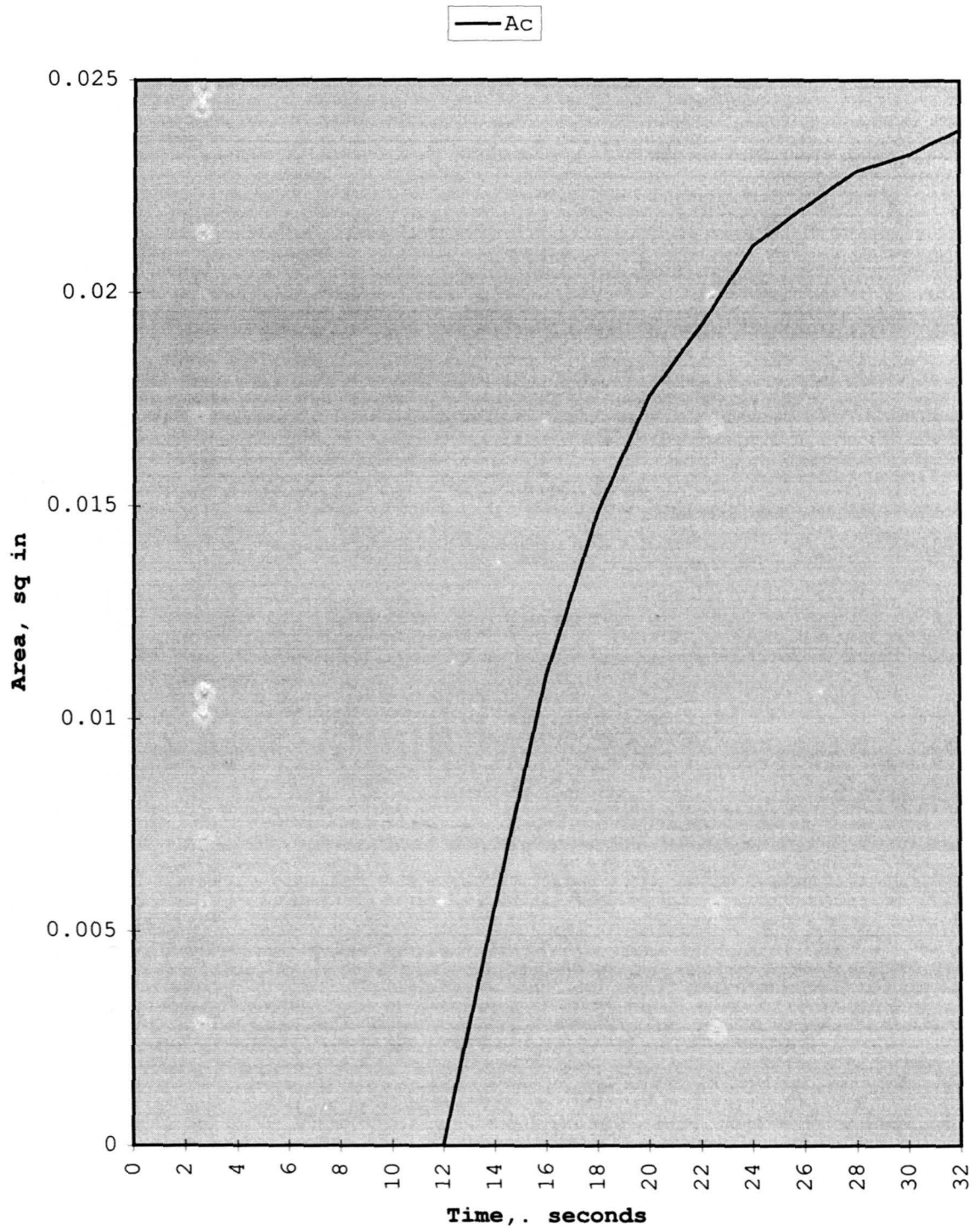


Figure 7.18: Tempering valve model, hot supply temperature increase, orifice area

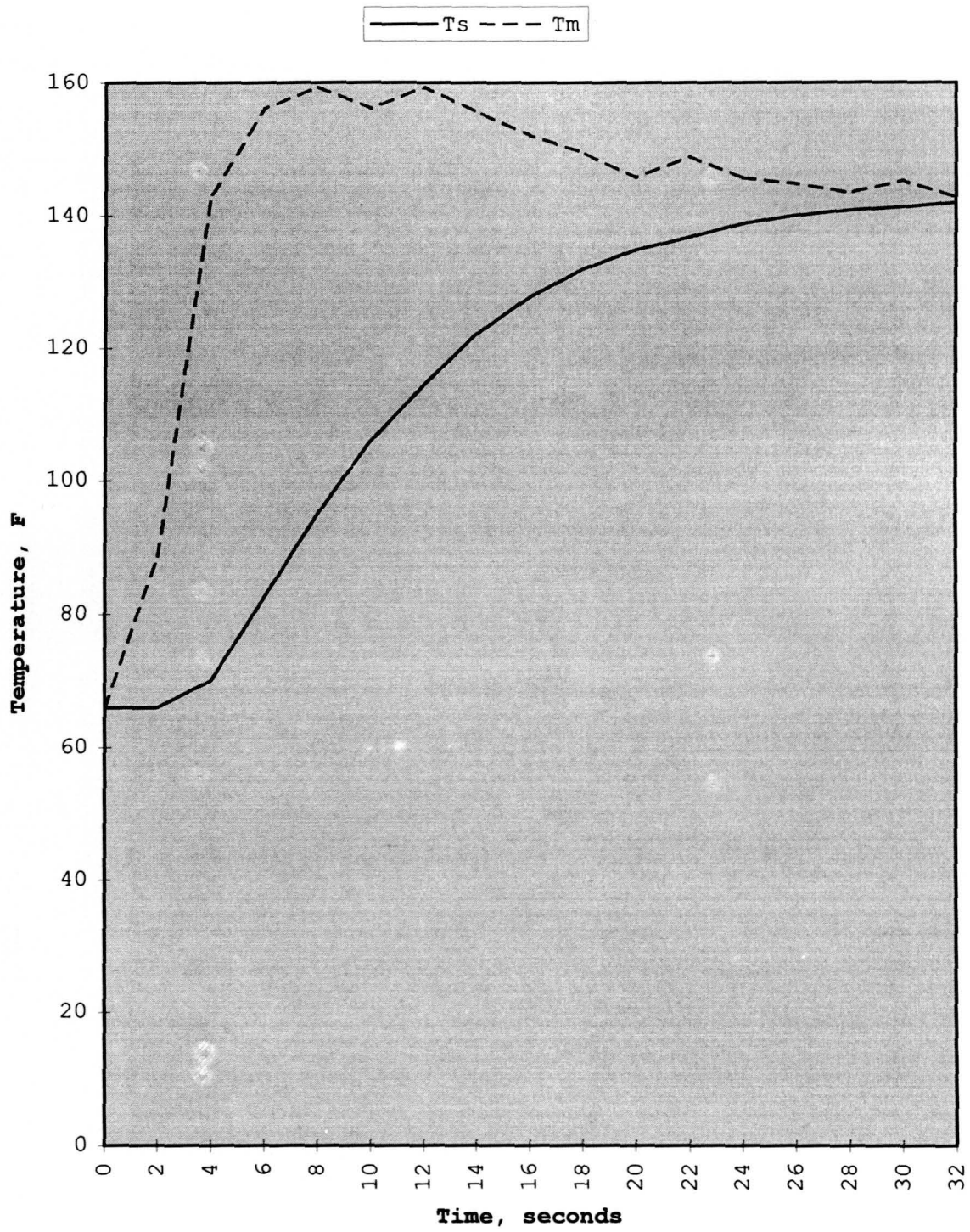


Figure 7.19: Tempering valve model, hot supply temperature increase, mix and thermostat temperature

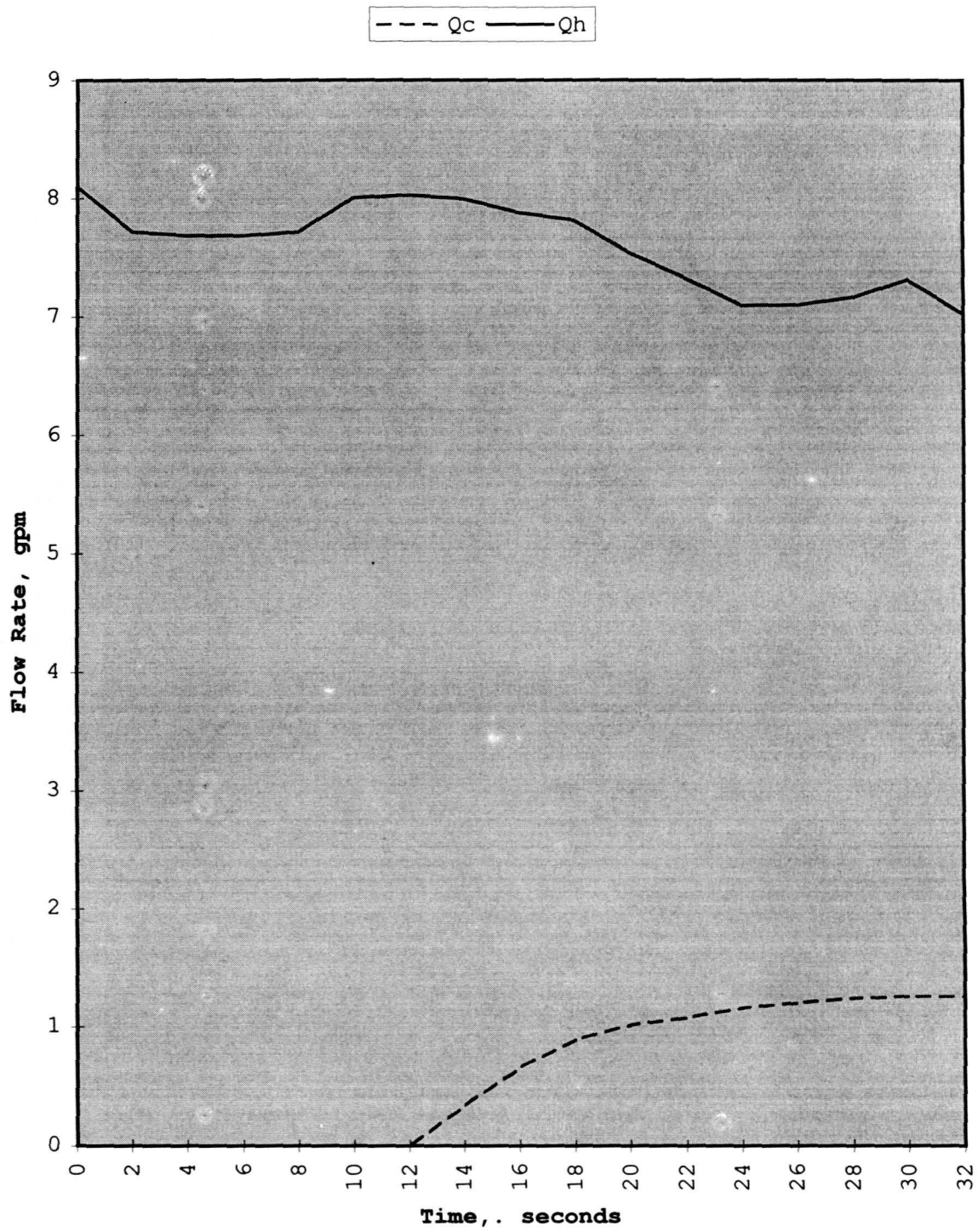


Figure 7.20: Tempering valve model, hot supply temperature increase, supply flow rates

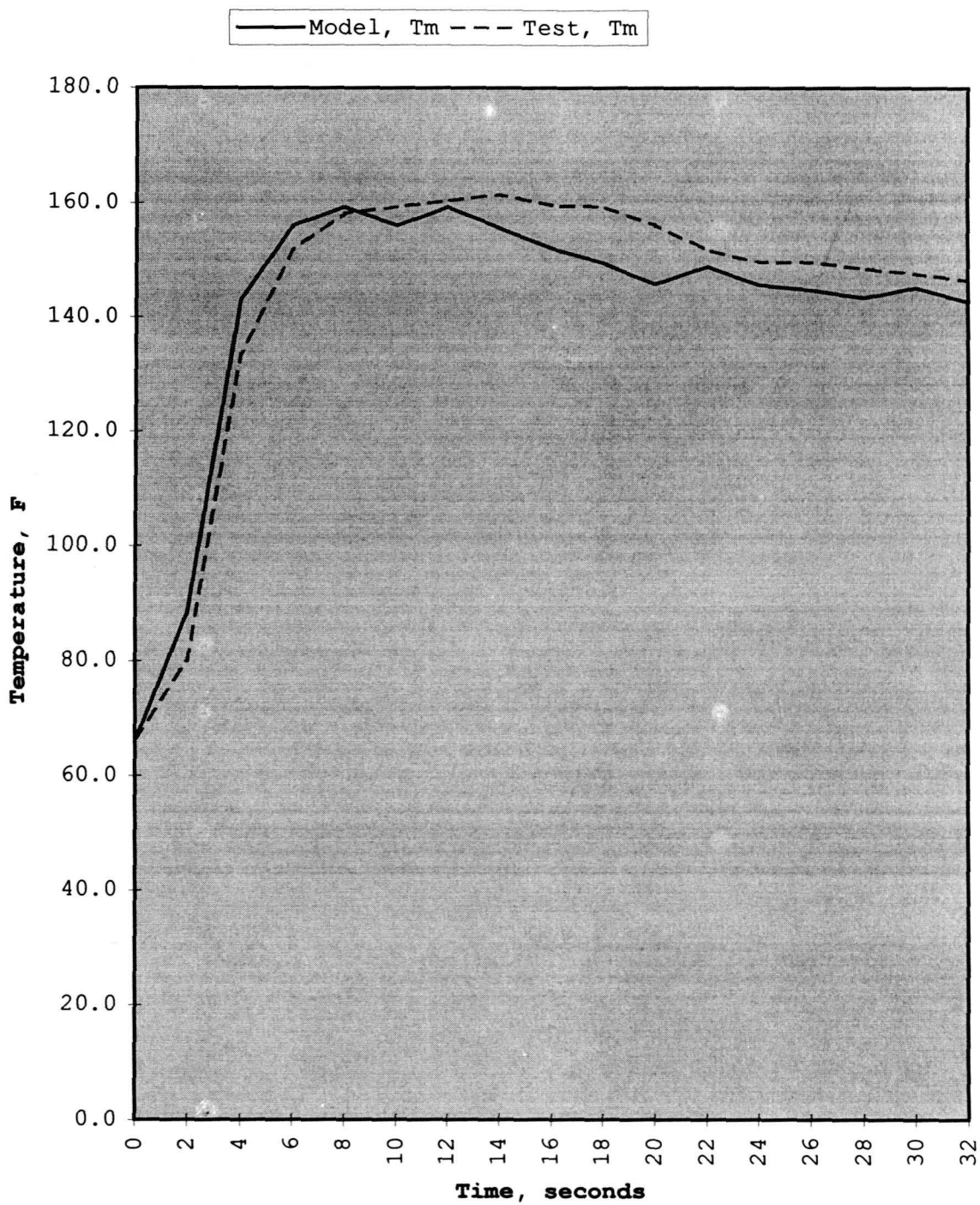


Figure 7.21: Tempering valve test and model, hot supply temperature increase, mix temperature

CHAPTER 8. ANTI-SCALD VALVES

Anti-Scald valves are designed to be installed at the point of use to prevent hot water scald injuries. The valve is installed at the exit of the faucet spigot or immediately in front of the shower head. As the temperature of the mixed water is increased a thermostatic device reacts to this change. When a certain temperature is reached, the valve automatically shuts off the water flow. This type of valve is specifically designed to be installed at the point of use, thus addressing the scald hazard of hot water. This type of valve is a consumer product and does not require adjustments or regularly scheduled maintenance by the owner or a qualified contractor.

Valve Design

A commercially available anti-scald valve intended for a shower head was obtained which allows the user to screw the valve directly to the shower arm and then attach the shower head. The valve instructions claim the anti-scald device provides the same anti-scald protection as expensive pressure balancing mixing valves. It also uses an actuator to automatically shut off the water flow when the water temperature reaches 114 °F. The instructions state

the valve is a full flow valve and will not restrict or interfere with shower performance. It states furthermore that the valve is self-cleaning with built in anti-clog features.

Figure 8.1 is a cross sectional view of the anti-scald valve. The key components of the valve are: 1) the valve body having a mix supply input and a shower output connection, 2) an actuator flow cage, 3) a secondary flow cage, 4) an actuator ball and spring, 5) a pressure relief valve ball and spring, 6) a cap, 7) a restart button and spring, and 8) an actuator return pin and spring.

The anti-scald valve is attached to the shower arm at the mix supply (shower water) input ("A") as shown in figure 8.2. The shower head is attached to the valve's male connector ("B"). There is an supply entry orifice ("C") which allows the shower water to enter the valve cavity.

Immediately after this orifice there is an actuator flow cage. This cage provides a housing for the actuator ball and spring and also provides openings to allow the shower water to flow into the valve cavity (see Figure 8.3). Water flows through the openings of the actuator flow cage and then axially into the secondary flow cage.

The secondary flow cage provides a seal with the valve body ("D") and separates the valve cavity into an entrance cavity and an exit cavity. On the exit cavity side, the secondary flow cage has openings to allow the shower water to flow out of the valve exit orifice ("E"). The secondary flow cage also provides a valve seat for the actuator ball.

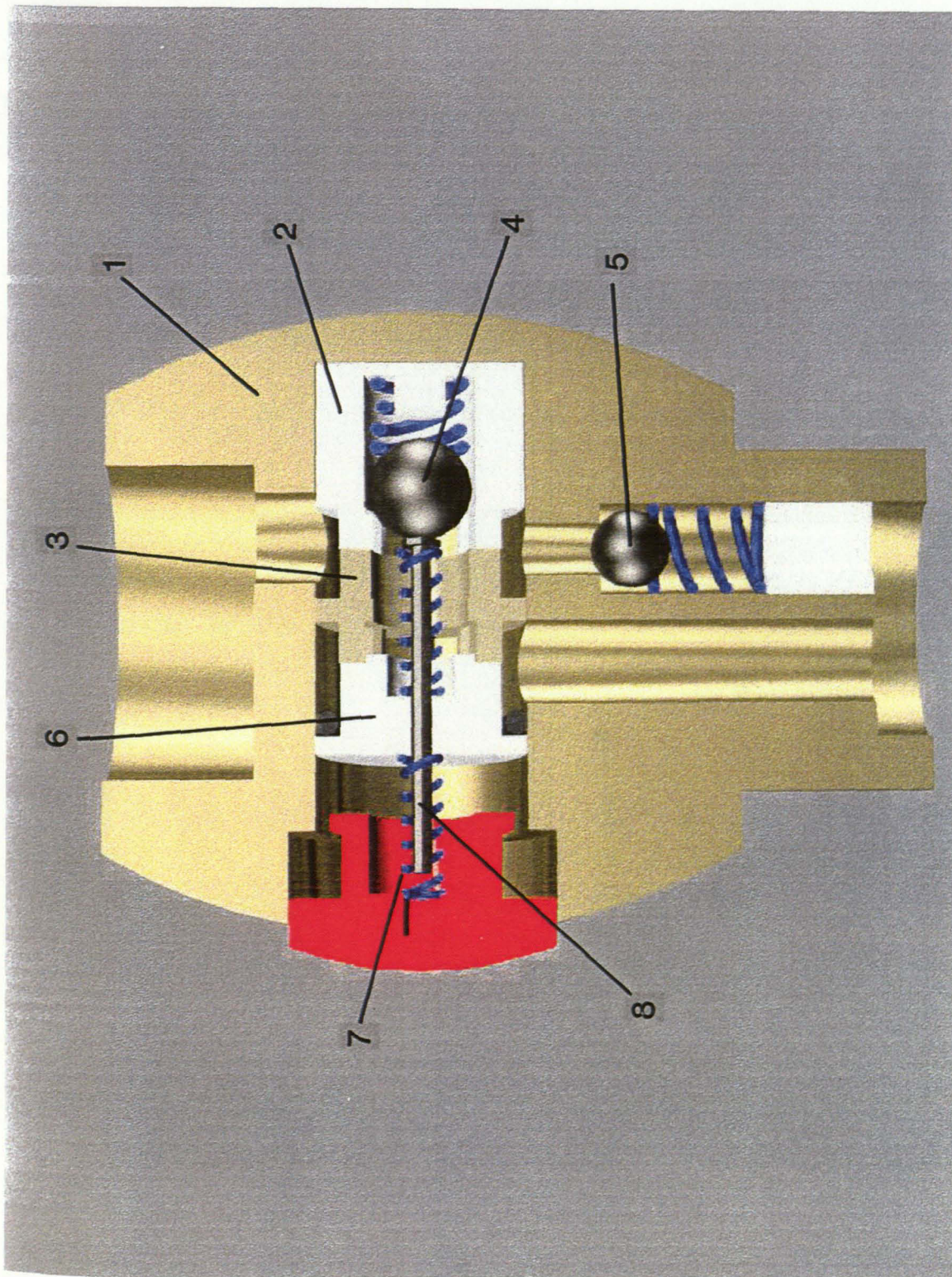


Figure 8.1: Cross section view of anti-scald valve

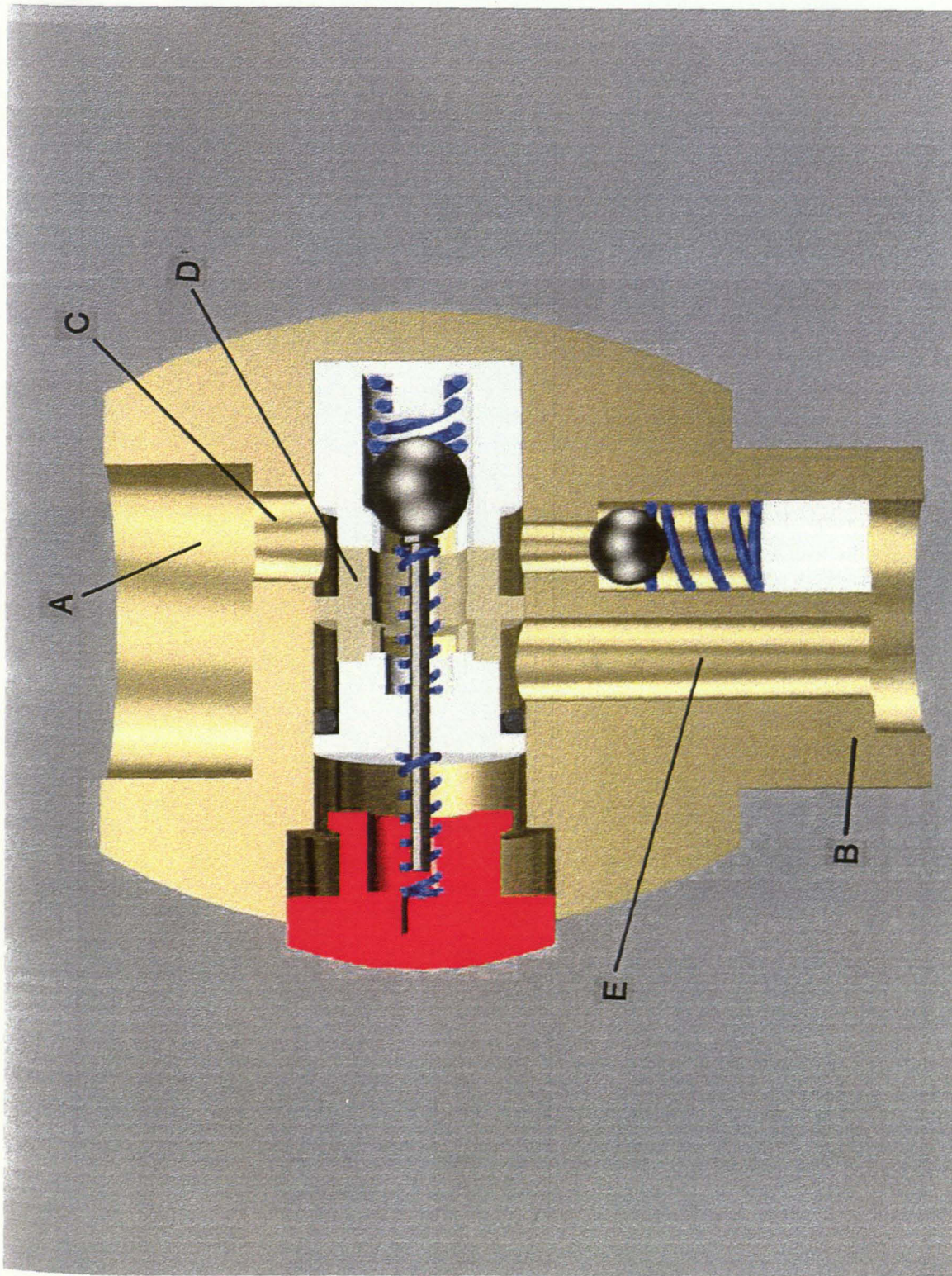


Figure 8.2: Anti-scald valve system components

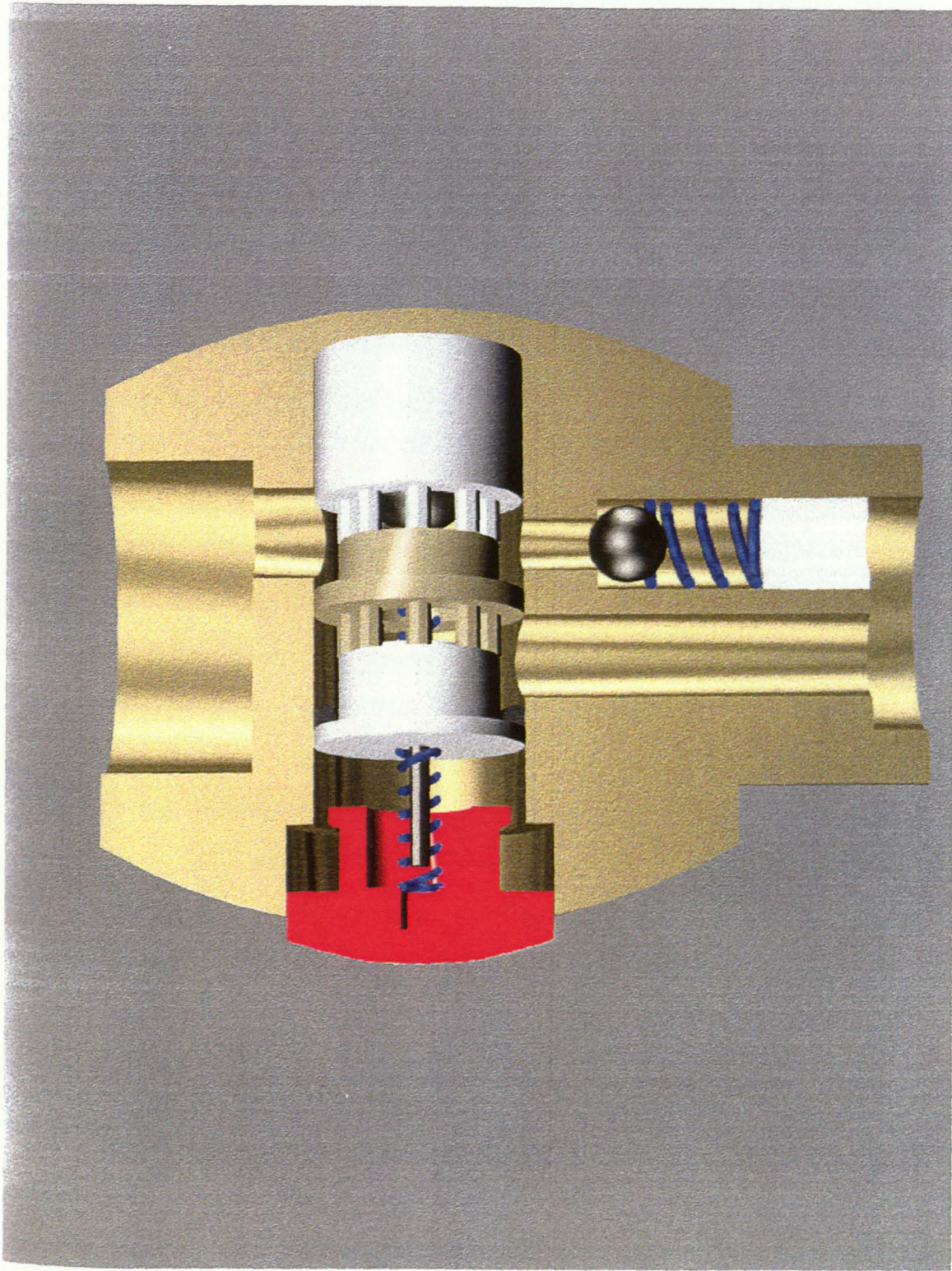


Figure 8.3: Anti-scald valve cage housing design

As water flows through the valve the temperature of the actuator ball and the actuator spring react to the changing temperature of the shower water. The actuator spring increases in length as the temperature of the spring material is increased. As the length of the spring increases, the actuator ball is moved into the flow of the shower water.

At a specific temperature, the actuator spring will move the actuator ball into the supply flow until the major diameter of the ball is directly exposed to the flow. At this point, the pressure on the side of the actuator spring changes from the static pressure of the flow to the stagnation pressure of the flow. The actuator ball is thus accelerated against the secondary flow cage valve seat and stops the water flow.

The restart button allows the user to force the actuator ball from the secondary flow cage valve seat. This allows water to flow through the valve. If the temperature of the supply flow is reduced, the supply flow will cool the actuator spring and allow the valve to return to a free flow state. If the valve is allowed to cool sufficiently, the restart button allows the user to force the actuator ball from the valve seat, relieve the back pressure on the valve and return the valve to a free flow state. The valve cap seals the valve cavity and also provides a bearing surface for the actuator pin.

System Modeling

Modeling of this system entails the summation of the forces on the actuator ball. Summing the forces on the actuator ball in the horizontal plane yields the following equation:

$$mx'' = F_{rs} - F_{as} + f + A(P_{rs} - P_{as}) \quad (8.1)$$

where:

m = Mass of the actuator ball, slugs

F_{rs} = Force due to the return spring, lbf

F_{as} = Force due to the actuator spring, lbf

f = Frictional force of the return pin in the cap bearing,
lbf

A = Cross sectional area of the actuator ball, ft^2

P_{rs} = Fluid pressure on the return spring side of the ball,
psf

P_{as} = Fluid pressure on the actuator spring side of the ball,
psf

The position of the actuator ball will be defined from a position where the actuator spring is fully compressed; at this point $x = 0$. As the ball moves from this position, there is a specific distance where the ball moves into the flow of the supply water, but does not affect the cross sectional area of the secondary flow cage. The actuator ball intersects the edge of the orifice area when x is equal to 0.030 inches. During this period of motion, $0 < x < 0.030$, the static fluid pressure on the return

spring side of the ball is not affected by the position of the actuator ball in the secondary flow cage. Thus, the equation of motion for the actuator ball is:

$$mx'' = F_{rs} - F_{as} + f + A*(P_{rs} - P_{as}) \quad (8.1)$$

As the ball moves into the secondary flow cage orifice, the area of the orifice is reduced by the actuator ball causing an increase in fluid velocity (see Figure 8.2). The increase in fluid velocity reduces the static pressure on the return spring side of the actuator ball. During this period of motion when $x > 0.030$ inches, the orifice area of the secondary flow cage is:

$$A_c = \pi*(rc^2 - rp^2) - ra^2*\cos[(ra - x)/ra] \quad (8.3)$$

where:

A_c = Orifice area of the secondary cage, ft^2

rc = Radius of the secondary cage, ft

rp = Radius of the restart pin, ft

ra = Radius of the actuator ball, ft

x = Position of the actuator ball, ft

Figure 8.4 graphs the orifice area of the secondary cage as a function of x . During this period of motion the static pressure on the return spring side of the actuator ball is:

$$P_{rs}' = P_s + \rho[(V_s^2 - V_o^2)/2] \quad (8.4)$$

where:

P_{rs}' = Static Pressure at the secondary orifice, psf

P_s = Static Pressure at the supply entrance orifice, psf

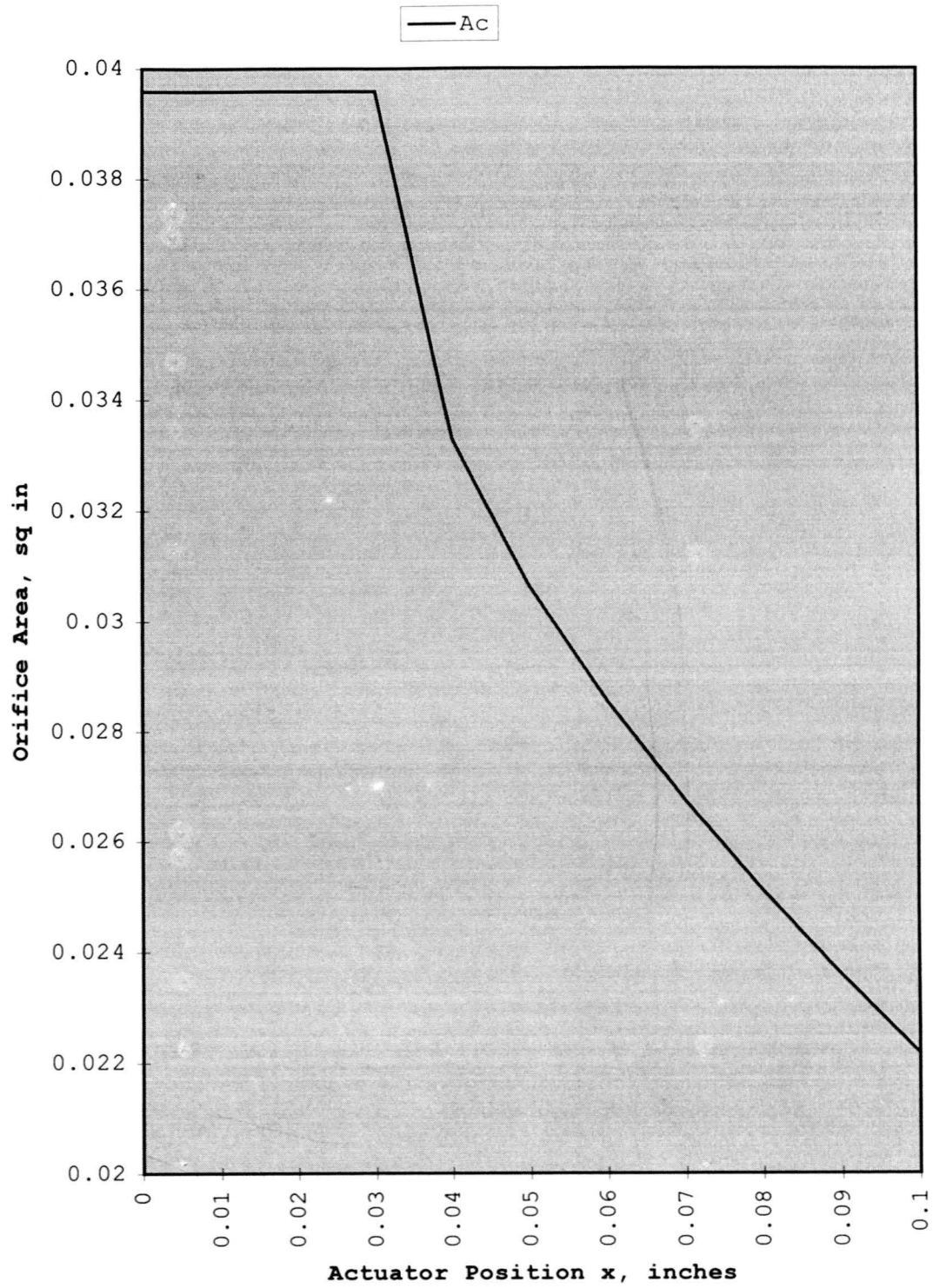


Figure 8.4: Valve orifice area as a function of actuator position

ρ = Density of the supply mix, slugs/ft³

V_s = Velocity of the mix at the supply entrance orifice, ft/s

V_o = Velocity of the mix at the secondary orifice, ft/sec

Thus, the equation of motion for the actuator ball is:

$$mx'' = F_{rs} - F_{as} + f + A^*(P_{rs}' - P_{as}) \quad (8.2)$$

The major diameter of the actuator ball is in the supply flow when x is equal to 0.065 inches. When the major diameter reaches this position, the stagnation pressure on the actuator spring side of the ball will equal:

$$P_{ast} = P_s + \rho[(V_s^2)/2] \quad (8.5)$$

where:

P_{ast} = Stagnation Pressure, psf

P_s = Static Pressure at the supply entrance orifice, psf

ρ = Density of the supply mix, slugs/ft³

V_s = Velocity of the mix at the supply entrance orifice, ft/s

At the point where $x = 0.065$ inches, the following is the equation of motion for the actuator ball:

$$mx'' = F_{rs} - F_{as} + f + A^*(P_{rs}' - P_{ast}) \quad (8.6)$$

The valve was disassembled to characterize its operation. The actuator spring was placed in water at various temperatures and the total length of the spring was recorded. Table 8.1 summarizes the results.

Table 8.1: Thermostat length as a function of temperature

| | | | | |
|------------------|-------|-------|-------|-------|
| Temperature (°F) | 75 | 100 | 110 | 124 |
| Length (inches) | 0.190 | 0.205 | 0.220 | 0.270 |

Assuming the relationship of the thermostat length is a linear function of temperature, the data was characterized by an equation using a least squares data fit. The equation for the length of the spring is:

$$L = 0.0561 + 0.00168 * T_s \quad (8.7)$$

where:

L = Free length of the spring, inches

T_s = Temperature of the spring, °F

Figure 8.5 plots the raw data and the resulting equation from the least squares data fit.

Data was then taken of the length of the spring as it was exposed to a hot water bath. The length of the spring reached its final length in 3 seconds; accurate measurement of the spring length during its expansion was not conducted. Since the spring reached its final length in 3 seconds, the time constant for the spring is 1 second; therefore, the characteristic equation for the length of the spring is:

$$L = L_f - (L_f - L_o) * e^{-1t} \quad (8.8)$$

where:

L = Free length of spring, inches

Lf = Length of spring at the convective environment
temperature, inches

Lo = Initial length of spring, inches

t = Time, seconds

The spring rate for the actuating spring and the return spring pin were evaluated and found to be:

$$k_{as} = 27 \text{ lb/in}$$

$$k_{rs} = 6 \text{ lb/in}$$

Figure 8.6 graphs the force of the actuating spring as a function of the actuator position (x) and of temperature. Figure 8.7 graphs the force of the return spring as a function of x. An evaluation was conducted for the position of the actuating ball ranging from $0 < x < 0.030$ inch. During this period the following equation governs the motion of the ball:

$$m\ddot{x} = F_{rs} - F_{as} + f + A*(P_{rs} - P_{as}) \quad (8.1)$$

This equation is plotted in Figure 8.8 as a function of x and for various temperatures. When the graphed function crosses the x axis, a point of equilibrium is reached for the actuator ball. Thus, this equation of motion holds for actuating spring temperatures up to approximately 90°F.

An evaluation was conducted for the position of the actuating ball ranging from $0.030 < x < 0.065$ inch. During this period the following equation governs the motion of the ball:

$$m\ddot{x} = F_{rs} - F_{as} + f + A*(P_{rs}' - P_{as}) \quad (8.2)$$

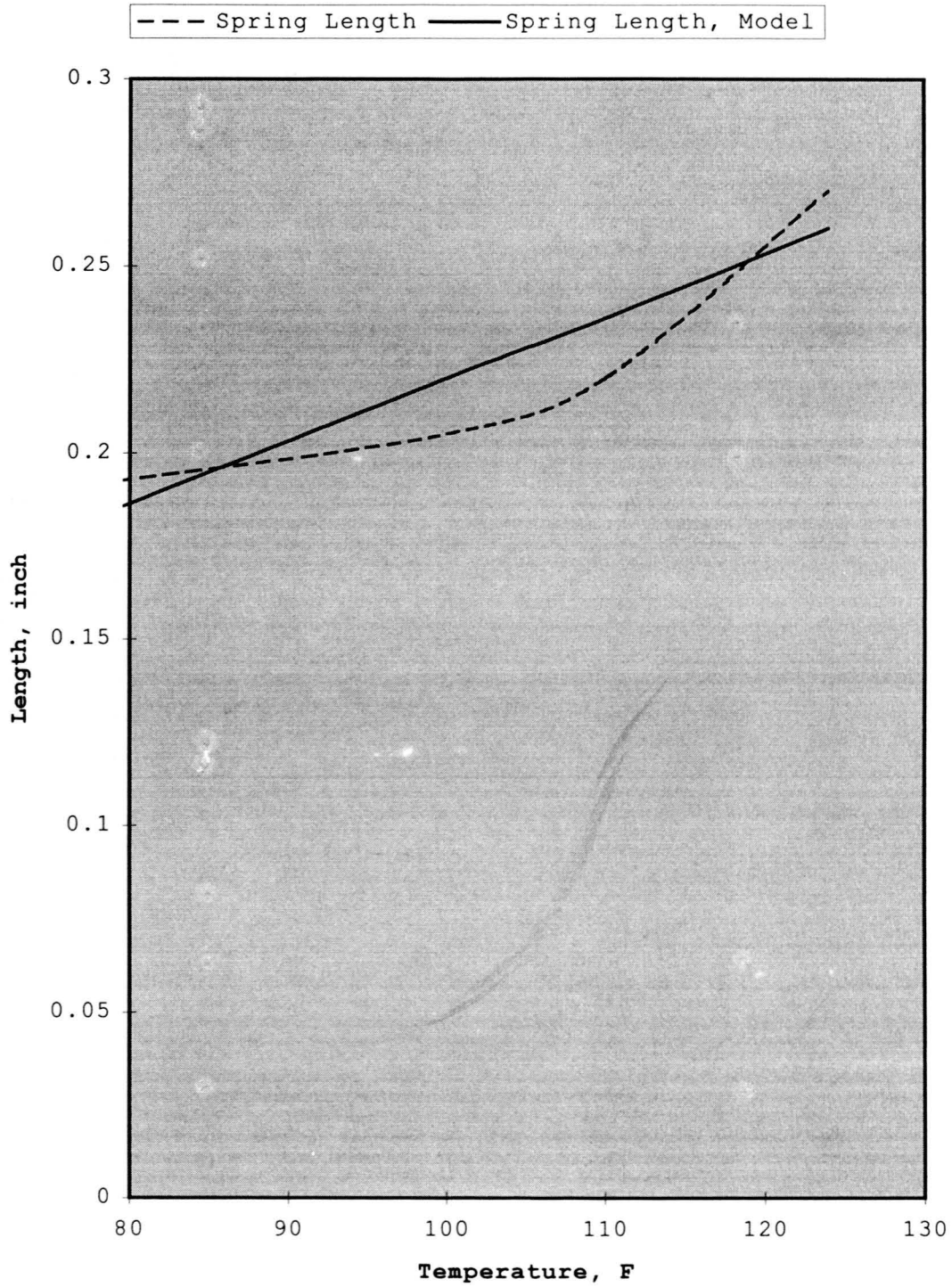


Figure 8.5: Actuator spring length as a function of temperature, test and model

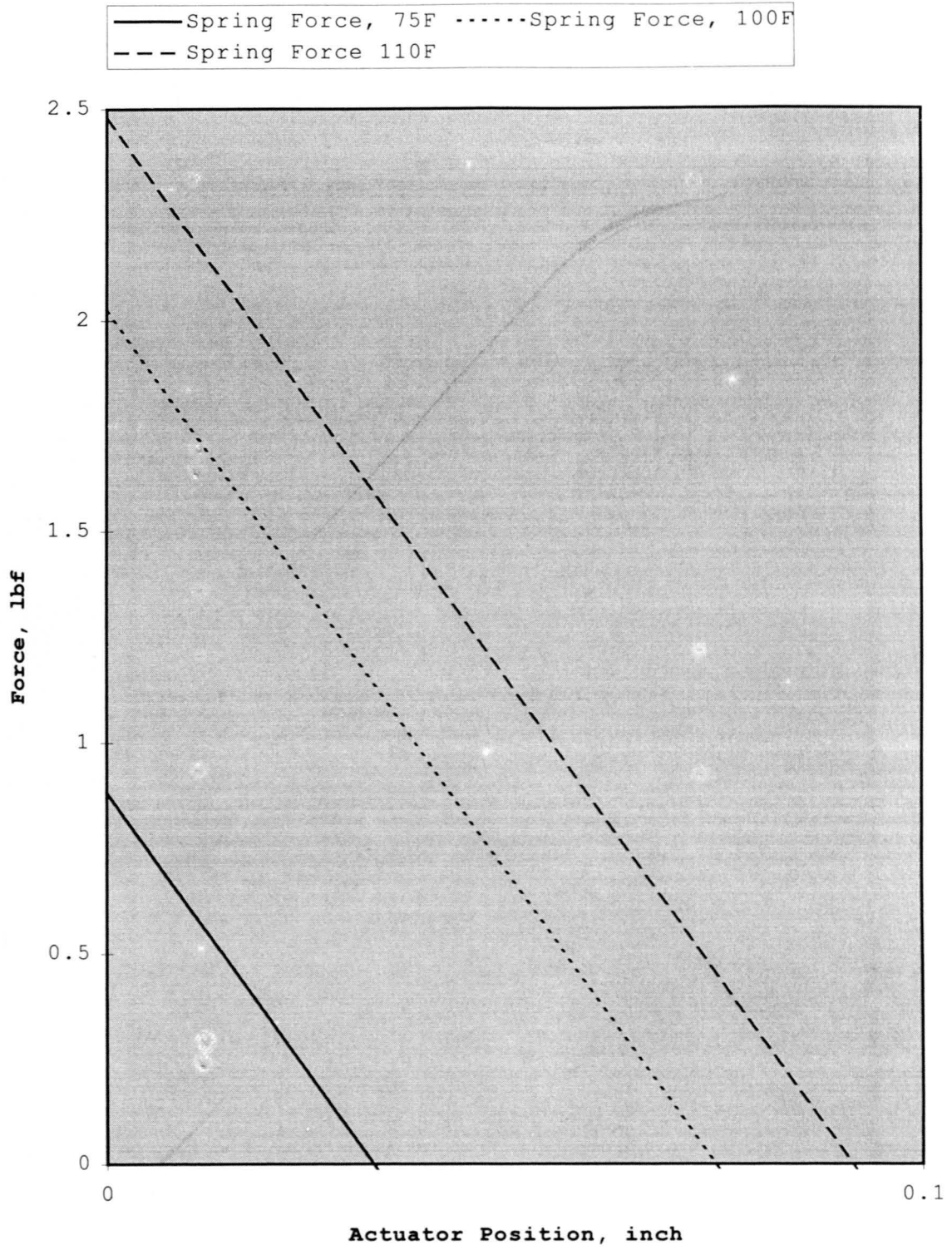


Figure 8.6: Actuator spring force as a function of actuator position, model

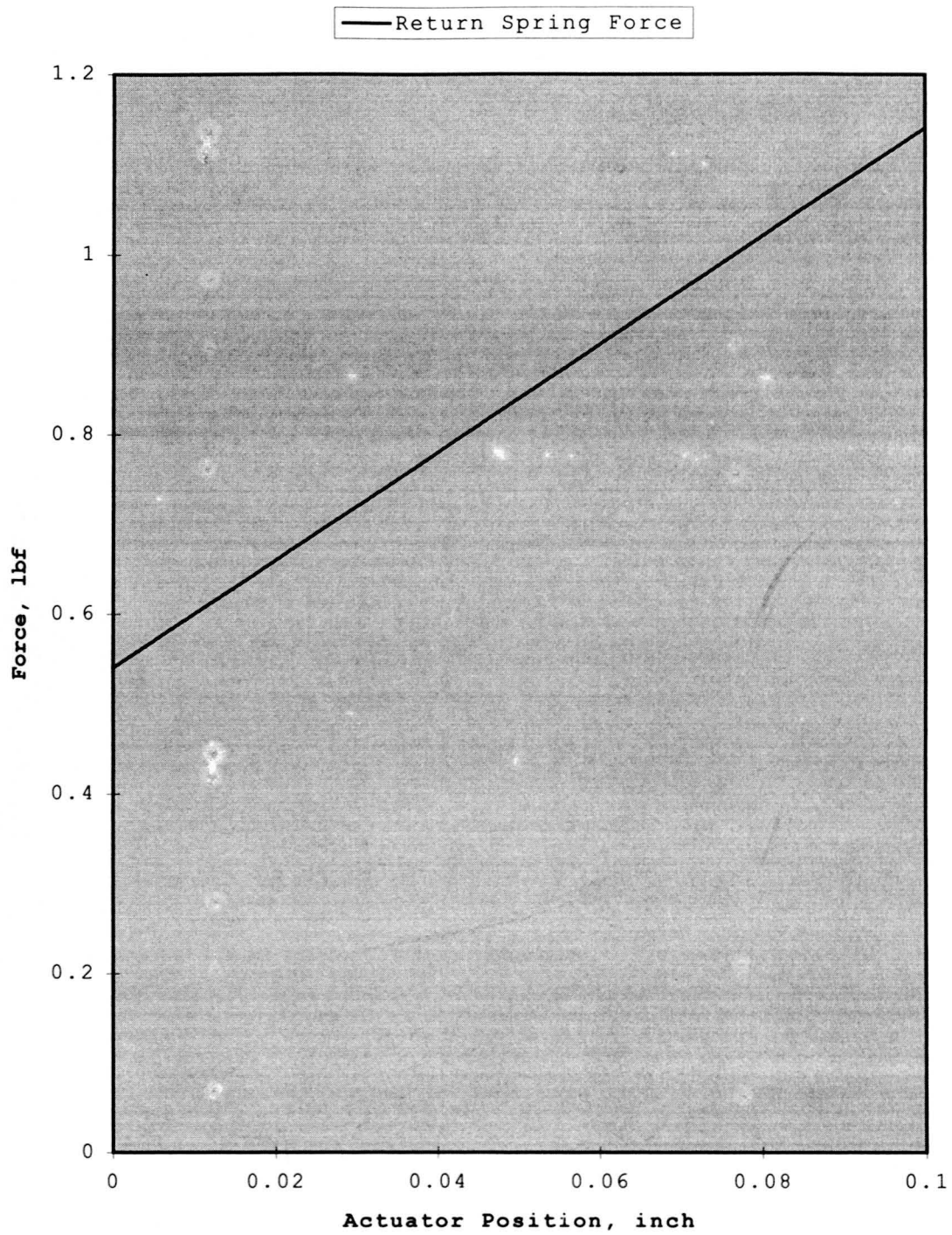


Figure 8.7: Return spring force as a function of actuator position, model

This equation is plotted in Figure 8.9 as a function of x and for various temperatures. Where the function crosses the x axis is the point of equilibrium for the actuator ball. Thus, this equation of motion holds for actuating spring temperatures up to approximately 112°F.

An evaluation was conducted for the position of the actuating ball ranging when $x > 0.065$ inch. At this position, the following equation governs the motion of the ball:

$$mx'' = F_{rs} - F_{as} + f + A^*(P_{rs}' - P_{as}) \quad (8.6)$$

At $x = 0.064$ inches, a mix pressure of 20 psi, pressure out of the valve of 2 psi, and a spring temperature of 111.5°F, the actuator ball is in equilibrium. At $x = 0.065$ inches and a spring temperature of 111.5°F the stagnation pressure results in an acceleration of the actuator ball toward the valve seat. Applying these conditions to equation 8.6, the acceleration of the actuator ball is 4607 ft/s². The actuator ball moves a total of 0.042 inches to reach the valve seat, this takes approximately 0.0043 seconds.

The flow equation for the valve is based upon relationships developed by Keller [1978] for orifices, and relationships developed by Fox and McDonald [1978] for sudden contractions and expansions. The following is the flow equation for the anti-scald valve:

$$Q_m = \{ [2*(P_m - P_o)] / (\rho * \Psi) \}^{0.5} \quad (8.9)$$

where:

P_m = Mix pressure into the valve, psf

P_o = Pressure out of the valve, psf

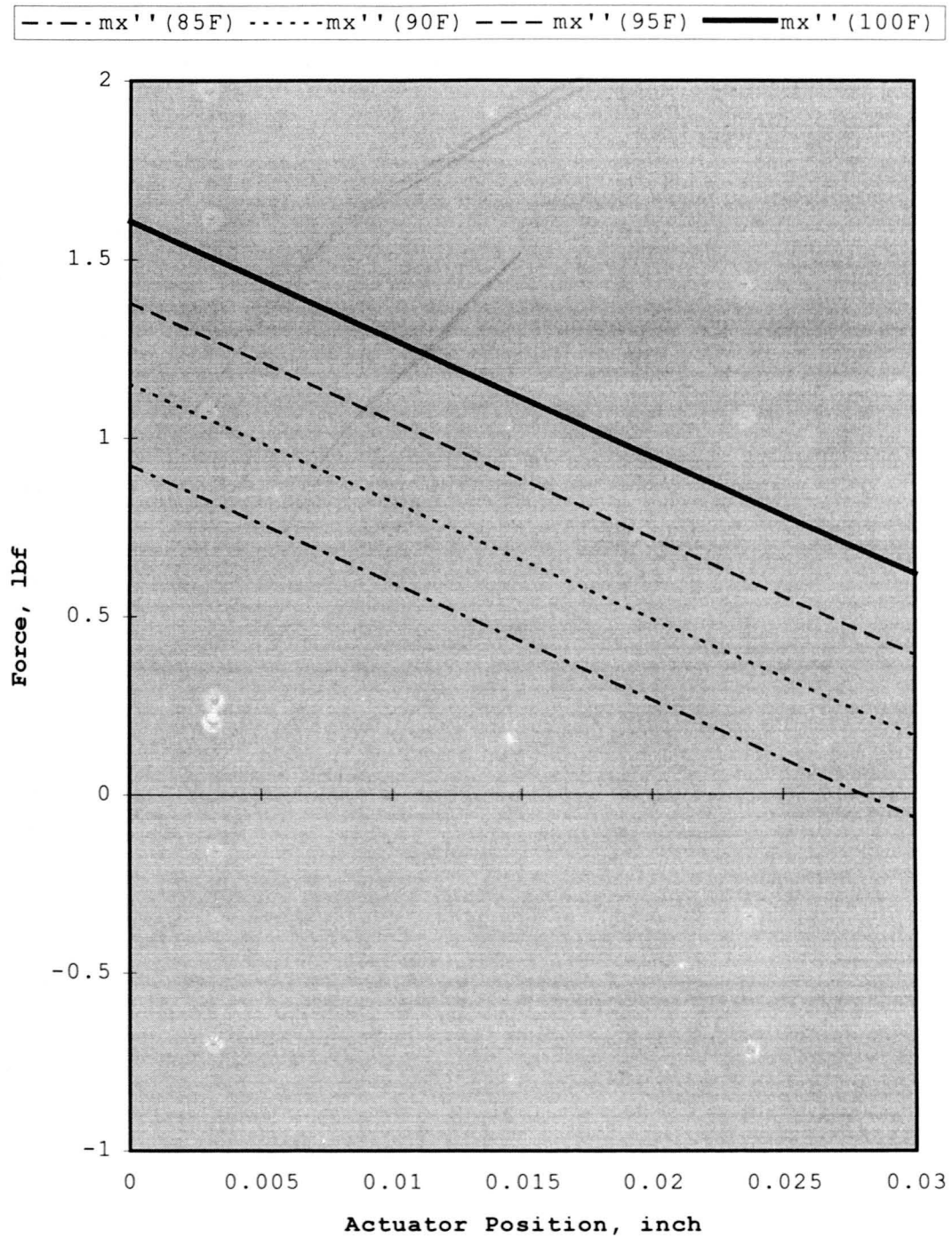


Figure 8.8: Actuator equilibrium equation as a function of position ranging from $0.00 < x < 0.030$, model

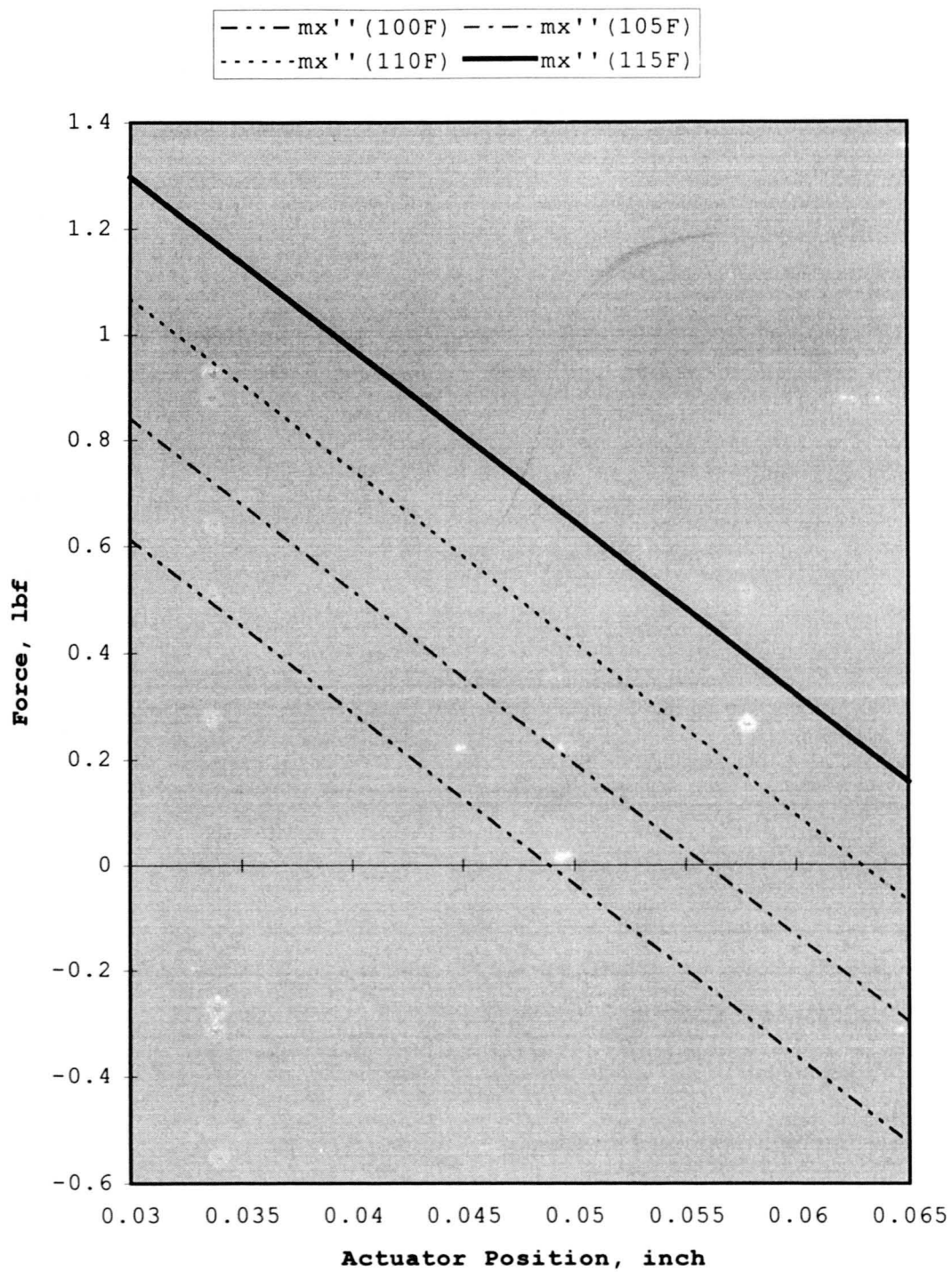


Figure 8.9: Actuator equilibrium equation as a function of position ranging from $0.03 < x < 0.065$, model

ρ = Density of the mix, slugs/ft³

$$\Psi = 1/(Ac \cdot C)^2 + Kc1/(A1)^2 + Ke2/(A2)^2 + 1/(Ac1 \cdot C)^2 + 1/(Ac2 \cdot C)^2$$

Ac = Orifice area of the secondary cage, ft²

C = Orifice coefficient (0.59)

Kc1 = Contraction coefficient for the valve inlet

A1 = Area of valve inlet, ft²

Ke2 = Expansion coefficient for the valve outlet

A2 = Area of valve outlet, ft²

Ac1 = Area of cage 1 orifice, ft²

Ac2 = Area of cage 2 orifice, ft²

System Testing

Tests were conducted on the anti-scald valve to obtain characteristic flow curves for the valve and to obtain information on the dynamic response of the valve. Figure 8.10 is a plot of the test results of the input mix temperature to the valve. A steady state condition is established at the location of the "Y" axis. During this test, the temperature of the mix supply is gradually increased until the valve actuator stops the flow of water to the shower head. Figure 8.11 is a plot of the mix pressure and is the pressure of the mix entering the valve. The valve stops the flow of

water between the time of 23:08:53 (hours, minutes, seconds) and 23:09:03 (hours, minutes, seconds) where the mix pressure spikes above 50 psi; this is the point where the actuator ball moves to the valve seat. Figure 8.12 is a plot of the hot and cold supply flow that develops into the mix flow for the valve.

Based on the characteristic equations developed for the anti-scald valve, the dynamic response of the valve was modeled. The test supply pressure and temperature will be used in the characteristic equations to evaluate the response of the valve. With a slow gradual temperature rise of the mix flow into the valve, the position of the actuator ball is dictated by the following force equilibrium equation as x approaches 0.065 inches:

$$mx'' = F_{rs} - F_{as} + f + A*(P_{rs}' - P_{as}) \quad (8.2)$$

For this equation, mx'' is a function of the actuator spring temperature and the actuator ball position (x). To calculate the steady state flow conditions using the characteristic equations, an iterative approach may be applied. An estimate is made of the actuator position (x). The force equilibrium equation 8.2 is evaluated. If the force is positive, the actuator position is decreased. If the force is negative, the actuator position is increased. The actuator position could be evaluated with a standard differential equation solver or by graphical methods given specific mix and output pressures. The expression may also be graphed for various actuator spring temperatures to identify when mx'' is equal to zero at an actuator ball position of 0.065 inch. This process will produce the mix temperature at which the anti-scald valve will close. Figure 8.13 graphs this equation as a

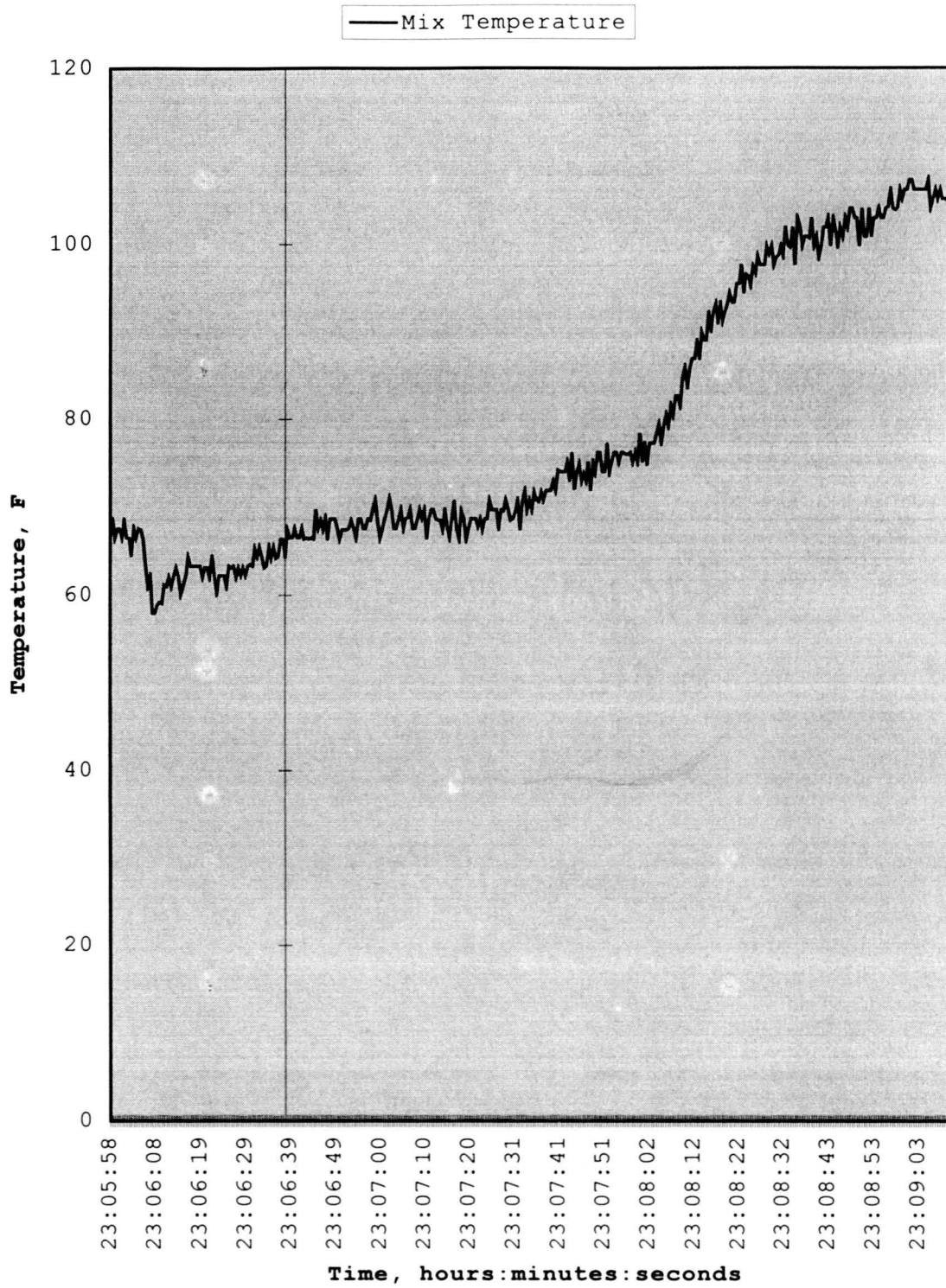


Figure 8.10: Anti-Scald valve test, gradual temperature increase, supply and mix temperature

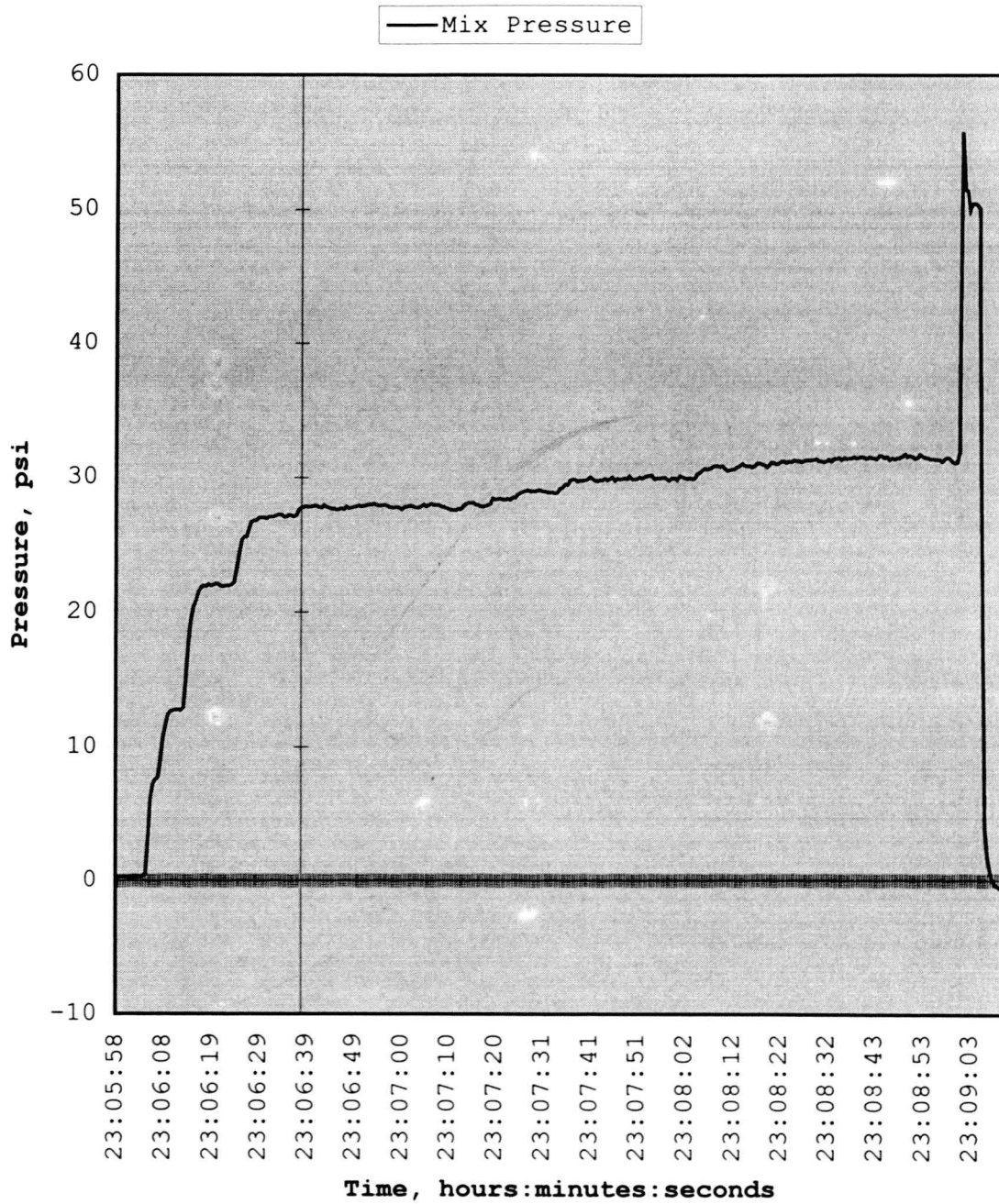


Figure 8.11: Anti-Scald valve test, gradual temperature increase, mix pressure

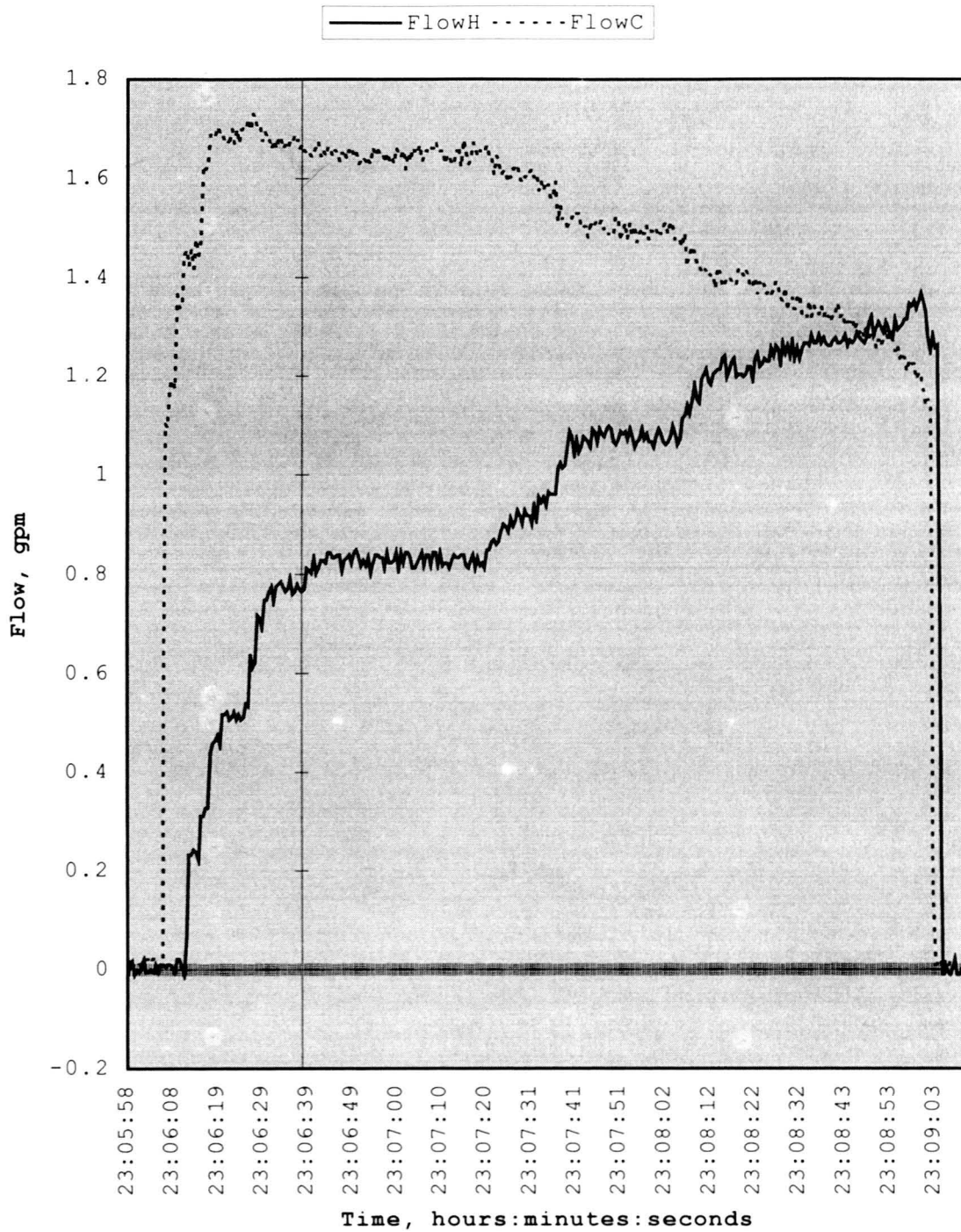


Figure 8.12: Anti-Scald valve test, gradual temperature increase, supply flow

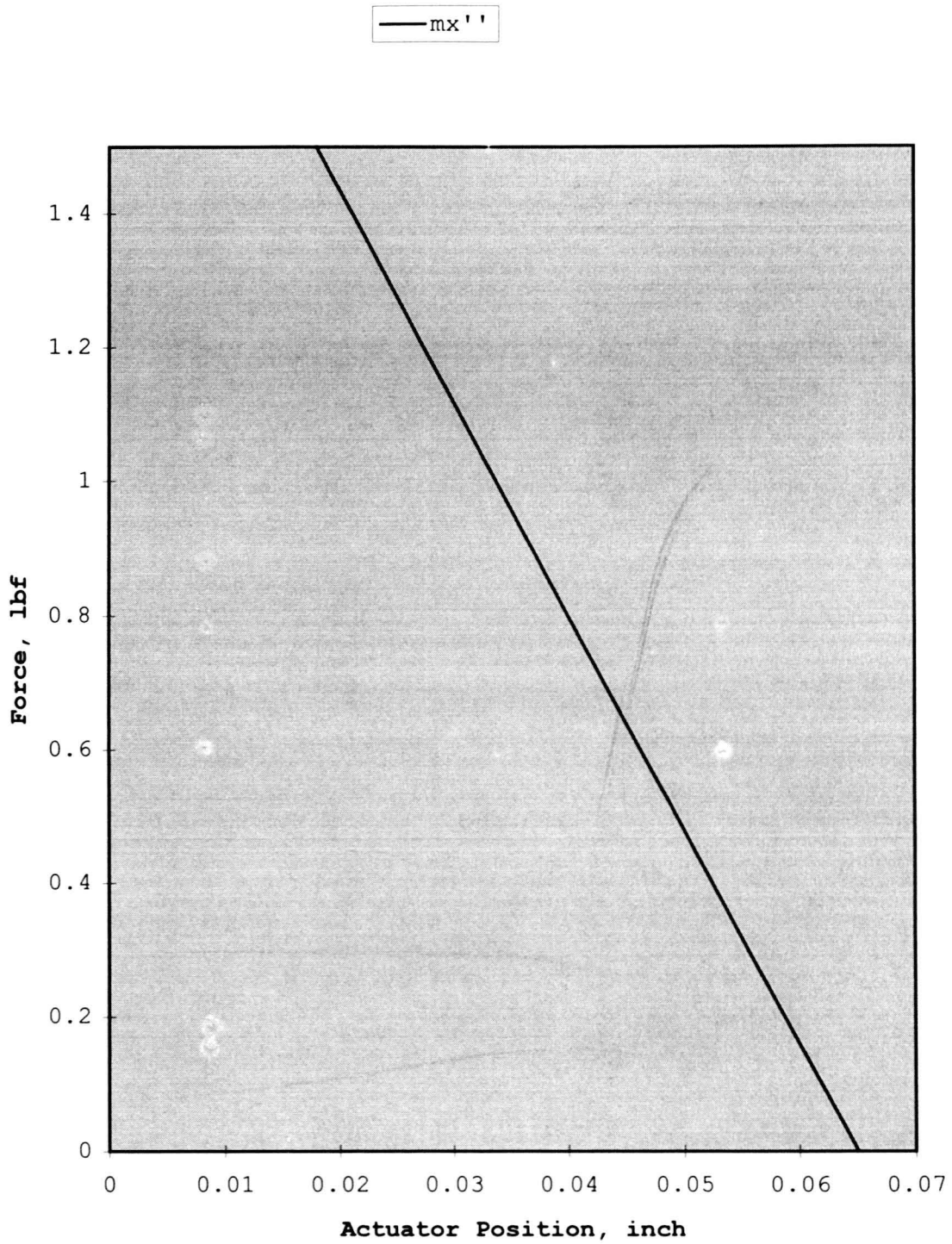


Figure 8.13: Anti-Scald valve model, force equation for the actuator ball, actuator spring temperature 108.5 °F

function of actuator position at a mix pressure of 30 psi and an actuator spring temperature of 108.5 °F. The anti-scald valve closed in the test at 106.5 °F.

Tests were conducted to record the response of the valve given a step change in the mix supply temperature. Supply pressure was not changed and the mix temperature was raised increasing the mix temperature to the anti-scald valve. Figure 8.14 is a graph of the mix supply temperature during the test. A steady state condition is established at the location of the "Y" axis. Figure 8.15 is a graph of the mix supply pressure during the test. The mix supply was turned to a full hot flow condition at 14:21:23.

The test pressure and temperature supplies will be used in the characteristic equations to evaluate the dynamic response of the valve. Given an initial set of steady state flow and pressure conditions, the mix supply temperature is changed. Given the following at time $t < 0$:

$$P_m = 20 \text{ psi}$$

$$T_m = 91^\circ\text{F}$$

For the flow at time $t = 0$:

$$Q_m = \{ [2 * (P_m - P_o)] / (\rho * \Psi) \}^{0.5} \quad (8.9)$$

$$Q_m = 1.86 \text{ gpm}$$

Based upon the pressure and temperature of the mix, and the temperature of the actuator spring, the position of the actuator may be evaluated by the iterative process discussed earlier. The actuator position at $t = 0$ is 0.0363 inches. Based on a time increment of 1 second, the supply mix pressure and the supply mix

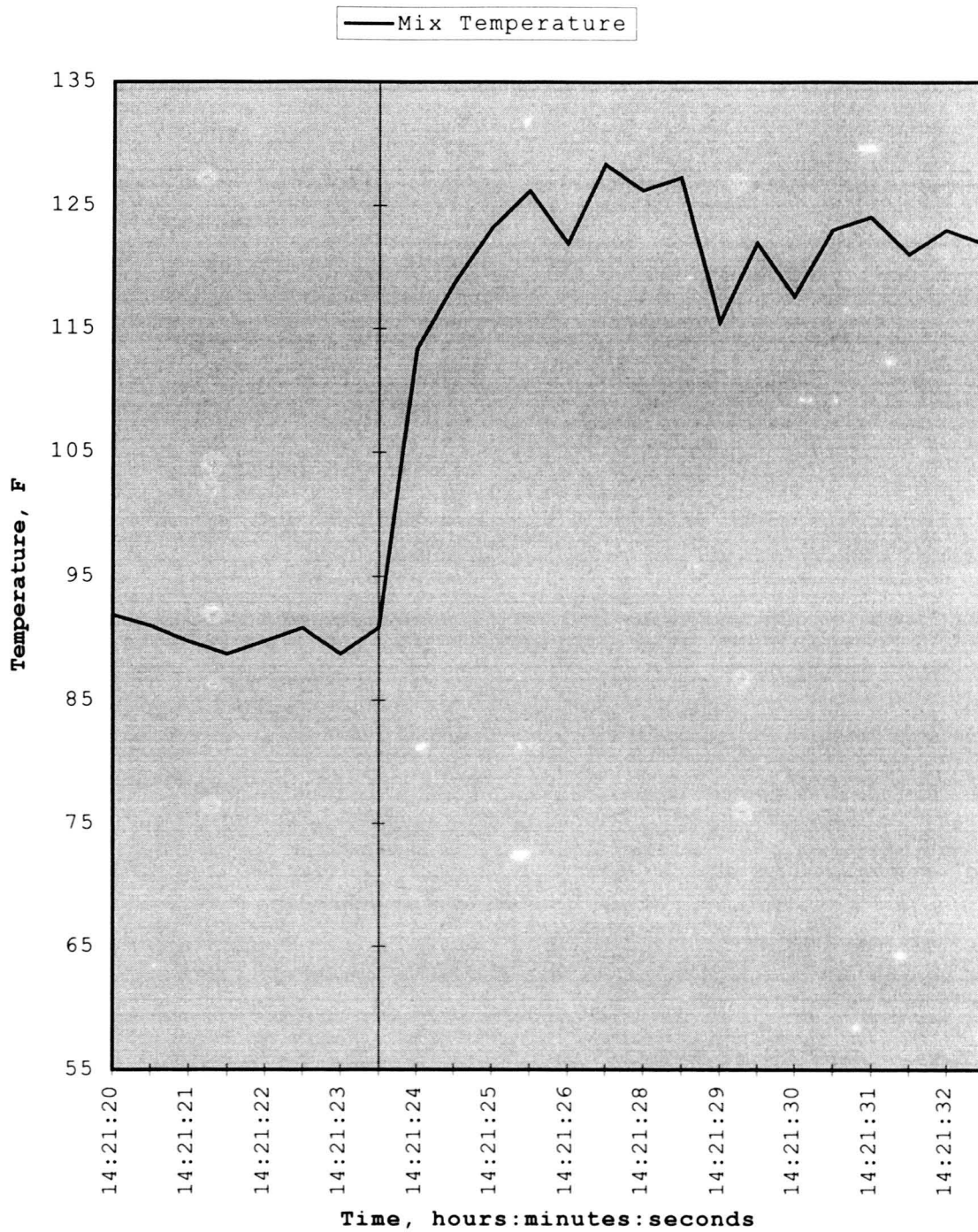


Figure 8.14: Anti-Scald valve test, increase in mix temperature, mix temperature

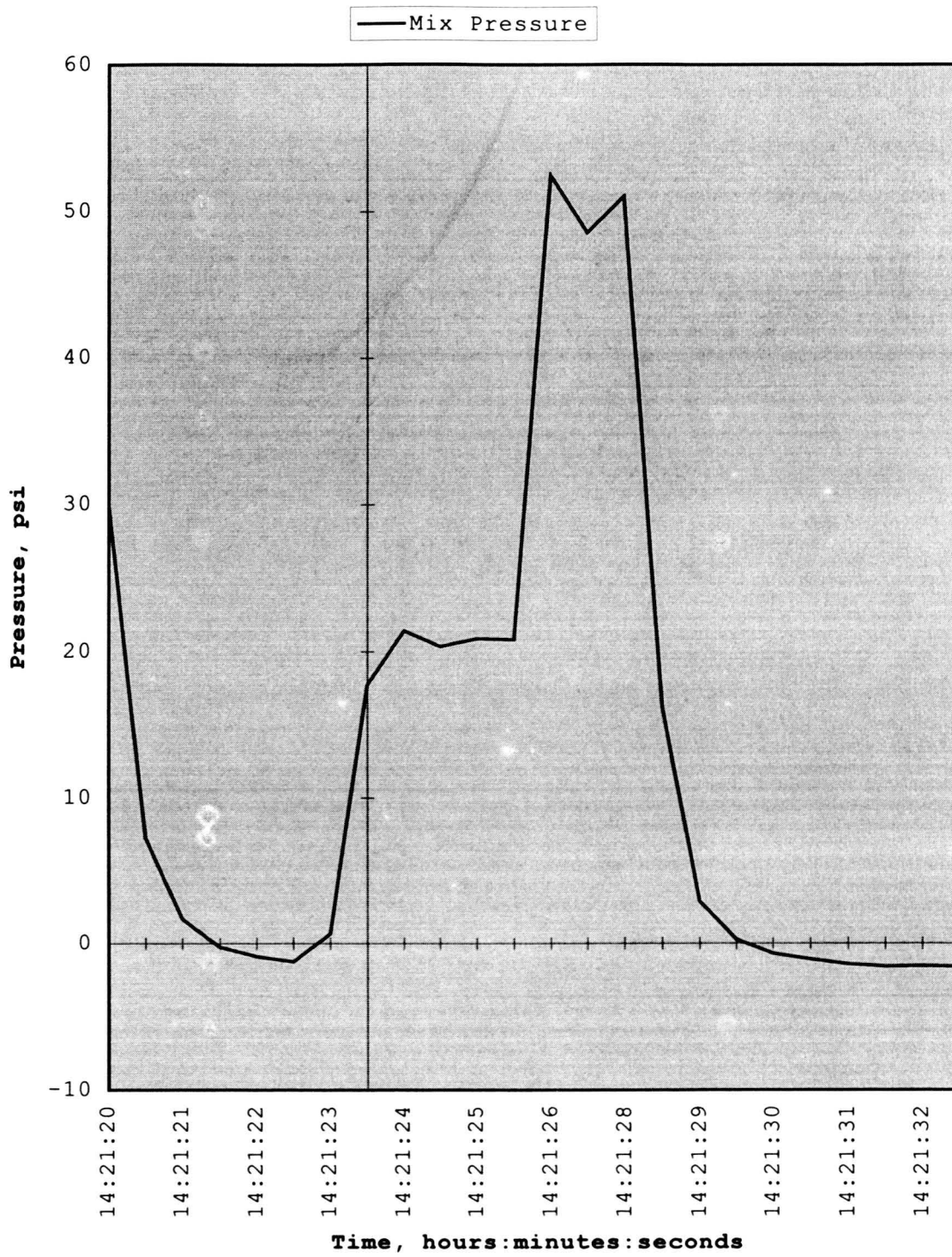


Figure 8.15: Anti-Scald valve test, increase in mix temperature, mix pressure

temperature, the length of the actuator spring may be calculated using equation 8.8 and the position of the actuator ball may then be evaluated using equations 8.1 or 8.2. This process is repeated until the actuator position of 0.065 inch is reached. At this position, the mix flow creates a stagnation pressure behind the actuator ball and the ball accelerates towards the valve seat at 3838 ft/s^2 . Figure 8.16 graphs the mix temperature and the actuator spring temperature based upon the characteristic equations, and Figure 8.17 graphs the actuator position. Figure 8.18 compares the supply mix pressure found in the test and predicted by the model. Figure 8.19 compares the supply mix flow found in the test and predicted by the model. The model predicts that the valve will close in 2 seconds, the test found that the valve closed between 2 and 2.5 seconds.

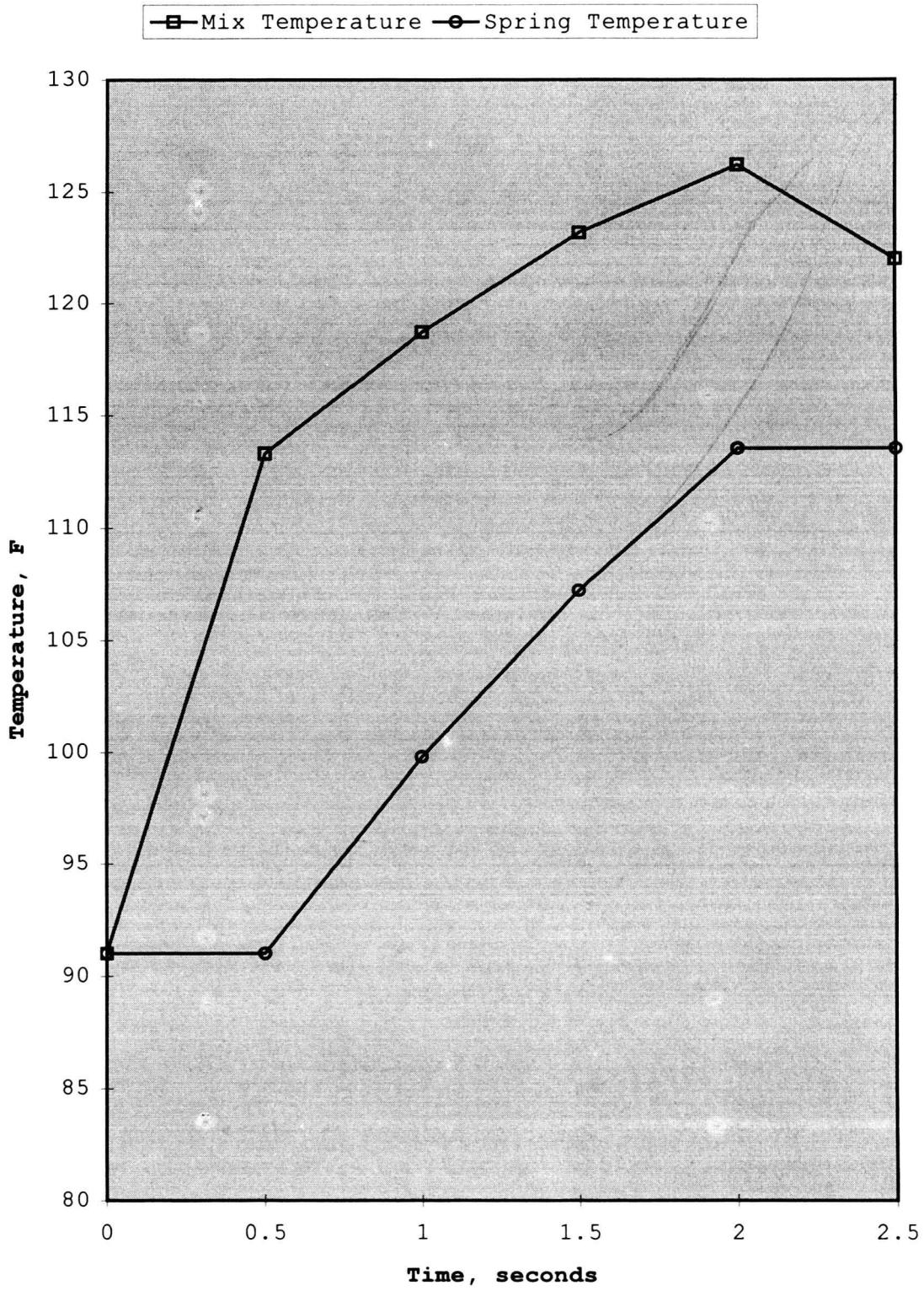


Figure 8.16: Anti-Scald valve model, increase in mix temperature, mix and actuator spring temperature

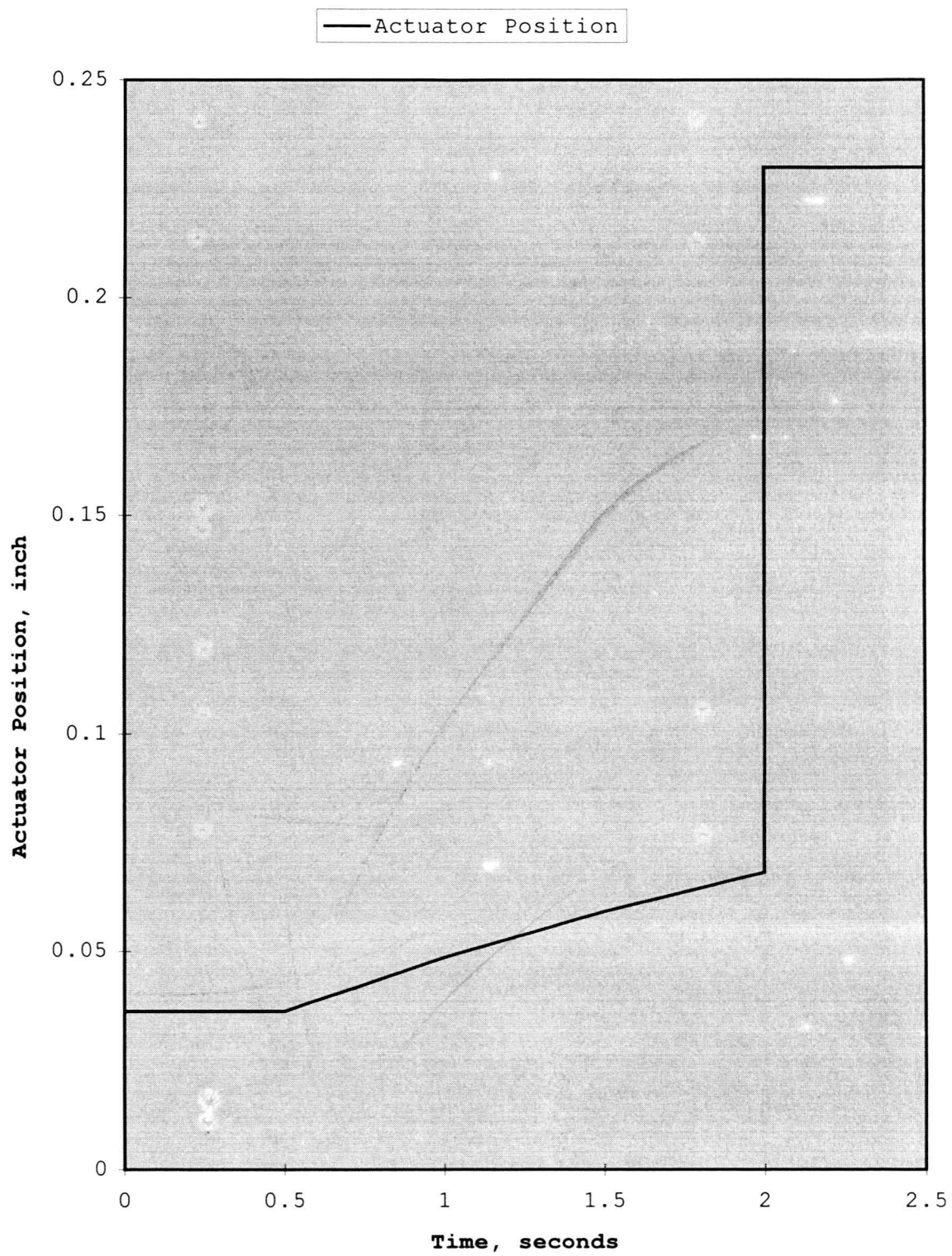


Figure 8.17: Anti-Scald valve model, increase in mix temperature, actuator position

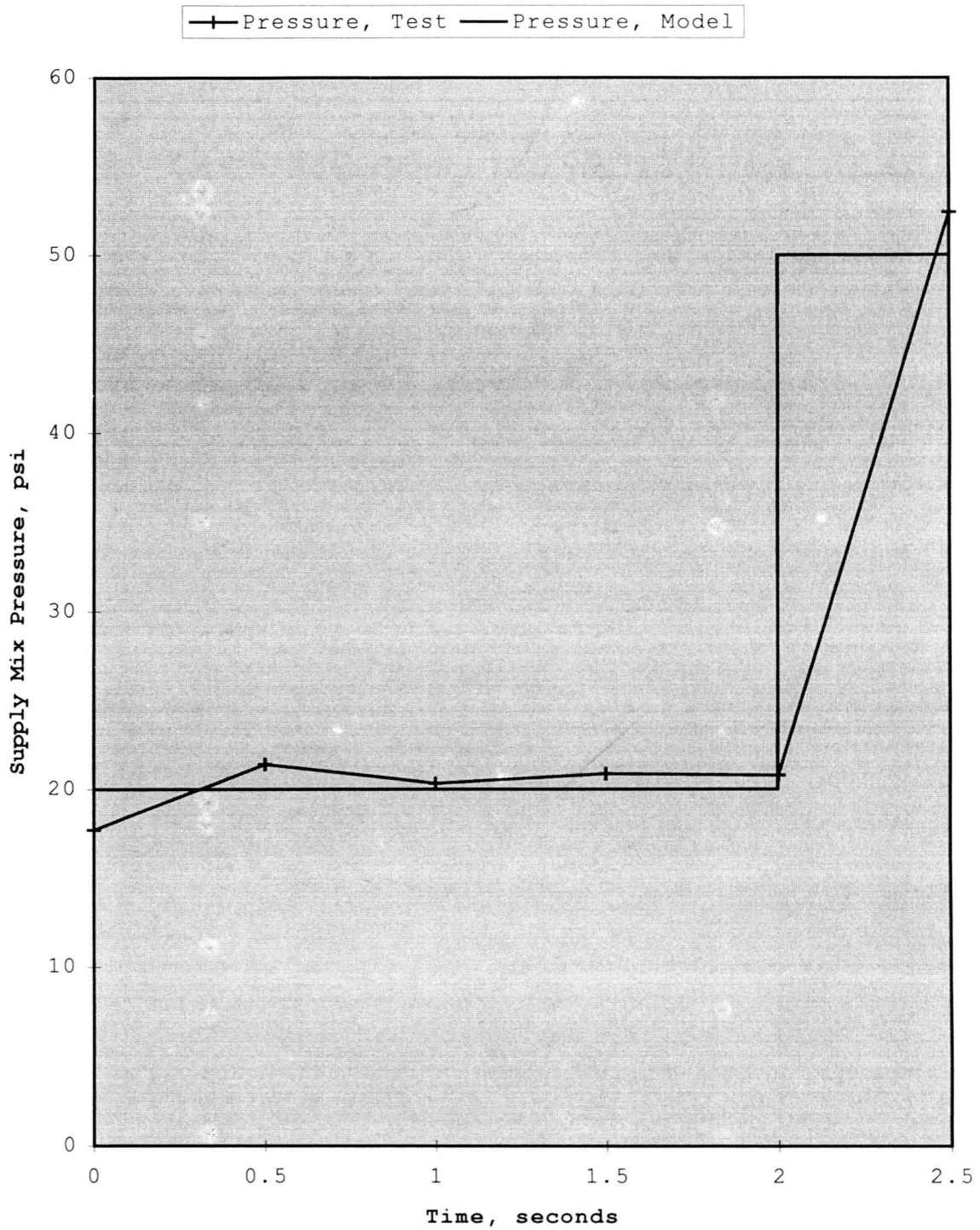


Figure 8.18: Anti-Scald valve test and model, increase in mix temperature, supply mix pressure

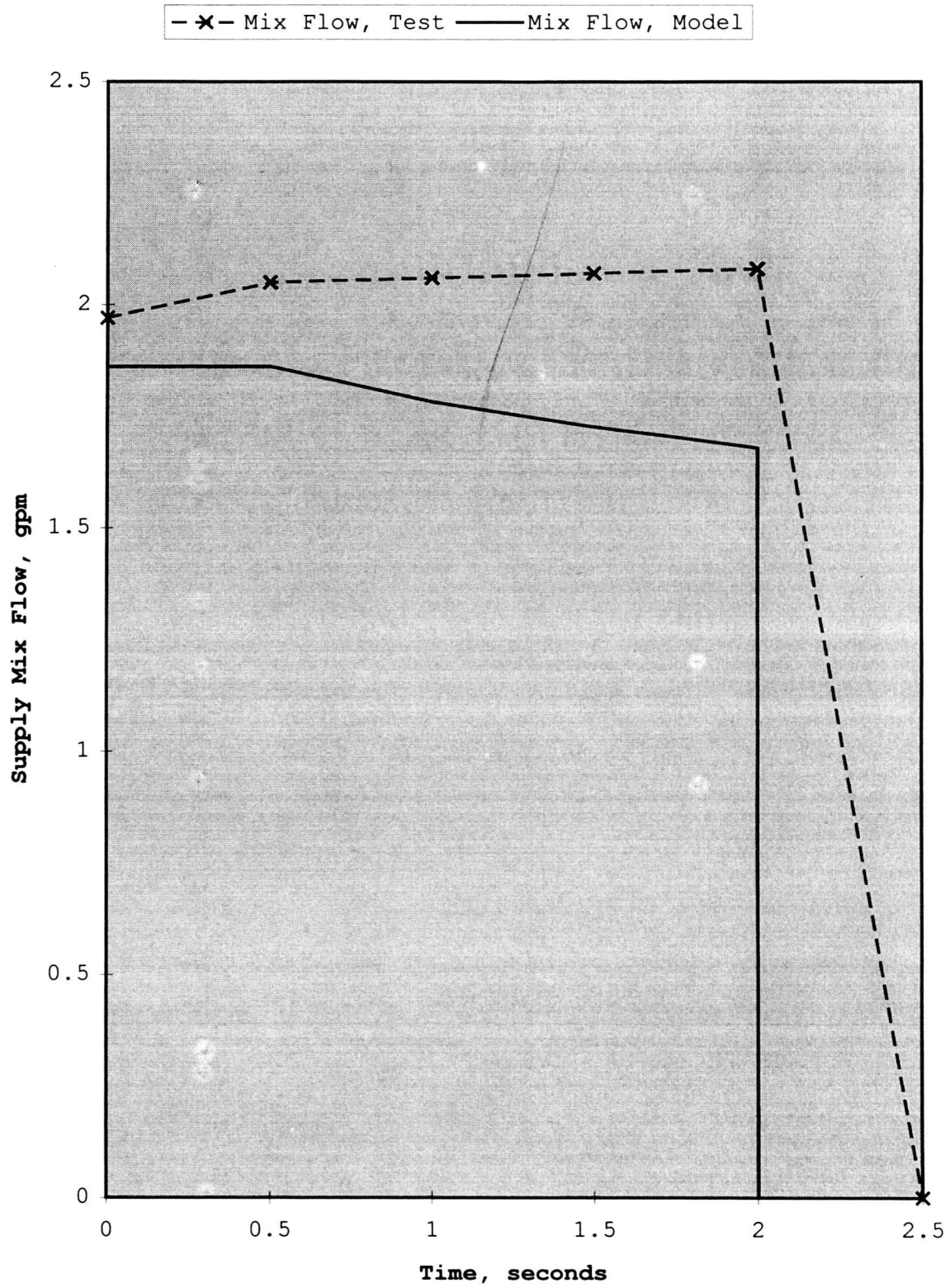


Figure 8.19: Anti-Scald valve test and model, increase in mix temperature, supply mix flow

CHAPTER 9. THERMOSTATIC MIXING VALVES

Automatic mixing valves are designed to minimize the effects of outlet water temperature changes due to both inlet pressure changes and inlet temperature changes. These types of valves are installed at the point of use and are typically used for bath and shower valves. Automatic mixing valves combine the design features and functions that are found with pressure balanced valves and with tempering valves. Combining both of these characteristics into the valve increases the valve mechanical complexity. It also increases the price to the consumer. This type of valve will require adjustment and testing during installation and will require periodic inspection and maintenance.

Maintenance of the valve may be required in several instances: when the water heater control temperature is changed, if there is failure of other temperature controlling devices in the plumbing system, and when there are contaminants that affect the operation of the valve.

Valve Design

A commercially available automatic mixing bath and shower valve was obtained. The valve design has two controls, one to

adjust the temperature of the mix water and one control to open and close the flow of water through the valve. The installer must adjust the valve to deliver water at a maximum temperature. A manufacturer instructs the installer that both hot and cold water must be available to properly install and adjust the valve. The instructions direct the installer to adjust the valve to a maximum mix temperature of 112°F. The valve face-plate has temperature readings from 95°F to 105°F and the valve handle will rotate a maximum of 180 degrees. Their instructions do not include any recommendations to the installer or the user on periodic cleaning or maintenance of the valve.

Figure 9.1 is a cross sectional view of the mixing valve. The key components of the valve assembly are: 1) a valve body, 2) a spool housing, 3) a spool casing, 4) a spool, 5) a thermostat assembly, 6) an adjustment nut and, 7) a valve handle.

Hot and cold half inch copper supply lines are attached to the inlet of the valve body ("A" and "B" respectively in Figure 9.2). Hot and cold water enters the casting assembly and initially flows through screen filters and backflow check valves (not shown in figure). The hot supply water flows through cast channel "B" and cold supply water flows through cast channel "C" to the spool housing cavity. The supply water flows through orifices in the spool housing cavity "E" and then through the inlet orifice of the spool casing "F". The spool travels axially in the casing and its position determines the inlet orifice area for both the hot and cold supply flow. The supply water then travels out of the spool outlet

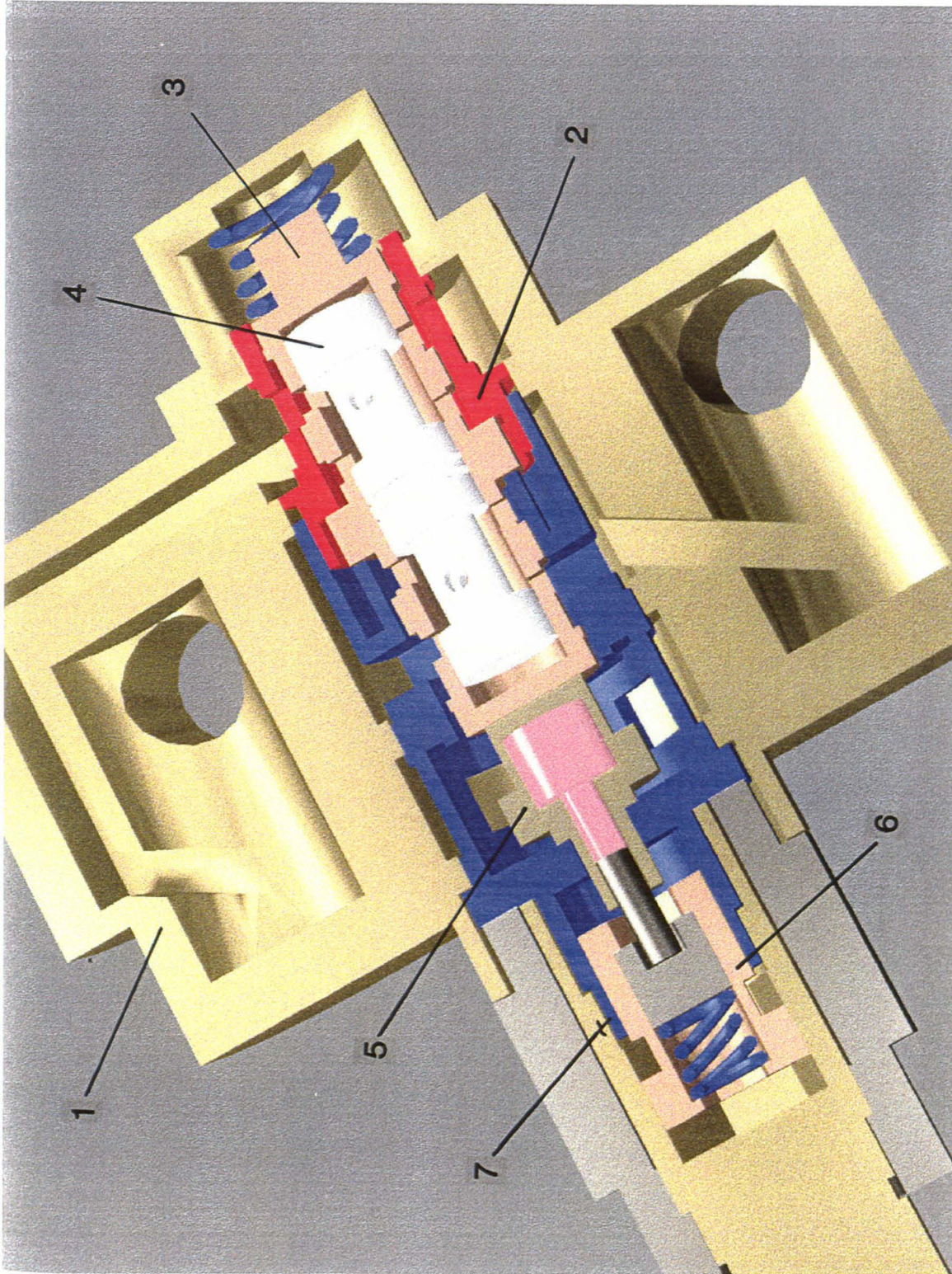


Figure 9.1: Cross section view of mixing valve

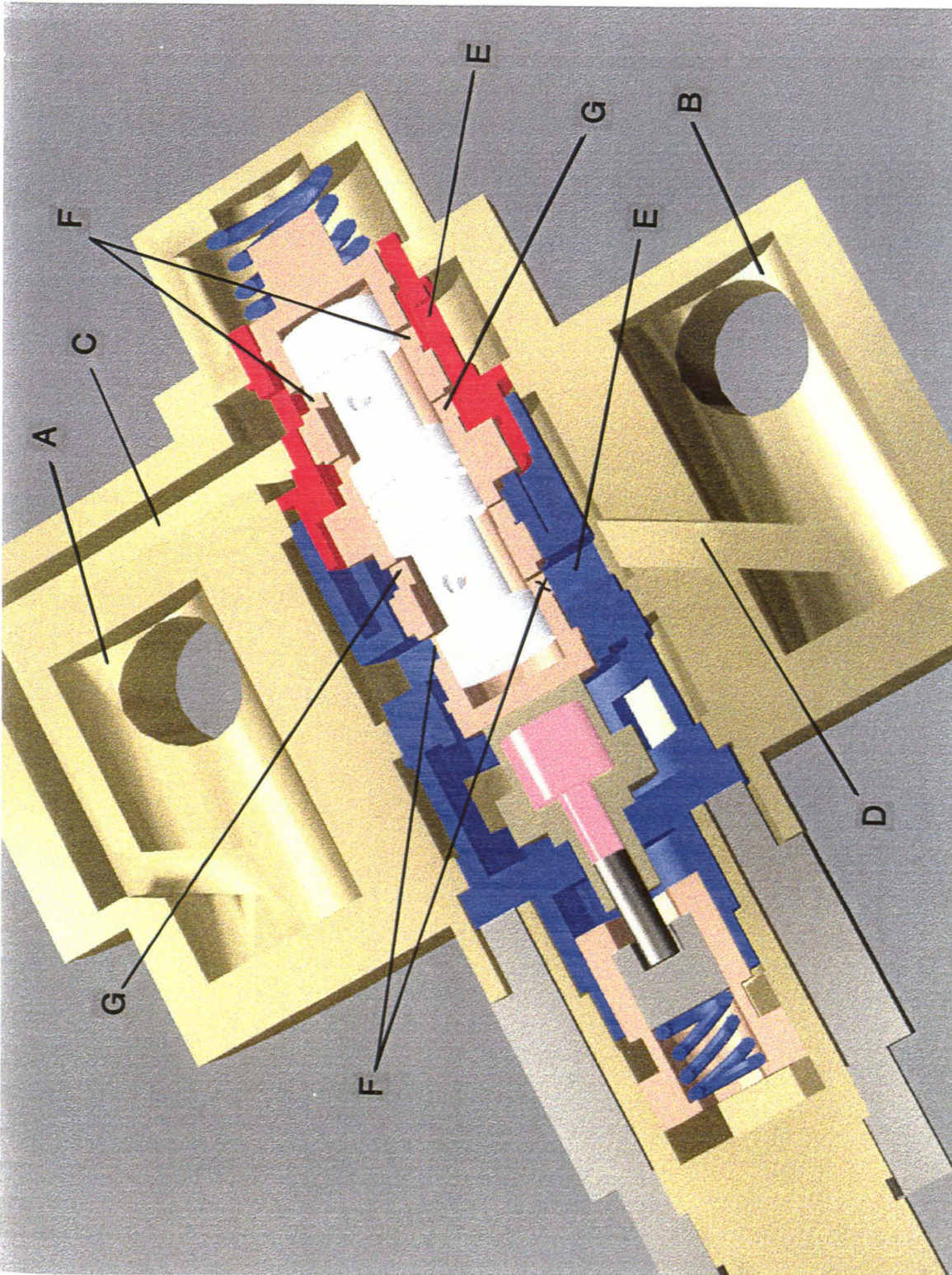


Figure 9.2: Cross section view of mixing valve components

orifice "G". The end of the valve with the adjustment handle will be referred to as the front of the valve.

The spool casing is positioned axially in the spool housing by the position of the valve handle and by the effective length of the thermostat. As the valve handle is rotated counterclockwise, the adjustment nut rotates away from the spool. This allows the spool casing to move towards the front of the valve. The nut moves axially 0.030 inch when turning the handle 180 degrees. As the temperature of the thermostat assembly increases, the length of the assembly increases and moves the spool casing towards the back of the valve.

The hot and cold supply flows out of the spool casing exit orifice and then flows through an area between the spool casing and the spool housing ("H" in Figure 9.3). As the spool casing moves axially in the valve, the flow area for the hot and cold supply is affected. The total travel for the spool casing is approximately 0.060 inch.

When the travel of the spool casing is as far towards the front of the valve as possible, the axial length of the flow area for the cold supply flow is 0 inches and the axial length for the hot supply flow is 0.060 inches. When the travel of the spool casing is as far towards the rear of the valve as possible, the axial length of the flow area for the cold supply flow is 0.060 inches and the axial length for the hot supply flow is 0 inches.

Once the supply flow passes this variable flow area, the hot and cold water are mixed and travel axially toward the front of the valve. The mix flows through an orifice ("I") prior to flowing

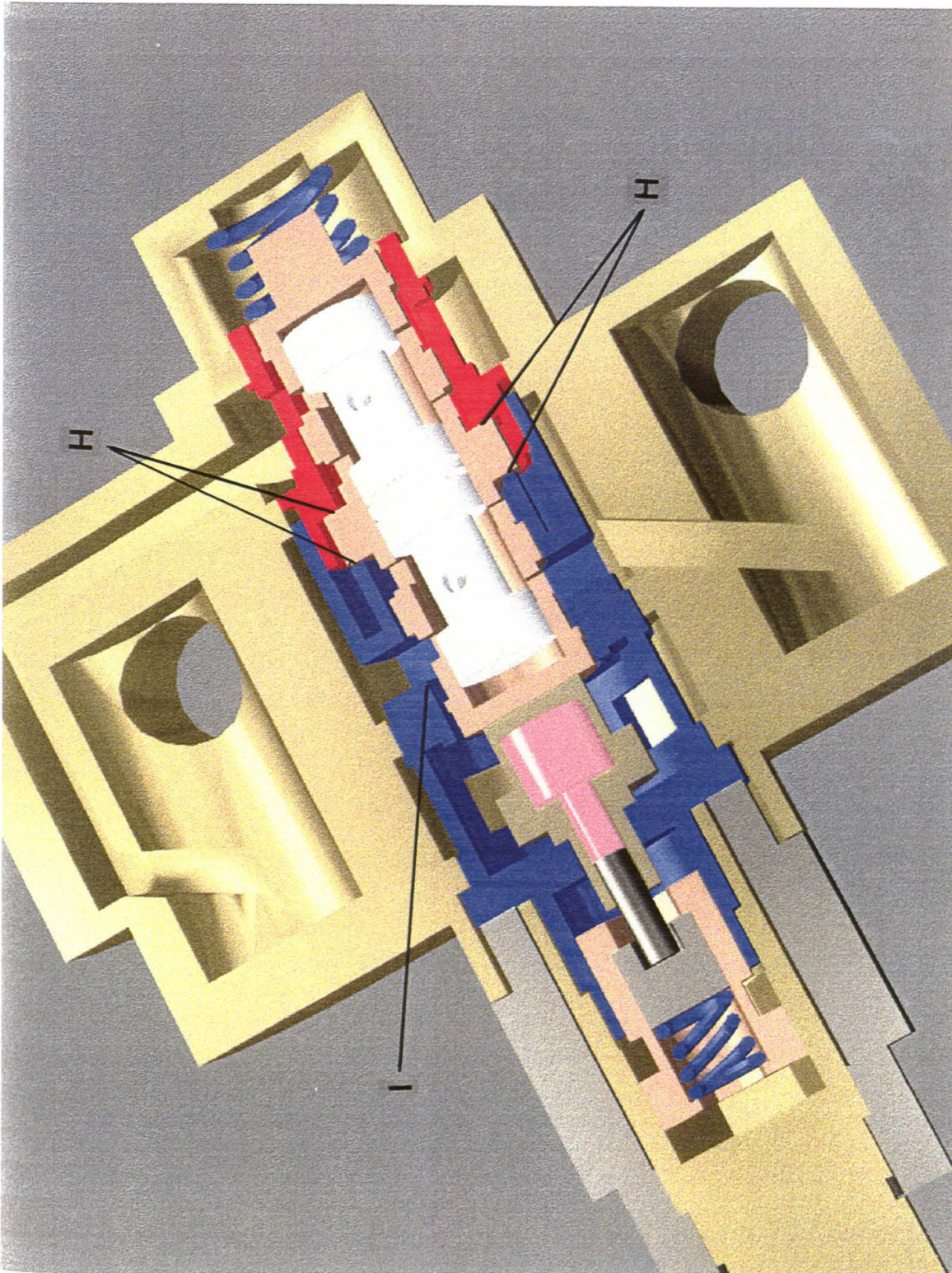


Figure 9.3: Cross section view of mixing valve

around the thermostat assembly. At this point, the mix travels out of the spool housing, through an exit orifice in the casting, and to the valve that controls the mix flow to the shower head.

System Modeling

The modeling assumptions include incompressible flow, the utilization of contraction and expansion coefficients and equations as defined by Fox and McDonald [1978], and the utilization of orifice coefficients and flow equations as defined by Keller [1978]. The model will include: 1) the head loss from the sudden expansion from the supply line into the valve casting, 2) the head loss from the sudden contraction from the casting into the filter and check valve, 3) the head loss from the sudden expansion from the filter and check valve into the valve cavity, 4) the head loss at the spool housing inlet orifice, 5) the head loss at the spool casing inlet orifice 6) the head loss at the spool casing outlet orifice, 7) the head loss in the variable area between the spool casing and the spool housing, 8) the head loss in the spool housing axial orifice, 9) the head loss in the spool housing exit orifice, 10) the head loss in the casting outlet orifice and, 11) the head loss in the flow control orifice.

The spool casing inlet and outlet orifices will vary depending on the position of the spool. When the spool is centered axially in the spool casing, this position will be defined as $x_s = 0$ inches. The total travel of the spool may range from $-0.060 < x_s < 0.060$

inches. The spool inlet and outlet areas are dependent upon the position of the spool and therefore are a function of x . The spool orifices are rectangular openings. The effective orifice area is determined by the position of the spool as the spool lands passes by the rectangular orifice (see items "F" and "G" in Figure 9.2). For the cold supply flow the spool inlet orifice area may be defined as follows:

$$A_{sci} = N_i * L * W * (0.06 - x_s) / .12 \quad (9.1)$$

where:

A_{sci} = Area of spool cold inlet, ft^2

N_i = Number of inlet orifices

L = Orifice length, ft

W = Orifice width, ft

x_s = Spool position, inches

For the cold water spool outlet, the orifice area may be defined as follows:

$$A_{sco} = N_o * L * W \quad \text{For } -0.60 < x_s < 0 \quad (9.2)$$

$$A_{sco} = N_o * L * W * (0.12 + x_s) / 0.12 \quad \text{For } 0 < x_s < 0.06 \quad (9.3)$$

where:

A_{sco} = Area of spool cold outlet, ft^2

N_o = Number of outlet orifices

L = Orifice length, ft

W = Orifice width, ft

x_s = Spool position, inches

For the hot supply flow, the spool inlet orifice area may be defined as follows:

$$\text{Ashi} = \text{Ni} * \text{L} * \text{W} * (0.06 + \text{xs}) / .12 \quad (9.4)$$

where:

Ashi = Area of spool hot inlet, ft²

Ni = Number of inlet orifices

L = Orifice length, ft

W = Orifice width, ft

xs = Spool position, inches

For the hot water spool outlet, the orifice area may be defined as follows:

$$\text{Asho} = \text{No} * \text{L} * \text{W} \quad \text{For } 0 < \text{xs} < 0.06 \quad (9.5)$$

$$\text{Asho} = \text{No} * \text{L} * \text{W} * (0.12 - \text{xs}) / 0.12 \quad \text{For } -.060 < \text{xs} < 0 \quad (9.6)$$

where:

Asho = Area of spool hot outlet, ft²

Ni = Number of outlet orifices

L = Orifice length, ft

W = Orifice width, ft

xs = Spool position, inches

The spool valve has 4 inlet and 4 outlet orifices for both the hot and cold supply lines. As the spool moves axially in the spool casing, the effective area of the inlet and outlet orifices are affected. The area of the spool casing supply inlets and outlets are graphed in Figure 9.4 and Figure 9.5.

The flow area between the spool casing and the spool housing for the hot and cold supply water is a function of the spool casing position. When the spool casing is positioned as far to the front of the valve as possible, the cold supply flow area is 0. If the

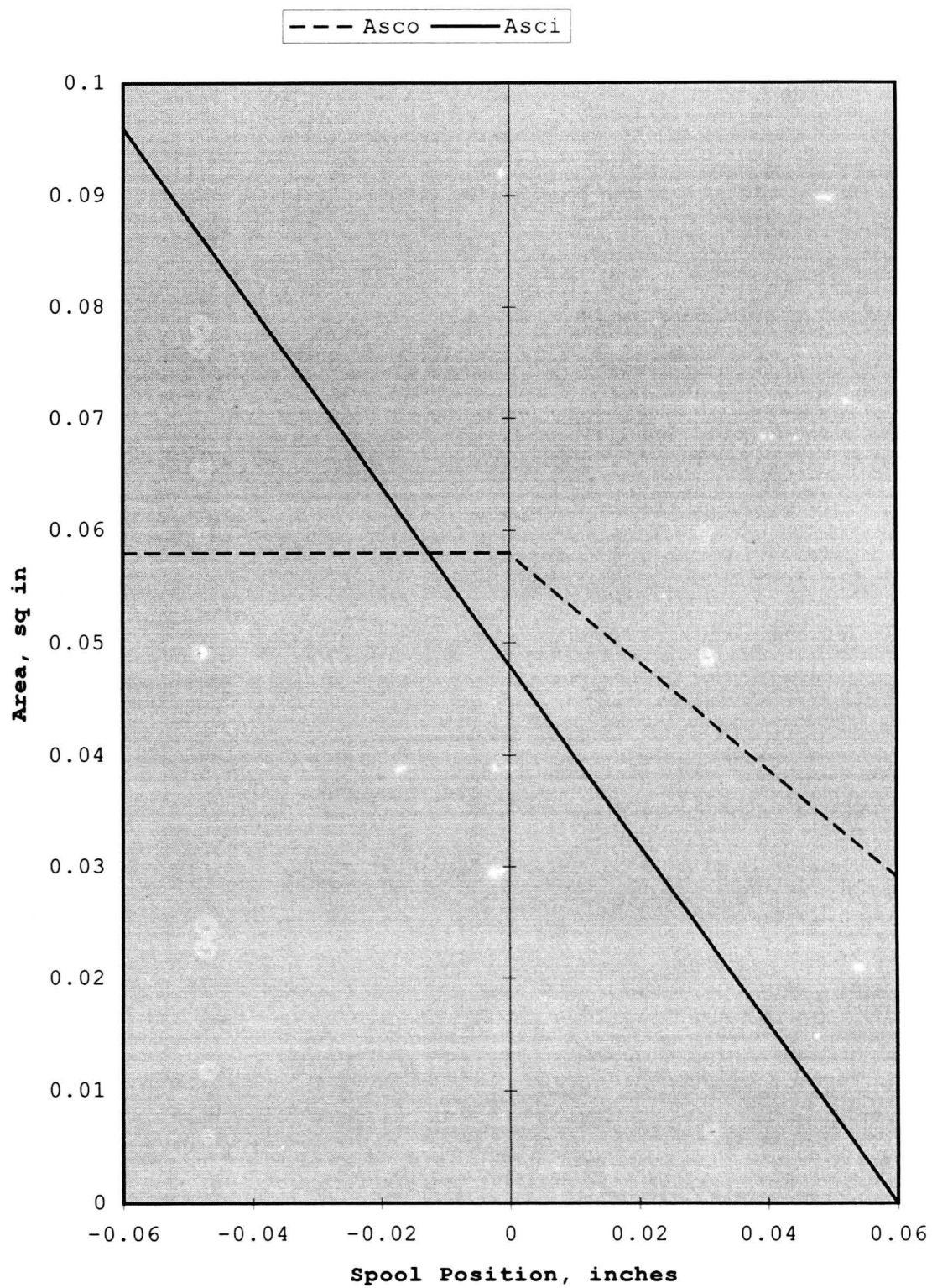


Figure 9.4: Spool casing cold supply inlet and outlet area, model

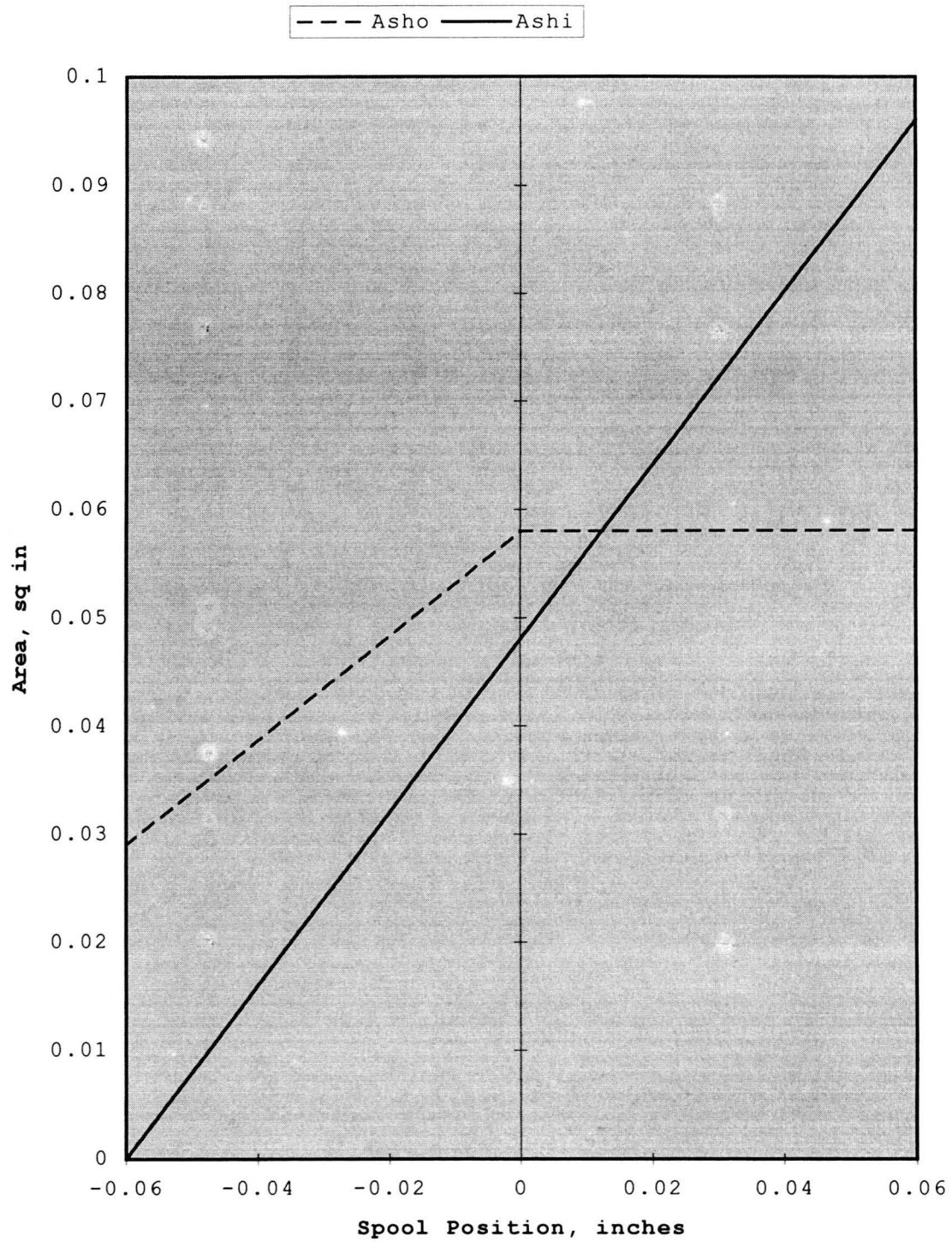


Figure 9.5: Spool casing hot supply inlet and outlet area, model

thermostat assembly is adjusted to be flush with the spool casing at a temperature of 95°F, a relationship between the valve handle position, the thermostat length, and the spool case position may be obtained. At this position, the thermostat assembly position will be defined as $x_t = 0$. The total travel of the spool casing is from 0 inches to 0.06 inches. The cold supply flow area may be defined as follows:

$$A_{ct} = \pi * D_c * (x_t - \theta * P_n / 180) \quad (9.7)$$

where:

A_{ct} = Area for cold supply flow, ft^2

D_c = Diameter of spool casing at flow area, ft

θ = Valve handle position (varies from 0 to 180 degrees)

P_n = Adjustment nut thread pitch, inches

x_t = Spool casing position, inches

The hot supply flow area may be defined as follows:

$$A_{ht} = \pi * D_c * (0.021 - x_t + \theta * P_n / 180) \quad (9.8)$$

where:

A_{ht} = Area for hot supply flow, ft^2

The thermostat assembly of the mixing valve was removed to characterize its operation. The assembly was placed in water at various temperatures, and the total length of the assembly was recorded. Table 9.1 summarizes the results.

Assuming a linear relationship between the length of the thermostat assembly and its temperature, the relationship is

characterized by the following equation using a least squares data fit:

$$L = 1.0547 + 0.00151 \cdot T_s \quad (9.9)$$

where:

L = Length of the thermostat assembly, inches

T_s = Temperature of the thermostat, °F

Table 9.1: Thermostat Length as a Function of Temperature

| | | | | | | | | | | |
|------------------|------|------|------|------|------|------|------|------|------|------|
| Temperature (°F) | 70 | 80 | 88 | 100 | 110 | 120 | 132 | 145 | 165 | 190 |
| Length (inches) | 1.15 | 1.17 | 1.18 | 1.21 | 1.23 | 1.25 | 1.27 | 1.29 | 1.20 | 1.32 |

Figure 9.6 is a plot of the raw data and characteristic equation.

Experimental data was then taken of the length of the thermostat assembly as the thermostat was exposed to 190°F water. Table 9.2 summarizes the results.

Assuming negligible internal resistance to the flow of heat and that the solid is uniform and varies only with time, the following characterizes the data using a least squares data fit:

$$L = L_f - (L_f - L_o)e^{-.151 \cdot t} \quad (9.10)$$

where:

L = Length of the thermostat assembly, inches

L_f = Length of the thermostat at the convective environment

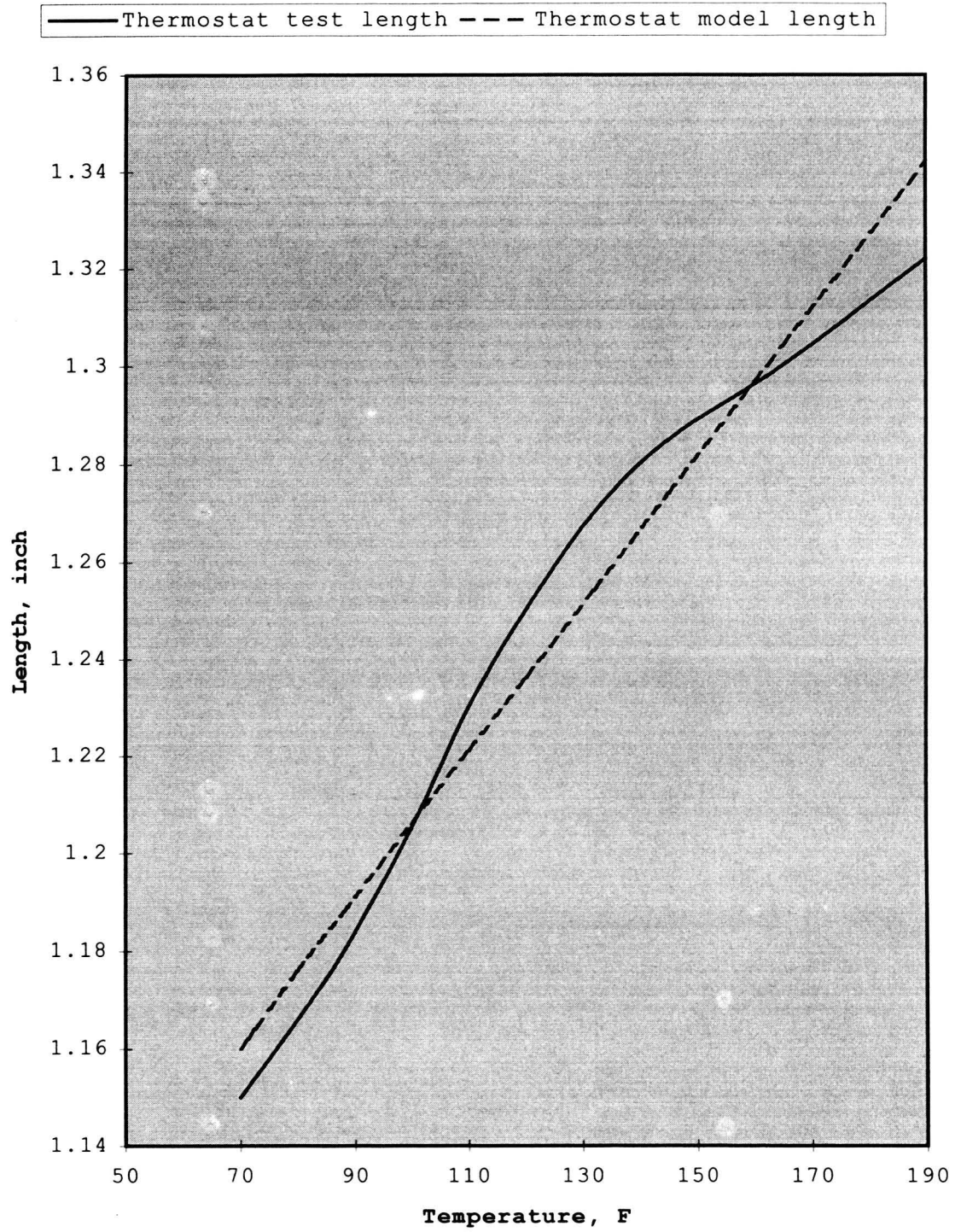


Figure 9.6: Thermostat length as a function of temperature, test and model

temperature, inches

L_0 = Initial length of thermostat, inches

t = time exposed to the convective environment, sec

Table 9.2 - Thermostat Length as a Function of Time and ΔT

| | | | | | |
|-----------------------|------------------|--|--|--|--|
| $L_0^1 = 1.15$ inches | $L_f^2 = 1.322$ | | | | |
| $T_0^3 = 70$ °F | $T_f^4 = 190$ °F | | | | |

| | | | | | |
|-----------------|------|------|------|------|------|
| Time (seconds) | 0 | 3 | 6 | 12 | 30 |
| Length (inches) | 1.15 | 1.20 | 1.25 | 1.30 | 1.32 |

¹ L_0 = Initial thermostat length, inches

² L_f = Final thermostat length, inches

³ T_0 = Initial thermostat temperature, °F

⁴ T_f = Final thermostat temperature, °F

Figure 9.7 is a plot of the raw data and the following characteristic equation using a least squares data fit:

$$T_s = T_f - (T_f - T_0)e^{-.151*t} \quad (9.11)$$

The length of the thermostat assembly may now be related to the spool casing position. Assuming that the adjustment nut is adjusted against the thermostat assembly to deliver 113°F at $\theta = 180$ degrees, the following is the relationship between the temperature of the thermostat assembly and x_t :

$$x_t = (1.0547 + .00151 * T_s) - 1.1867 \quad (9.12)$$

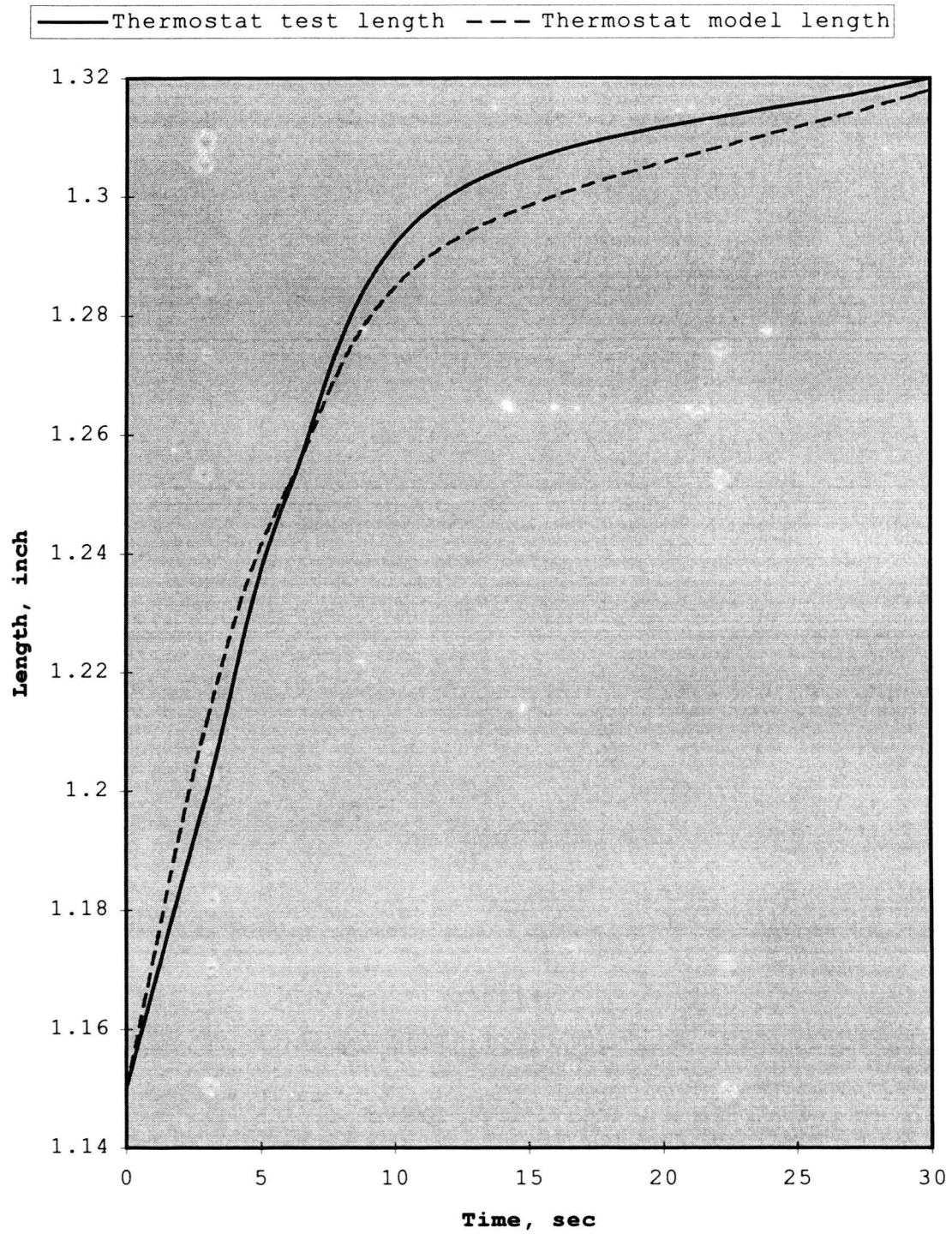


Figure 9.7: Thermostat dynamic reaction to a 190°F water bath, test and model

where:

x_t = Position of thermostat assembly, inches

T_s = Temperature of the thermostat assembly, °F

The hot and cold supply flow area may now be calculated for various positions of the valve handle ($0^\circ < \theta < 180^\circ$) and the temperature of the thermostat assembly. Figure 9.8 graphs the hot and cold supply flow area as a function of the thermostat temperature at valve handle positions equal to 0, 90 and 180 degrees.

To define the characteristic equation for the mixing valve the following system variables are defined:

P_c = Cold input supply pressure to the valve, psf

P_h = Hot input supply pressure to the valve, psf

P_m = Mix output pressure to the shower head or tub spout, psf

θ = Valve Handle Position, degrees

x_s = Spool position, inches

Q_c = Cold water supply flow, ft³/sec

Q_h = Hot water supply flow, ft³/sec

P_{sc} = Pressure on cold supply side of spool, psf

P_{sh} = Pressure on hot supply side of spool, psf

P_{cc} = Pressure in spool housing where hot and cold supplies
mix

ρ = Density of water, slugs/ft³

C = Orifice Coefficient

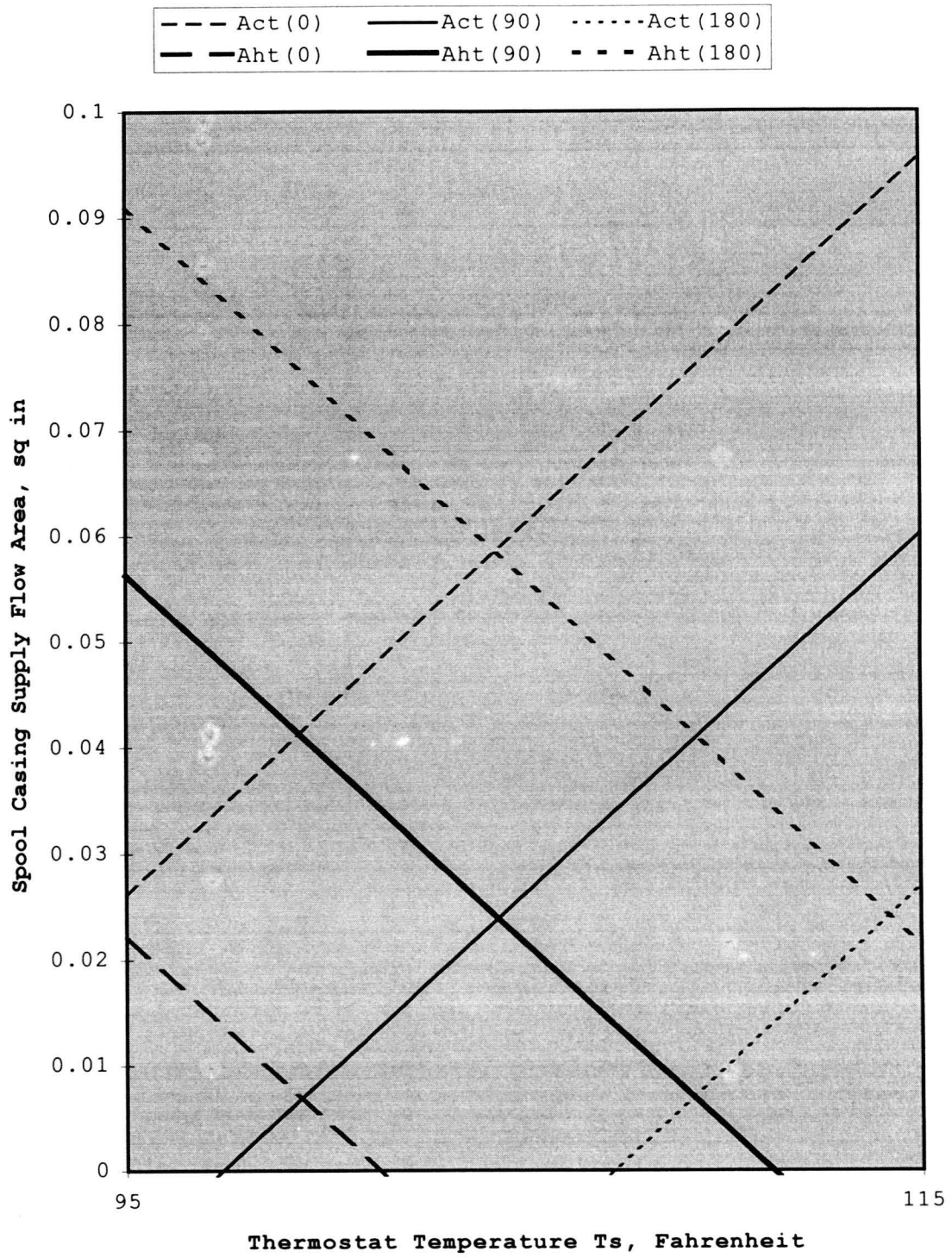


Figure 9.8: Hot and cold supply flow area as a function of thermostat length and valve handle position

A_o = Area of Orifice, ft^2

D_p = Hot and cold supply and mix output pipe diameter, ft

A_s = Area of spool which supply pressure acts upon, ft^2

M_s = Mass of spool, slugs

The flow for the cold supply line may be written:

$$Q_c = \{ [2 * (P_c - P_{cc})] / [\rho * (\Lambda_1 + \Lambda_c)] \}^{0.5} \quad (9.13)$$

where:

$$\Lambda_1 = [K_{e1}^{0.5} / A_p]^2 + [K_{c2}^{0.5} / A_2]^2 + [K_{e3}^{0.5} / A_3]^2 + \quad (9.14)$$

$$[1 / (C_4 * A_4)]^2$$

$$\Lambda_c = [1 / (C * A_{sci})]^2 + [1 / (C * A_{sco})]^2 + [1 / (C * A_{ct})]^2 \quad (9.15)$$

K_{e1} = Expansion coefficient for head loss 1

A_p = Supply pipe area, ft^2

K_{c2} = Contraction coefficient for head loss 2

A_2 = Area for head loss 2, ft^2

K_{e3} = Expansion coefficient for head loss 2

A_3 = Area for head loss 3, ft^2

C_4 = Orifice coefficient for head loss 4

A_4 = Orifice area for head loss 4, ft^2

C = Orifice coefficient for spool inlet, outlet and spool casing area

A_{sci} = Spool inlet area for cold supply, ft^2

Asco = Spool outlet area for cold supply, ft²

Act = Spool casing flow area for cold supply, ft²

In a similar fashion, the flow for the hot supply line may be written:

$$Q_h = \{ [2 * (P_h - P_{cc})] / [\rho * (\Lambda_1 + \Lambda_h)] \}^{0.5} \quad (9.16)$$

where:

$$\Lambda_h = [1 / (C * A_{shi})]^2 + [1 / (C * A_{sho})]^2 + [1 / (C * A_{ht})]^2 \quad (9.17)$$

Ashi = Spool inlet area for hot supply, ft²

Asho = Spool outlet area for hot supply, ft²

Aht = Spool casing flow area for hot supply, ft²

In a similar fashion, the flow for the mix out of the valve may be written:

$$Q_m = \{ [2 * (P_{cc} - P_s)] / [\rho * (\Lambda_o)] \}^{0.5} \quad (9.18)$$

where:

$$\Lambda_o = [1 / (C_8 * A_8)]^2 + [1 / (C_9 * A_9)]^2 + [1 / (C_{10} * A_o)]^2 \quad (9.19)$$

P_s = Shower head pressure, psf

C₈ = Orifice coefficient for head loss 8

A₈ = Orifice area for head loss 8, ft²

C₉ = Orifice coefficient for head loss 9

A₉ = Orifice area for head loss 9, ft²

C₁₀ = Orifice coefficient for head loss 10

A_o = Orifice area for head loss 10, ft^2

The variables Λ_c and Λ_h are a function of the spool position, x_s , the thermostat assembly temperature, T_s , and the valve handle position θ . Figure 9.9 graphs Λ_c and Λ_h as a function of T_s for handle positions of 0 degrees, 90 degrees and 180 degrees, and the spool position $x_s = 0$ inches.

For the cold supply side of the valve the following equation defines the cold supply side spool pressure:

$$P_{sc} = P_c - (Q_c^2 * \rho * \Lambda_{cs}) / 2 \quad (9.20)$$

where:

$$\Lambda_{cs} = \Lambda_1 + \Lambda_c - [1 / (C * A_{ct})]^2 \quad (9.21)$$

Similarly for the hot supply side of the valve the following equation defines the hot supply side spool pressure:

$$P_{sh} = P_h - (Q_h^2 * \rho * \Lambda_{hs}) / 2 \quad (9.22)$$

where:

$$\Lambda_{hs} = \Lambda_1 + \Lambda_h - [1 / (C * A_{ht})]^2 \quad (9.23)$$

Summing forces axially on the spool defines the differential equation of motion for the spool.

$$M_s * x'' = A_s * (P_{sc} - P_{sh}) - c x' - f_s \quad (9.24)$$

where:

M_s = Mass of the spool, slugs

x'' = Acceleration of the spool, ft/s^2

x' = Velocity of the spool, ft/s

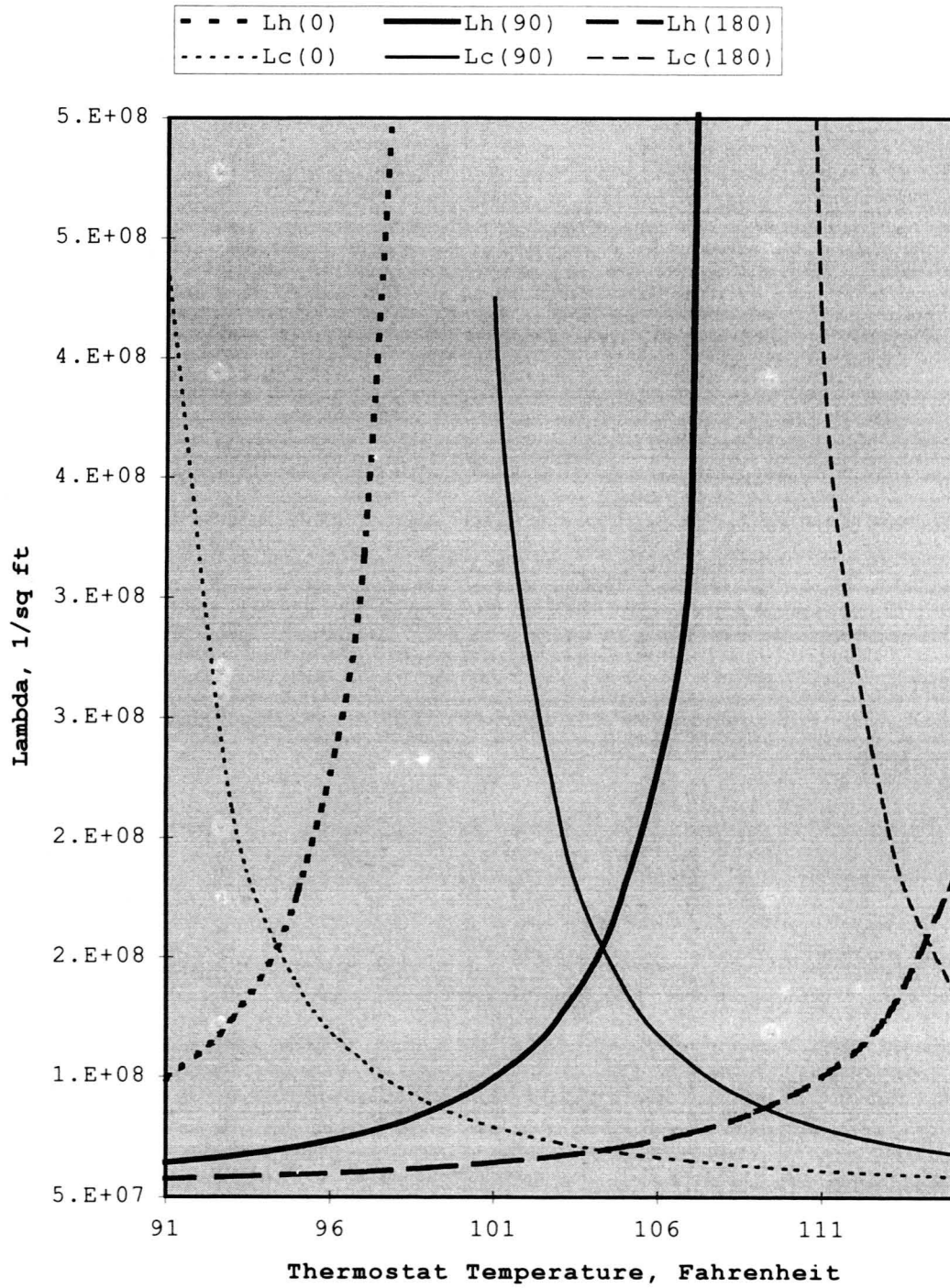


Figure 9.9: Λ plotted as a function of thermostat temperature

A_s = Area of the spool, ft^2

P_{sh} = Pressure on the spool due to the hot supply water, psf

P_{sc} = Pressure on the spool due to the cold supply water, psf

c = Damping coefficient due to relative motion of the spool,
slugs/sec

f_s = Frictional force on the spool ($\mu * M_s * g$)

Once again a coefficient of friction (μ) of 0.08 will be used in this modeling. The damping coefficient will be varied in the modeling to evaluate the effects on the motion of the spool. Expanding the equation by inserting the expanded form of P_{sh} and P_{sc} gives:

Summing the forces axially results in:

$$x'' = \frac{A_s * (Q_c^2 * \rho * A_{cs} - Q_h^2 * \rho * A_{hs})}{M_s} - \frac{c * x'}{M_s} - \mu * g \quad (9.25)$$

This is the equation of motion for the spool and involves solving a nonlinear differential equation. In this equation x'' is a function of the spool position, the valve handle position and the temperature of the thermostat assembly.

The following equation defines the relationship between the hot and cold supply water flow, hot and cold supply water temperature, and the resulting mix flow and temperature:

$$T_m = \frac{Q_c * T_c + Q_h * T_h}{Q_m} \quad (9.26)$$

where:

Q_m = Mix output flow, ft^3/sec

T_m = Temperature of the mix output flow, °F

Q_c = Cold supply flow, ft³/sec

T_c = Temperature of the cold supply flow, °F

Q_h = Hot supply flow, ft³/sec

T_h = Temperature of the hot supply flow, °F

Figure 9.10 graphs the mix temperature, T_m , as a function of the thermostat assembly temperature for a spool position $x_s = 0$ inches and for handle positions equal to 0, 90 and 180 degrees. Plotting the thermostat assembly temperature against T_s identifies points of equilibrium between the mix temperature and the thermostat assembly temperature. The graph identifies three equilibrium points: 1) at 96°F where the valve handle position is at 0 degrees, 2) at 104.5°F where the valve handle is at 90 degrees, and 3) at 113°F where the valve handle position is at 180 degrees.

To calculate the steady state flow conditions using the characteristic equations, an iterative approach is required. First, estimates are made of: 1) the pressure in the spool housing where the hot and cold supplies mix (P_{cc}), 2) the spool position (x_s), and 3) the thermostat temperature (T_s). An estimate is made of the pressure of the common mixing cavity (P_{cc}) and of the thermostat temperature (T_s). Flow calculations of the hot water supply, cold water supply and the mix output are calculated using equations 9.13, 9.16 and 9.18. Based on the supply and mix flows, the estimated pressure in the common mixing cavity (P_{cc}) may be updated. If the mix flow is lower than the combination of the hot

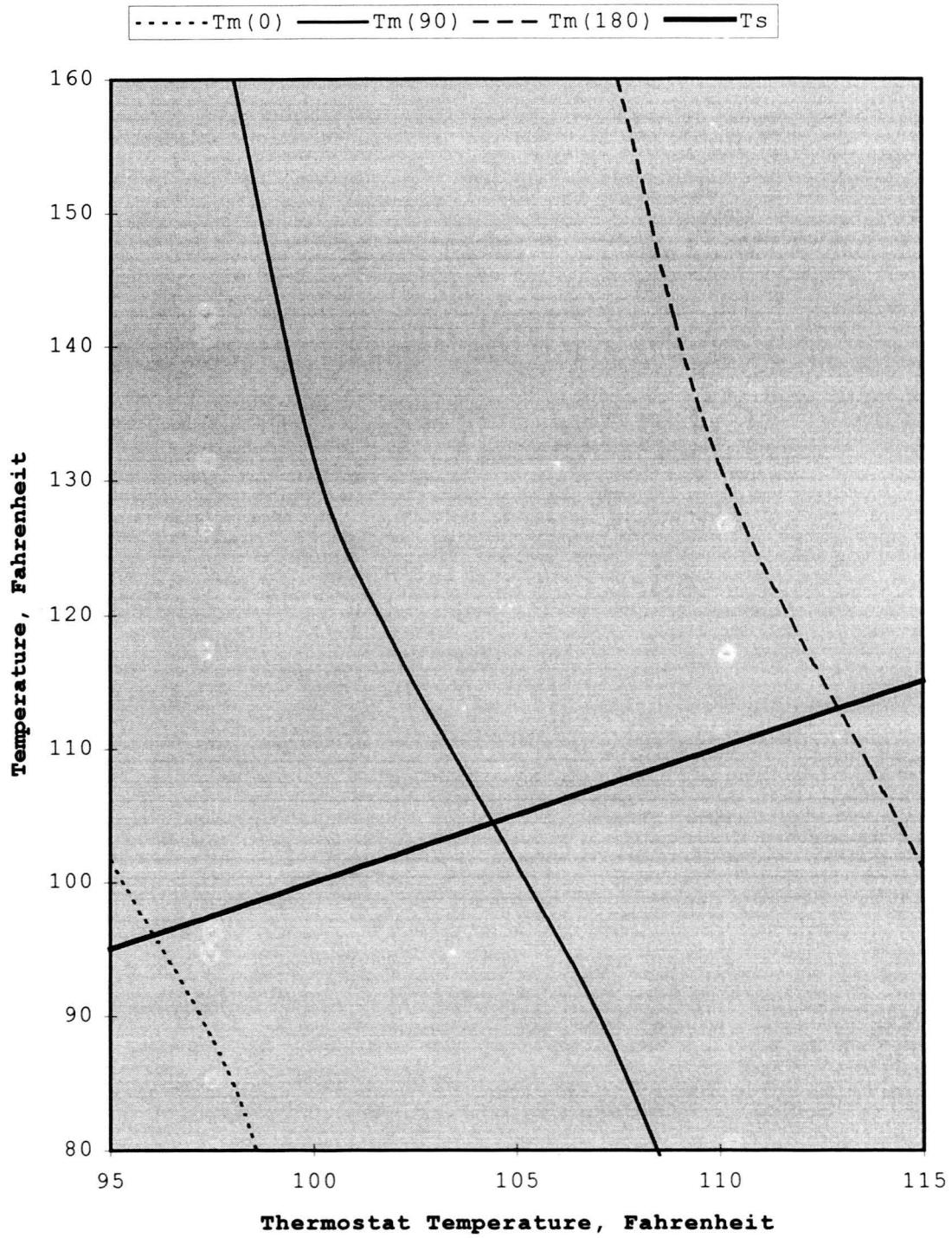


Figure 9.10: Mix temperature as a function of thermostat temperature, model

and cold supply flow, P_{cc} is increased. If the mix flow is higher than the combination of the hot and cold supply flow, P_{cc} is decreased. The mix temperature is calculated utilizing equation 9.26. The thermostat temperature is then compared to the mix temperature. If the thermostat temperature is higher than the mix temperature, the thermostat temperature is lowered. If the thermostat temperature is lower than the mix temperature, the thermostat temperature is raised. The hot and cold supply spool pressure is calculated using equations 9.20 and 9.22. If the hot supply spool pressure is higher than the cold supply spool pressure, x_s is decreased. If the hot supply spool pressure is lower than the cold supply spool pressure, x_s is increased. This process is repeated until the hot and cold supply flow rates are equal to the mix flow rate, until the cold supply spool pressure is equal to the hot supply spool pressure, and until the thermostat temperature is equal to the mix temperature.

System Testing

Tests were conducted on the mixing valve to obtain characteristic flow curves for the valve and to obtain information on the dynamic response of the valve.

Tests were conducted to record the response of the valve given a change in the cold water supply pressure. Steady state pressure, temperature and flow conditions were established prior to changing the cold water supply pressure; the valve temperature adjustment

handle was set at 180 degrees. The upstream shut off valve for the cold water supply was then partially closed to produce a cold supply pressure drop. Supply temperature was not changed and the cold supply pressure was dropped. Figure 9.11 graphs the hot and cold supply pressure as a function of time. A steady state condition is established at the location of the "Y" axis. Figure 9.12 graphs the supply flow and Figure 9.13 graphs the hot supply, cold supply and mix temperature.

The test pressure and temperature supplies will be used in the characteristic equations to evaluate the dynamic response of the valve. Given the initial set of steady state flow and pressure conditions, the hot and cold supply flows, the thermostat temperature and the spool position were evaluated using the iterative process outlined in the modeling section of this chapter.

For a sudden supply pressure drop (step function) in the cold supply flow, the previous equations for Q_c (9.13), Q_h (9.16), Q_m (9.18), P_{sc} (9.20), P_{sh} (9.22), T_s (9.11), T_m (9.26), and x'' (9.25) will be used as time is incremented by 0.0005 seconds. A standard differential equation solver cannot be used since the common mix pressure is unknown and must be established through an iteration process. The following equations will be used to calculate the velocity and position of the spool.

$$x'(t+0.0005) = x'(t) + 0.0005 \cdot x''(t) \quad (9.27)$$

$$x(t+0.0005) = x(t) + 0.0005 \cdot [x'(t) + x'(t+0.0005)]/2 \quad (9.28)$$

The effects of friction on the movement of the spool are negligible when compared to forces due to the pressure differences on the spool and were eliminated from the calculation. A damping

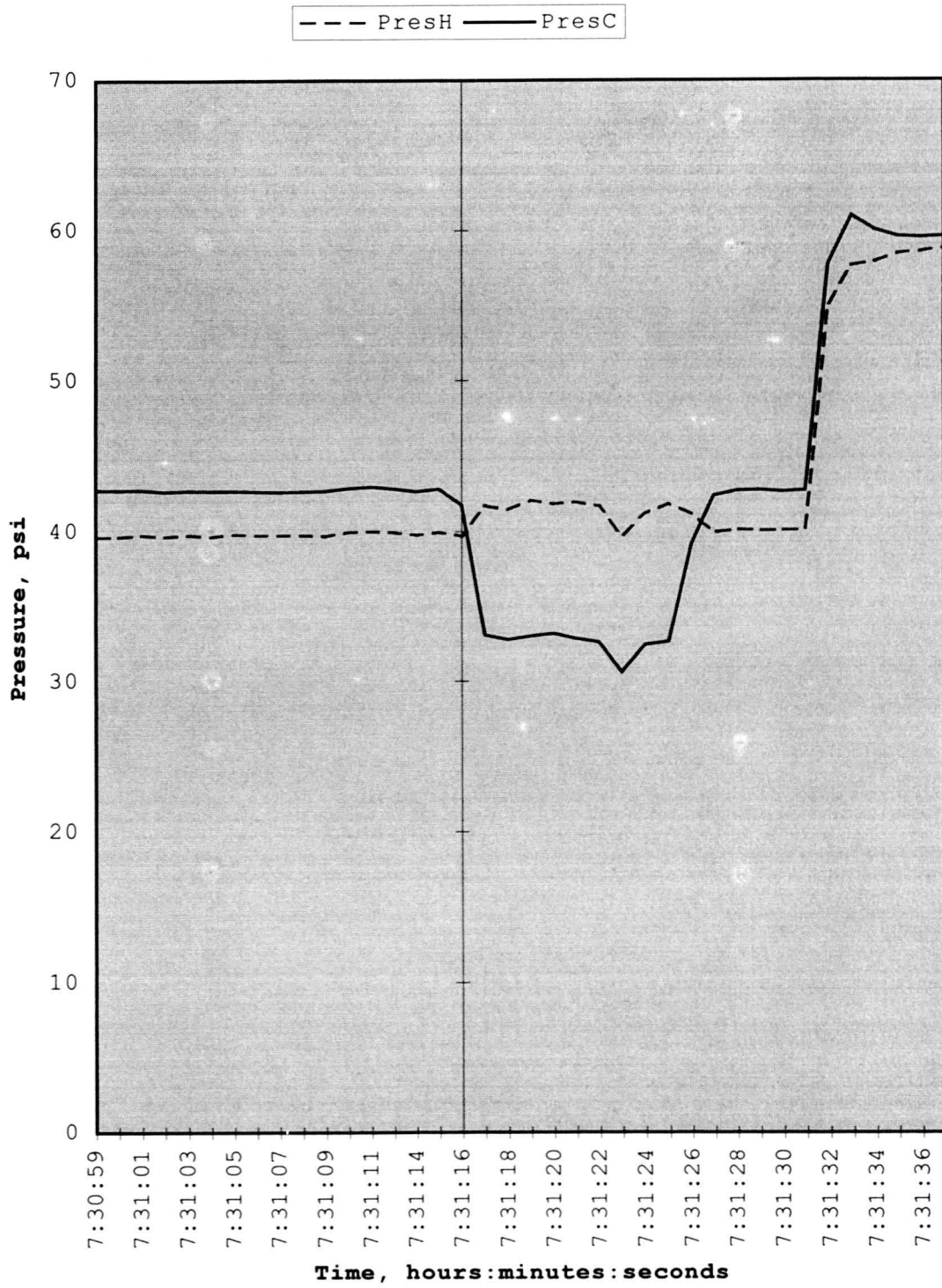


Figure 9.11: Mixing valve test, cold supply pressure drop, supply pressure

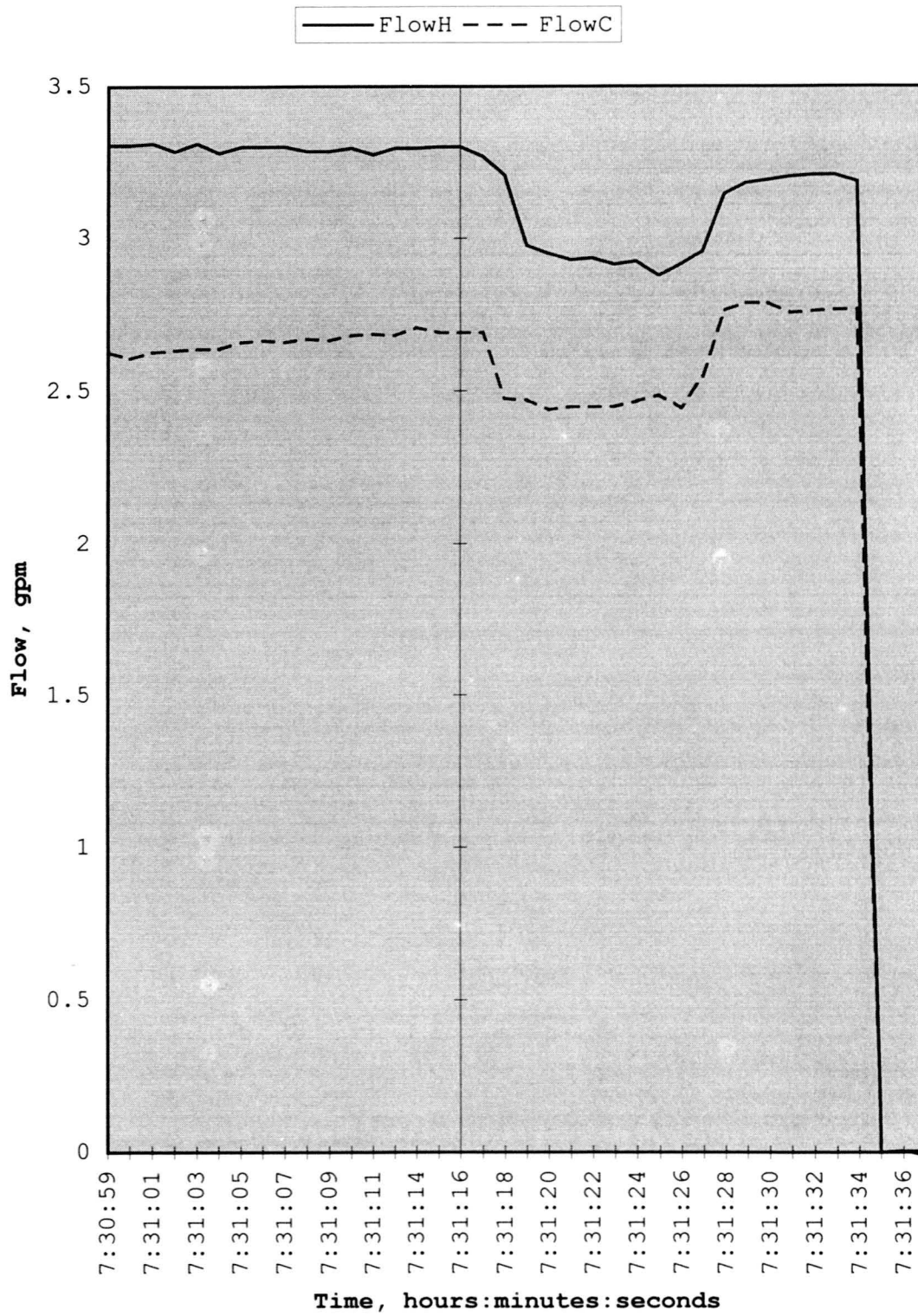


Figure 9.12: Mixing valve test, cold supply pressure drop, supply flow

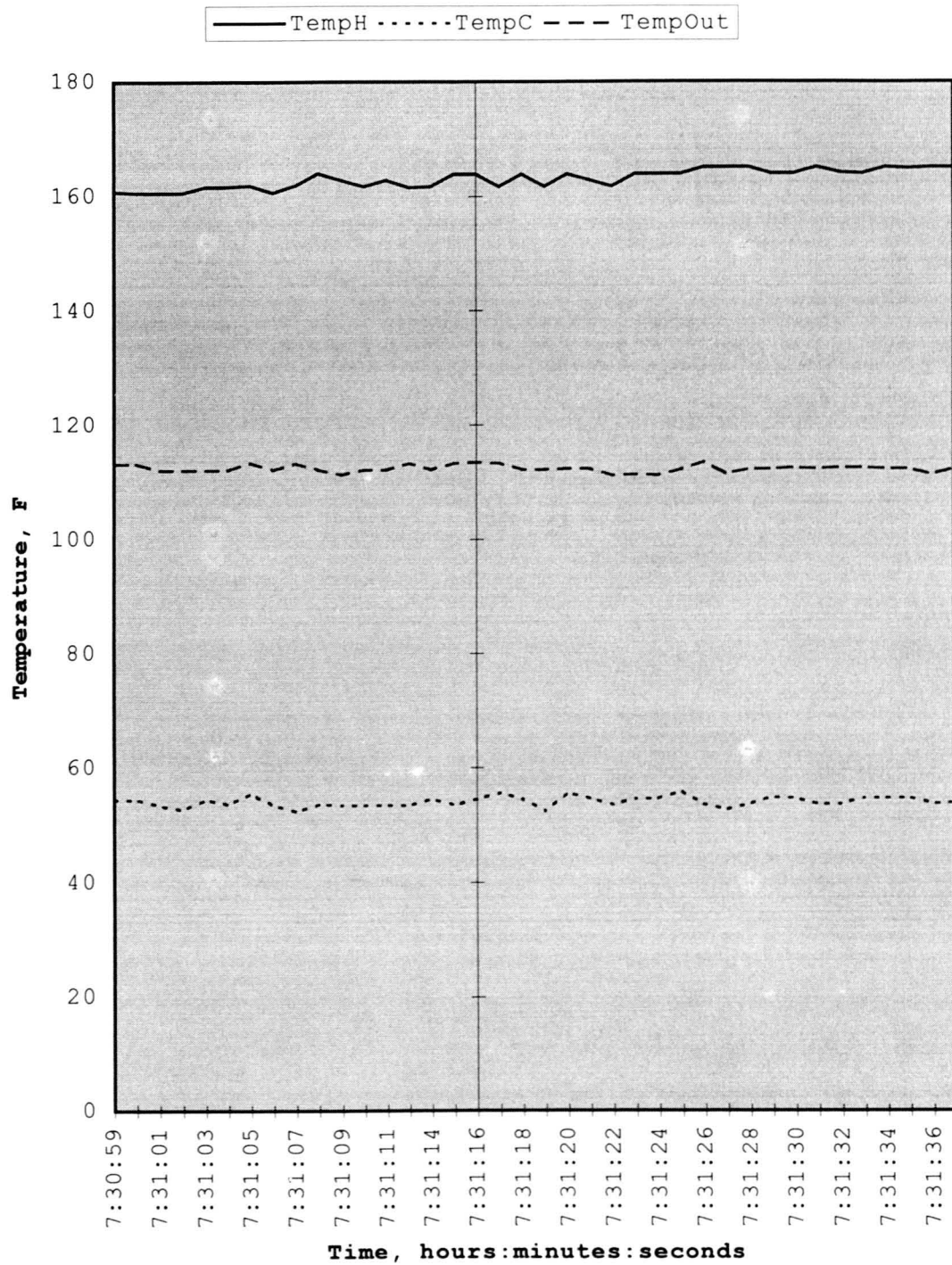


Figure 9.13: Mixing valve test, cold supply pressure drop, supply and mix temperature

coefficient of $0.04/M_s$ (where M_s is the mass of the spool) was used in the characteristic equations. The reaction time of the spool to the pressure drop is less than 0.005 second. The reaction time of the thermostat assembly is several orders of magnitude larger. As a result, the dynamic response was evaluated with a focus on the spool reaction, then the dynamic response was evaluated with a focus on the thermostat assembly reaction. A summary of the results for the first 0.0045 seconds may be found in Table 9.3. Spool pressure is graphed as a function of time in Figure 9.14, spool acceleration is graphed in Figure 9.15, spool velocity is graphed in Figure 9.16, spool position is graphed in Figure 9.17, hot and cold supply flow are graphed in Figure 9.18, and the resulting mix and thermostat temperature are graphed in Figure 9.19.

Table 9.3 Mixing valve response, cold supply pressure drop
(spool response in 0.0045 seconds)

| Time (sec) | X'' (ft/s ²) | X' (in/s) | X (in) | Q_c (gpm) | P_{sc} (psi) | Q_h (gpm) | P_{sh} (psi) | T_s (°F) | T_m (°F) |
|---------------|-------------------------------|----------------|-------------|----------------|-------------------|----------------|-------------------|---------------|---------------|
| -0.0005 | 0 | 0.00 | 0.0150 | 2.17 | 34.24 | 2.64 | 34.22 | 113.5 | 113.5 |
| 0.0000 | -5709 | 0.00 | 0.0150 | 1.83 | 26.90 | 2.73 | 35.38 | 113.5 | 119.5 |
| 0.0005 | 999 | -34.26 | 0.0064 | 1.89 | 28.09 | 2.68 | 34.50 | 113.5 | 118.1 |
| 0.0010 | 2642 | -28.26 | -0.0092 | 1.97 | 29.41 | 2.55 | 32.00 | 113.5 | 115.6 |
| 0.0015 | 2332 | -12.41 | -0.0194 | 2.07 | 29.93 | 2.39 | 29.33 | 113.5 | 113.5 |
| 0.0020 | 852 | 1.58 | -0.0221 | 2.01 | 30.04 | 2.34 | 28.41 | 113.5 | 112.7 |
| 0.0025 | -475 | 6.70 | -0.0200 | 2.01 | 29.96 | 2.38 | 29.12 | 113.5 | 113.3 |
| 0.0030 | -664 | 3.85 | -0.0174 | 2.00 | 29.84 | 2.43 | 29.94 | 113.5 | 114.0 |
| 0.0035 | -256 | -0.14 | -0.0164 | 2.00 | 29.80 | 2.44 | 30.21 | 113.5 | 114.2 |
| 0.0040 | 84 | -1.67 | -0.0169 | 2.00 | 29.82 | 2.44 | 30.08 | 113.5 | 114.1 |
| 0.0045 | 168 | -1.17 | -0.0176 | 2.00 | 29.85 | 2.43 | 29.87 | 113.5 | 113.9 |

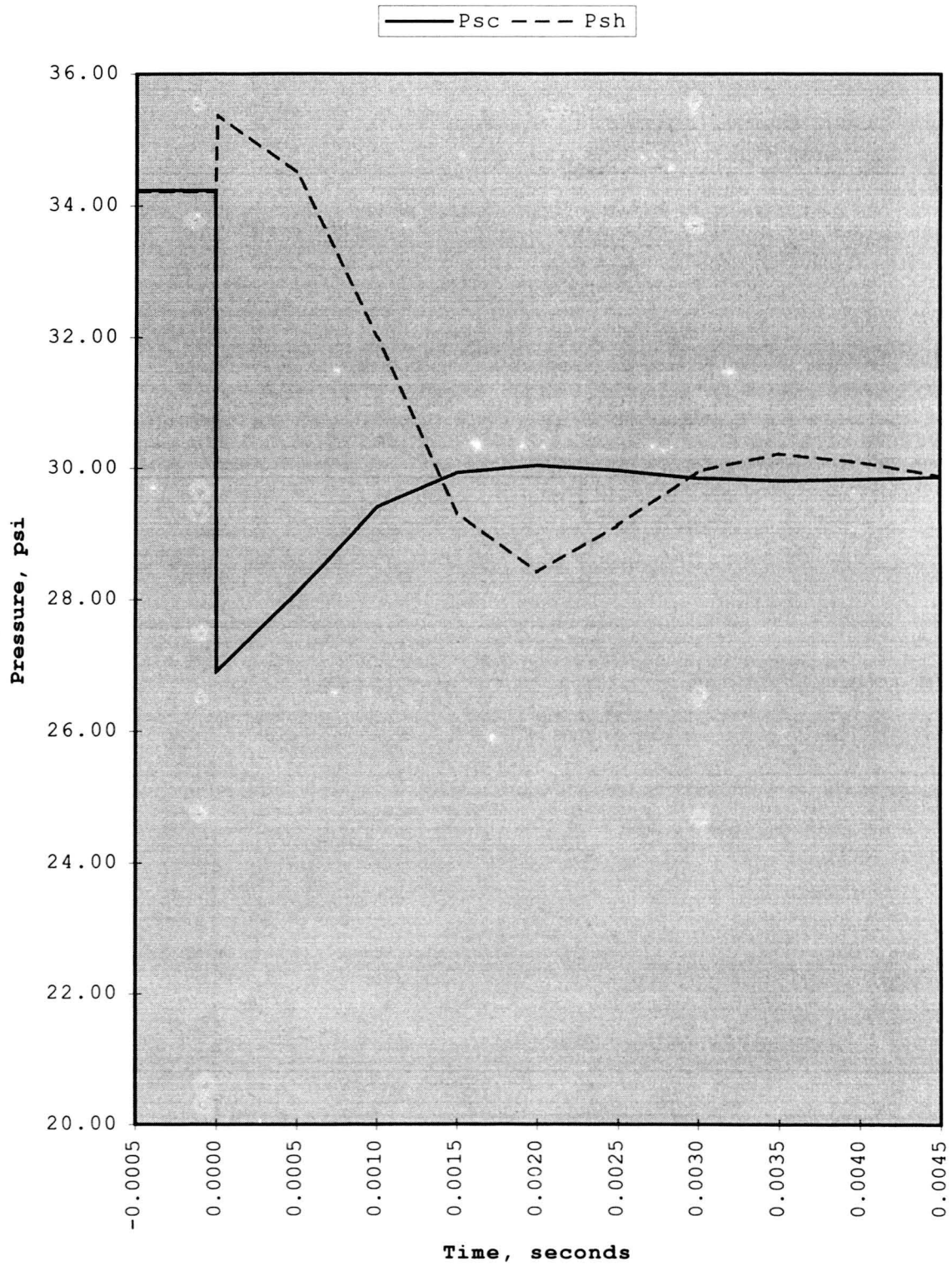


Figure 9.14: Mixing valve model, cold supply pressure drop, spool pressure

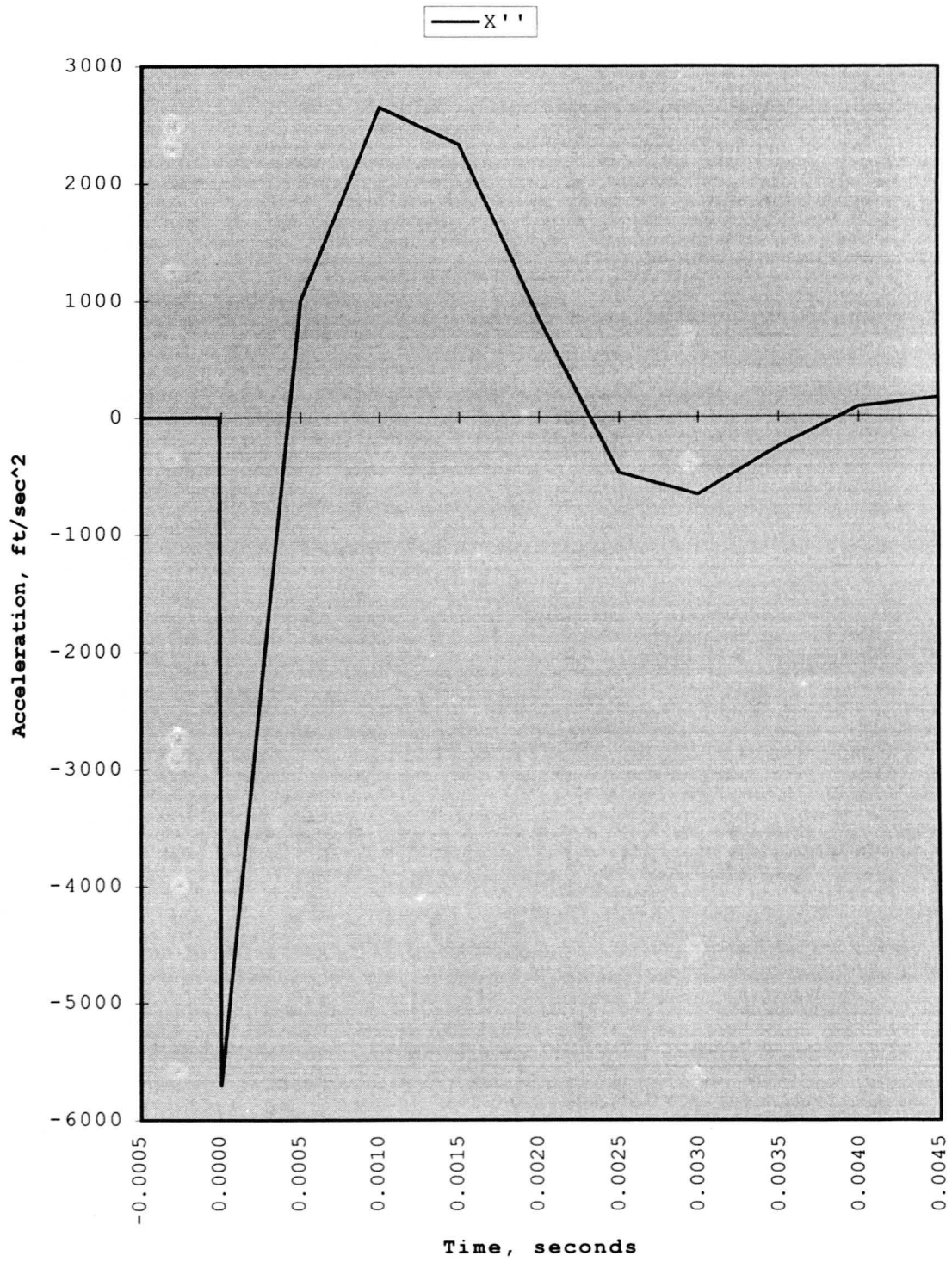


Figure 9.15: Mixing valve model, cold supply pressure drop, spool acceleration

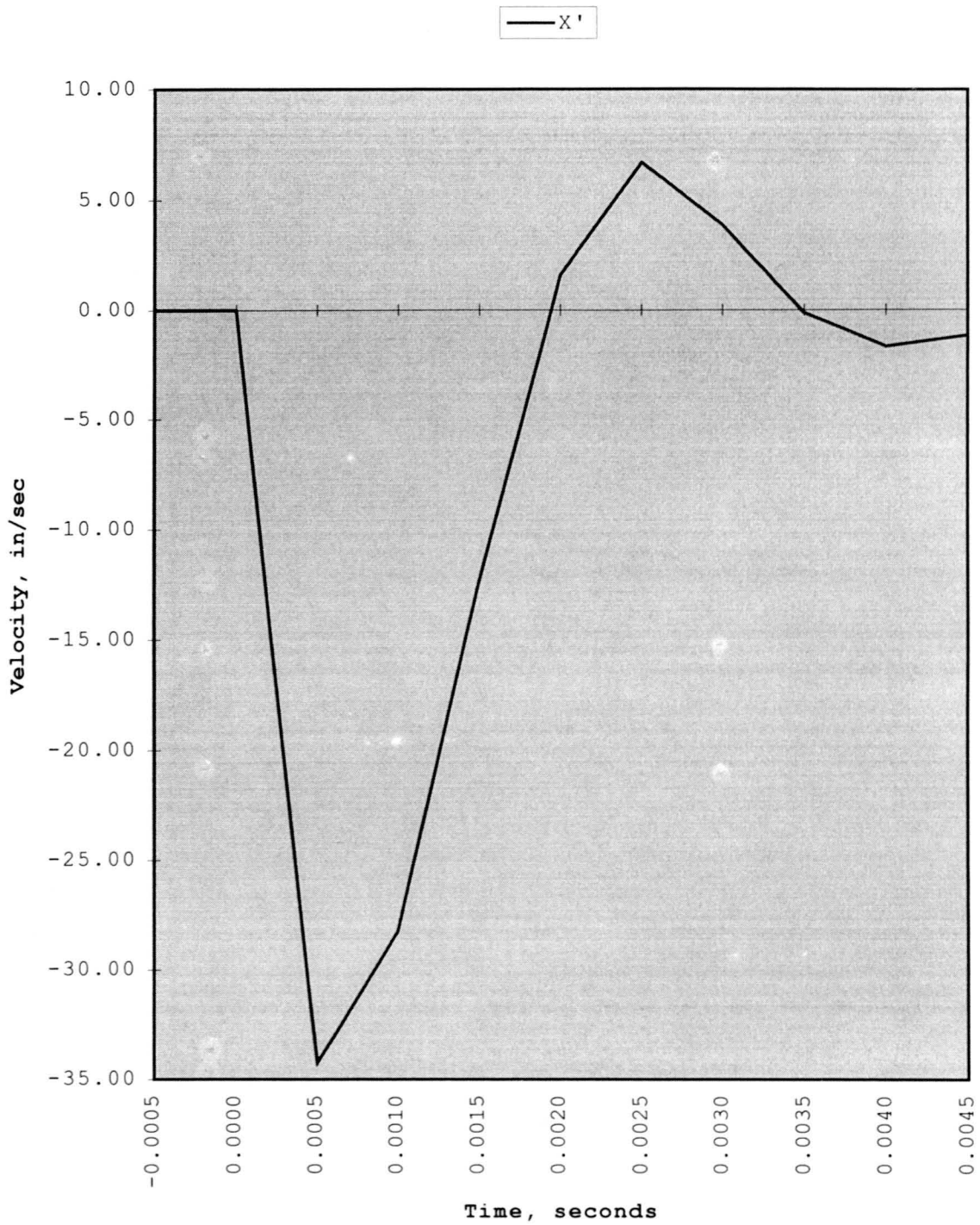


Figure 9.16: Mixing valve model, cold supply pressure drop, spool velocity

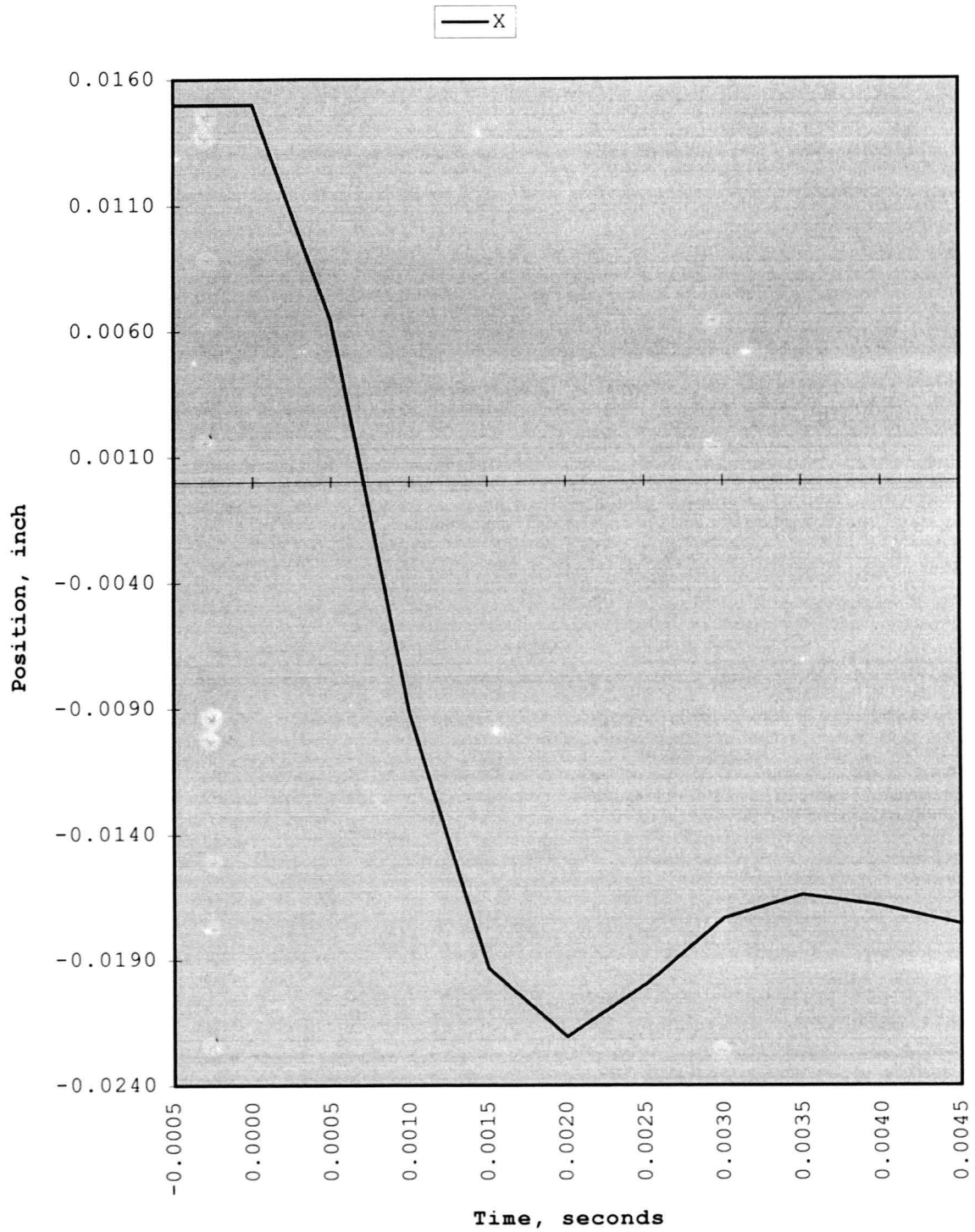


Figure 9.17: Mixing valve model, cold supply pressure drop, spool position

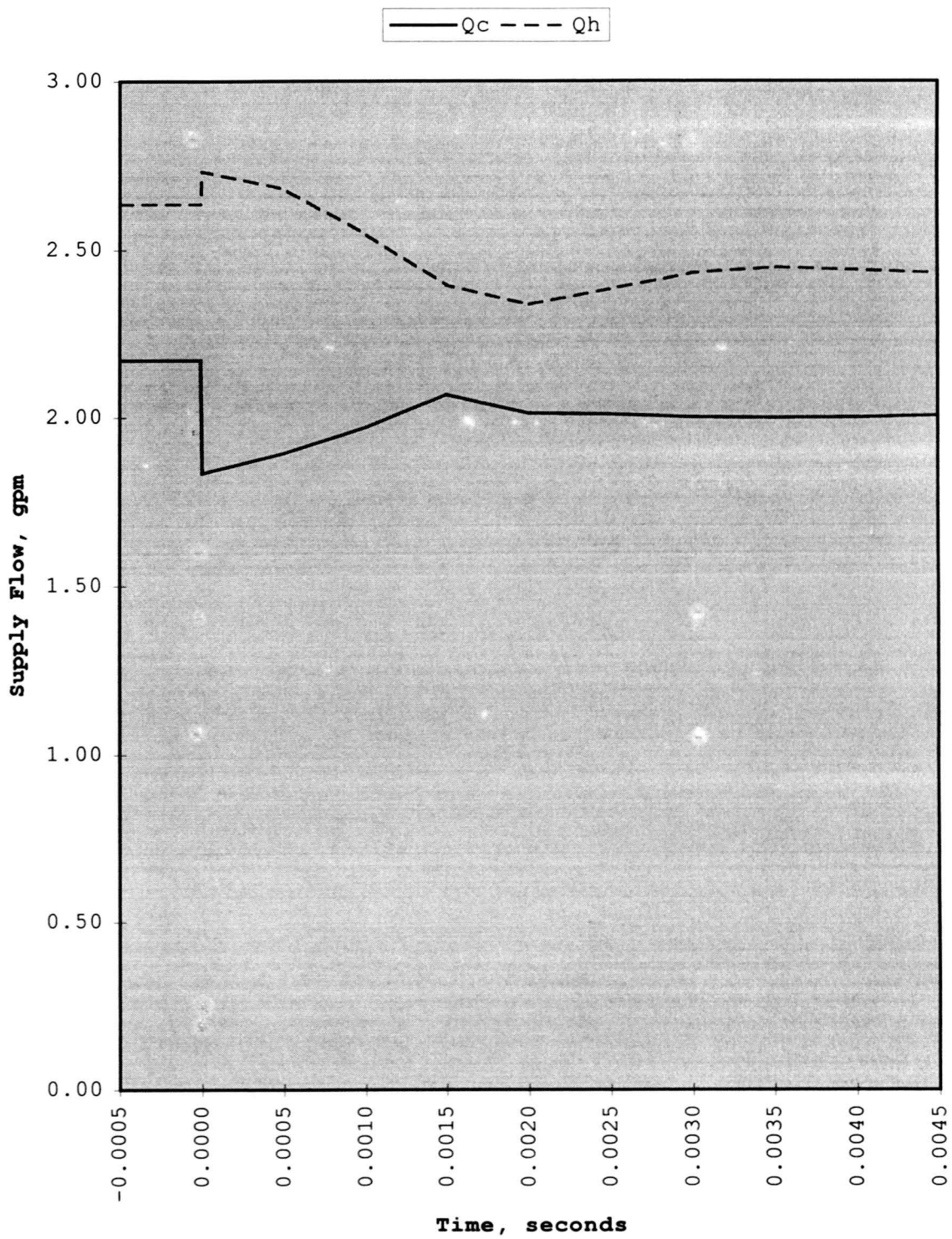


Figure 9.18: Mixing valve model, cold supply pressure drop, supply flow

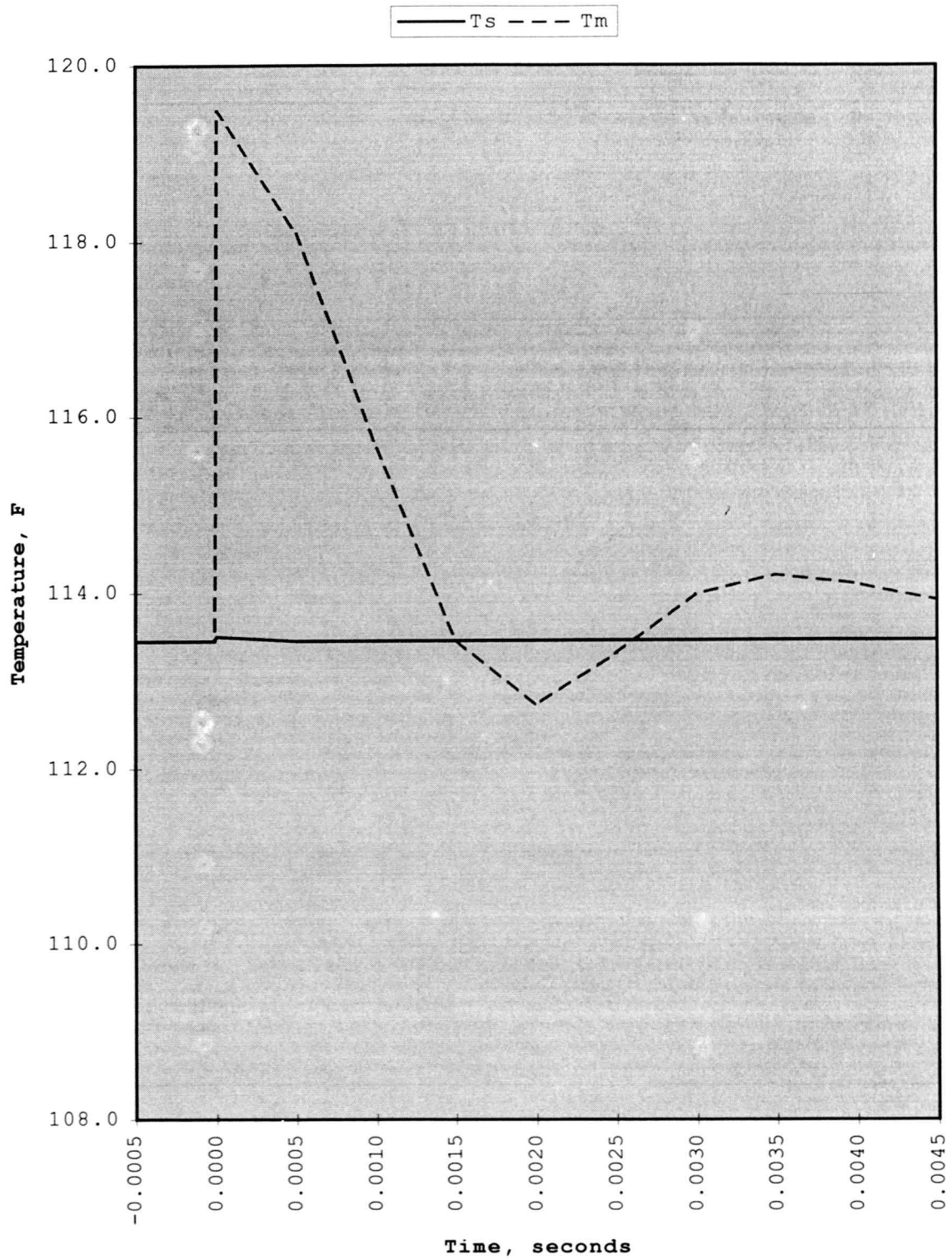


Figure 9.19: Mixing valve model, cold supply pressure drop, mix and thermostat temperature

Table 9.4 is a summary of the results for the first 9 seconds after the cold supply pressure drop. Spool position and spool case position are graphed as a function of time in Figure 9.20, hot and cold supply flow is graphed in Figure 9.21, and the resulting mix and thermostat temperature are graphed in Figure 9.22.

Figure 9.23 graphs the test and model results of the hot and cold supply flow. The test showed a decrease in both the hot and cold supply flow of approximately 8-9% of the flow rate; the model also showed a drop in both the hot and cold supply flow rates of 8-9%. Figure 9.24 graphs the tests and model results of the mix temperature. The model predicts a drop in mix temperature of approximately 0.5°F. The test results again reflect temperature fluctuations of +/- 1.5°F the mix temperature.

Table 9.4 Mixing valve response, cold supply pressure drop
(thermostat response in 9 seconds)

| Time (sec) | Xs (in) | Xc (in) | Qc (gpm) | Qh (gpm) | Ts (°F) | Tm (°F) |
|---------------|------------|------------|-------------|-------------|------------|------------|
| -0.005 | 0.015 | 0.051 | 2.17 | 2.64 | 113.5 | 113.5 |
| 0.000 | 0.015 | 0.051 | 1.83 | 2.73 | 113.5 | 119.5 |
| 0.005 | -0.018 | 0.051 | 2.00 | 2.43 | 113.5 | 113.9 |
| 1.000 | -0.018 | 0.051 | 2.01 | 2.41 | 113.5 | 113.5 |
| 2.000 | -0.018 | 0.051 | 2.01 | 2.41 | 113.5 | 113.5 |
| 3.000 | -0.018 | 0.051 | 2.01 | 2.41 | 113.5 | 113.5 |
| 4.000 | -0.018 | 0.051 | 2.01 | 2.41 | 113.5 | 113.5 |
| 5.000 | -0.018 | 0.051 | 2.01 | 2.41 | 113.5 | 113.5 |
| 6.000 | -0.018 | 0.051 | 2.01 | 2.41 | 113.5 | 113.5 |
| 7.000 | -0.018 | 0.051 | 2.01 | 2.41 | 113.5 | 113.5 |
| 8.000 | -0.018 | 0.051 | 2.01 | 2.41 | 113.5 | 113.5 |
| 9.000 | -0.018 | 0.051 | 2.01 | 2.41 | 113.5 | 113.5 |

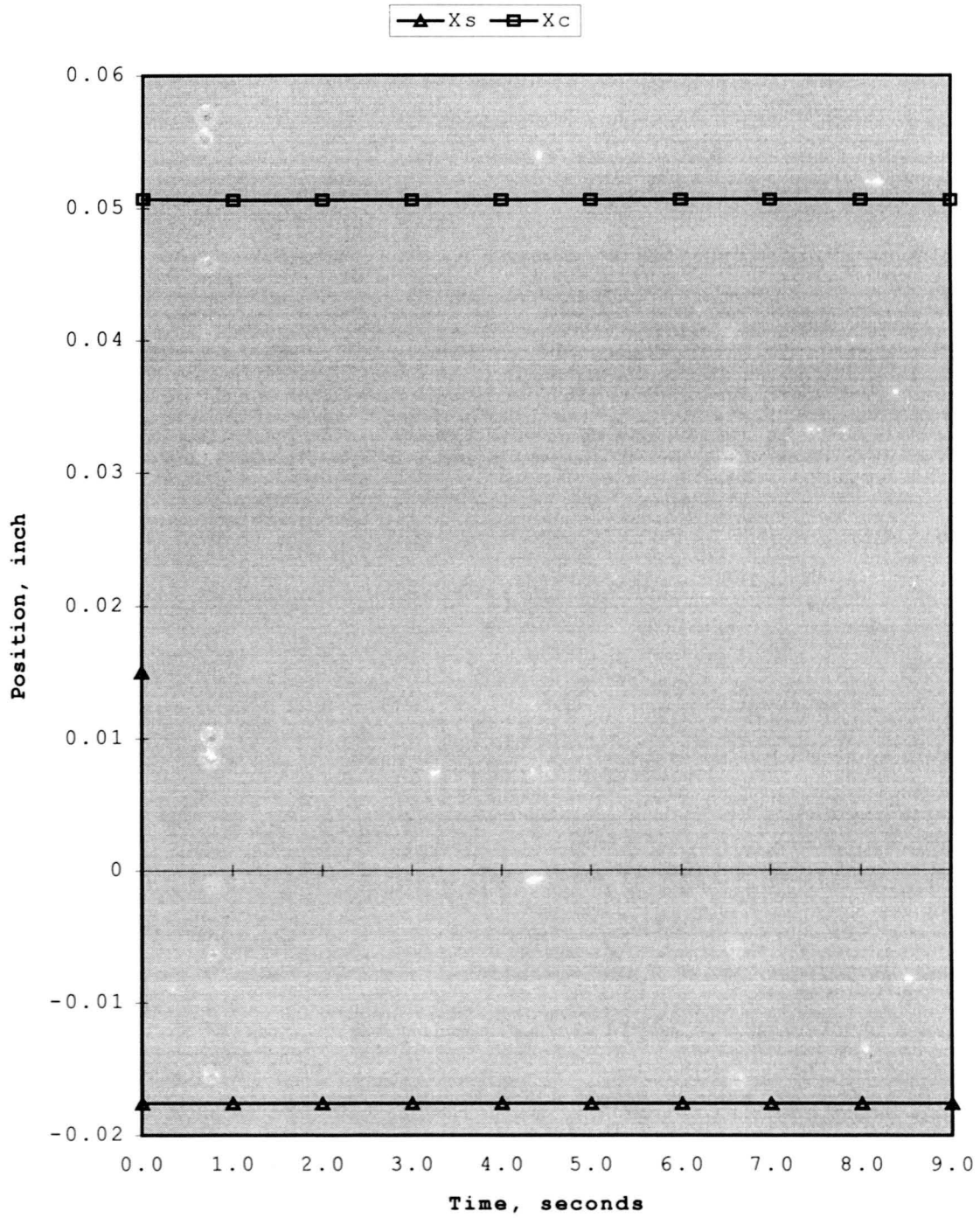


Figure 9.20: Mixing valve model, cold supply pressure drop, spool and spool casing position

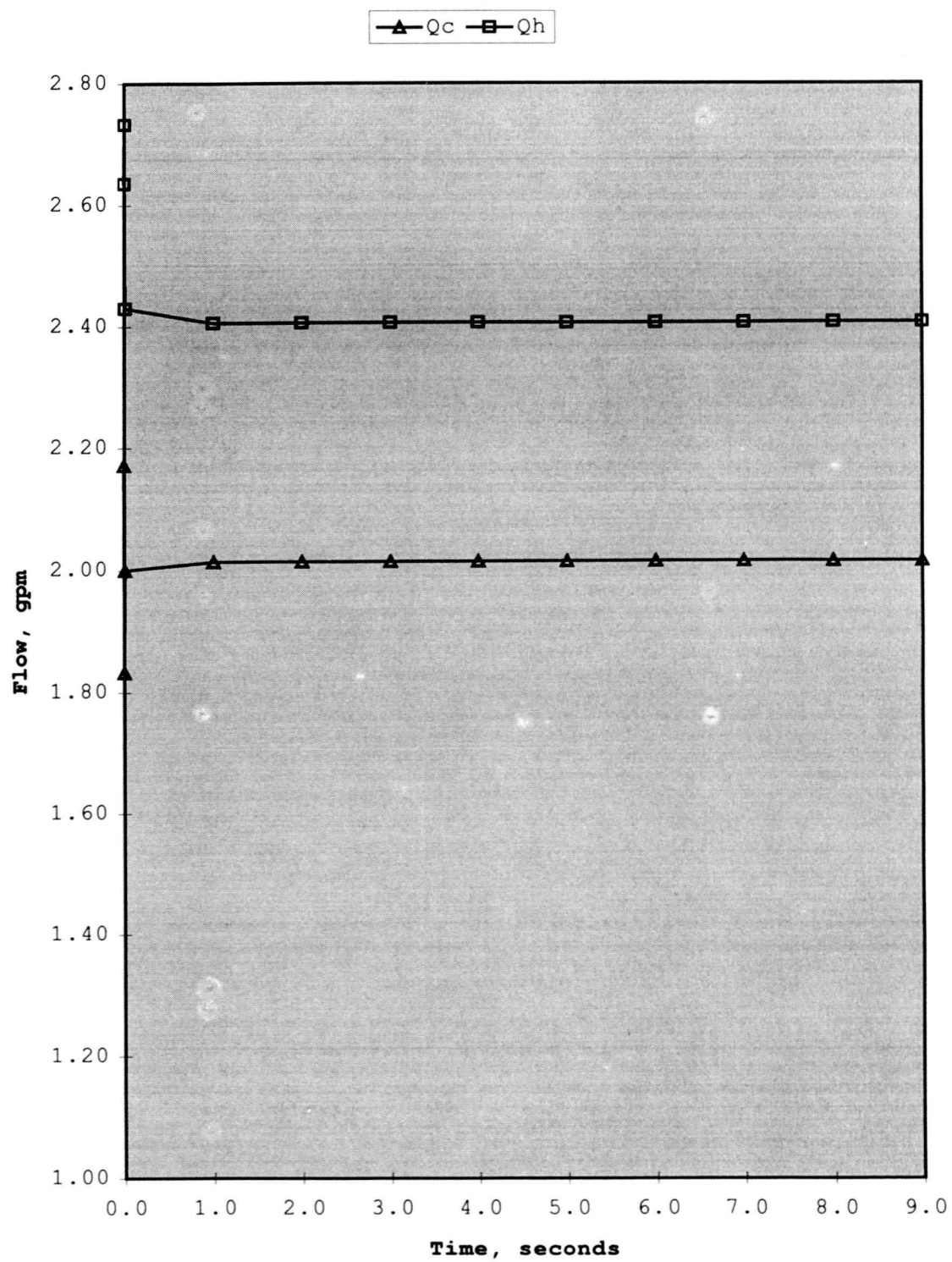


Figure 9.21: Mixing valve model, cold supply pressure drop, supply flow

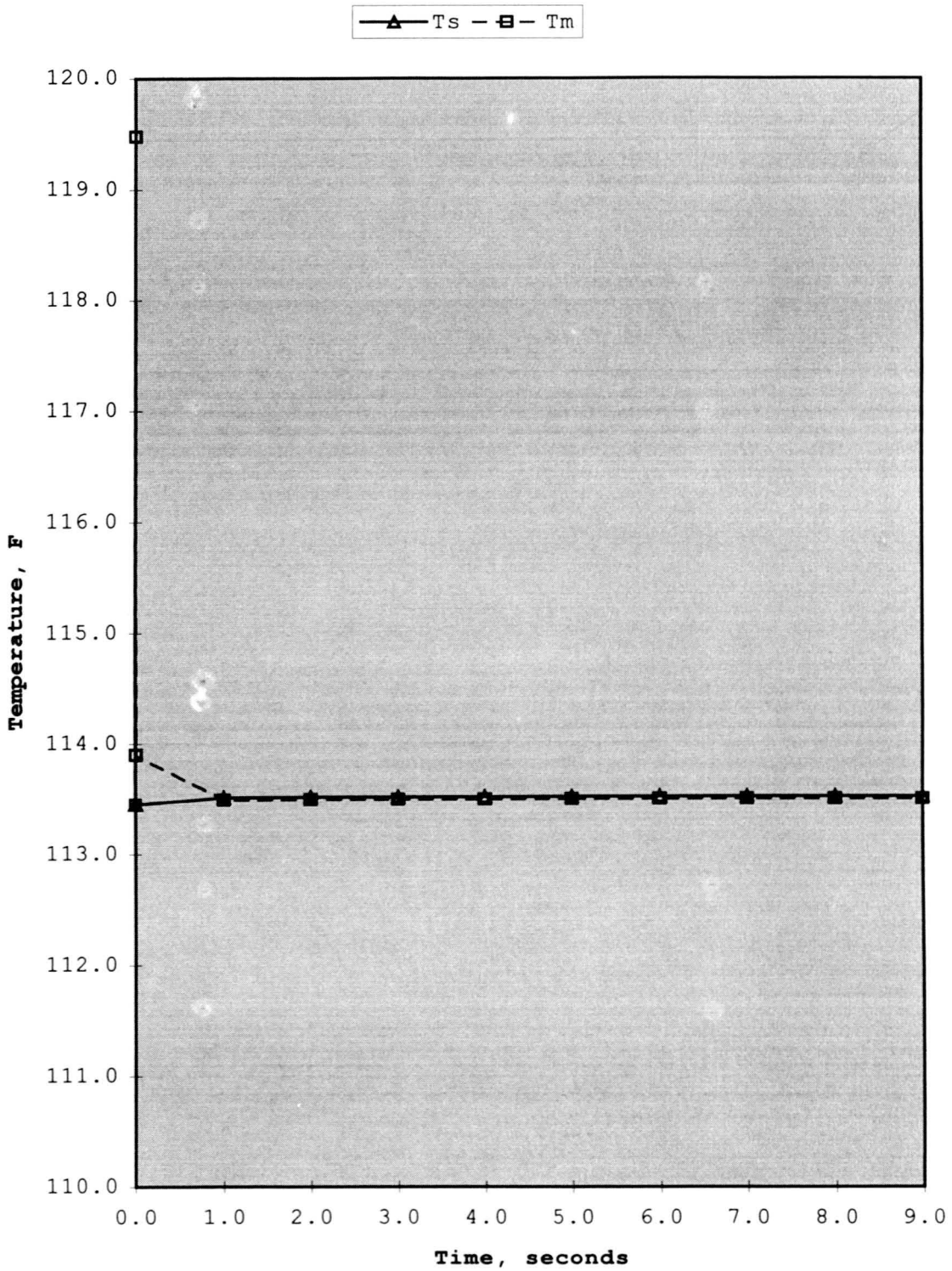


Figure 9.22: Mixing valve model, cold supply pressure drop, mix and thermostat temperature

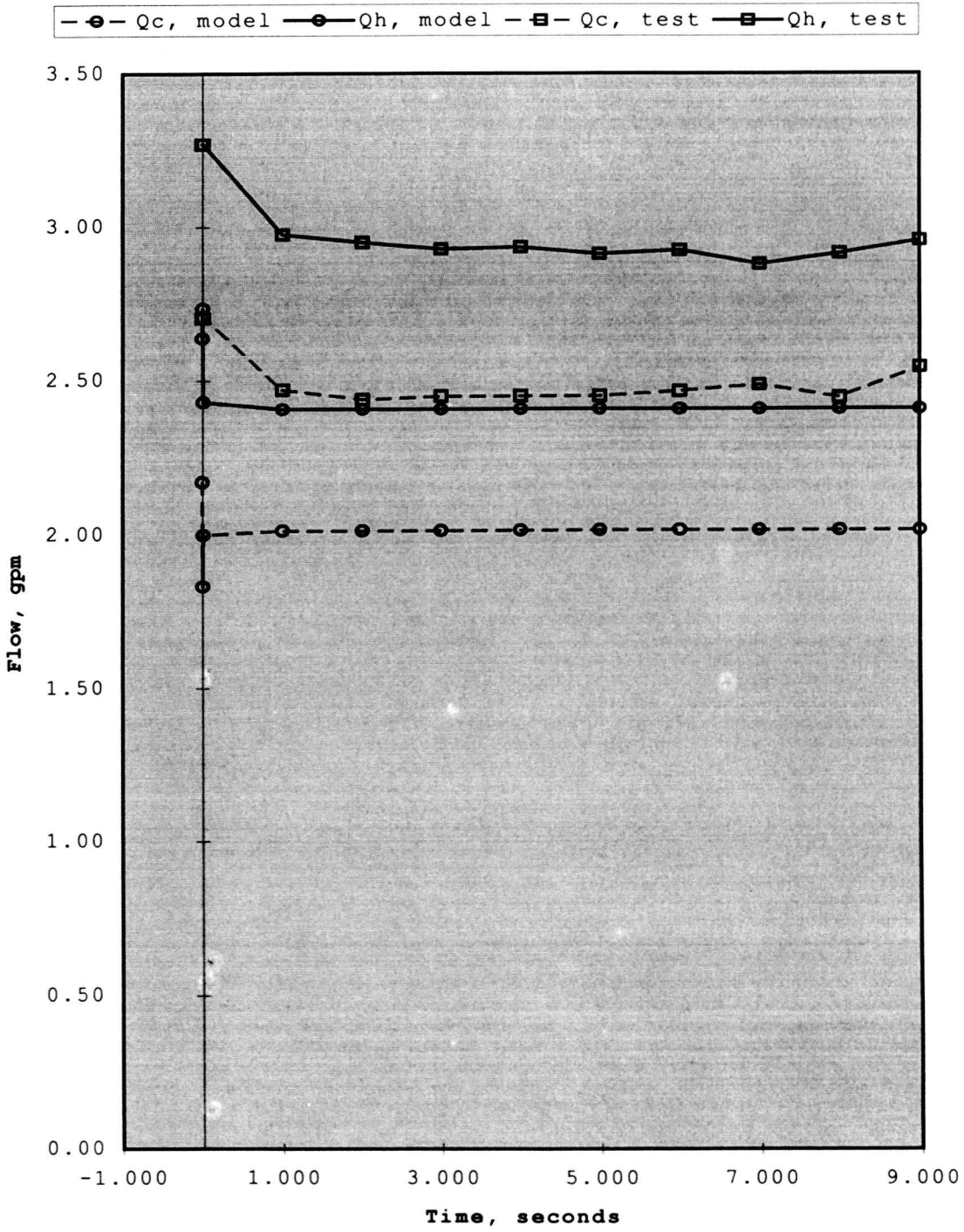


Figure 9:23: Mixing valve test and model, cold supply pressure drop, supply flows

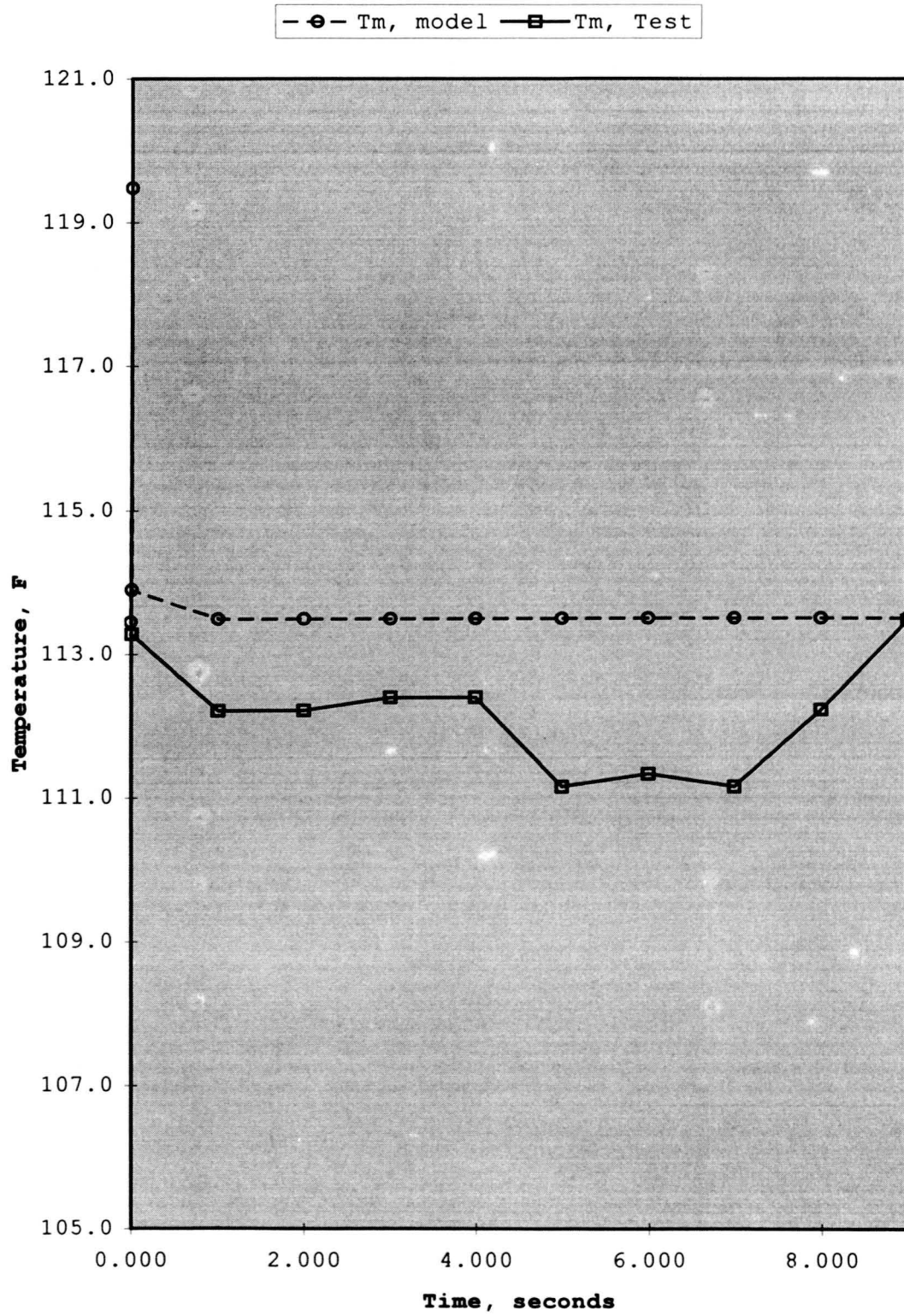


Figure 9:24: Mixing valve test and model, cold supply pressure drop, mix temperature

Tests were conducted to record the response of the mixing valve given a change in the hot water supply temperature. Steady state pressure, temperature and flow conditions were established prior to changing the hot water supply temperature. The temperature of the hot water supply was allowed to reach room temperature prior to the test. The water heater was set to deliver water at approximately 160°F. The valve handle was then turned to 180 degrees. Supply pressure was not changed during the test. Figure 9.25 graphs the hot and cold supply temperature and the resulting mix temperature. Figure 9.26 graphs the supply pressure of the hot and cold supplies. Figure 9.27 is a graph of the supply flow.

The following is the model for the response of the valve given an initial set of steady state flow, pressure and temperature conditions found in the test and then increasing the hot water supply temperature. Given the following at time $t = 0$:

$$P_c = 44.7 \text{ psi}$$

$$T_c = 61 \text{ }^\circ\text{F}$$

$$P_h = 37.7 \text{ psi}$$

$$T_h = 121 \text{ }^\circ\text{F}$$

$$P_s = 2.3 \text{ psi}$$

For steady state flow at time $t = 0$ the cold flow is:

$$Q_c = \{ [2 * (P_c - P_{cc})] / [\rho * (\Lambda_1 + \Lambda_c)] \}^{0.5} \quad (9.13)$$

Similarly for the hot supply flow:

$$Q_h = \{[2*(P_h - P_{cc})]/[\rho*(\Lambda_l + \Lambda_h)]\}^{0.5} \quad (9.16)$$

The combined mix flow is:

$$Q_m = \{[2*(P_{cc} - P_s)]/[\rho*(\Lambda_o)]\}^{0.5} \quad (9.18)$$

The temperature of the mix is:

$$T_m = \frac{Q_c * T_c + Q_h * T_h}{Q_c + Q_h} \quad (9.26)$$

The spool pressure on the cold supply flow is:

$$P_{sc} = P_c - (Q_c^2 * \rho * \Lambda_{cs})/2 \quad (9.20)$$

The spool pressure on the hot supply flow is:

$$P_{sh} = P_h - (Q_h^2 * \rho * \Lambda_{hs})/2 \quad (9.22)$$

The iterative approach outlined in this chapter was used to determine the steady state flow conditions. After establishing the steady state conditions of the valve, a time increment was selected (0.5 seconds was selected for this model), the process is repeated for time increments of $\Delta t = 0.5$ seconds with new supply and shower pressures and new supply temperatures.

A summary of the results from this evaluation may be found in Table 9.5. Spool position and spool case position are graphed as a function of time in Figure 9.28, hot and cold supply flow are graphed in Figure 9.29. The hot and cold supply, resulting mix, and the thermostat temperature are graphed in Figure 9.30.

Figure 9.31 graphs the tests and model results of the mix temperature. The model predicted a mix temperature increase of approximately 4°F; the test results showed a temperature increase of

approximately 3°F. Figure 9.32 graphs the test and model results of the hot and cold supply flow. The model predicted a cold supply flow increase of approximately 1.2 gpm and a hot supply flow decrease of approximately 0.8 gpm. The test results showed a cold supply flow increase of approximately 1.7 gpm and a hot supply flow decrease of approximately 0.7 gpm.

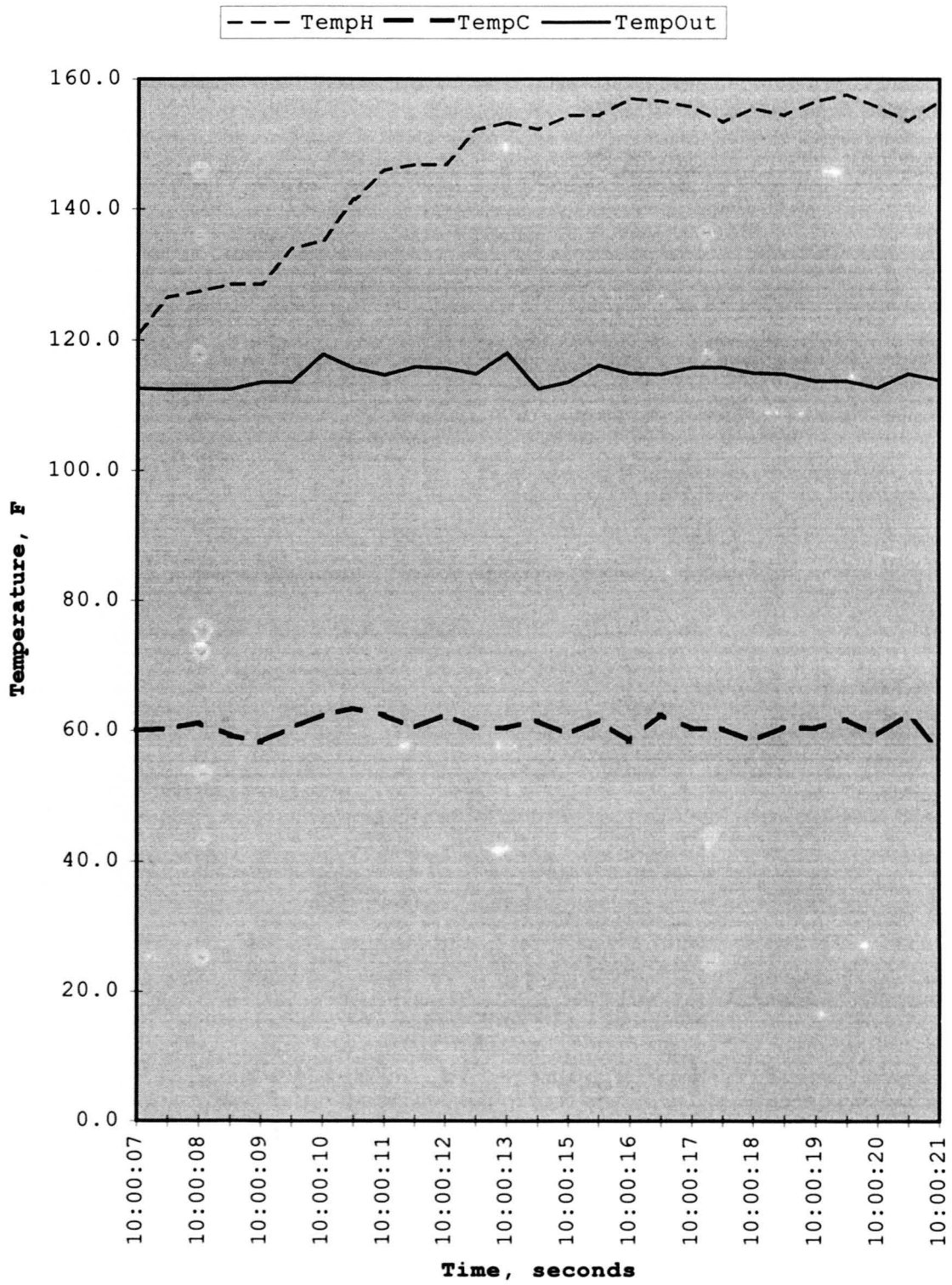


Figure 9.25: Mixing valve test, hot supply temperature increase, supply and mix temperatures

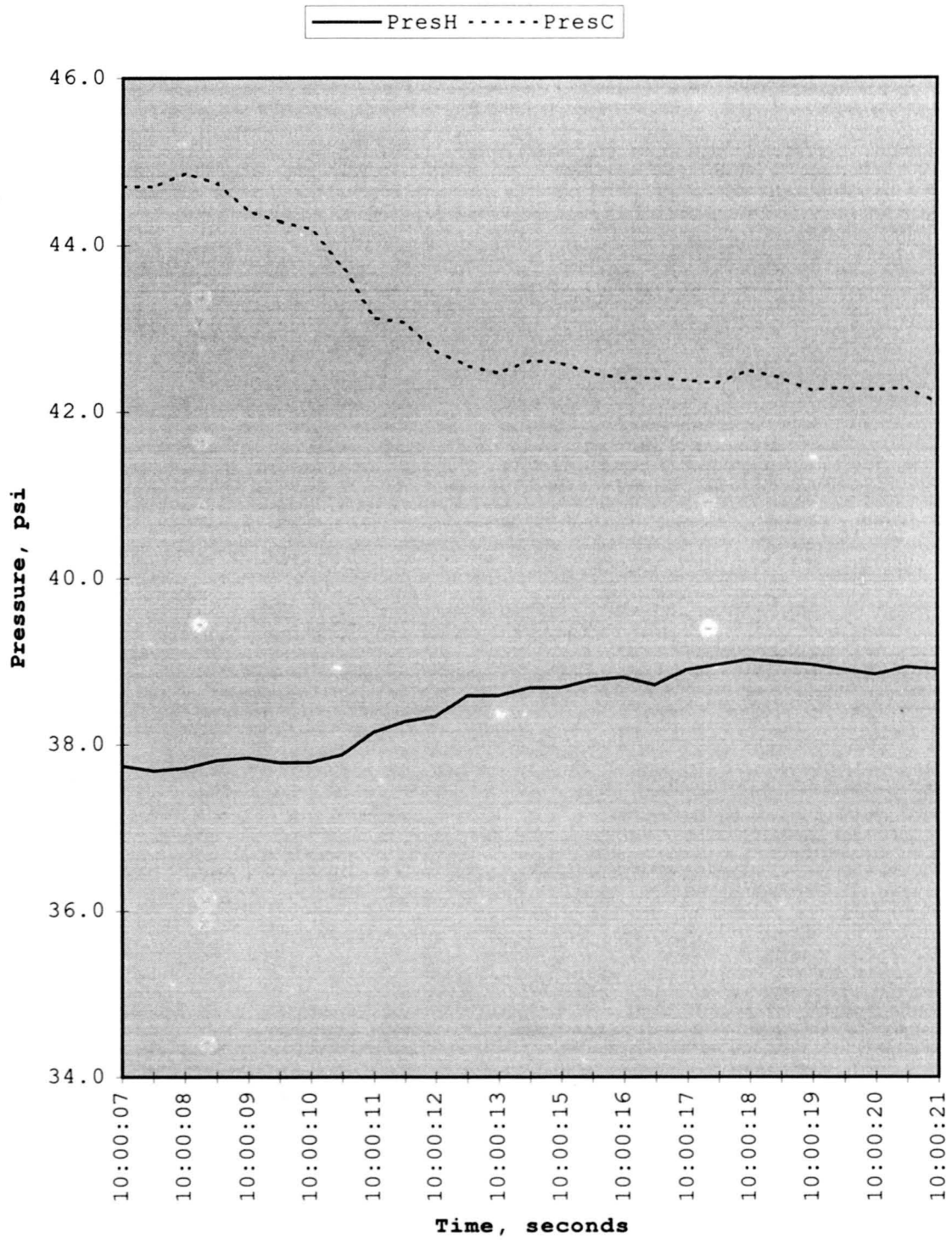


Figure 9.26: Mixing valve test, hot supply water temperature increase, supply pressure

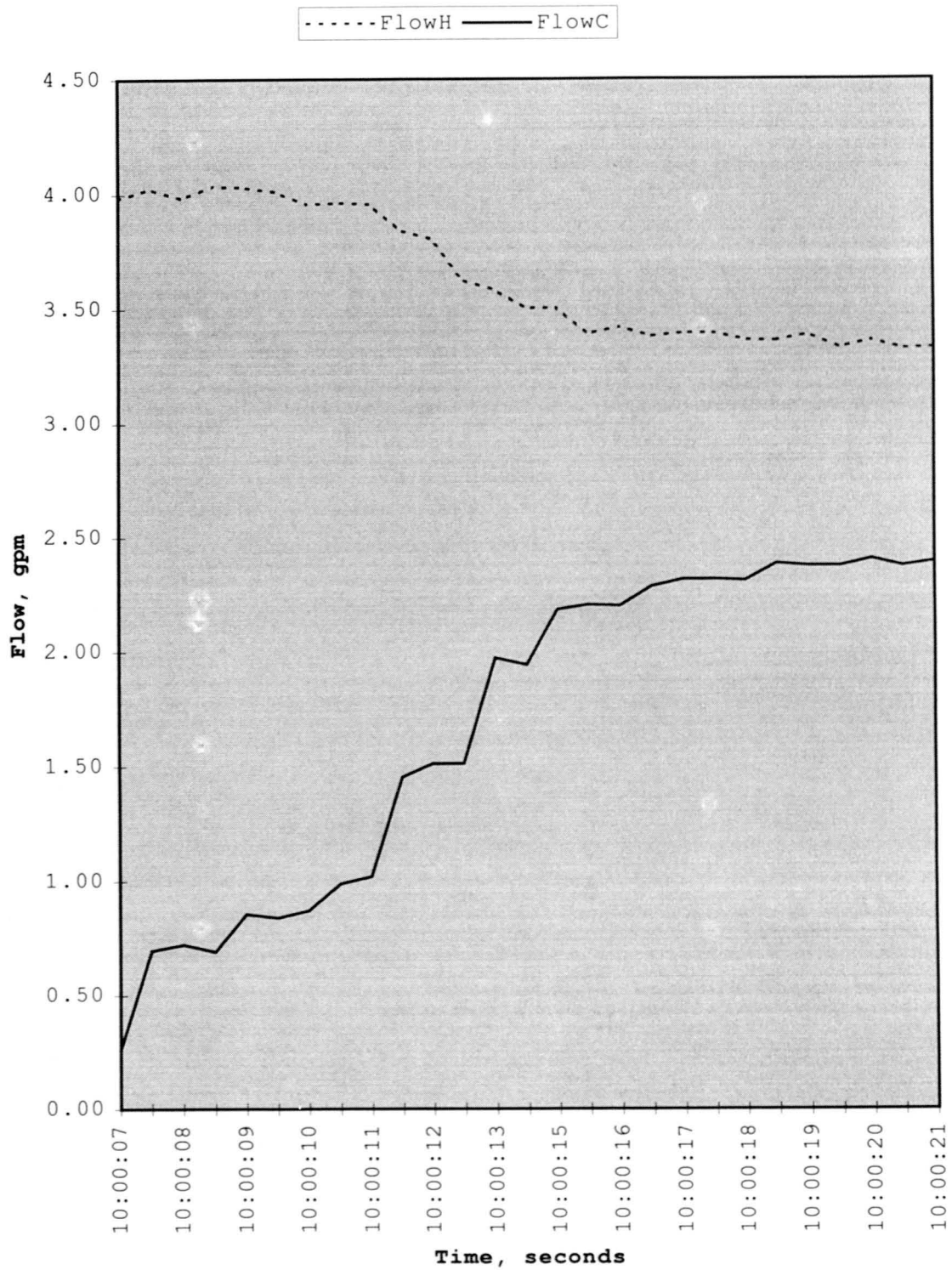


Figure 9.27: Mixing valve test, hot supply water temperature increase, supply flow

Table 9.5 Mixing valve response, hot supply temperature increase

| Time (sec) | Xs (in) | Xc (in) | Qc (gpm) | Tc (°F) | Qh (gpm) | Th (°F) | Ts (°F) | Tm (°F) |
|---------------|------------|------------|-------------|------------|-------------|------------|------------|------------|
| 0.0 | 0.0450 | 0.0041 | 1.01 | 61 | 3.52 | 121.0 | 109.5 | 109.5 |
| 0.5 | 0.0447 | 0.0041 | 1.01 | 61 | 3.52 | 126.6 | 109.4 | 111.9 |
| 1.0 | 0.0439 | 0.0043 | 1.07 | 61 | 3.48 | 127.5 | 110.1 | 111.9 |
| 1.5 | 0.0431 | 0.0045 | 1.11 | 61 | 3.46 | 128.5 | 110.3 | 112.1 |
| 2.0 | 0.0423 | 0.0047 | 1.16 | 61 | 3.43 | 128.5 | 110.4 | 111.4 |
| 2.5 | 0.0419 | 0.0048 | 1.19 | 61 | 3.41 | 133.9 | 110.5 | 115.1 |
| 3.0 | 0.0398 | 0.0053 | 1.31 | 61 | 3.34 | 135.2 | 110.8 | 114.3 |
| 3.5 | 0.0382 | 0.0057 | 1.40 | 61 | 3.28 | 141.5 | 111.1 | 117.4 |
| 4.0 | 0.0353 | 0.0064 | 1.57 | 61 | 3.18 | 145.9 | 111.5 | 117.9 |
| 4.5 | 0.0324 | 0.0071 | 1.73 | 61 | 3.07 | 146.8 | 112.0 | 115.9 |
| 5.0 | 0.0304 | 0.0075 | 1.83 | 61 | 3.00 | 146.8 | 112.3 | 114.3 |
| 5.5 | 0.0295 | 0.0078 | 1.88 | 61 | 2.96 | 152.2 | 112.4 | 116.8 |
| 6.0 | 0.0273 | 0.0082 | 1.99 | 61 | 2.89 | 153.3 | 112.7 | 115.6 |
| 6.5 | 0.0258 | 0.0086 | 2.06 | 61 | 2.83 | 152.2 | 113.0 | 113.8 |
| 7.0 | 0.0254 | 0.0087 | 2.08 | 61 | 2.81 | 154.4 | 113.0 | 114.7 |
| 7.5 | 0.0245 | 0.0088 | 2.12 | 61 | 2.78 | 154.4 | 113.1 | 114.0 |
| 8.0 | 0.0241 | 0.0089 | 2.14 | 61 | 2.76 | 156.9 | 113.2 | 115.0 |
| 8.5 | 0.0231 | 0.0091 | 2.19 | 61 | 2.73 | 156.5 | 113.3 | 114.0 |
| 9.0 | 0.0228 | 0.0092 | 2.20 | 61 | 2.72 | 155.6 | 113.4 | 113.2 |
| 9.5 | 0.0228 | 0.0092 | 2.20 | 61 | 2.72 | 153.3 | 113.4 | 113.4 |
| 10.0 | 0.0236 | 0.0090 | 2.17 | 61 | 2.74 | 155.5 | 113.3 | 113.8 |

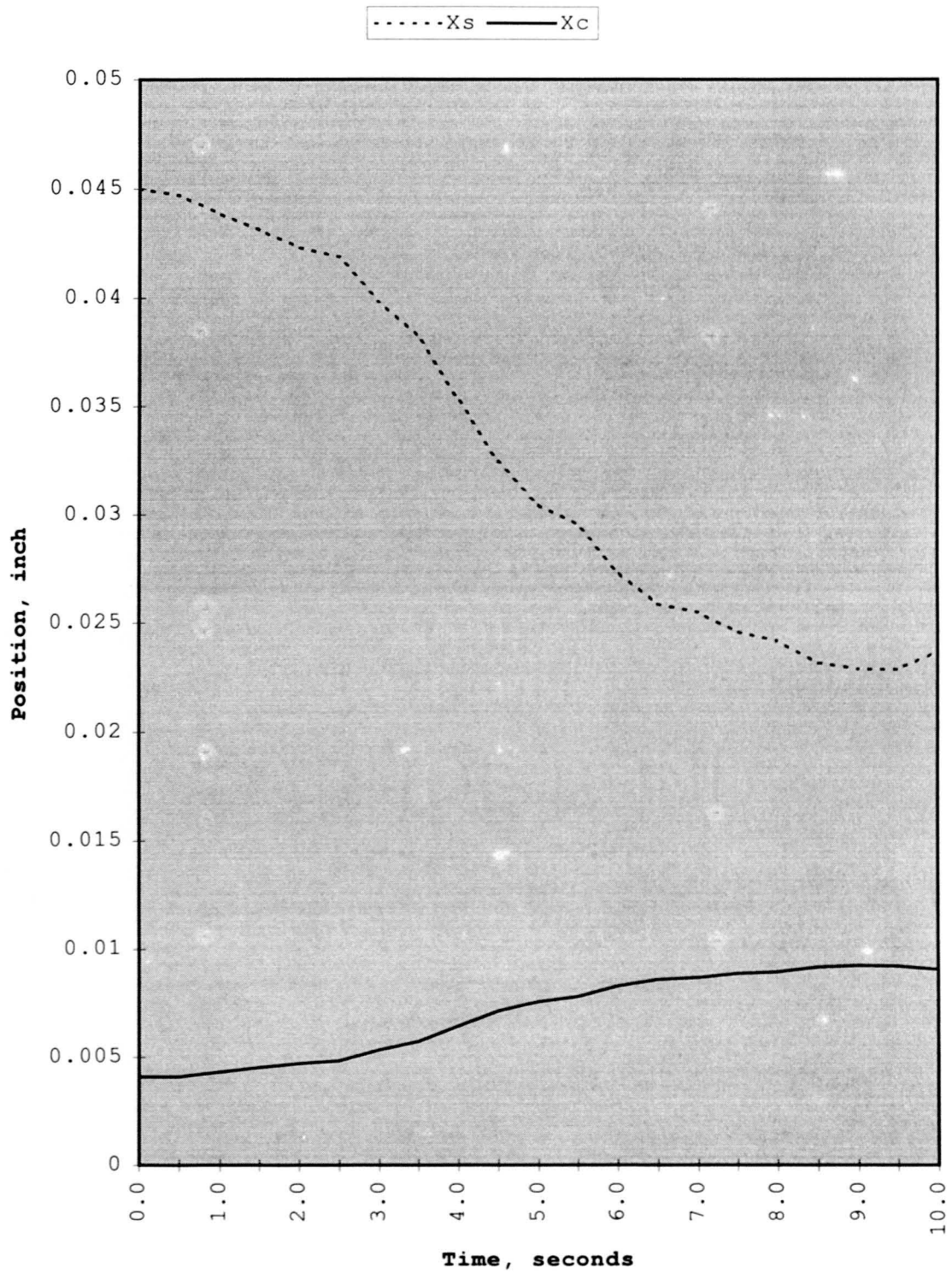


Figure 9.28: Mixing valve response, hot supply temperature increase, spool and case position

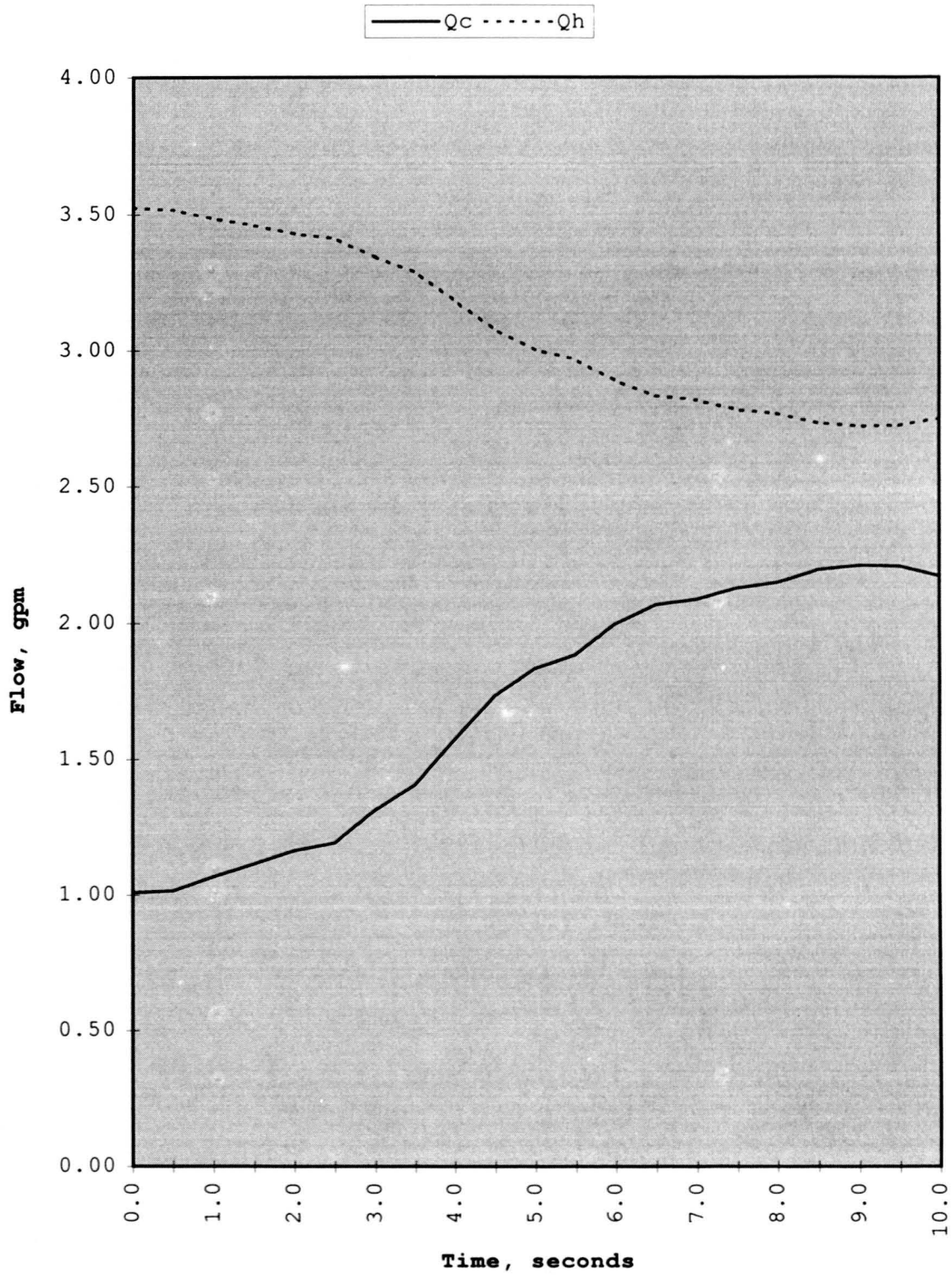


Figure 9.29: Mixing valve response, hot supply temperature increase, supply flow

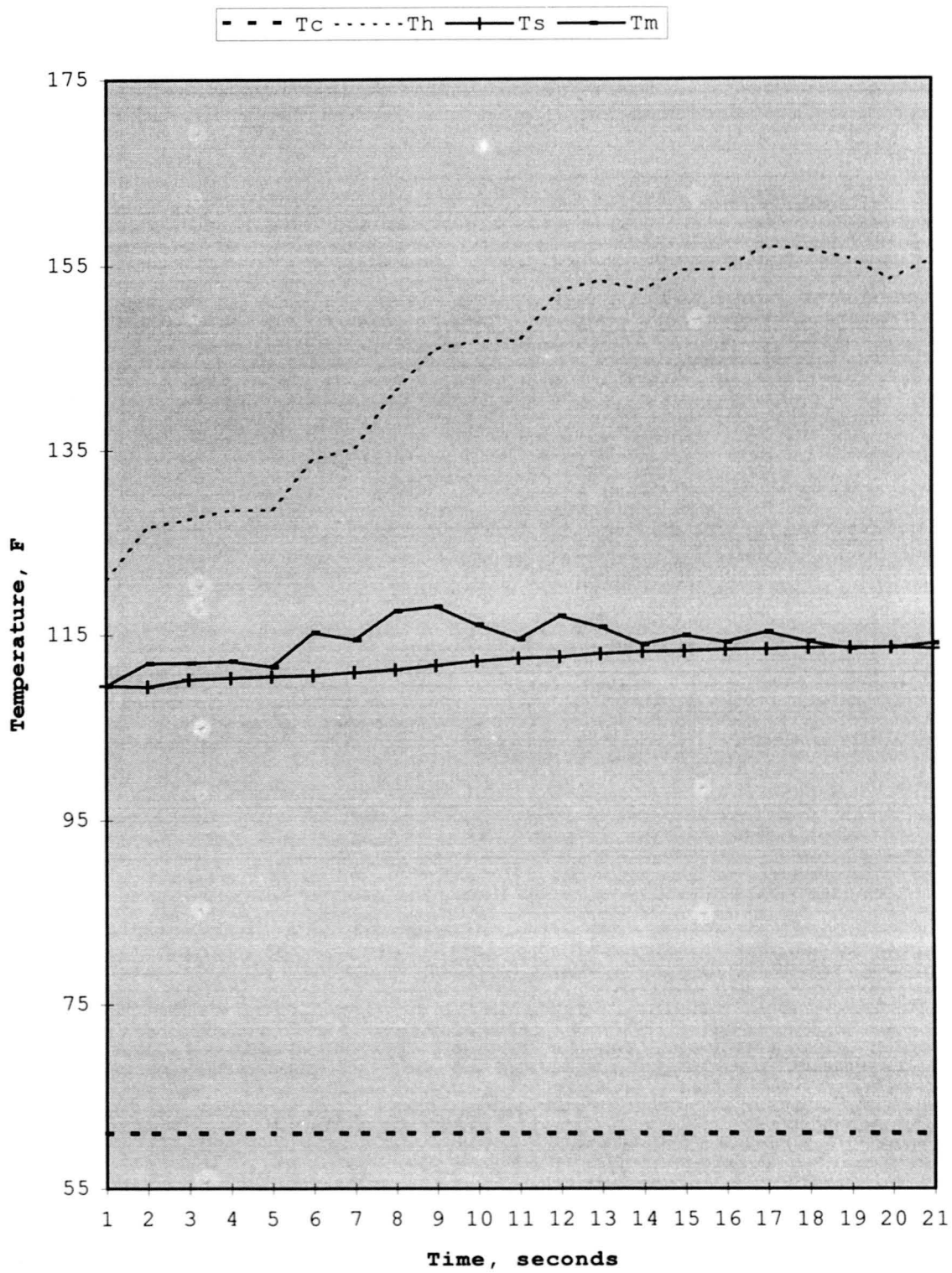


Figure 9.30: Mixing valve model, hot supply temperature increase, supply, mix and thermostat temperature

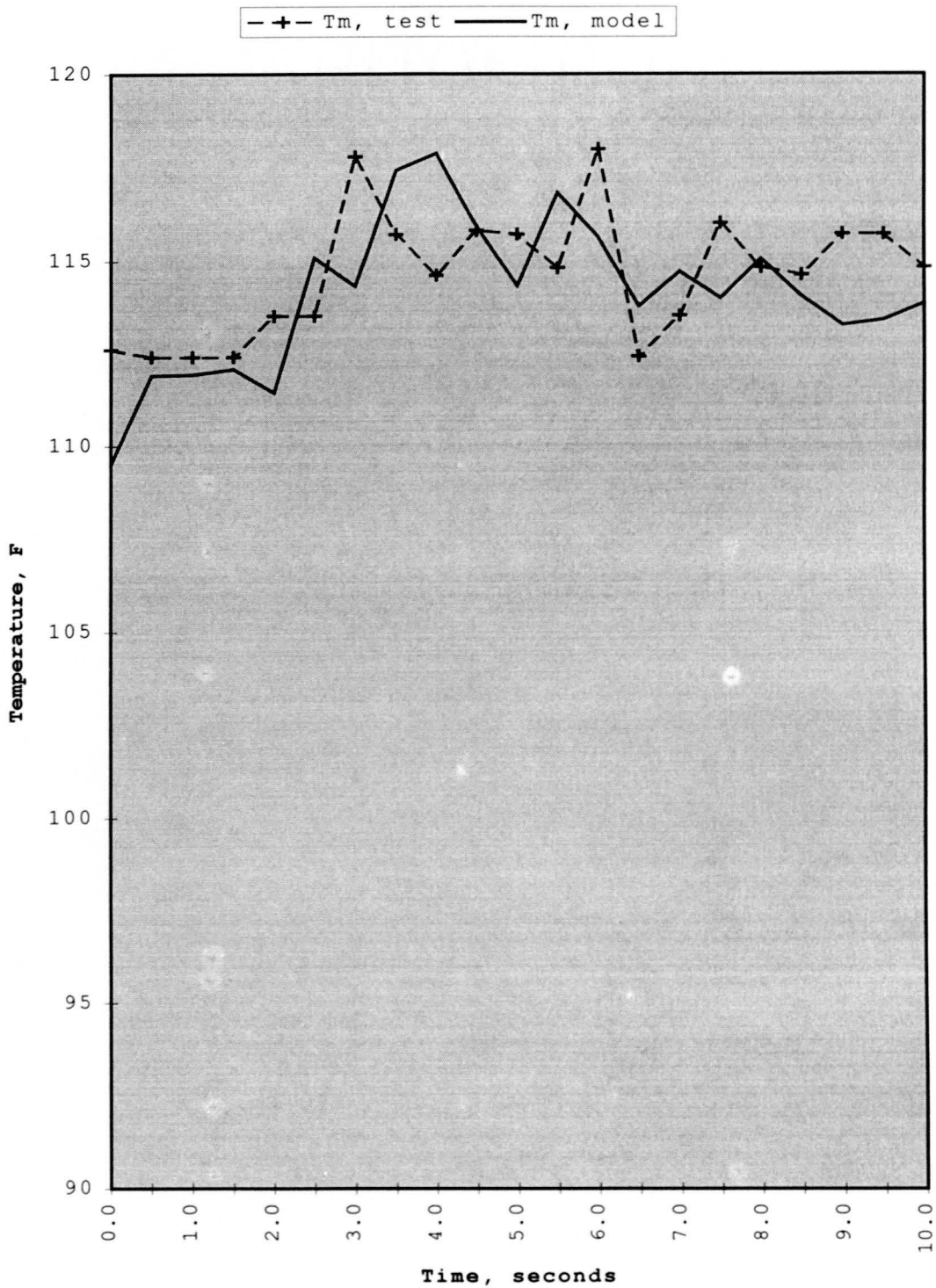


Figure 9.31: Mixing valve test and model, hot supply temperature increase, mix temperature

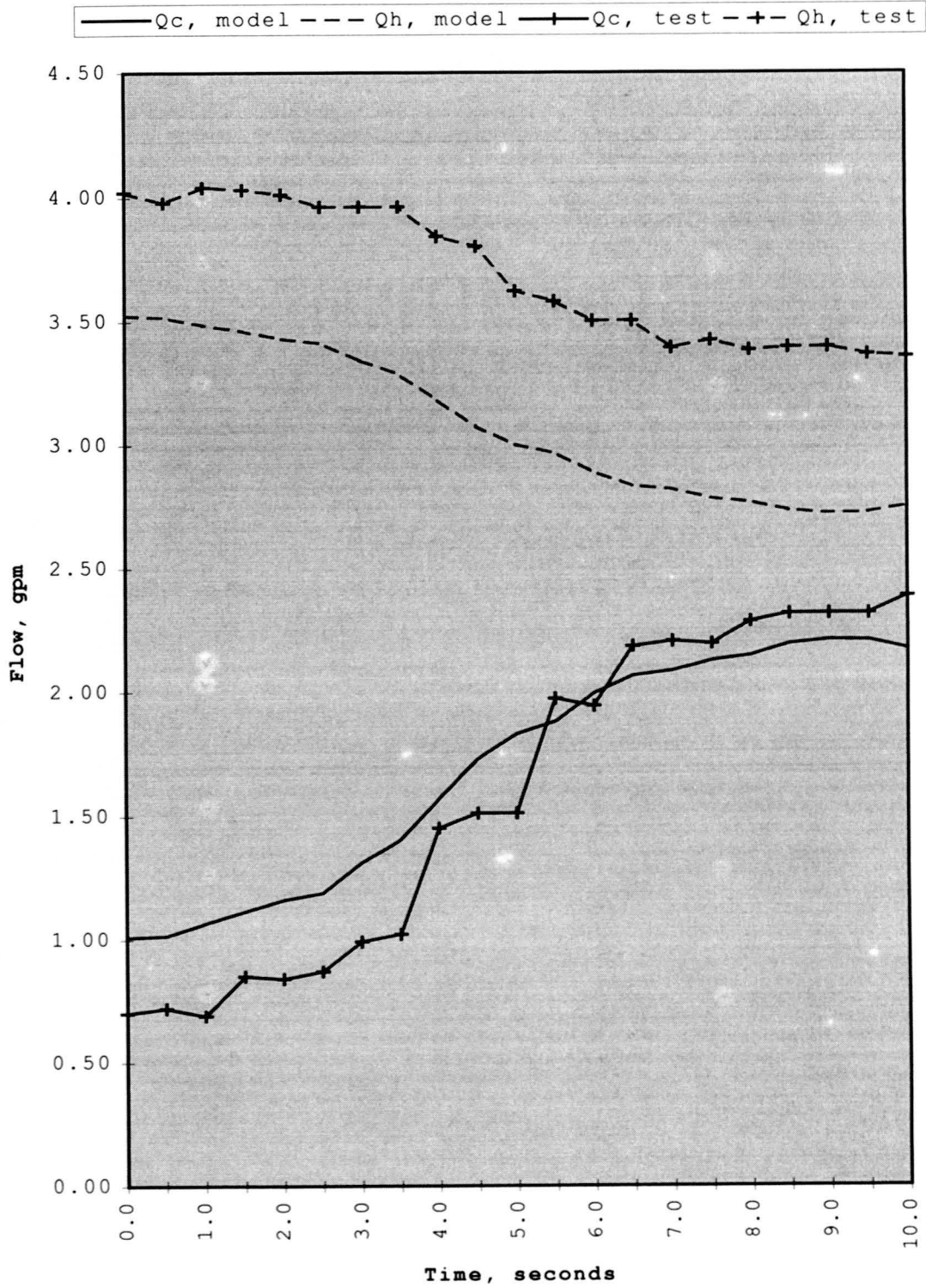


Figure 9.32: Mixing valve test and model, hot supply temperature increase, supply flow rates

CHAPTER 10. CONCLUSIONS

The objectives of this research were to develop mathematical models using differential equations to characterize the dynamic response of each of the subject valves, to develop a methodology to test the valves, and to evaluate the capability of each of the valves to control output water temperature based on changes in supply temperature and pressure.

Characteristic mathematical models were generated for each of the subject valves: mixing, pressure balance, tempering and anti-scald valves. The models did characterize the operation and dynamic response of each of the systems reasonably well.

When the steady state supply temperature conditions were changed on the pressure balance valve, the model predicted no change in supply flow rates with a change in supply flow temperature; this was verified in the valve temperature test (Figures 6.20 and 6.21). When steady state supply pressure conditions were changed on the pressure balance valve, the model predicted a mix temperature increase of 0.8°F; the valve test showed an average increase in mix temperature of 0.9°F (Figure 6.31).

When the steady state supply temperature conditions were changed on the tempering valve, the model predicted a mix temperature increase of 76.6°F in 32 seconds; the valve test showed

an increase in mix temperature of 80°F in 32 seconds (Figure 7.21). When the steady state supply pressure conditions were changed on the tempering valve, the model predicted a mix temperature increase of approximately 3.2°F, the valve test showed a mix temperature increase of 4°F (Figure 7.14).

When the steady state supply temperature conditions were gradually increased on the anti-scald valve, the model predicted the valve would close at 108.5°F; the valve test showed that the valve closed when the mix temperature was 106.5°F (Figures 8.10 and 8.13). When the steady state supply temperature was given a dramatic increase in mix temperature, the model predicted the valve would close in 2 seconds; the valve test showed that the valve closed between 2.0 and 2.5 seconds (Figure 8.18).

When the steady state supply pressure conditions were changed on the mixing valve, the model predicted the valve would keep the mix temperature at 113.5°F; the valve test showed that the average mix temperature did not change from 112.5°F (Figure 9.24). When the steady state supply temperature conditions were changed on the mixing valve, the model predicted the mix temperature would increase approximately 4°F over in 10 seconds; the valve test showed that the average mix temperature increased 1.8°F (Figure 9.31)

The models did not address head losses which occur in the valves when the hot and cold water supplies were mixed. Improvements on the models could be made by testing each of the valve components and applying actual loss coefficients to each of the models.

A test environment was established that was representative of plumbing systems found in a residential hot and cold water potable plumbing system. It reflected and conformed to the recommended test configuration described in the American Society of Sanitary Engineering standards. Pressure, temperature and flow sensors allowed accurate data to be obtained for each of the supply flows into the valves and for the mix out of the valve.

Both modeling of the valves and test results showed that the automatic mixing valve had the best performance in controlling the output water temperature when there are changes in supply temperature and pressure. The pressure balance valve performed as well as the mixing valve in controlling the output water temperature when there was a change in supply pressure. The tempering valve did respond to changes in both pressure and temperature, but the dynamic response was slow compared to the other valves. The anti-scald valve had no effect on controlling the output water temperature, but was capable of shutting off the flow of water at specific mix supply pressure and temperatures. The valves which are to be installed at the point of use exhibited the best dynamic response to limit the temperature and/or flow of water.

Recommendations for Future Work

An improved understanding of the flow characteristics across the various valve components (check valves, mixing chambers) could offer a better understanding of valve performance. Modeling of the system using compressible flow, variable fluid properties such as

viscosity and density, and using differential equations to characterize the flow may lead to an improvement in predicting the flow characteristics of the valves.

Research into thermally sensitive springs and actuators and the capability to obtain reliable, repeatable and cost effective components during the manufacturing process could be investigated further.

REFERENCES

- ANSI Z21.10.1 1993. Gas Water Heaters Volume I, Automatic Storage Type Water Heaters With Inputs of 75,000 Btu Per Hour or Less. *ANSI Standard Z21.10.1-1993*, United States of America Standards Institute, New York.
- ANSI Z21.23 1993. Gas Appliance Thermostats. *ANSI Standard Z21.23-1993*, United States of America Standards Institute, New York.
- ASSE No. 1016, 1990. Performance Requirements for Individual Thermostatic Pressure Balancing and Combination Control For Bathing Facilities. *ASSE Standard No. 1016*, American Society of Sanitary Engineering For Plumbing and Sanitary Research, Bay Village, Ohio.
- ASSE No. 1017, 1979. Performance Requirements for Temperature Actuated Mixing Valves For Primary Domestic Use. *ASSE Standard No. 1017*, American Society of Sanitary Engineering For Plumbing and Sanitary Research, Bay Village, Ohio.
- ASTM F444-88, 1988. Standard Consumer Safety Specification for Scald-Preventing Devices and Systems in Bathing Areas. *ASTM Standard F444-88*. American Society for Testing and Materials Committee on Standards, Philadelphia, Pennsylvania.
- ASTM F445-88, 1988. Standard Consumer Safety Specification for Thermal-Shock-Preventing Devices and Systems in Showering Areas. *ASTM Standard F444-88*. American Society for Testing and Materials Committee on Standards, Philadelphia, Pennsylvania.
- BOCA National Plumbing Code, 1996. *Building Officials and Code Administrators International, Inc.*, Country Club Hills, Illinois.
- Colgate-Palmolive Company, 1991. Questions Consumers Ask Most Often About Laundry. Consumer Information From Colgate-Palmolive. New York, New York.
- Feldman, K.W. 1983. Help Needed on Hot Water Burns. *Pediatrics*, Vol. 71, No. 1, January 1983.
- Fox, R.W. and McDonald, A.T. 1978. Introduction to Fluid Mechanics. John Wiley & Sons, Inc., New York, New York.

- Furry, M.S. 1965. Detergents for Home Laundering. US Government Printing office, *United States Department of Agriculture Home and Garden Bulletin No. 49*, Washington, D.C.
- General Electric Company, 1990. GE Automatic Clothes Washer Model WWA5636M Use and Care Guide. Louisville, Kentucky.
- General Electric Company, 1978. GE Automatic Dishwasher Model SD1200 Installation Instructions. Louisville, Kentucky.
- Hogben, L. 1987. Elementary Linear Algebra. West Publishing Company, St. Paul, Minnesota.
- Karlekar, B.V. and Desmond, R.M. 1977. Engineering Heat Transfer. West Publishing Company, St. Paul, Minnesota.
- Keller, G.R. 1978. Hydraulic System Analysis. *Hydraulics & Pneumatics Magazine*, Cleveland, Ohio.
- KitchenAid, Inc. 1989. KitchenAid Clothes Washer Model KAWE850V Use and Care Guide. St. Joseph, Michigan.
- KitchenAid, 1977. KitchenAid Regency and Deluxe Portable Dishwashers Use and Care Guide. Hobart Corporation, Troy, Ohio.
- Knauer, V.H. 1974. Consumer News. *Department of Health, Education and Welfare*, Vol. 4, No. 2, April 15, 1974.
- LemMon, J. 1982. Maytag Encyclopedia of Home Laundry. Western Publishing Company, Inc., Newton, Iowa.
- Lever Brothers Company, 1991. ALL Automatic Dishwasher Detergent Instructions. New York, New York.
- Maytag, 1993. Factors Affecting Dishwashing Results. Focus on Consumer Education. Newton, Iowa.
- Mettitt, H.E. 1967. Hydraulic Control Systems. John Wiley & Sons, Inc., New York, New York.
- Moritz, A.R. and F.C. Hendriques, Jr. 1947. Studies of Thermal Injuries - The Relative Temperature of Time and Surface Temperature in the Causation of Cutaneous Burns. *The American Journal of Pathology*, September 1947, Vol 23:695.
- National Standard Plumbing Code, 1987. *National Association of Plumbing-Heating-Cooling Contractors*, Falls Church, Virginia.
- Peet, L.J.; Pickett, M.S.; Arnold, M.G.; Wolf, I.H. 1975. Household Equipment. John Wiley & Sons, Inc., New York, New York.

- Procter & Gamble, 1986. Cascade Automatic Dishwasher Detergent Instructions. Cincinnati, Ohio.
- Roper, 1989. Roper Dishwasher Model 8587 and 8597 Marketing Brochure. Roper Appliances, Benton Harbor, Michigan.
- Sanitation in Home Laundering, 1971. US Government Printing office, *United States Department of Agriculture Home*, Washington, D.C.
- Sears, Roebuck and Company, 1992. Sears Kenmore Dishwasher Part No. 3369796 Dishwasher Installation Instructions. Chicago, Illinois.
- Speed Queen Company, 1987. Speed Queen Handbook to Better Automatic Washing. Ripon, Wisconsin.
- Steele, Alfred. 1988. Temperature Limits in Service Hot Water Systems. *American Society of Plumbing Engineers Research Foundation Research Report 88-01*, 1988, Westlake, California.
- Tappan, 1992. Tappan Dishwasher and Trash Compactor Collection Brochure. White Consolidated Industries, Dublin, Ohio.
- Uniform Plumbing Code, 1994. *International Association of Plumbing and Mechanical Officials*, Walnut, California.
- Whirlpool Corporation, 1991. Whirlpool Dishwasher Model DU8500XX Use and Care Guide. Benton Harbor, Michigan.
- Whirlpool Corporation, 1979. Whirlpool Laundry Guide for Whirlpool Automatic Washers. Benton Harbor, Michigan.